DOT/FAA/TC-15/6

Federal Aviation Administration
William J. Hughes Technical Center
Aviation Research Division
Atlantic City International Airport
New Jersey 08405

A Quantitative Assessment of Conventional Nondestructive Inspection Techniques for Detecting Flaws in Composite Laminate Aircraft Structures

March 2016

Final Report

U.S. Department of Transportation
Federal Aviation Administration

NOTICE

Technical Report Documentation Page

1. Report No.	2. Government Accession No.	3. Recipient's Catalog No.
DOT/FAA/TC-15/6		

4. Title and Subtitle	5. Report Date
A QUANTITATIVE ASSESSMENT OF CONVENTIONAL NONDESTRUCTIVE INSPECTION TECHNIQUES FOR DETECTING FLAWS IN COMPOSITE LAMINATE AIRCRAFT STRUCTURES	March 2016
	6. Performing Organization Code
7. Author(s) Dennis P. Roach, Thomas M. Rice, and Kirk A. Rackow	8. Performing Organization Report No.
9. Performing Organization Name and Address Sandia National Laboratories FAA Airworthiness Assurance Center Box 5800 MS-0615 Albuquerque, NM 87185	10. Work Unit No. (TRAIS)
	11. Contract or Grant No. DTFA03-95-X-900002
12. Sponsoring Agency Name and Address U.S. Department of Transportation Program Management and Information Branch 950 L'Enfant Plaza, S.W. 5th Floor Washington, DC 20024	13. Type of Report and Period Covered Final Report
	14. Sponsoring Agency Code AFS-320

15. Supplementary Notes

The Federal Aviation Administration William J. Hughes Technical Center Aviation Research Division CORs were Dave Galella and David Westlund.

16. Abstract

The aircraft industry continues to increase its use of composite materials, most notably in the area of principle structural elements. This expanded use, coupled with difficulties associated with the damage tolerance analysis of composites, has placed greater emphasis on the application of accurate nondestructive inspection (NDI) methods. Traditionally, a few ultrasonic-based inspection methods have been used to inspect solid laminate structures. Recent developments in more advanced NDI techniques have produced a number of new inspection options. Many of these methods can be categorized as wide area techniques that produce two-dimensional flaw maps of the structure. An experiment has been developed to assess the ability of both conventional and advanced NDI techniques to detect voids, disbonds, delaminations, and impact damage in adhesively bonded composite aircraft structures. A series of solid laminate, carbon composite specimens with statistically relevant flaw profiles are being inspected using conventional, handheld pulse echo ultrasonic testing (PE UT) and resonance, as well as new NDI methods that have recently been introduced to improve sensitivity and repeatability of inspections. The primary factors affecting flaw detection in laminates included in this study are material type, flaw profiles, presence of complex geometries like taper and substructure elements, presence of fasteners, secondarily bonded joints, and environmental conditions. One phase of this effort used airline personnel to study probability of detection (POD) in the field and to formulate improvements to existing inspection techniques. In addition, advanced NDI methods for laminate inspections—such as thermography, shearography, scanning PE UT, ultrasonic spectroscopy, and phased array UT—were applied to quantify the improvements achievable through the use of more sophisticated NDI. This report presents the composite laminate experiment design and POD results for conventional NDI as deployed at aircraft maintenance depots. A companion report will provide the results from the advanced NDI testing.

17. Key Words	18. Distribution Statement
Nondestructive inspection, Honeycomb composites, Solid laminate composites, Probability of detection, Disbonds, Delaminations, Impact	This document is available to the U.S. public through the National Technical Information Service (NTIS), Springfield, Virginia 22161. This document is also available from the Federal Aviation Administration William J. Hughes Technical Center at actlibrary.tc.faa.gov.

19. Security Classif. (of this report)	20. Security Classif. (of this page)	21. No. of Pages	22. Price
Unclassified	Unclassified	301	

Form DOT F 1700.7 (8-72) Reproduction of completed page authorized

ACKNOWLEDGEMENTS

This program is sponsored by the Federal Aviation Administration (FAA) William J. Hughes Technical Center under the direction of the technical monitor, Dave Galella. The approach used in this effort was formulated in concert with the Commercial Aircraft Composite Repair Committee Inspection Task Group (CACRC-ITG), which consisted of the team members listed below. The contributions of this team are gratefully acknowledged.

<u>CACRC-ITG (at time of experiment planning)</u>
Gerry Doetkott, Northwest Airlines
Alex Melton, Northwest Airlines (now Delta Air Lines)
Richard Watkins, Delta Air Lines
Tom Dreher, United Airlines®, now Rolls-Royce®
Robert Stevens, United Airlines
Bruce Garbett, Airbus® Industries
John Hewitt, Airbus Industries
Jim Hofer, The Boeing Company™
Jeff Kollgaard, The Boeing Company™
Glae McDonald, US Airways®
Kirk Rackow, Sandia National Laboratories Airworthiness Assurance NDI Validation Center (AANC)
Dennis Roach, Sandia National Laboratories AANC

The authors would like to recognize the data acquisition support provided by others at the Sandia Laboratories AANC, including Stephen Neidigk, Randy Duvall, and Tony Delong. Thanks go to those who provided FAA oversight and extensive guidance on this effort: Dave Galella, FAA Project Manager, and Rusty Jones, FAA Senior Technical Specialist in Nondestructive Inspection. Thanks also to Wayne Weisner, of Olympus, and Jeff Register, of General Electric, for their equipment support and to Eric Chesmar and his United Airlines colleagues for their assistance in test specimen production.

Finally, the authors would like to thank the following maintenance facilities for participating in this experiment: All Nippon Airways®, American Airlines®, Cathay Pacific Airlines, China Airlines™, Continental Airlines® (pre-merger with United), Delta Air Lines (Atlanta and Minneapolis facilities), Federal Express® (Los Angeles and Memphis facilities), Goodrich Aerospace, Japan Airlines, Northwest Airlines (pre-merger with Delta), Singapore Airlines, Taikoo Aircraft, Thai Airways, United Airlines, and US Airways.

TABLE OF CONTENTS

LIST OF FIGURES

LIST OF TABLES

LIST OF SYMBOLS, ABBREVIATIONS, AND ACRONYMS

2D	Two-dimensional
a	Flaw length
a_c	Critical flaw size
a_d	Minimum detectable flaw size
a_p	Maximum permissible flaw size
A&P	Airframe and powerplant
AANC	Airworthiness Assurance NDI Validation Center
AC	Advisory Circular
ARP	Aerospace Recommended Practice
BN	Bullnose
BVID	Barely visible impact damage
CACRC	Commercial Aircraft Composite Repair Committee
CAL	Calibration
CG	Complex geometry
CT	Constant thickness
DTA	Damage tolerance analysis
FAA	Federal Aviation Administration
FBH	Flat bottom hole
FS	Flaw signal
FSH	Full screen height
GE	General Electric
GRI	Grafoil insert
ITG	Inspection Task Group
LFBT	Low frequency bond test
MAUS	Mobile Automated Scanner
MIA	Mechanical impedance analysis
MRO	Maintenance and repair organization
NDI	Nondestructive inspection
NDT	Nondestructive testing
OEM	Original equipment manufacturer
OJT	On-the-job training
PE	Pulse echo
PE UT	Pulse-echo ultrasonic testing
P_L	Limit load
POD	Probability of detection
$POD_{[90]}$	Probability of detection of 90%
$POD_{[90/95]}$	Probability of detection of 90% with 95% confidence
RDC	Ramp damage checker
RDCE	Ramp damage check experiment
S/N	Signal-to-noise ratio
SLE	Solid laminate experiment
ST	Simple taper
STL	Simple taper lower
STU	Simple taper upper
UT	Ultrasonic testing

EXECUTIVE SUMMARY

The rapidly growing use of composites on commercial airplanes, coupled with the potential for economic savings associated with their use in aircraft structures, has increased the demand for composite materials technology. Inspecting these composite structures is a critical element in assuring their continued airworthiness. Typical damage encountered in composite structures includes: (1) disbonds and delaminations stemming from normal flight loads, (2) fluid ingress, (3) impact damage, (4) lightning strikes, (5) deterioration from contact with fluids, such as paint strippers or hydraulic fluids, and (6) extreme heat and ultraviolet exposure. Each of these elements can produce hidden damage that may be difficult to visually detect yet are detrimental to the strength of the structure.

The Federal Aviation Administration Airworthiness Assurance NDI Validation Center (FAA-AANC) at Sandia National Laboratories completed a study to evaluate the performance of conventional inspection methods as applied to flaw detection in solid composite laminate structures. Input from the aviation industry was received from the Commercial Aircraft Composite Repair Committee Inspection Task Group (CACRC-ITG). This experiment assessed the ability of conventional nondestructive inspection (NDI) techniques, as deployed at aircraft maintenance facilities, to detect voids, disbonds, delaminations, and impact damage in adhesively bonded composite aircraft structures. A series of solid laminate, carbon composite specimens with statistically relevant flaw profiles were inspected using conventional, handheld pulse echo ultrasonic testing (PE UT) to evaluate the sensitivity and repeatability of this inspection method. This program used airline personnel to study probability of detection (POD) in the field and formulate improvements to existing inspection techniques. After a sufficient number of inspectors completed the experiment, industry-wide performance curves showing the probability of detection versus flaw size were established to determine how well current inspection techniques are able to reliably find flaws in composite laminate structures.

In total, over 70 inspectors from 14 airlines and 2 maintenance and repair organizations (MRO) participated in this experiment. The inspections emphasized flaw detection methods applicable to solid laminate structures ranging from 12–64 plies thick. This study was driven by a desire to improve aircraft safety. Airlines and original equipment manufacturers (OEM) can use these results to guide NDI deployment and training, define what flaws/damage can be reliably found by inspectors, and reduce the human factors issues to effect improved NDI performance in the field. Overall, the results from this study produced input and recommendations to the FAA regarding guidance (e.g., Advisory Circulars) that can enhance the composite inspection process.

The Solid Laminate Experiment (SLE) includes a set of 15 carbon-graphite composite laminate test specimens that contain engineered flaws (disbonds, interply delaminations, and impact damage). The test specimens include approximately 200 flaws with sufficient unflawed regions to allow for an assessment of false calls. To implement a realistic experiment, it was necessary to design representative specimens that include a full spectrum of variables found on composite aircraft structures. This included the different construction scenarios, such as various ply thicknesses, different substructure thicknesses, the presence of fasteners, bonding methods for substructure (co-cured and secondarily bonded), and geometry issues (e.g., curved surfaces, small access regions, taper/ply drop-offs) that can make inspections difficult. Another important factor in the specimen design was to determine the most prevalent flaw types found on this type of structure and to develop ways to engineer representative flaws. Other isolated POD information derived from this study includes flaw detection performance in selected areas, such as substructure regions or tapered areas. These results can be compared to inspection results from other categories (e.g., constant thickness regions) to pinpoint the greatest challenges associated with composite NDI. Five NDI feedback specimens were also produced. These feedback specimens contain all of the same construction and flaw types as those found in the blind POD tests specimens. The flaw profiles in the NDI feedback specimens were provided to each inspector so that they could become comfortable with the inspection demands before moving on to the blind POD specimens.

While the size of flaw, or damage, that must be detected is affected by many parameters (e.g., structure type, location on aircraft, stress, and fatigue levels), the general goal for composite inspections is to detect flaws that are 1″ diameter or larger. Many of the NDI reference standards in OEM NDT manuals use 1″ diameter flaws to guide equipment set-up. In addition, the CACRC-ITG members generally concur that 1″ flaw detection provides a good center point for this SLE.

The purpose of the SLE was to determine the minimum flaw size for which there is a 95% confidence that the POD is at least 90% ($POD_{[90/95]}$). Therefore a range of flaw sizes from 0.25″ to 2″ was used. From the data collected, POD versus flaw size curves were generated and the intersect with the 95% threshold determined.

In addition, a customized POD experiment was produced from the SLE and is called the ramp damage check experiment (RDCE). The purpose of the RDCE is to assess new, ultrasonic-based “go/no go” equipment that the OEMs plan to allow airlines to deploy at airports and other nonscheduled maintenance depots using NDI and non-NDI aircraft maintenance personnel. The equipment can be deployed whenever visual clues or other events that warrant closer scrutiny of a composite laminate structure occur. Ground personnel, with appropriate training on such equipment, will set up the equipment in accordance with OEM-supplied procedures and then make an assessment of the region in question.

POD curves were produced for each inspector, as well as the resulting cumulative POD curve for both the thin (12–20 ply) and the thick (20–32 ply) laminate experiments. The curves show the variation within the group of inspectors that completed each experiment. In the thin (12–20 ply) laminate experiment, the best performing inspector produced a $POD_{[90/95]}$ = 0.53″ diameter flaw, the worst inspector produced a $POD_{[90/95]}$ = > 3.00″ diameter, and the overall cumulative result was a $POD_{[90/95]}$ = 1.29″ diameter. For the thick (20-32 ply) laminate experiment, the best performing inspector produced a $POD_{[90/95]}$ = 0.54″ diameter, the worst inspector produced a $POD_{[90/95]}$ = > 3.00″ diameter, and the cumulative result was a $POD_{[90/95]}$ = 0.82″ diameter. When all results are combined into a comprehensive composite solid laminate flaw detection experiment, it was determined that an inspector deploying a handheld, PE UT method can achieve an overall $POD_{[90/95]}$ level when the flaw, or damage, is approximately 1.0″ in diameter. This indicates that a flaw of approximately 1.0″ in diameter could be reliably detected (within the industry standard of 90% POD with a 95% confidence) by an inspector using manually deployed pulse echo ultrasonic equipment to inspect a composite structure in the 12–32 ply skin thickness range (plus substructures which make the total lay-up a maximum of 64 plies).

Detection of flaws in the presence of substructure elements, either in the bond line or substructure itself (e.g., stringer, frame), are the most challenging. The complexity of the PE UT waveform increases drastically in the areas of substructure elements. In addition, the added signal penetration requirement and associated porosity increase, coupled with reflections from dissimilar materials (resin or bond lines vs. composite laminates), create lower amplitude signals. This decreases the signal-to-noise ratios so that flaw signals are more difficult to discern. Overall, false calls were not deemed to be a problem. In fact, depending on the tolerance of the airline or MRO to revisit sites to make final determinations on flaw calls, it seems that inspectors could possibly set their thresholds slightly lower to possibly improve flaw detection while only slightly increasing the number of false calls. This would mean that the number of false calls could increase above the current overall numbers of one false call per 17 $ft.^2$, but the POD could be improved.

When participants were directed to particular inspection regions—simulating occasions when impact or other visible surface features indicate a need for a local inspection—they were able to improve their flaw detection well beyond that produced in an open, wide area inspection mode (e.g., SLE). The overall results calculated from all experiment participants and all flaws contained in the RDCE revealed a $POD_{[90/95]} = 0.78''$ diameter for this type of focused, go/no go inspection.

The RDCE showed that untrained people could receive basic training and properly deploy the go/no go NDI equipment if they focus sufficient attention on detail. However, the user must properly set up the equipment for the subsequent inspections to be effective. Limitations in the application of the go/no go devices were identified.

Multiple human factors issues and technical inspection challenges were highlighted and recommendations were produced to guide efforts to improve NDI performance. Specific procedural improvements were identified for the deployment of both conventional PE UT as well as the Ramp Damage Checker by Olympus and Bondtracer™ by General Electric (GE®). These can be readily integrated into NDI procedures in OEM nondestructive testing (NDT) manuals.

Currently, the lack of routine exposure to composite inspections makes it difficult for inspectors to maintain the necessary level of expertise. It is recommended that OEMs, or some other aviation agency, design a set of composite specimens—much like the NDI feedback specimens used in this experiment—for inclusion in aircraft NDI shops. Added exposure to available flaw specimens is viewed as a way to keep inspectors ready, well trained, and current on composite inspections.

This experiment provides overall POD values for inspecting composite laminate structures so that the aviation industry can: (1) better understand what type of damage detection is possible for specific inspection scenarios, (2) adjust inspection procedures to optimize performance, and (3) intelligently enhance inspector preparation and training to generate the performance improvements possible with optimized NDI deployment, sufficient knowledge of the inspection idiosyncrasies, and increased exposure to realistic composite inspection demands. Improvements in this critical PE-UT NDI technique could help detect damage in its early stages, thus improving safety and reducing the costs associated with the restoration of a larger affected area.

1. INTRODUCTION AND BACKGROUND

1.1 OVERVIEW OF SOLID LAMINATE EXPERIMENT

The rapidly increasing use of composites on commercial airplanes, coupled with the potential for economic savings associated with their use in aircraft structures, has increased the demand for composite materials technology. Inspecting these composite structures is a critical element in assuring their continued airworthiness. The Federal Aviation Administration Airworthiness Assurance NDI Validation Center at Sandia National Laboratories (FAA-AANC) completed a study to evaluate the performance of conventional and advanced inspection methods as applied to flaw detection in solid composite laminate structures. Input from the aviation industry was received from the Commercial Aircraft Composite Repair Committee Inspection Task Group (CACRC-ITG).

The aircraft industry continues to increase its use of composite materials, most notably in the area of principle structural elements. The extreme damage tolerance and high strength-to-weight ratio of composites have motivated designers to expand the role of fiberglass and carbon graphite in aircraft structures. This has placed greater emphasis on the development of improved nondestructive inspection (NDI) methods that are more reliable and sensitive than conventional NDI and the optimization of current inspection practices. The FAA-AANC has been pursuing this goal via a host of studies addressing the inspection of composite structures. Through the AANC's participation in the CACRC-ITG, this team has been investigating the performance of conventional inspection methods and determining the need for improved inspections of composite structures.

The FAA-AANC conducted the Solid Laminate Experiment (SLE) to assess flaw detection in composite laminate aircraft structures. The SLE involves the use of a set of composite laminate test specimens (see figure 1) containing engineered flaws that were shipped to airlines and third-party maintenance depots to acquire flaw detection data from aviation industry inspectors. The experiment required approximately 2–3 days of each inspector's time. In general, inspectors were asked to locate and size hidden flaws in the test specimens. After a sufficient number of inspectors completed the experiment, industry-wide performance curves were established to determine how well current inspection techniques are able to reliably find flaws in composite laminate structure. In total, over 70 inspectors from 14 airlines and 2 maintenance and repair organizations (MRO) participated in this experiment. The test program was intended to evaluate the technical capability of the inspection procedures and the equipment (i.e., NDI method). Evaluation of inspector-specific or environment-specific factors associated with performing this inspection were not the primary objective of this experiment; however, key insights regarding measures to improve inspection performance were obtained. The inspections emphasized flaw detection methods applicable to solid laminate structures ranging from 12–64 plies thick. The results are published in this report as industry-wide performance measures and all links to specific aircraft maintenance depots have been removed.

The CACRC-ITG completed an effort to develop solid laminate and honeycomb NDI reference standards [1] to aid in the uniform and optimum application of aircraft NDI techniques. As a follow-on activity, the CACRC-ITG completed a multi-year study to assess flaw detection capabilities in composite honeycomb structure. A natural extension of these efforts is to assess flaw detection capabilities in composite laminate structure. This document summarizes the experiment purpose, the test variables included in the study, experiment planning issues, the set of test specimen designs, and a comprehensive set of results from this experiment.

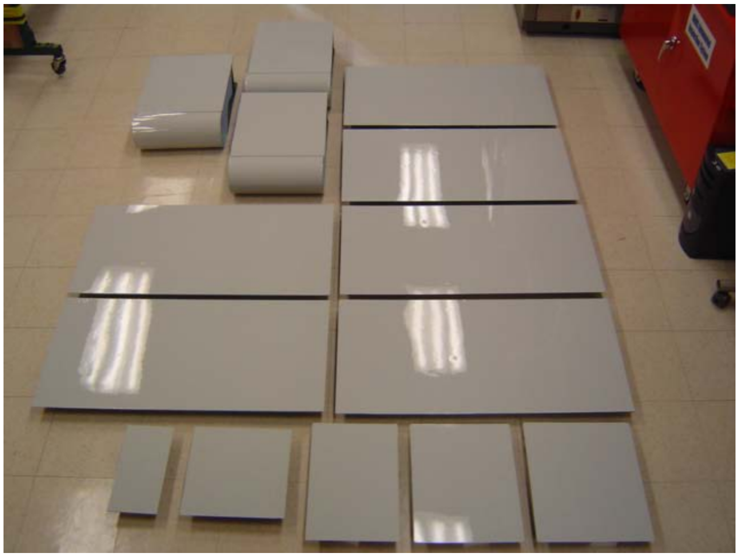

Figure 1. Subset of the 15 painted solid laminate test specimens and 5 feedback specimens

This experiment uses a series of solid laminate composite specimens with statistically relevant flaw profiles to evaluate flaw detection using pulse echo ultrasonic testing (PE UT) and other advanced NDI methods. These tests are being conducted using nondestructive testing (NDT) equipment that the inspectors are experienced in using for this type of inspection. The effort focuses on understanding the factors influencing the performance of NDI methods (device and inspector) when applied to the inspection of solid laminate composites. The primary factors included in this study that affect NDI are composite materials, flaw profiles, thickness of structure, geometry of structure, presence of substructure elements, presence of bond lines, presence of fasteners, sealed joints, skin over honeycomb substructure, and environmental conditions. The phase of the study described here used airline personnel to study PE UT inspections with a POD experiment in the field to formulate improvements for this critical inspection method.

The main reasons for this experiment are to: (1) optimize composite laminate inspection procedures, (2) determine in-service flaw detection capabilities of conventional NDI methods and measure potential for improvements through the application of advanced NDI methods and equipment, (3) compare results from handheld devices with results from scanning systems (focus on A-scan vs. C-scan and human factors issues in large area coverage), and (4) provide additional information on laminate inspections for the “Composite Repair NDT/NDI Handbook” (ARP 5089). The motivations for the SLE will be discussed in greater detail in section 2.

The assessment of advanced NDI methods was achieved from the extension of this study beyond conventional PE-UT to include new NDI equipment and methods that are in development or are being proposed for application to aircraft inspections. Results from this testing will quantify the degree of improvements possible through the integration of more advanced NDI techniques and improved procedures. This report includes the results from the application of conventional PE UT inspection methods.

1.2 INCREASING USE OF COMPOSITES IN AIRCRAFT STRUCTURES

Composite materials are increasingly becoming the material of choice for aircraft designers because of their global benefits. Engineers estimate that building comparable fuselages with aluminum would take thousands of components and fasteners, and would require extensive tooling and dozens of technicians. Additionally, an aircraft would weigh about 20% more and consume more fuel. Through the use of composite technology construction, engineers can cut the number of parts in an assembly in half. This results in significant cost savings. Other benefits of composite technology include lower acquisition costs, lower operating costs, as well as improved maintainability, reliability, and durability.

New transport and commuter category aircraft, such as the Boeing 787 and Airbus A380, are being produced with much of their structure composed of composite materials. Typical damage encountered in composite structures includes: (1) disbonds and delaminations stemming from normal flight loads, (2) fluid ingress, (3) impact damage, (4) lightning strikes, (5) deterioration from contact with fluids, such as paint strippers or hydraulic fluids, and (6) extreme heat and ultraviolet exposure. Each of these elements can produce hidden damage that may be difficult to visually detect but which is detrimental to the strength of the structure.

The expanded use of composite materials on aircraft has driven a number of FAA-AANC programs to validate and aid the associated inspection process. References 1–3 describe a successful effort to develop an industry-wide set of composite reference standards. The standards are being used in NDI equipment calibration for damage assessment and post-repair inspection of commercial aircraft composites. Final review of these honeycomb and solid laminate standards was completed and several aircraft manufacturers have already adopted these standards into their maintenance manuals. The activity described in this report complements the composite reference standard development effort. The purpose of this experiment was to assess the ability of conventional and emerging NDI techniques to inspect for flaws in representative composite structures. The SLE experiment established the sensitivities and limitations of applicable NDI methods. Other observations accumulated during the test program will allow for inspection improvements via optimized procedures and practices.

Figures 1–5 depict the increasing use of composite materials in aircraft manufacture and highlight some of the principal structural elements that are now being fabricated from composite laminate materials. Figures 6 and 7 show several finished composite aircraft components. They underscore the degree of complexity associated with these structures and the size of components that are being fabricated from composites.

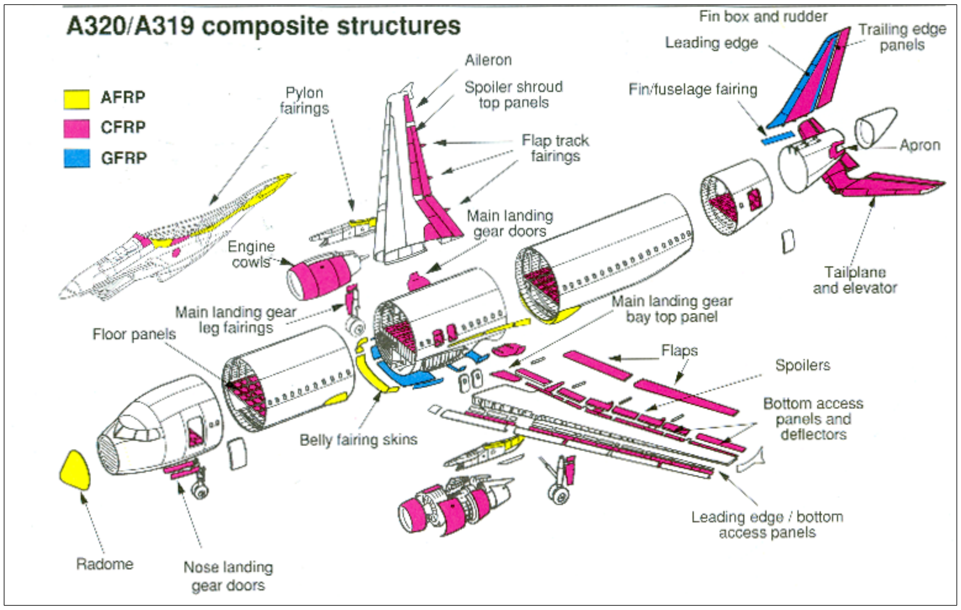

Figure 2. Use of composite structures on Airbus 320 series aircraft

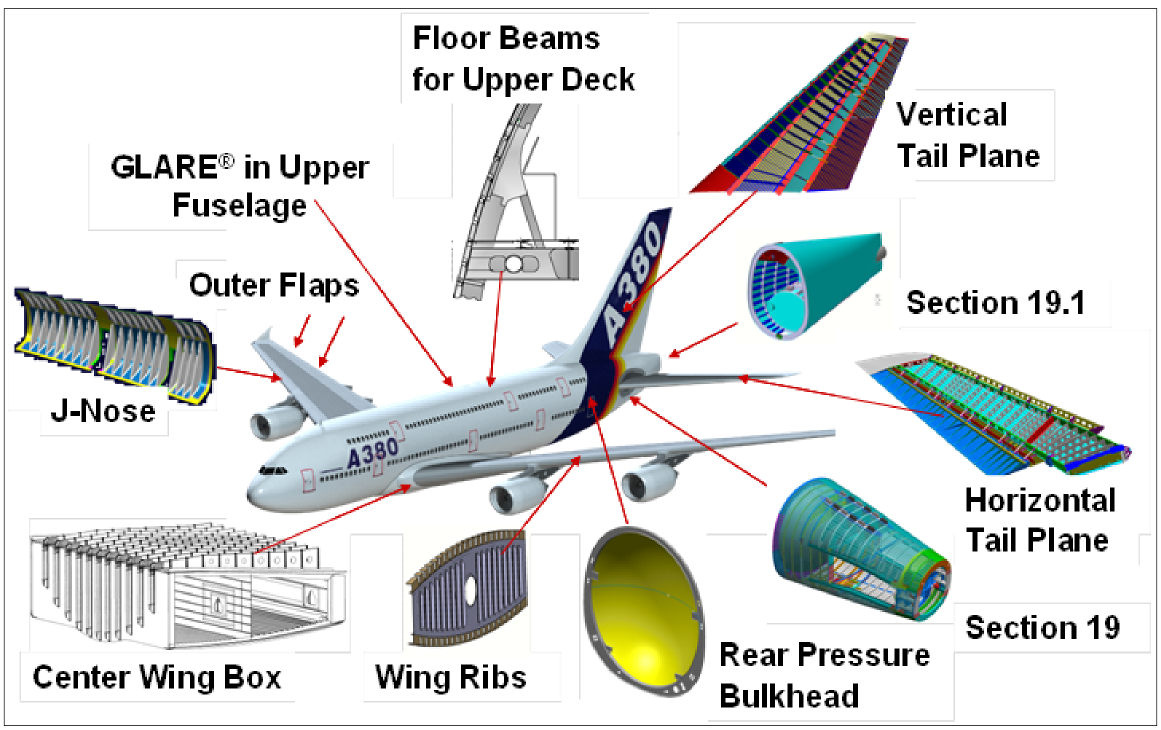

Figure 3. Major composite structures on Airbus A380 aircraft

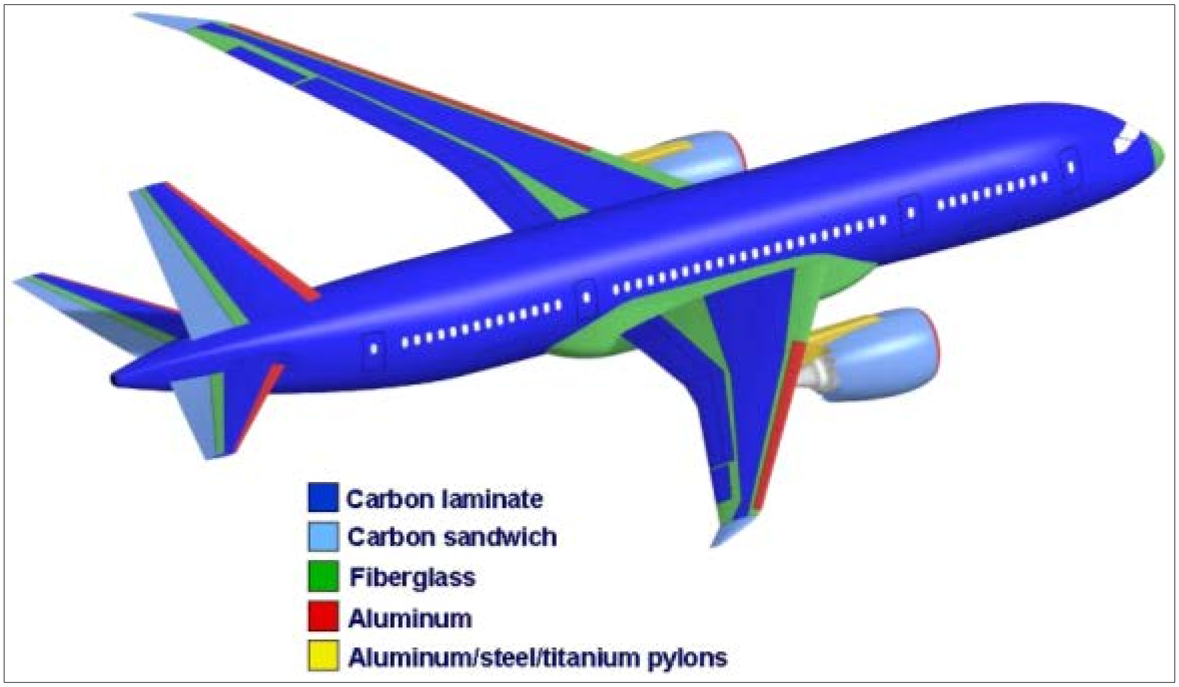

Figure 4. Summary of composite structures on Boeing 787 aircraft

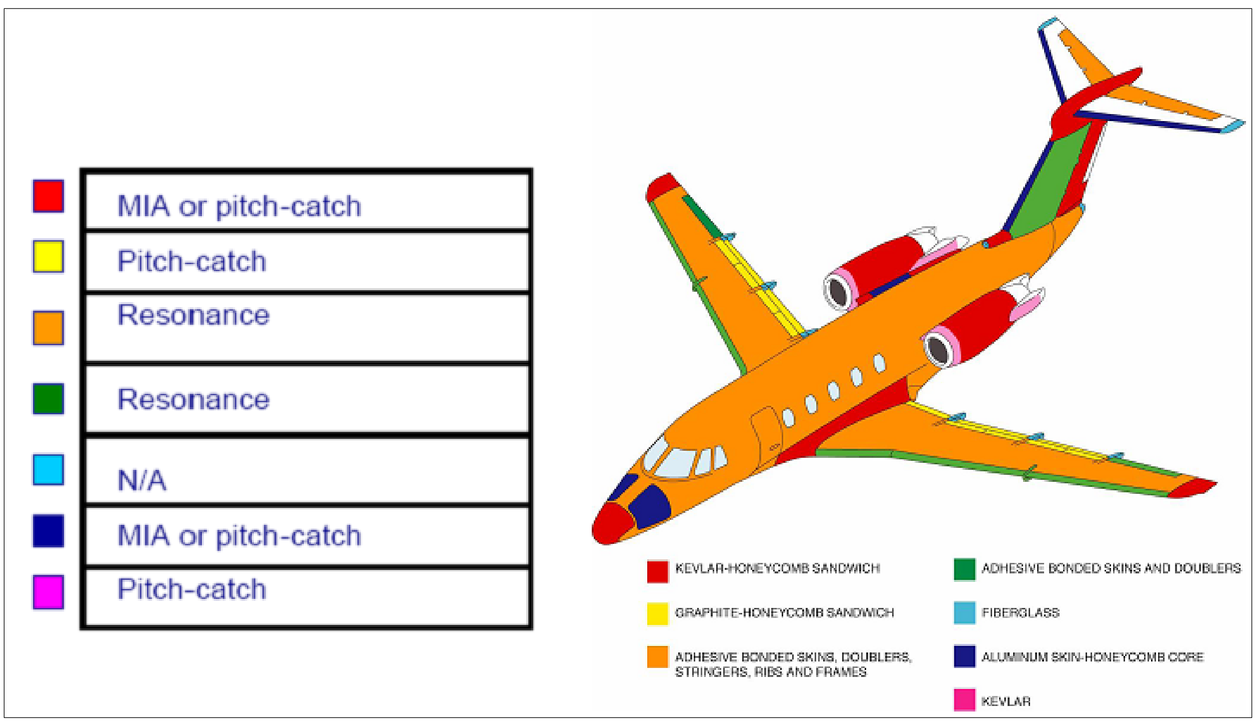

Figure 5. Summary of composite structures on Cessna Citation III aircraft and conventional NDI methods used to inspect them

Figure 6. Production of an all-composite fuselage section

Figure 7. Summary of advanced composite applications on A380 primary structures

1.3 BACKGROUND ON IN-SERVICE INSPECTION NEEDS FOR COMPOSITE STRUCTURES

As aircraft structural materials, composites have many advantages, including their high specific strength and stiffness, resistance to damage by fatigue loading, and resistance to corrosion. In addition, new analyses, operational experience, and aircraft safe-life extension programs may produce additional NDI requirements. The expanded use of composite structures, coupled with difficulties associated with the damage tolerance analysis (DTA) of composites, create a greater need for NDI methods that can effectively identify degradation and damage in composite structures. This must be balanced with the need for simple, low-cost NDI methods for detecting damage in composite structures and repair configurations. Recent developments in advanced NDI techniques have produced a number of new inspection options. Many of these methods can be categorized as wide area techniques that produce two-dimensional (2D) flaw maps of the structure. New inspection techniques that are available today, or will be in the immediate future, hold promise for reducing the direct maintenance costs while improving the capacity for detecting damage. Improved NDI techniques could help detect damage in its early stages, thus improving safety and reducing costs associated with the restoration of a larger affected area. A more thorough discussion on the in-service inspections needs for composite aircraft structures is provided in section 2.

The reliability, safety, and availability of aircraft can be improved, if deemed necessary, through the application of more sophisticated NDI methods and/or enhanced procedures for conventional NDI and improved training of maintenance personnel. This study compared the results from a wide array of NDI methods and identified limitations and optimum applications for specific inspection methods. This report addresses the application of conventional PE UT NDI methods to establish an aviation industry performance baseline for flaw detection capability. The performance of advanced NDI methods will be addressed in a forthcoming report.

1.4 DAMAGE TOLERANCE APPROACH TO ESTABLISH INSPECTION INTERVALS

Today’s transport category aircraft were designed using the damage tolerance approach by which they can meet continuing structural airworthiness requirements for their design lifetime. This approach is predicated on the use of an effective inspection and corrective maintenance program that effectively ensures structural integrity over the life of the aircraft. Damage tolerance is the attribute of the structure that permits it to retain its required residual strength without detrimental structural deformation for a period of use after the structure has sustained a given level of fatigue, corrosion, and accidental or discrete source damage. The maintenance program may be adjusted to reflect real time operational experience and analytical findings through the use of modern analysis tools, testing, and trends assessment of historical operation. Effective maintenance programs can ensure that airplane structures continue to meet the required ultimate strength, fatigue, and damage tolerance requirements.

Inspection requirements (sensitivity and inspection intervals) are driven by DTA. However, the multiple plies of composite material, composite lamina (anisotropic) response characteristics, and adhesive layers make the analysis quite complex and hinder the calculation of an exact DTA. It is difficult to determine the effects of flaw size and the point at which a flaw size/location becomes critical. This is especially true of disbond, delamination, and porosity flaws. Thus, an increased emphasis is placed on quantifying the probability that a flaw of a particular size and location will be detected by a piece of NDI equipment. In any surveillance of aircraft structure, there are three main aspects to the inspection requirements: (1) the DTA, which determines the flaw onset and growth data (especially critical flaw size information), (2) the sensitivity, accuracy, and repeatability of NDI techniques, which, in concert with the DTA, establish the minimum inspection intervals, and (3) the impediments with which the NDI techniques must contend while achieving the required level of sensitivity. In addition to this report, detailed discussions on damage tolerance assessments for composite materials are presented in references 4–8.

Damage tolerance refers to an aircraft structure's capacity to sustain damage, without catastrophic failure, until the component can be repaired or replaced. The Code of Federal Regulations (CFR) Part 25 specifies that the residual strength shall not fall below limit load, P_L, which is the load anticipated to occur once in the life of an aircraft. This establishes the minimum permissible residual strength $\sigma_P = \sigma_L$. To varying degrees, the strength of composite structures are affected by crack, disbond, and delamination flaws. The residual strength as a function of flaw size can be calculated. Figure 8 shows a sample residual strength diagram. The residual strength curve is used to relate this minimum permissible residual strength, σ_P, to a maximum permissible flaw size, a_P. The critical flaw size, a_c, is the flaw size that reduces the residual strength to the permissible residual strength.

A damage control plan is needed to safely address any possible flaws which may develop in a structure. NDI is the tool used to implement the damage control plan. Once the maximum permissible flaw size has been determined, flaw growth versus time or number of cycles is needed to properly apply NDI. Figure 9 contains a flaw growth curve that shows the total time, or cycles, required to reach a_P. It should be noted that a_d is the minimum detectable flaw size; a flaw smaller than a_d would likely be undetected and, thus, inspections performed in the time frame prior to n_d would be of little value. The time, or number of cycles, associated with the bounding parameters a_d and a_P is set forth by the flaw growth curve and establishes *H(inspection)*. Therefore, *H(inspection)* is defined as the number of cycles or amount of time during which a flaw grows from the minimum detectable size, a_d, to the maximum permissible size, a_p. Safety is maintained by providing at least two inspections during *H(inspection)* to ensure flaw detection between a_d and a_P.

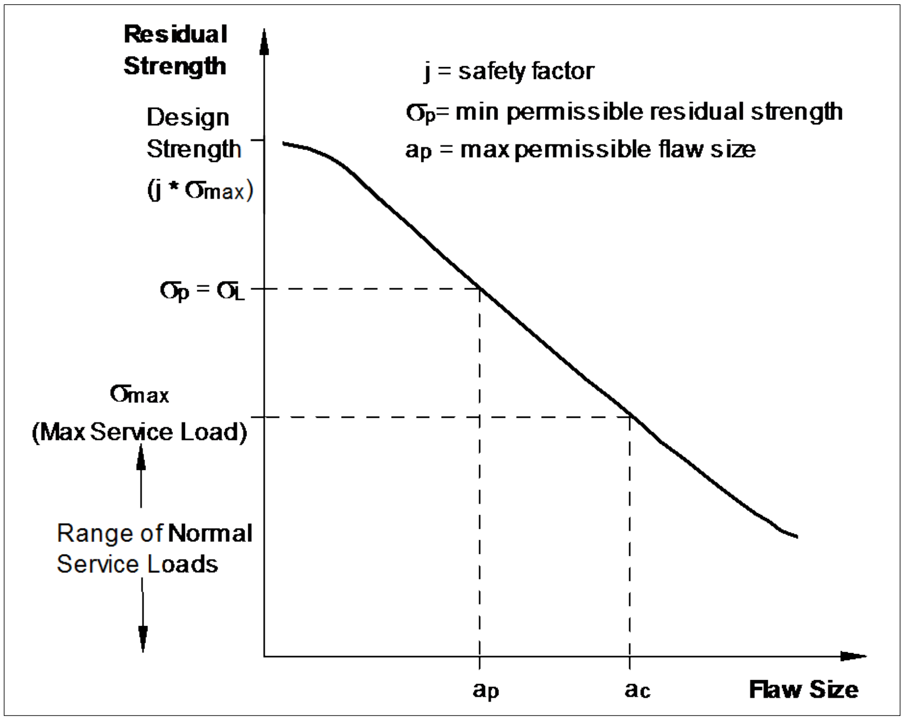

Figure 8. Residual strength curve

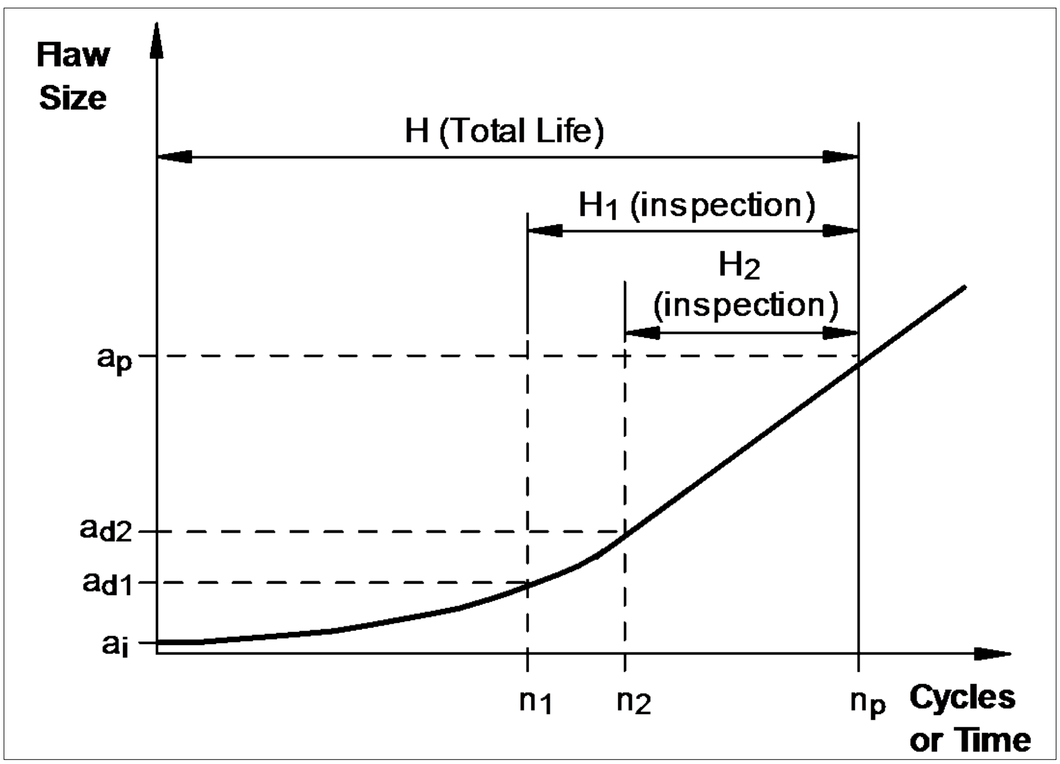

Figure 9. Crack growth curve showing time available for damage control

Figure 9 shows the significant effect that NDI sensitivity has on the required inspection interval. Two sample flaw detection levels a_d1, and a_d2, are shown along with their corresponding intervals $n1$ and $n2$. Because of the gradual slope of the flaw growth curve in this region, it can be seen that the inspection interval H_1*(inspection)* can be much larger than H_2*(inspection)* if NDI allows for a slightly better flaw detection capability. Because the detectable flaw size provides the basis for the inspection interval, it is essential that quantitative measures of flaw detection are performed for each NDI technique applied to the structure of interest. This quantitative measure is represented by a POD curve such as the one shown in figure 10. Regardless of the flaw size, the POD never quite reaches 1, which is equivalent to 100% POD. Inspection sensitivity requirements normally ask for a 90–95% POD at a_p. For any given inspection task, the POD is affected by many factors, such as: (1) the skill and experience of the inspector, (2) accessibility to the structure, (3) exposure of the inspection surface, and (4) confounding attributes, such as underlying structure or the presence of fasteners. Thus, the effects of circumstances on the POD must be accounted for in any NDI application and associated damage control plan. Figure 11 shows how increasingly difficult circumstances can degrade the POD of an NDI technique.

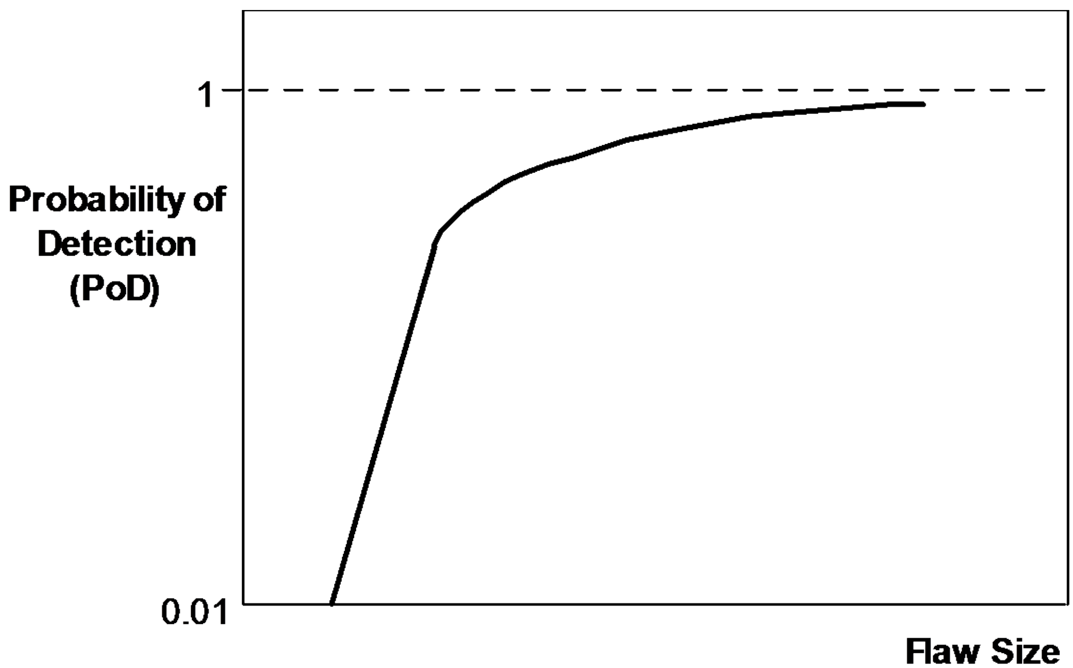

Figure 10. POD vs. flaw size

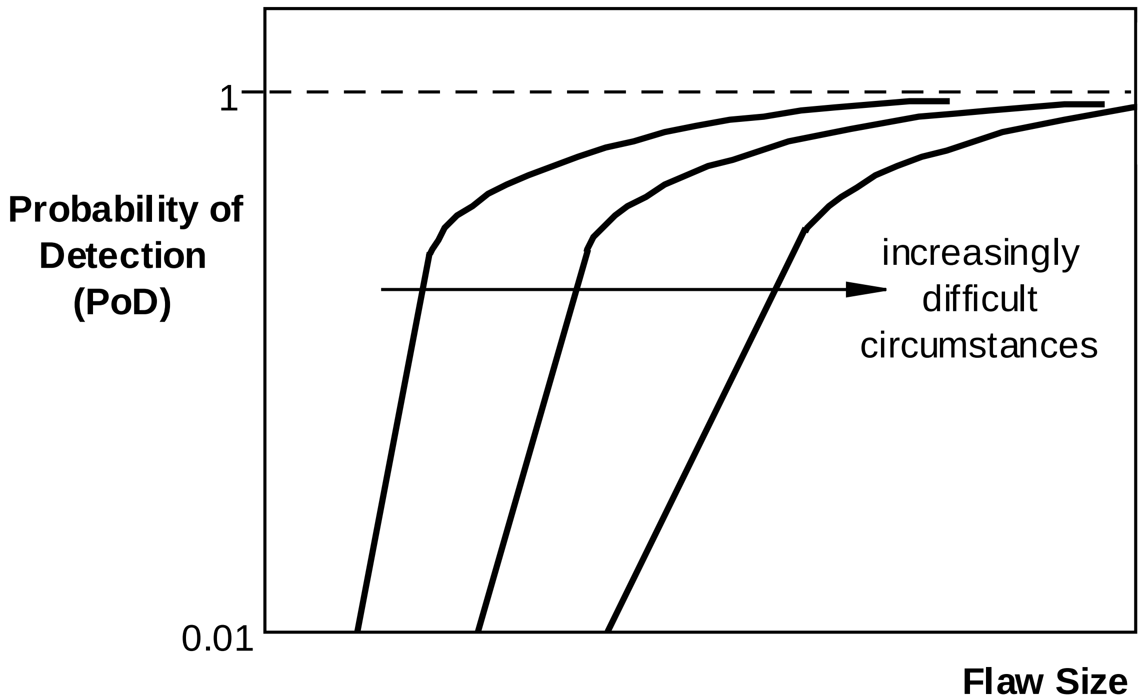

Figure 11. Effect of circumstances on POD

2. PURPOSE OF THE SLE

Composites have many advantages for use as aircraft structural materials, including their high specific strength and stiffness, resistance to damage by fatigue loading, light weight, and resistance to corrosion. The primary motivation for this program is to address the extensive and increasing use of composites on commercial aircraft and the associated increase in the array of NDI used to inspect them. Figure 12 shows how the use of composite materials has risen dramatically over the last decade. The end result of this experiment is an assessment of the NDI flaw detection capability in composite laminate structures, along with insights that can be used to improve the performance of composite inspection methods.

By using actual airline inspectors, it was possible to establish industry-wide NDI performance curves that quantify: (1) how well current inspection techniques are able to reliably find flaws in composite laminate structure and (2) the extent of improvements possible through the integration of more advanced NDI techniques and procedures. This report contains a comprehensive discussion on the performance of PE UT. The results from the advanced NDI testing, with comparisons to conventional PE UT, will be provided in a companion report.

The SLE goals included improving composite laminate inspection procedures and performance and developing structured comparisons between results from handheld inspection equipment and automated scanning systems. The latter item focuses on A-scan vs. C-scan data presentation and the human factors issues associated with inspections that cover large areas. Overall, the results from this study will provide input and recommendations to the FAA regarding guidance that can enhance the composite inspection process. Thus, this study is driven by a desire to improve aircraft safety. Airlines and original equipment manufacturers (OEMs) can use these results to guide NDI deployment and training, define what flaws/damage can be reliably found by inspectors, and reduce the human factors issues to produce improved NDI performance in the field.

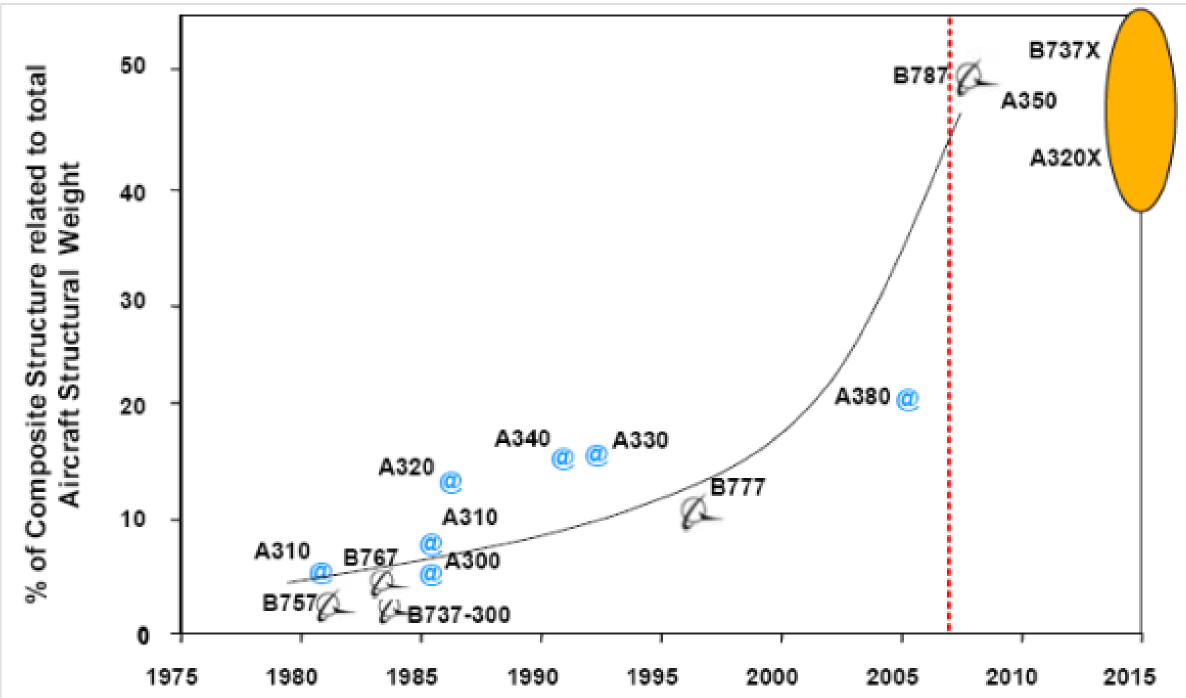

Figure 12. Expansion in use of composite materials in aircraft construction

The primary sources of damage to composite structures are:

- Normal and abnormal flight loads
- Fluid contamination and ingress
- Surface coating removal or erosion
- Impact (in-flight and on the ground):
  - hail, birds, tools, runway debris, tire separation, ground-handling equipment
- Lightning strikes
- Heat and ultraviolet light exposure
- Corrosion effects from adjacent metals in conductive joints (carbon materials)
- Maintenance errors

Figures 13–18 show sample damage found in composite structures. Information from one airline report indicates an average of eight composite damage events per aircraft with 87% of those stemming from impact. Figure 19 shows data relating the probability of an aircraft being impacted by runway debris alone. The data indicate probability of impact that reaches the 25–30% range. The costs associated with the repair of such impact damage averages $200,000 per aircraft. Another report indicates that fuselage damage is incurred every 1,000 flights in wide body aircraft and every 4,600 flights in narrow body aircraft.

The inspection challenges associated with the composite damage described above include:

- Subsurface delaminations and disbonds
- Hidden, subsurface damage
- Small amounts of moisture
- Cluster of damage in which each individual damage point is quite small
- Heat damage that affects resin matrix
- Weak bonds (manufacturing or environmentally induced)

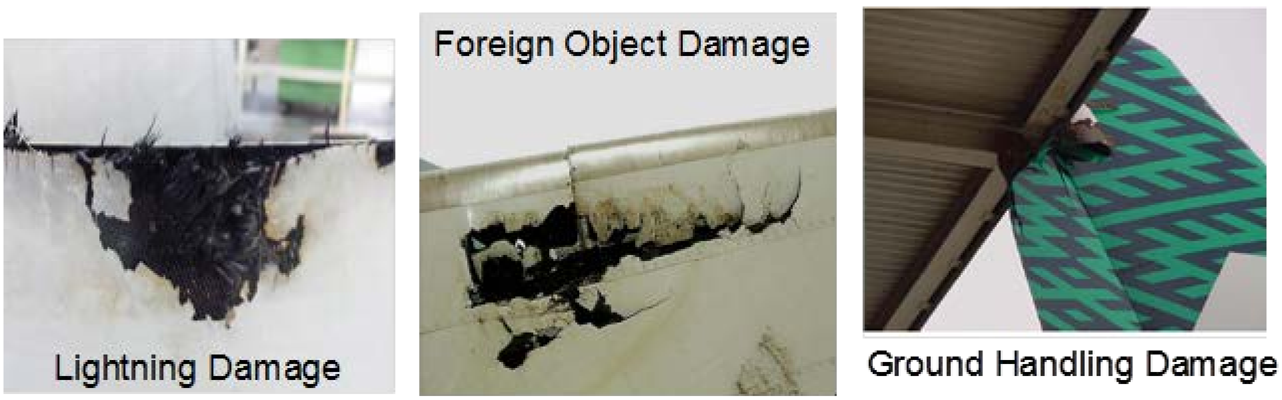

Figure 13. Sample sources of damage to composite structures

Figure 14. Sample damage from ground service vehicle impact

Figure 15. Sample damage from ground operations

Figure 16. Sample damage from impacts during flight

Figure 17. Sample damage from lightning strike

Water Ingress in Elevator

Disbonding at Skin-to-Honeycomb Interface

Figure 18. Sources of in-service damage to composite structures

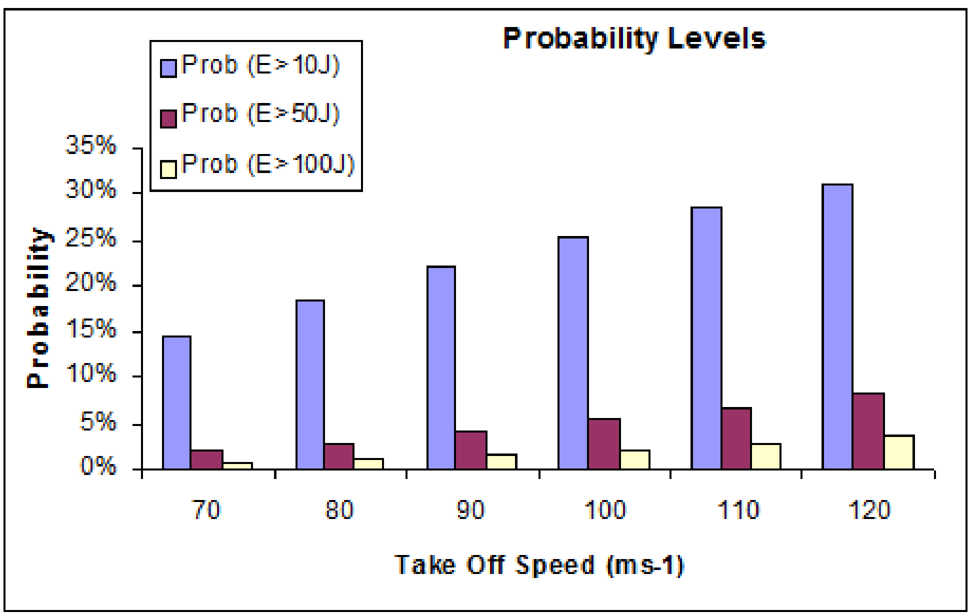

Typical Runway Debris

Source: Prof Paul Curtis, DERA/MSMA2/TR000702

Figure 19. Probability of impact energy as a function of takeoff speed (based on runway debris collected from four United Kingdom military air bases)

Impact damage can be especially hard to detect because this damage mode often produces subsurface damage while leaving no external surface demarcations or visual clues. Figures 20–22 describe the physics behind this impact damage scenario and include photos of this type of "blind" damage in both solid laminate and honeycomb structures. For example, hailstorm damage can produce subsurface interply delaminations while low-velocity, high-mass impacts (e.g., ground-handling equipment) can produce substructure damage (e.g., stringer-to-skin disbonds, frame fracture), both of which can be challenging to detect.

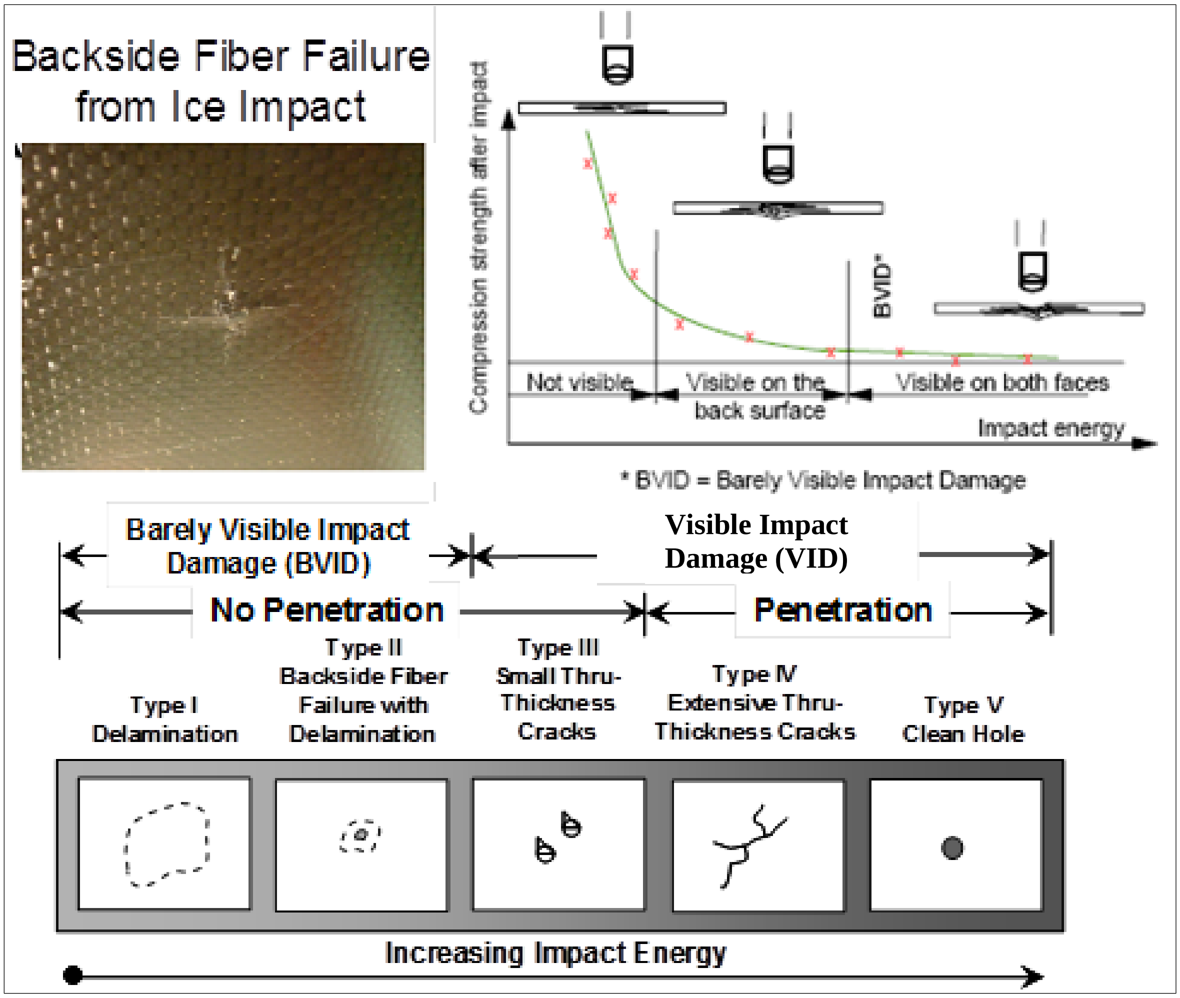

Figure 20. Effects of impact on composite structures

Source: Carlos Bloom (Lufthansa) & S. Waite (EASA)

Figure 21. Example of external impact creating minor surface demarcation but significant internal damage

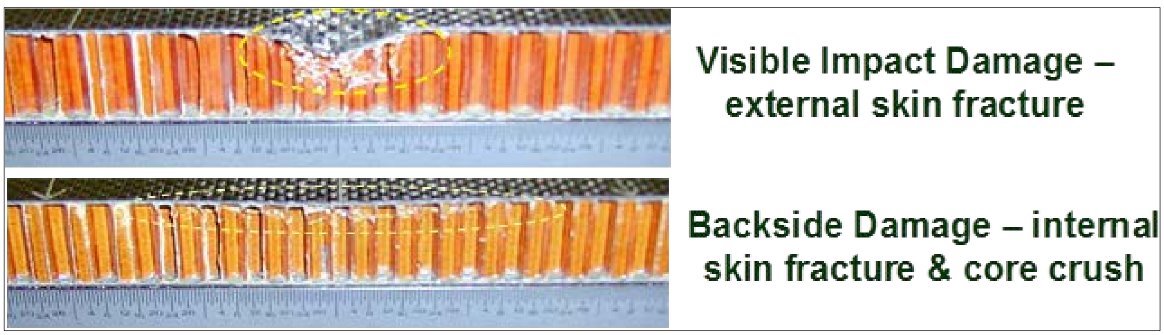

Figure 22. Comparison between visible and backside damage in honeycomb structures (crushed core and backside fiber fracture)

3. CONVENTIONAL INSPECTION METHODS FOR COMPOSITE LAMINATE STRUCTURE

In general, ultrasonic inspection uses high-frequency sound waves as a means of detecting anomalies in parts. Ultrasonic test equipment usually operates in the range of 200 KHz to 25 MHz. The speed with which the sound waves travel through a material is dependent on the composition and density of the material. The speed of sound as it passes through carbon graphite composite material is approximately 0.117 in/µs. Thus, the time it takes for an ultrasonic pulse to travel from the front surface to the back surface and back to the front surface of a 0.1″ thick composite laminate (0.2″ total travel) is approximately 1.7 µs. In PE UT inspections, short bursts of high-frequency sound waves are introduced into materials for the detection of surface and subsurface flaws in the material. The sound waves travel through the material with some attendant loss of energy (attenuation) and are reflected at interfaces. The reflected beam is displayed and then analyzed to define the presence and location of flaws. Sound is transmitted into the test item by means of a transducer. The reflected waves are then received by a transducer, often the same transducer for PE UT, and converted back into electrical signals for display.

3.1 A-SCAN MODE

Ultrasonic testing involves one or more of the following measurements: time of wave transit (or delay), path length, frequency, phase angle, amplitude, impedance, and angle of wave deflection (reflection and refraction). In conventional PE UT, pulses of high-frequency sound waves are introduced into a structure being inspected. A-Scan signals represent the response of the stress waves, in amplitude and time, as they travel through the material. As the waves interact with defects or flaw interfaces within the solid and portions of the pulse’s energy are reflected back to the transducer, the flaws are detected, amplified, and displayed on a computer screen. The interaction of the ultrasonic waves with defects and the resulting time versus amplitude signal produced on the computer screen depends on the wave mode, its frequency, and the material properties of the structure. Flaw size can be estimated by comparing the amplitude of a discontinuity signal with that of a signal from a discontinuity of known size and shape. Flaw location (depth) is determined from the position of the flaw echo along a calibrated time base. In the pitch-catch UT method, one transducer introduces a pressure wave into the specimen while a second detects the transmitted wave. A complex wave front is generated internally in the material as a result of velocity characteristics, acoustical impedance, and thickness. The time and amount of energy is affected by the changes in material properties, such as thickness, disbonds, and discontinuities. The mechanical vibration (ultrasound) is introduced into the specimen through a couplant and travels by wave motion through the specimen at the velocity of sound. If the pulses encounter a reflecting surface, some or all of the energy is reflected and monitored by the transducer. The reflected beam, or echo, can be created by any normal or abnormal (flaw) interface. Complete reflection, partial reflection, scattering, or other detectable effects on the ultrasonic waves can be used as the basis of flaw detection.

In most PE systems, a single transducer acts alternately as the sending and receiving transducer. If the pulses encounter a reflecting surface, some or all of the energy is reflected and monitored by the transducer. The reflected beam, or echo, can be created by any normal (e.g., in multilayered structures) or abnormal (flaw) interface. Figure 23 is a schematic of the PE technique. It shows the interaction of UT waves with various interfaces within a structure and the corresponding A-scan waveforms that are displayed on an ultrasonic inspection instrument. Complete reflection, partial reflection, scattering, or any other detectable effect on the ultrasonic waves can be used as the basis of flaw detection. In addition to wave reflection, other variations in the wave that can be monitored include: time of transit through the test piece, attenuation, and features of the spectral response (see figures 23 and 24). Sometimes it is advantageous to use separate sending and receiving transducers for PE inspection. The term “pitch-catch” is often used in connection with separate sending and receiving transducers. The degree of reflection depends largely on the physical state of the materials forming the interface. Cracks, delaminations, shrinkage cavities, pores, disbonds, and other discontinuities that produce reflective interfaces can be detected.

3.2 C-SCAN MODE: USE OF UT SCANNING TECHNOLOGY

It is sometimes difficult to clearly identify flaws using ultrasonic A-Scan signals alone. Small porosity pockets commonly found in composites, coupled with signal fluctuations caused by material nonuniformities, can create signal interpretation difficulties. Significant improvements in disbond and delamination detection can be achieved by taking the A-Scan signals and transforming them into a single C-Scan image of the part being inspected. C-scans are two-dimensional images (area maps) produced by digitizing the point-by-point signal variations of an interrogating sensor while it is scanned over a surface. A computer converts the point-by-point data into a color representation and displays them at the appropriate point in an image. Specific time gates can be set within the data acquisition software to focus on response signals from particular regions within the structure. C-Scan area views provide the inspector with data that are easier to use, are more reliable, and that recognize flaw patterns. This format provides a quantitative display of signal amplitudes or time-of-flight data obtained over an area. The X-Y position of flaws can be mapped and time-of-flight data can be converted and displayed by image processing equipment to provide an indication of flaw depth. A variety of PC-based manual and automated scanning devices can provide position information with digitized ultrasonic signals (figure 25).

The basic C-Scan system is shown schematically in figure 24. The scanning unit containing the transducer is moved over the surface of the test piece using a search pattern of closely spaced parallel lines. A mechanical linkage connects the scanning unit to X-axis and Y-axis position indicators that feed position data to the computer. The echo signal is recorded, as a function of its X-Y position on the test piece, and a color-coded image is produced from the relative characteristics of the sum total of signals received. A photograph of an automated (motorized) scanner, the Boeing Company's Mobile Automated Scanner (MAUS®) system, inspecting an aircraft fuselage section, is shown in figure 25. The entire ultrasonic C-Scan device is attached to the structure using suction cups connected to a vacuum pump. The unit is tethered to a remotely located computer for control and data acquisition. Figure 26 shows a comparison of A-scan signals from damaged and undamaged portions of a composite structure that were produced by the PE UT inspection method. The clear reflection peak produced by uninterrupted signal travel to the back wall in the "undamaged" A-scan signal should be noted and compared to the A-scan signal from the "damaged" region where the amplitude of the back wall signal is decreased and a new intermediate peak (reflection) is observed. Both of these A-scan changes indicate the presence of damage or other anomaly. Additional sample A-scan signals from PE UT inspections can be found in appendix A. Figure 27 shows a sample C-scan image (based on amplitude) from a PE UT inspection of a composite fuselage structure containing stringers and frame shear ties (see figure 25). Dark spots and irregularly shaped regions of nonuniform color indicate the presence of impact damage to this panel. The value of using 2D color coding, stemming from the sum total of the A-scan signals, to identify and size composite flaws is evident in this C-scan image. It is important to note here that this report contains a comprehensive discussion on the performance of PE UT. The results from the advanced NDI testing, including scanning systems that produce C-scan images, will be provided in a companion report.

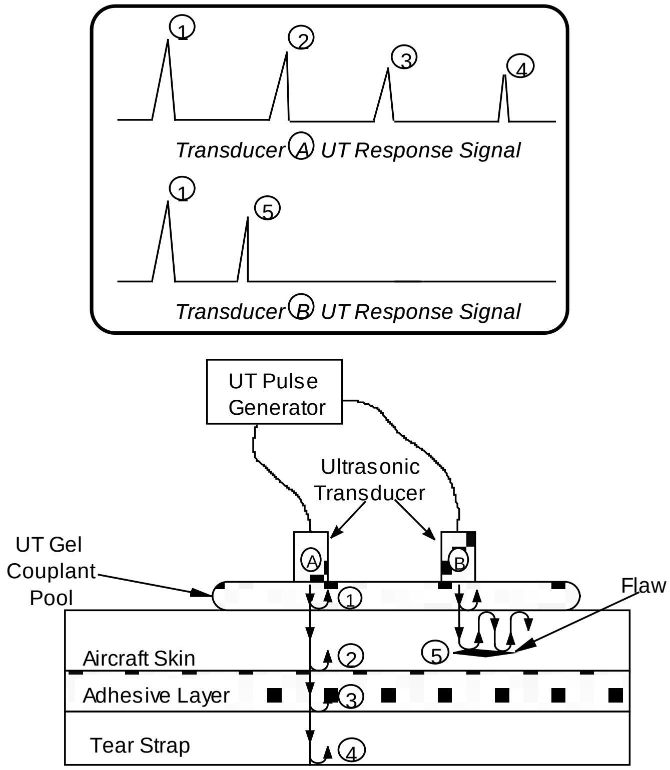

Figure 23. Schematic of PE UT and A-scan signal showing reflection of UT waves at assorted interfaces

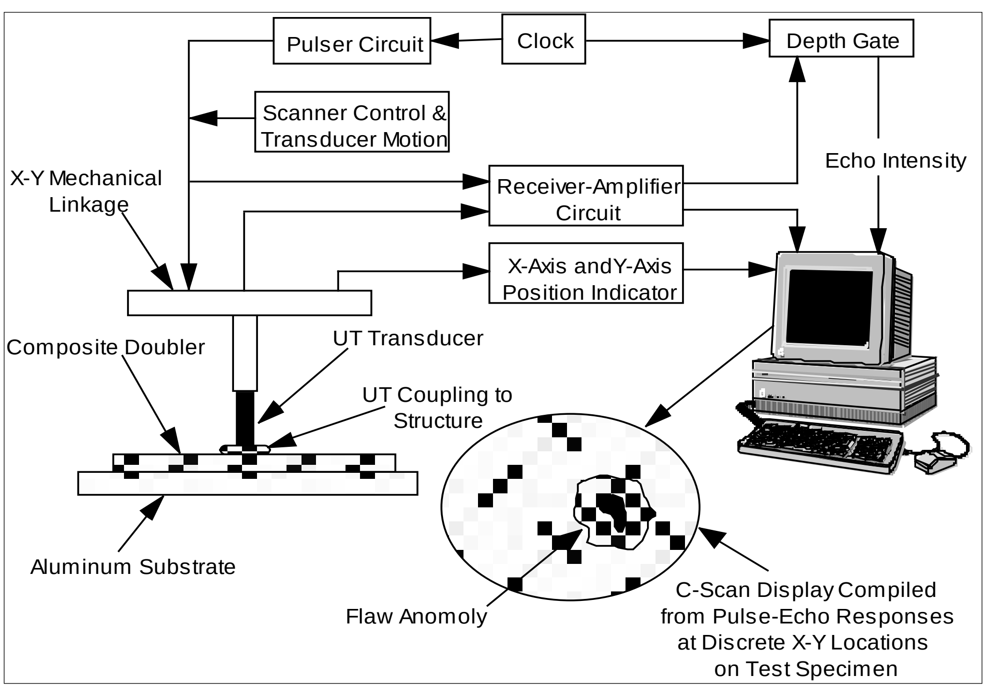

Figure 24. The C-scan setup for PE UT inspection

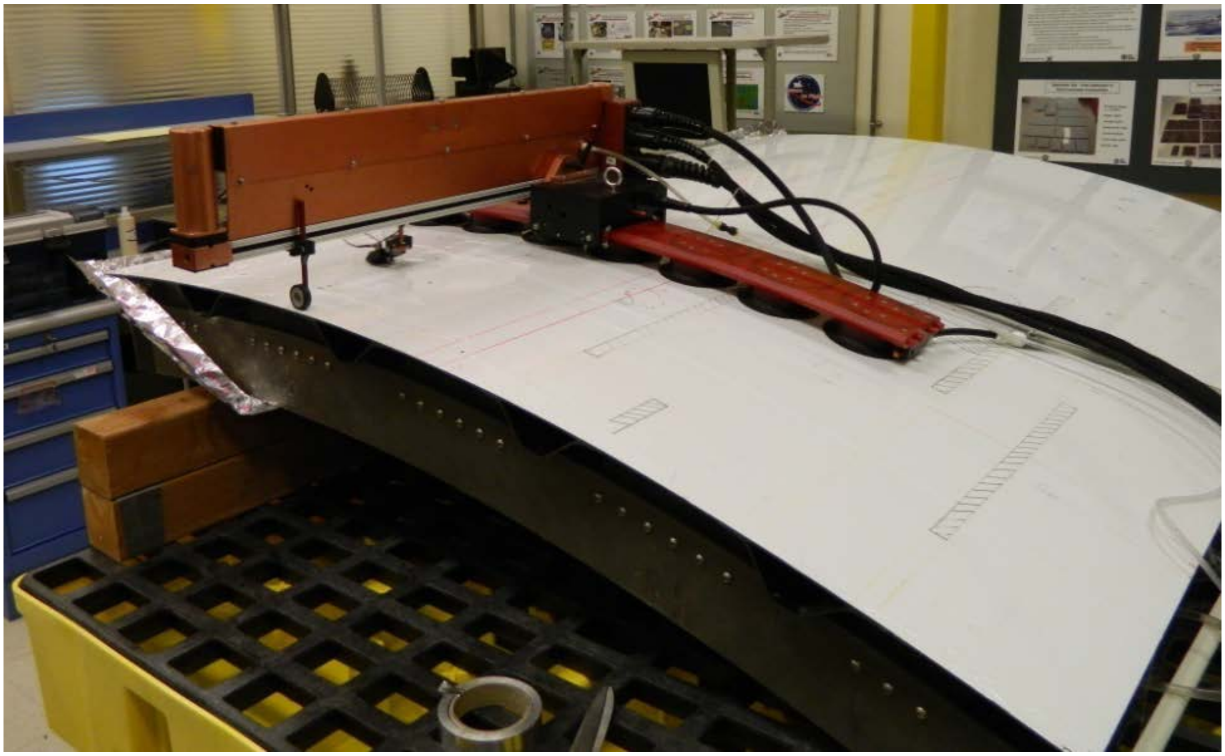

Figure 25. The MAUS® system

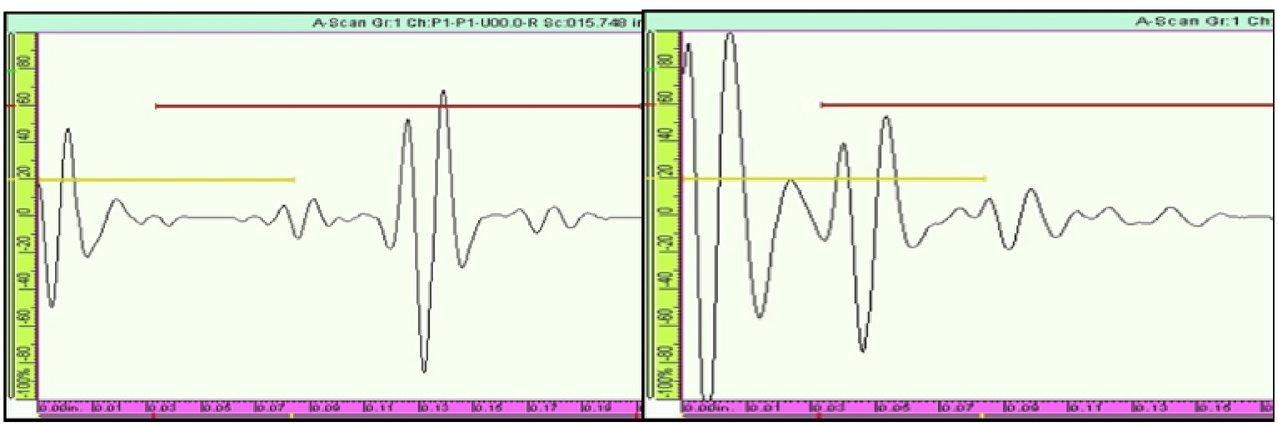

(a) (b)

Figure 26. Sample ultrasonic signals generated from (a) structure without damage and (b) structure with damage

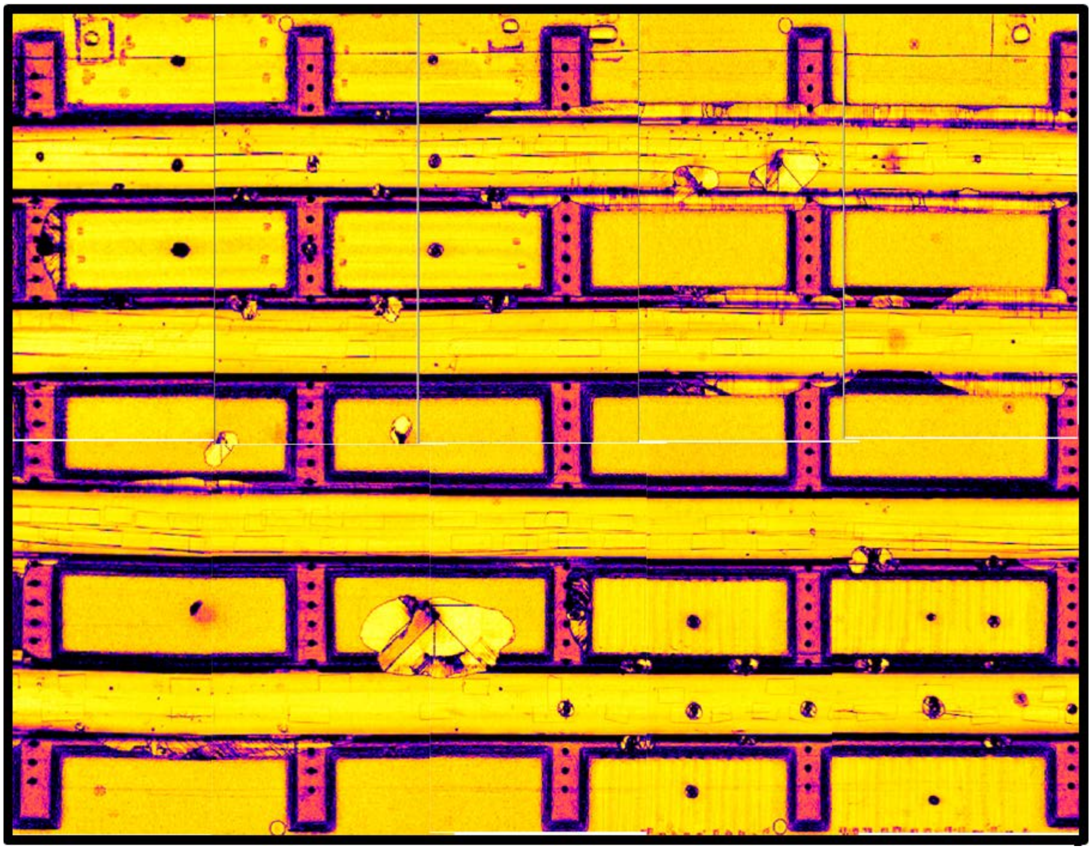

Figure 27. Sample C-scan produced by an automated ultrasonic scanning device

3.3 ULTRASONIC GO/NO GO DEVICES

Recently, two similar, ultrasonic-based devices were released for possible use by airline personnel: the Bondtracer™ by GE® and Ramp Damage Checker (RDC) by Olympus (see figure 28). These are both simplistic versions of standard PE UT equipment which, when properly calibrated on undamaged structure, can provide go/no go information regarding the presence of flaws in composite structures. One of the projected uses of this equipment would be at airport gates where non-inspectors with proper airline training could use these devices to determine if visual scuff marks (or other indicators, such as possible impact from equipment) are associated with actual damage to the composite laminate. Rather than displaying an A-scan signal as conventional PE UT devices do, these devices internally compare the calibration signal from a representative composite laminate with the current inspection signal to determine if the change in the inspection signal is sufficient to indicate damage. The Bondtracer™ changes its lights from green to red to indicate damage, whereas the Ramp Damage Checker changes its screen display from good to bad (see figure 28) to indicate the presence of damage. These devices are intended to be used in local inspection scenarios only when visual clues or other events occur which warrant additional inspection of a small region. The SLE was adapted to allow for the evaluation of these UT-based go/no go devices (see section 4).

General Electric – "Bondtracer" | **Olympus – "Ramp Damage Checker"**

Figure 28. Ultrasonic devices with go/no go capabilities used in ramp damage check experiment

4. THE SLE DESIGN

The FAA requested that the FAA-AANC conduct this experiment to make an overall assessment of flaw detection in composite laminate aircraft structures. The SLE includes a set of 15 composite laminate test specimens (see figure 29) that contain engineered flaws (disbonds, interply delaminations, and impact damage). Five NDI feedback specimens were also produced. These feedback specimens contain all of the same construction and flaw types as those found in the blind POD test specimens. The flaw profiles in the NDI feedback specimens were provided to each inspector to allow them to become comfortable with the inspection demands before proceeding to the blind POD specimens. Figure 1 shows the inspection surfaces on the set of painted specimens, whereas figure 29 shows the back side and unpainted surfaces of the same specimen set. The SLE was shipped to airlines and third-party maintenance depots to acquire flaw detection data from qualified aviation inspectors. The experiment required approximately 2–3 days of each inspector's time. In general, inspectors were asked to locate and size hidden flaws in the test specimens. The test program was intended to evaluate the technical capability of the inspector, the inspection procedures, and the equipment (i.e., the NDI method itself). The inspections emphasized flaw detection methods applicable to solid laminate structures ranging from 12–64 plies thick.

Figure 29. Subset of the 15 solid laminate test specimens and 5 NDI feedback specimens

This experiment used a series of solid laminate composite specimens with statistically relevant flaw profiles to evaluate flaw detection using PE UT and other NDI methods. These tests were conducted using NDI equipment that the inspectors were experienced in using for this type of inspection. The effort focuses on understanding the factors influencing the performance of NDI methods (device and inspector) when applied to the inspection of solid laminate composites. The experiment results evaluated inspection performance attributes including accuracy and sensitivity (flaw hits, misses, false calls, flaw sizing) and usability features such as versatility, portability, complexity, and inspection time (a human factors feature). This report includes the results from the application of conventional inspection methods (i.e., PE UT). A forthcoming companion report will discuss the results from the advanced NDI testing.

The primary factors affecting NDI included in this study are: composite materials, flaw profiles, geometry of structure, thickness of structure, presence of substructure elements, ply drop-off (taper), presence of bond lines, presence of fasteners, sealed joints, skin-over-honeycomb substructure, and inspection environment conditions. This phase of the study used airline personnel to study PE UT inspections with a POD experiment in the field to formulate improvements in this critical inspection method.

4.1 EXPERIMENT DESIGN GUIDELINES

Experiment Design Criteria:

- Conventional and advanced inspection techniques are being assessed
- Carbon plies will be used for all parts (carbon pre-preg, uniaxial tape). Some pre-cured carbon stringers will be secondarily bonded and some stringers will be co-cured
- Multiple stringers and create bays that have 2D ply taper should be used
- Specimens shall be cured as per the normal manufacture temperature-time cure profile. Laminates will be cured at 85 psi. Secondary bonds will be produced at vacuum bag pressure only
- The purpose of the honeycomb portion of specimens is to ascertain difficulties in recognizing the back wall echo in the presence of resin pools around the honeycomb edges
- Coatings—Inspection surface will be a painted production tool surface, as per normal part manufacture
- General OEM laminate inspection procedures are provided as guidance for inspectors
- Specimen drawings, similar to those found in OEM manuals, are provided to inspectors to aid in the interpretation of PE UT signals
- Test specimen designs include the variables that have been deemed to be the most important because they have the greatest effect on NDI (table 1)
- Approximately 200 flaws with sufficient unflawed regions shall be included to allow for the assessment of false calls
- For the most part, a minimum of a 2″ separation between flaws should be maintained to eliminate signal cross-talk; a few flaw pairs that are closely clustered should be included to study the ability to define the boundaries of flaws
- For the most part, a minimum of 0.50″ distance should be maintained from flaws to edge of panels; a few instances of flaws close to the edge should be included to study flaw detection near a natural edge

Final Specimen Matrix—Table 1 shows the final test specimen matrix and includes the different design variables integrated into each specimen. The specimen set consists of three bullnose (BN) specimens (BN1, BN2, and BN3), four complex taper specimens (CT1-A, CT1-B, CT2-A, & CT2-B), and eight simple taper specimens (ST1U-A, ST1L-

A, ST2U-A, ST2L-A, ST32-1, ST32-2, ST32-3, and ST32-4) for a total of 15 POD specimens

Table 1. Test specimen matrix with design variables for solid composite laminate flaw detection experiment

Engineered Specimens (Design Variables)					
Test Specimen	Design Variable 1	Design Variable 2	Design Variable 3	Design Variable 4	Design Variable 5
Bullnose 1 (BN1)	12 plies over honeycomb	24 plies over substructure	24 plies over radius	38 Ply Spar	N/A
Bullnose 2 (BN2)	12 plies over honeycomb	24 plies over substructure	24 plies over radius	38 Ply Spar	N/A
Bullnose 3 (BN3)	12 plies over honeycomb	24 plies over substructure	24 plies over radius	38 Ply Spar	N/A
Complex Taper 1 (CT1-A & CT1-B)	12 plies	20 plies	12 to 20 ply taper (.50″ step)	12 to 20 ply taper (.25″ step)	N/A
Complex Taper 2 (CT2-A & CT2-B)	12 plies	20 plies	12 to 20 ply taper (.50″ step)	12 to 20 ply taper (.25″ step)	N/A
Simple Taper 1 Upper (ST1U-A)	12 plies	20 plies	12 to 20 ply taper (.50″ step)	12 plies w/substructure	20 plies w/substructure
Simple Taper 1 Lower (ST1L-A)	12 plies	20 plies	12 to 20 ply taper (.50″ step)	12 plies w/substructure	20 plies w/substructure
Simple Taper 2 Upper (ST2U-A)	12 plies	20 plies	12 to 20 ply taper (.50″ step)	12 plies w/substructure	20 plies w/substructure
Simple Taper 2 Lower (ST2L-A)	12 plies	20 plies	12 to 20 ply taper (.50″ step)	12 plies w/substructure	20 plies w/substructure
Simple Taper New 32 (ST32-1 through ST32-4)	32 plies	20 to 32 ply taper (.50″ step)	32 plies w/substructure	N/A	N/A

The POD study breakdown shown in figure 30 depicts the breakdown in results where the overall goal is to determine POD level for composite laminate structures in general. This is an all-inclusive POD result determined from all the inspection results from a specific inspection technique (e.g., PE UT). Subset POD levels are results from the 12–20 ply laminates and the 20–32 ply laminates for a specific inspection method. This will also produce individual POD results for each inspector, which can then be used in a comparison to look at the variance within a specific inspection method.

It should be noted that the specimens have several discrete laminate thicknesses, substructures, and taper regions. Other isolated POD information to be derived from this study includes flaw detection performance in selected areas, such as substructure regions or tapered areas. These results can then be compared to inspection results from other categories (e.g., constant thickness [CT] regions) to pinpoint the greatest challenges associated with composite NDI.

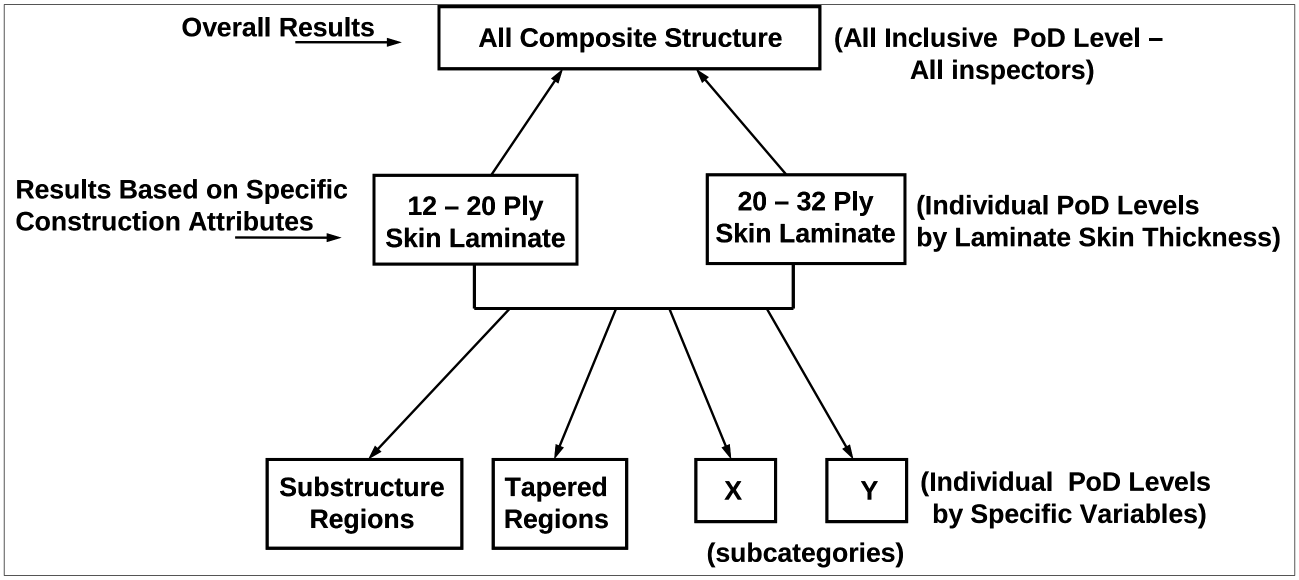

Figure 30. POD study breakdown to produce separate POD values related to specific inspection variables

All of the important variables are represented but cannot be individually uncoupled. As a result, it was desirable to distribute the construction variables (thickness, taper, honeycomb, fastened regions, secondarily bonded regions, and geometry) and flaws (size and depth) so that they would represent the distribution and impediments found in aircraft structure. A summary of the main experiment design considerations follows:

- The overall SLE can be broken down into two separate experiments. There is a thin laminate skin experiment with skins ranging from 12–20 plies (0.078″–0.130″ thick) and total thickness extending to 62 plies (0.406″) when the substructure is considered. There is also a thick laminate skin experiment with 32-ply skins (0.21″ thick) and total thickness extending to 58 plies (0.377″) when the substructure is considered

- Surface area and number of flaws (i.e., number of specimens) versus time for inspector to complete the tests using handheld probes—the goal was to produce experiments that could be completed in 2–3 days for the 12–20 ply thin laminate skin experiment (11 specimens) and in 1–2 days for the 20–32 ply thick laminate skin experiment (4 specimens)

- Disbonds were included between the laminate skin and substructure elements and delaminations were placed in both the laminate skin and substructure (stringers). Some premanufactured stringers were used, so flat-bottom holes were the only means of simulating delamination flaws in these stringers. In the cases where the substructure was co-cured with the skin, inserts were used for adding delamination flaws

- Boeing provided laminate inspection procedures for the B777 and Airbus provided laminate inspection procedures for the A300. These procedures were placed in the experiment protocols for inspector use

4.2 SPECIMEN DESIGN AND EXPERIMENT IMPLEMENTATION APPROACH

To implement a realistic experiment, it was necessary to design representative specimens that included a full spectrum of variables found on composite aircraft structures. This included the different construction scenarios, such as various ply thicknesses, different substructure thicknesses, bonding methods for substructure (co-cured and secondarily bonded), and geometry issues (taper/ply drop-offs) that can make inspections difficult. Another important factor in the specimen design was to determine the most prevalent flaw types found on this type of structure and to develop ways to engineer representative flaws. This included determining the various flaw sizes required for the statistical analysis.

While the size of the flaw, or damage, that must be detected is affected by many parameters (structure type, location on aircraft, stress, and fatigue levels), the general goal for composite inspections is to detect flaws that are 1″ diameter or larger. Many of the NDI reference standards in OEM NDT manuals use 1″ diameter flaws to guide equipment setup. In addition, the CACRC-ITG members generally concur that 1″ flaw detection provides a good center point for this SLE. Thus, the flaw sizes in the SLE design were established with a 1″ diameter at the center. Larger and smaller flaws were included so that POD values smaller than 1″ (as small as 0.25″) and POD values larger than 1″ (as large as 2″) could be ascertained.

4.2.1 Specimen and Flaw Types Used in the SLE

- Interply delaminations—tight and loose delaminations in which Grafoil inserts (GRI) simulated tight interply contact (kissing delaminations) and pillow inserts simulated loose interply contact (thin slide of entrapped air)

- Flat-bottom hole—larger delaminations simulated the presence of air gaps

- Pillow insert disbonds at substructure interface simulated tight contact but no adhesive strength (kissing disbonds)

- Pull tab disbonds simulating the presence of a variable air gap between the laminate and bonded substructure

- Impact damage subsurface damage but no surface demarcations. This was simulated with tapered flat bottom holes (FBHs) with stair-step sides (see figure 31, which compares normal impact damage morphology with the simulated version)

- Flaw Sizing—normal procedures and standards focus on flaw detection for 1″ diameter flaws and larger. However, this study also assessed performance for flaws as small as 0.25″ in diameter. Inspectors were told to use any positive indications to find flaws as small as 0.25″

in diameter." The flaw sizes used in this study were: 0.25″, 0.5″, 0.75″, 1″, 1.5″, and 2″ in diameter

- Flaw Depth—Some are included close to front and close to back surfaces and are hardest to detect; also, some along the midline are included which are located in CT and transition tapered regions

- Laminate Type—carbon graphite, uniaxial tape

- Laminate Thickness—panels have 12 (~.078″), 20 (~.130″), 24 (~.156″), and 32 (~.229″) ply laminate skins which include both CT and tapered regions. Ply steps in taper areas are 0.25″ step per ply (12–20 ply specimens) and 0.5″ step per ply (12–20 and 20–32 ply specimens). The substructure elements included in the test specimens had thicknesses of 0.075″, 0.125″, 0.192″, 0.225″, and 0.250″

- Test Specimen Size—some large enough to highlight need for scanners; some small and complex enough to make scanning difficult or unnecessary (see appendix D, Summary of SLE Test Specimens)

- Test Specimen Geometry—include flat surfaces, angled surfaces, and curved surfaces; complex geometry (CG) on the inside (substructure, taper, fasteners, etc.) and smooth surface on the outside

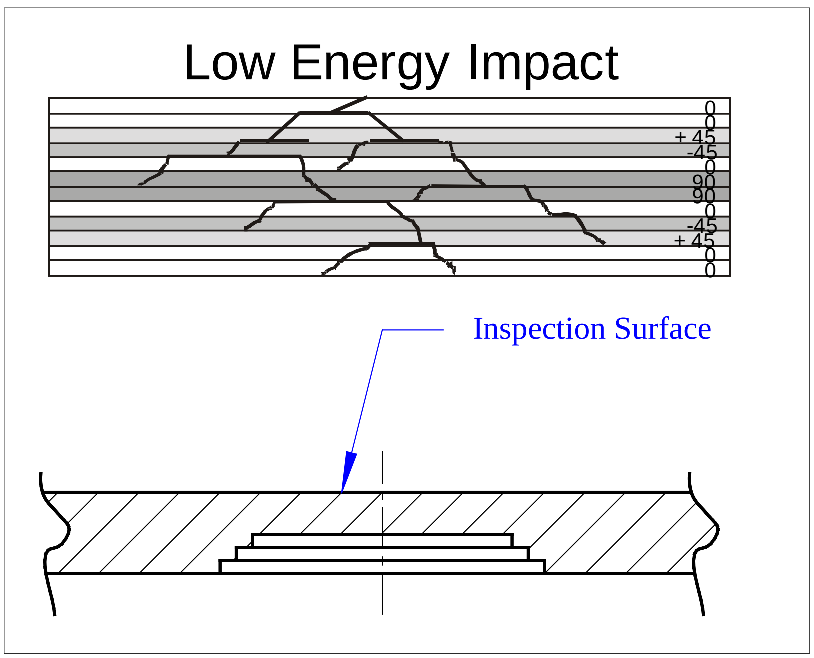

Figure 31. Simulated impact damage (laminate cross-section)

4.2.2 Application of NDI

- NDI feedback specimens, with known flaw profiles, were inspected first to allow the inspectors to become familiar with the inspection demands of the experiment

- The PE UT inspection technique was applied in a blind mode to the set of POD specimens to study hits, misses, false calls, and flaw sizing. Experimenter information packets and face-to-face briefings were provided for procedural guidance and to ensure uniformity of results

- The experiment investigated the full range of human factors issues, including inspection coverage methods and effects of the inspection environment

- Test specimen characterization was conducted with knowledge of flaw locations to determine quantitative signal-to-noise (S/N) ratios. The ability to achieve successful flaw detection was then inferred by studying S/N levels at various threshold levels

- Two Inspection Categories—a valid cumulative POD curve for an inspection device requires results from a minimum of 10 inspectors using that device or inspection method. Two NDI categories were considered in the SLE: conventional (results provided in this report) and advanced NDI (results provided in separate forthcoming report). It should be noted that, to break down some of the important inspection variables (e.g., flaw detection in the presence of CG), more than 10 inspectors were required for a single inspection device. This will be discussed further in section 6

- Inspection Device—for the most part, the inspectors used their own NDI equipment. Experiment monitors allowed access to acceptable inspection devices to be used for this testing (i.e., equipment met Boeing and Airbus specifications) and the inspectors made the final choice based on availability and familiarity with that equipment. Some testing with nonstandard devices was conducted (see discussions on ramp damage check experiment) to form a basis of comparison with results obtained using conventional PE UT devices

- Training—Equipment and experiment familiarization was achieved through the use of NDI feedback specimens or solid laminate training specimens. The feedback specimens were representative of the test specimens that were subsequently tested in blind mode. Figures 32–37 contain engineering drawings and sample photos of the set of five NDI feedback specimens. These specimens, along with the flaw location drawings, were sent out in advance of the experiment to allow the inspectors to learn about NDI equipment responses. Experiment monitors also provided one-on-one briefings (see appendices A and B) to aid in the proper deployment of the equipment just prior to beginning the blind flaw detection tests

- Experimenter Briefing—an SLE experimenter information packet (appendix A) and SLE experimenter briefing packet (appendix B) were provided to each participant. Face-to-face airline briefing sessions were completed at each site prior to beginning the NDI tests. To ensure maximum uniformity in information provided to participants, all team members who were experiment monitors attended one of the airline briefing sessions provided by the FAA-AANC

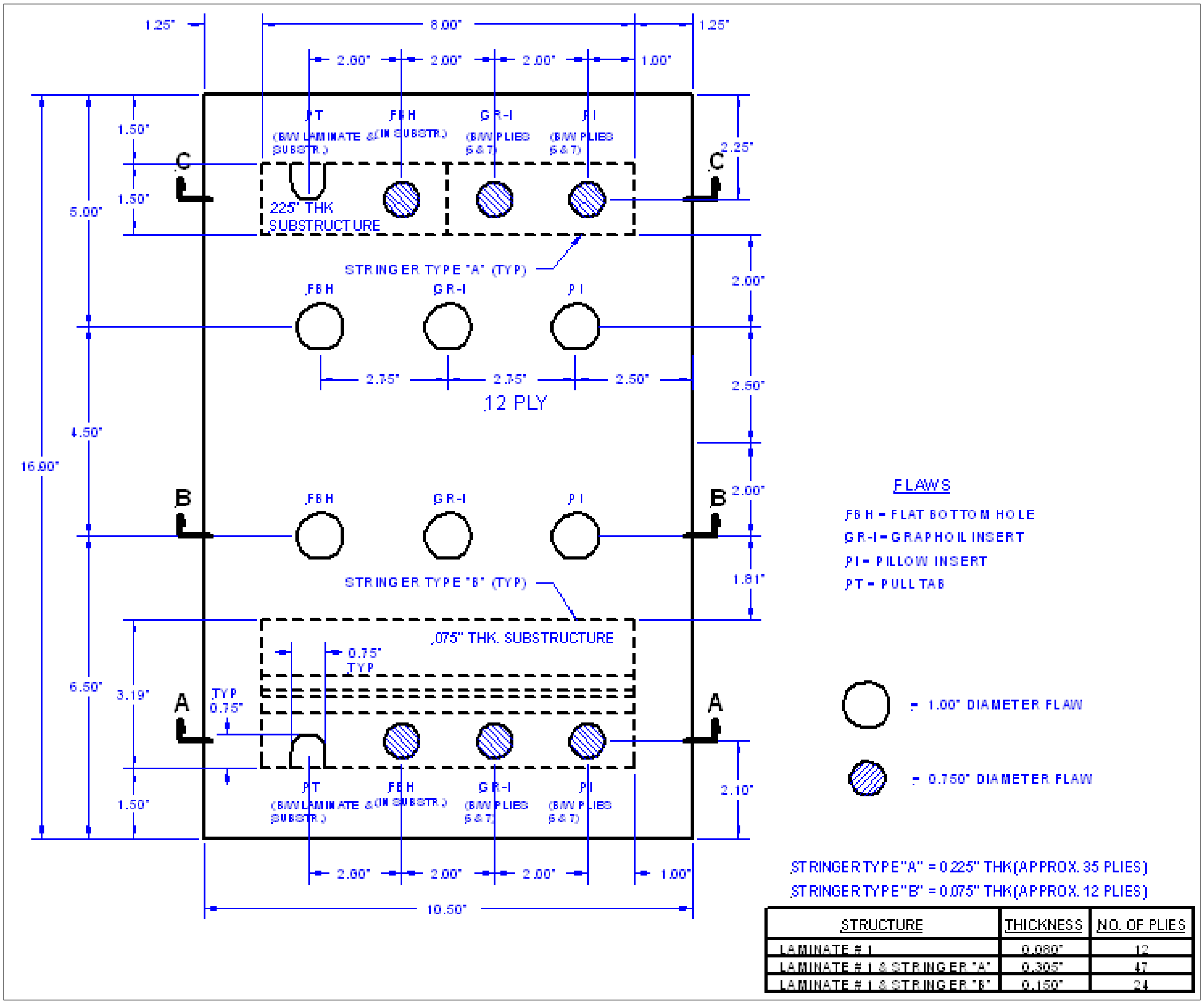

Figure 32. Final design of 12-ply training/feedback specimen

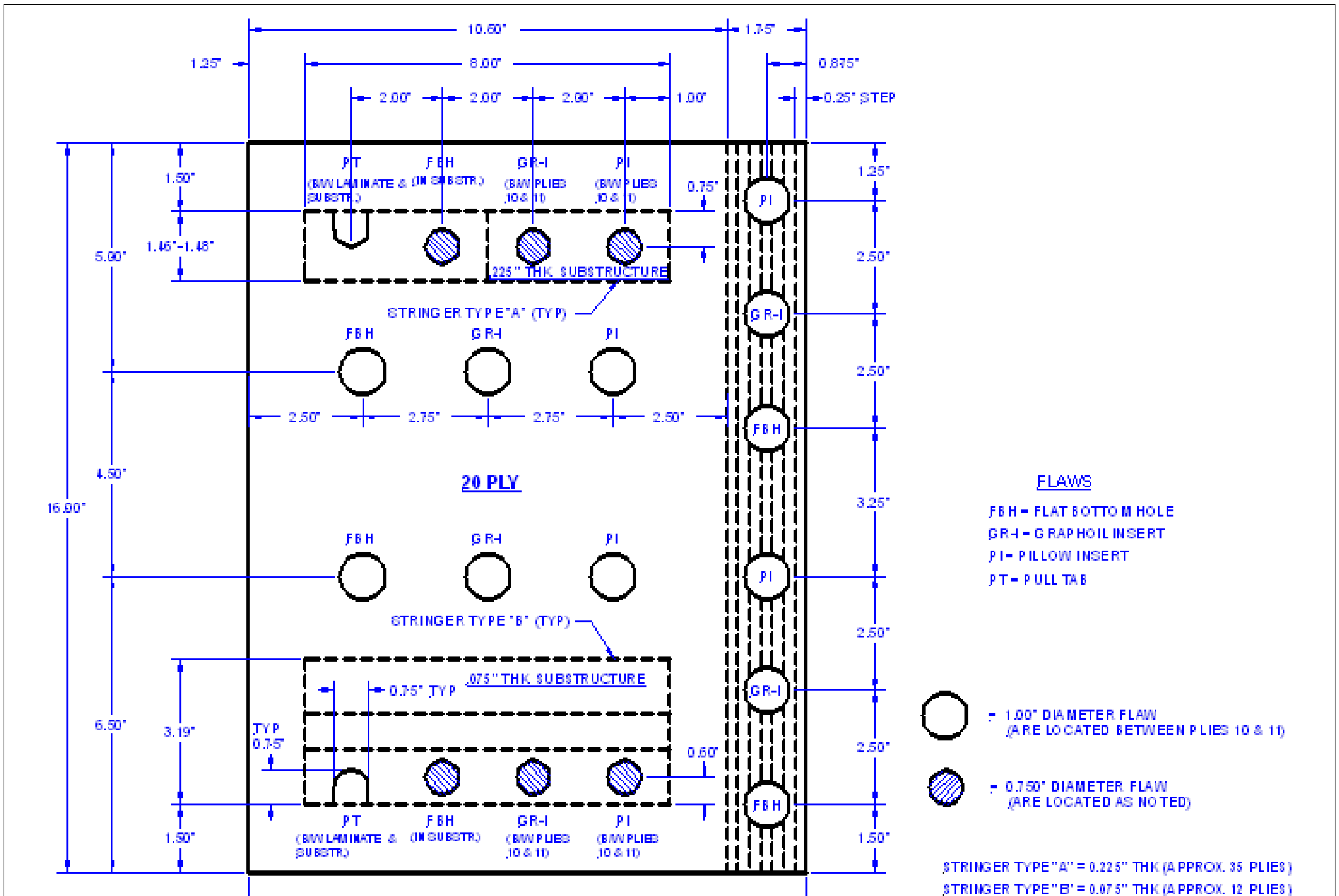

STRUCTURE	THICKNESS	NO. OF PLIES
LAMINATE # 2	0.130"	20
LAMINATE # 2 & STRINGER "A"	0.355"	55
LAMINATE # 2 & STRINGER "B"	0.205"	32

Figure 33. Final design of 20-ply training/feedback specimen with taper

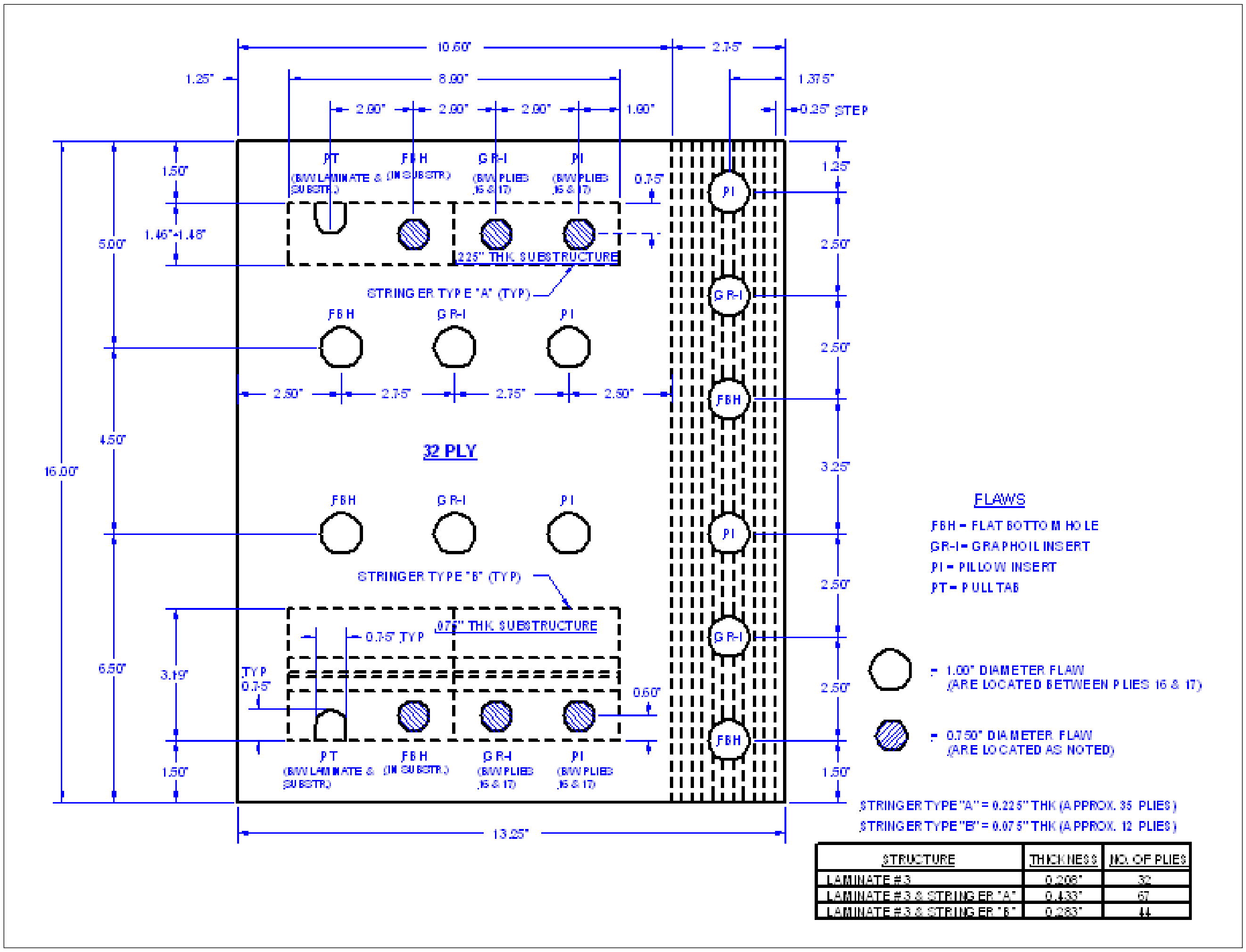

Figure 34. Final design of 32-ply training/feedback specimen with taper

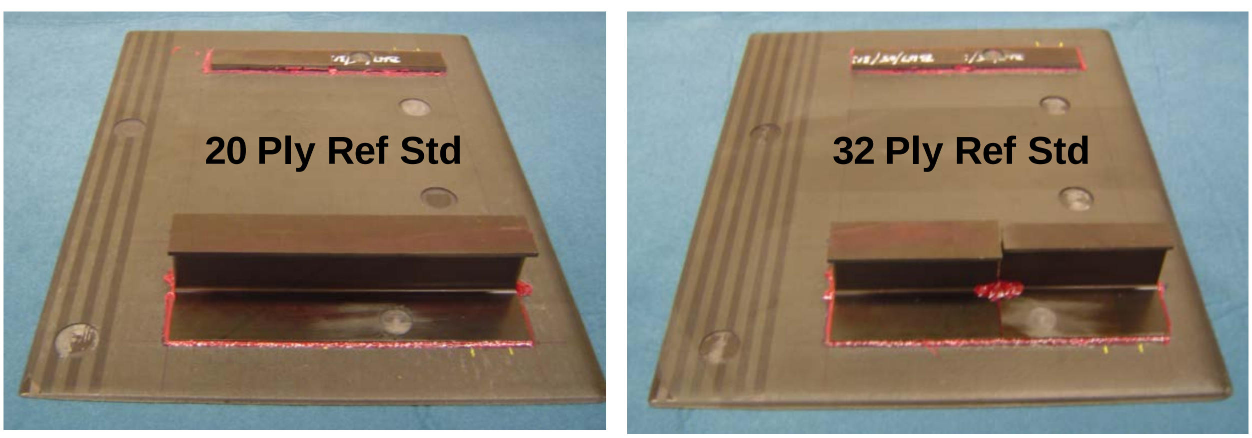

Figure 35. 20- and 32-ply NDI feedback specimens used by inspectors prior to starting the blind POD inspections (backside view)

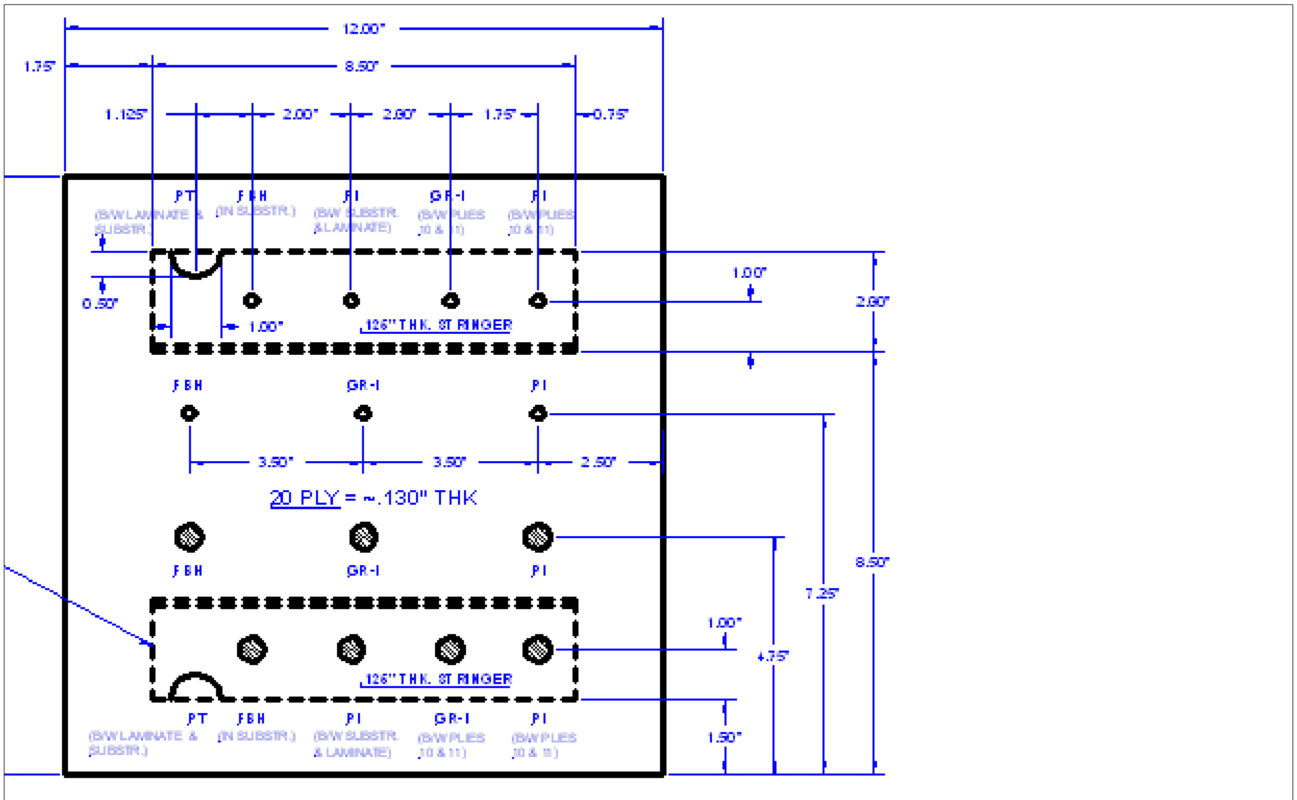

STRUCTURE	THICKNESS	NO. OF PLIES
LAMINATE # 1	0.130"	20
LAMINATE & STRINGER	0.255"	39

Figure 36. Final design of second 20-ply training/feedback specimen without taper and different substructure and smaller flaws

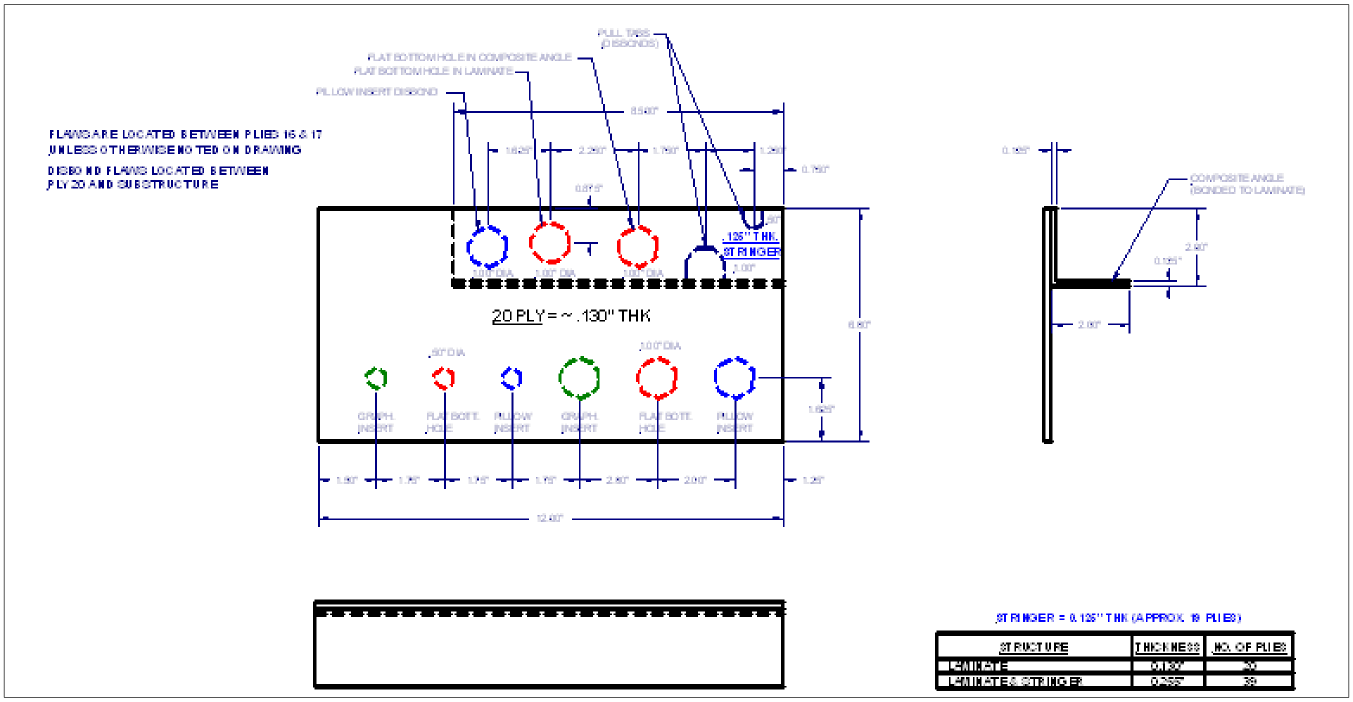

Figure 37. Final design of third 20-ply training/feedback specimen

4.2.3 Test Specimen Designs

- Test Specimen Types—proper flaw spacing and sufficient area for assessing false calls produced a need for 15 specimens broken down into four complex taper specimens, four 12–20 ply ST specimens, four 32-ply ST specimens, and three BNs. These different specimen types are shown in figures 37–43. There are a total of 11 specimens in the thin laminate experiment and 4 specimens in the thick laminate experiment

- Engineered Solid Laminate Test Specimens – (see also table 1)

  - BN Specimens—inspection area = 5.5 ft^2 each; total of 16.5 ft^2

  - Complex Taper Specimens—inspection area = 1.3 ft^2 each; total of 5.2 ft^2

  - ST Specimens (12–20 plies)—inspection area = 3.1 ft^2 each; total of 12.4 ft^2

  - Thin Laminate Experiment—total Inspection Area for 12–20 ply = 34.1 ft^2

  - ST Specimens (20–32 plies) = 3.0 ft^2 each; total of 12.0 ft^2

  - Thick Laminate Experiment—total Inspection Area for 20–32 ply = 12.0 ft^2

- Figure 38 shows the two types of ply tapers and how they were integrated with the substructure elements. The specimens contained both simple (one-directional) tapers and complex (two-directional) tapers.

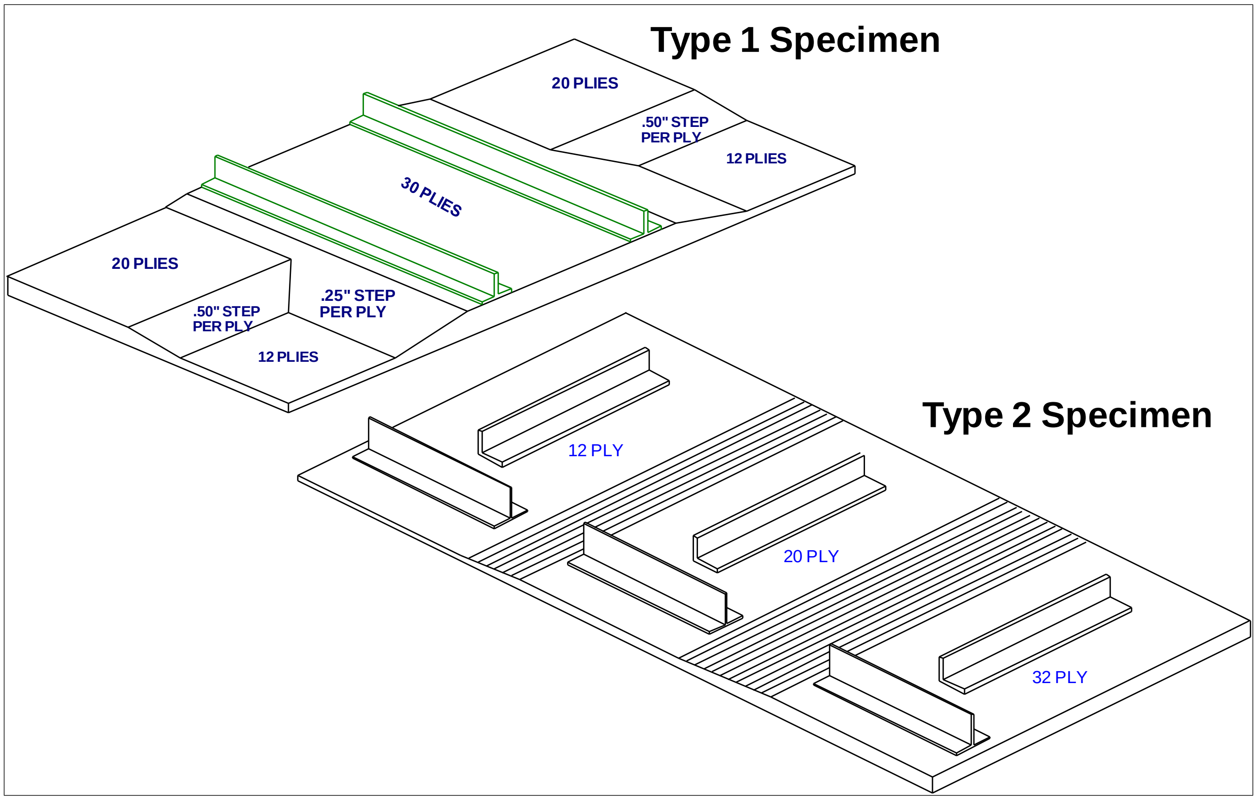

Figure 38. Solid composite laminate specimens with substructure and single (type 1) or dual (type 2) ply tapers on the back side

- Curved Specimens With Honeycomb—figure 39 shows the BN specimen design. It includes honeycomb regions in the top and bottom skins to study the inspection impediment of honeycomb under thick laminates. Flaws have been placed in the transition region where the laminate splits around the honeycomb. The rounded section in the front was produced separately and fastened into place as shown. The aft spar is a prefabricated C-section and is sealed and fastened. Flaws were placed in the fastened and sealed regions of the spar attachment joint. This specimen is approximately 5.5 ft^2 and there are three specimens of this design for a total inspection area of 16.5 ft^2.

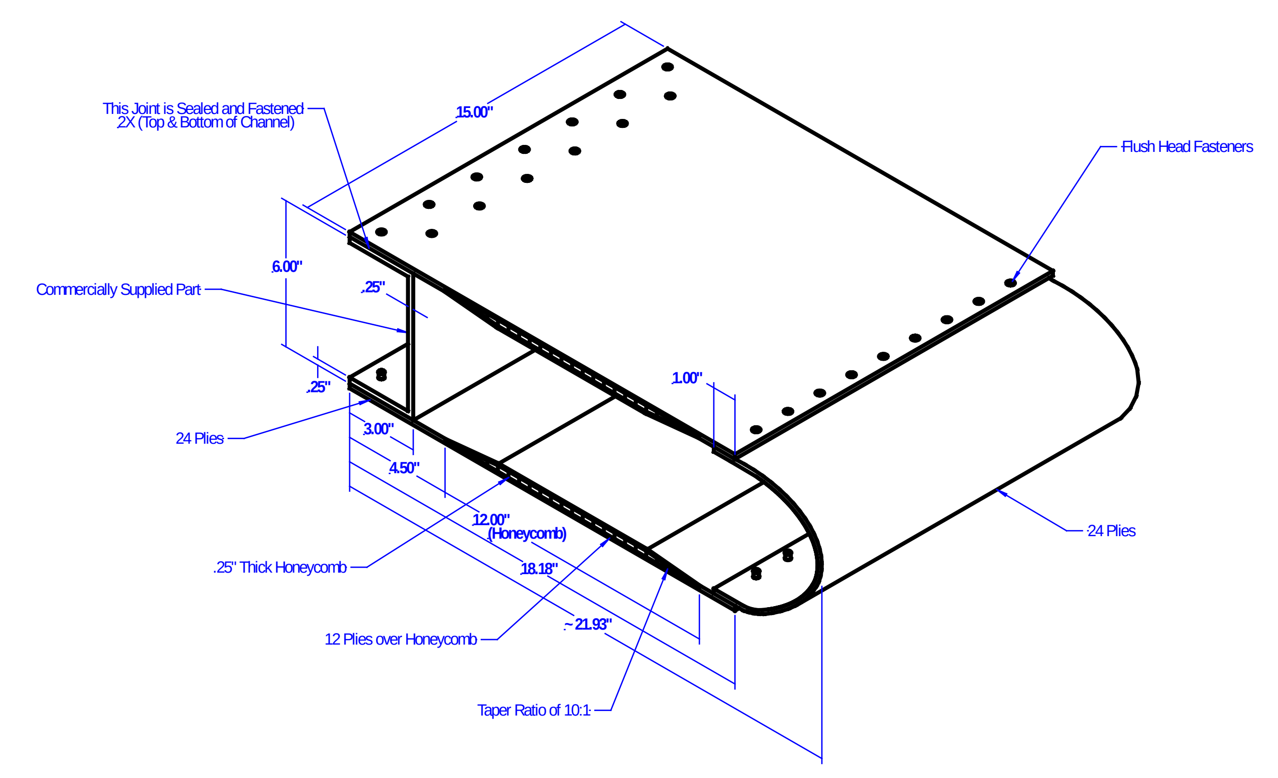

Figure 39. BN test specimen drawing

- Thin and Thick Laminates with Taper—figures 40–44 show the designs for this specimen type. Figures 40 and 41 highlight the complex double taper inspection challenge that is included in the study. Figures 42 and 43 show the simple taper designs that provide more surface area of CT as well as substructure stringer/rib regions that contain secondary bonds.

- Co-Cured and Secondarily Bonded Construction—several stringers were supplied by Airbus, Boeing, and a manufacturer of prefabricated, composite structures. These items were secondarily bonded to the laminate skins using a film adhesive (see figures 42 and 43). Figure 44 shows a substructure panel design that is similar to the panels in figures 42 and 43, with the main differences being the number of plies in the skin and the fact that the substructure are co-cured, versus secondarily bonded, in the thick laminate specimens. Flaws in the substructure elements include disbonds at the skin interface and delaminations (FBHs and inserts) in the structure itself.

- Inspection Area—the complex (double) taper specimens (shown in figures 42 and 43) provide 5.2 ft^2 of inspection area, the simple taper specimens (see figures 43 and 44; thin laminates) provide approximately 12.4 ft^2 of inspection area, and the simple taper specimens (figure 44; thick laminates) provide 12 ft^2 of inspection area. The total experiment consisted of a total of 46.1 ft^2 of inspection area. Inspectors completed the 11 specimens in the thin laminate skin experiment in 2–3 days and completed the four specimens in the thick laminate skin experiment in 1–2 days.

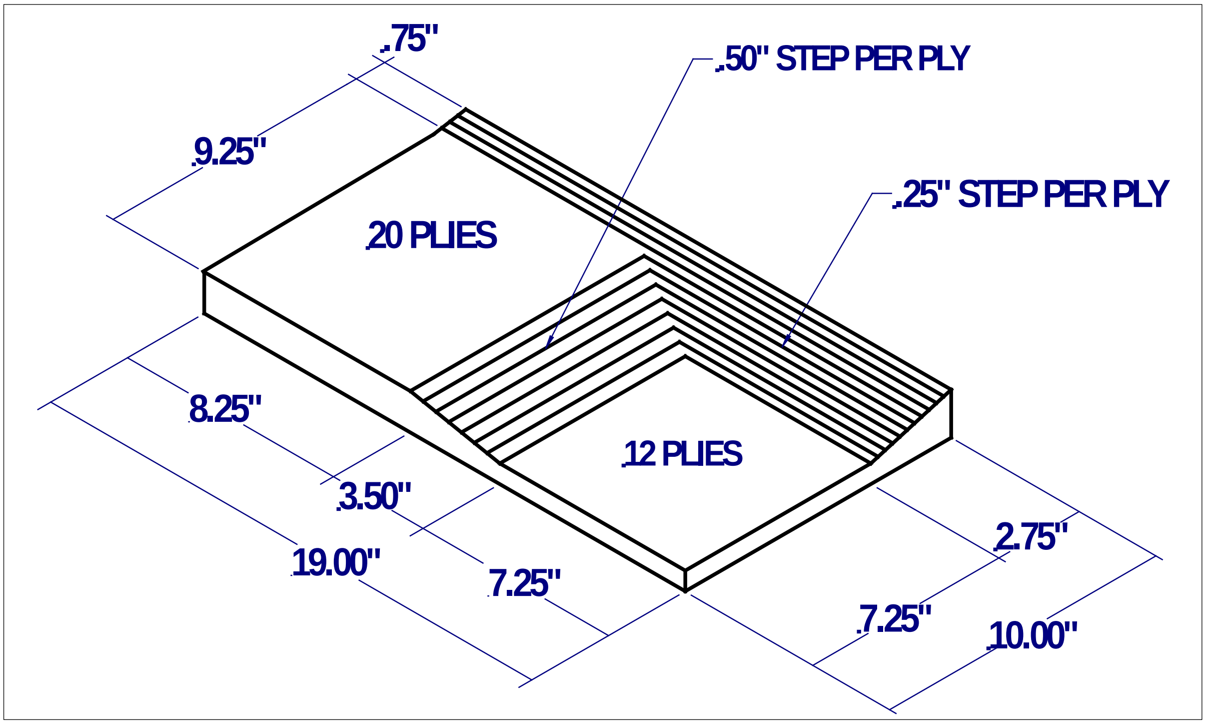

Figure 40. Complex taper “A” test specimen drawing

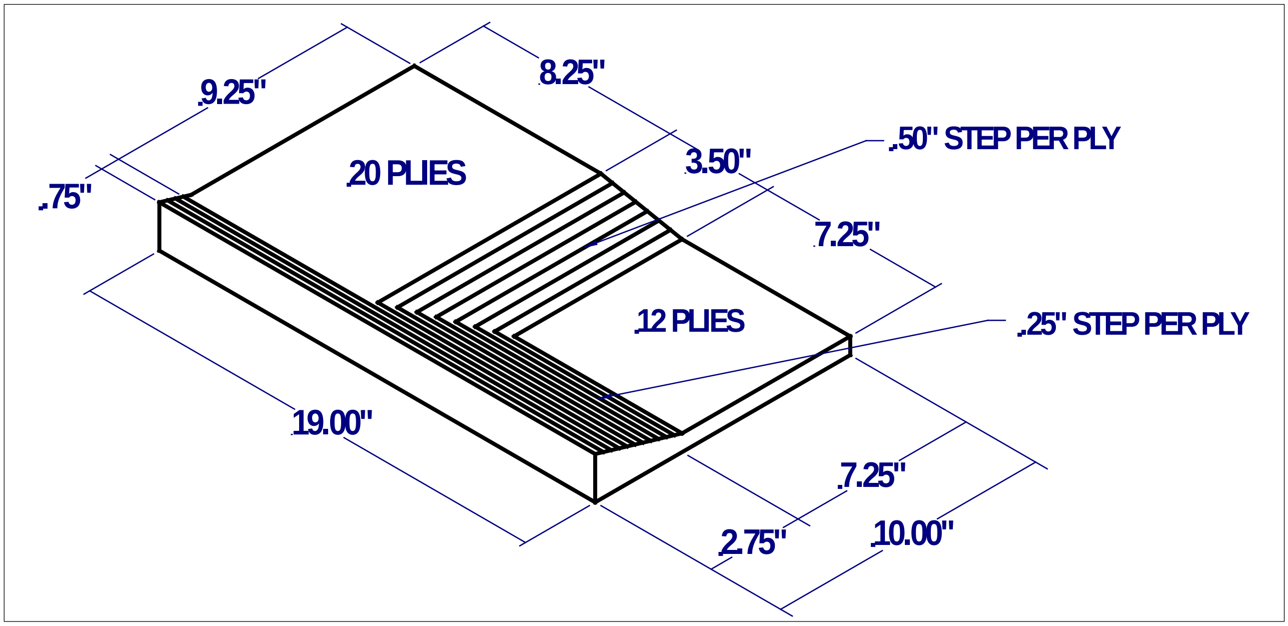

Figure 41. Complex taper “B” test specimen drawing

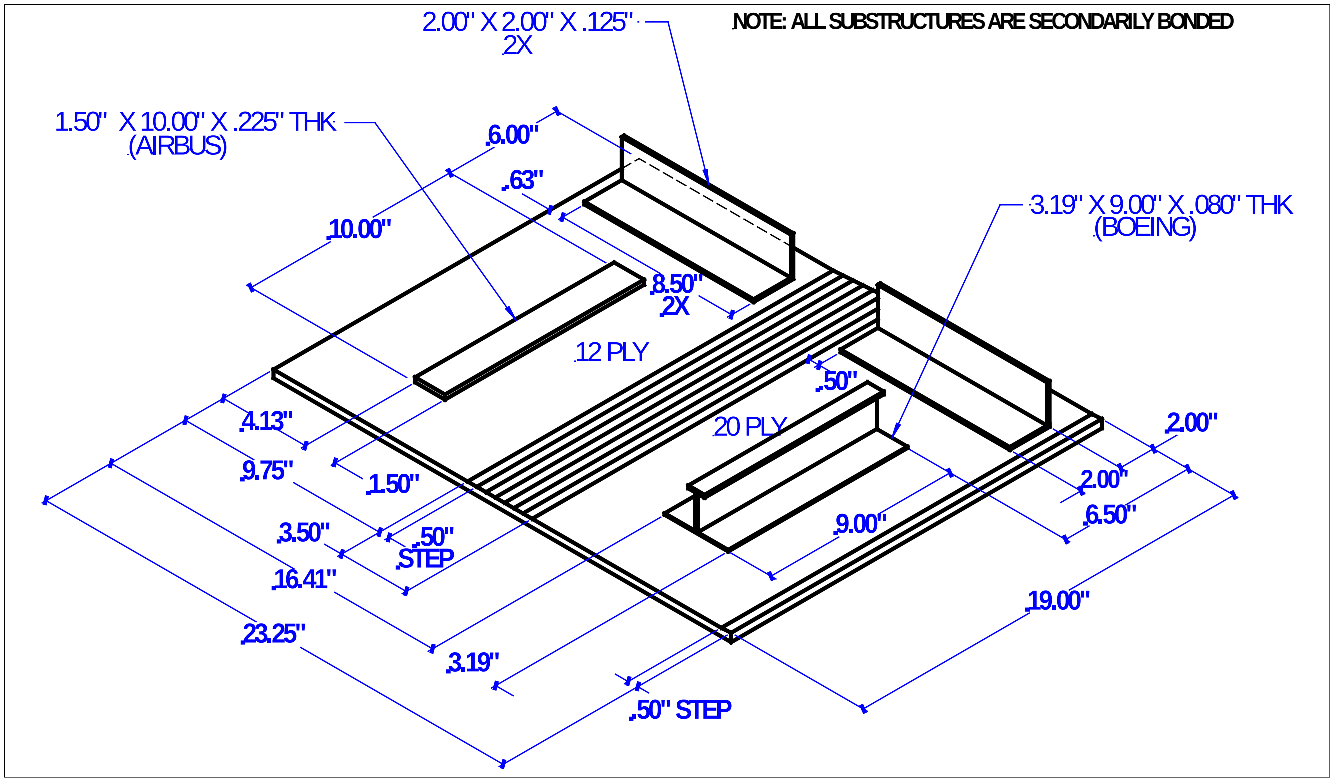

Figure 42. Simple taper upper test specimen drawing (12–20 plies)

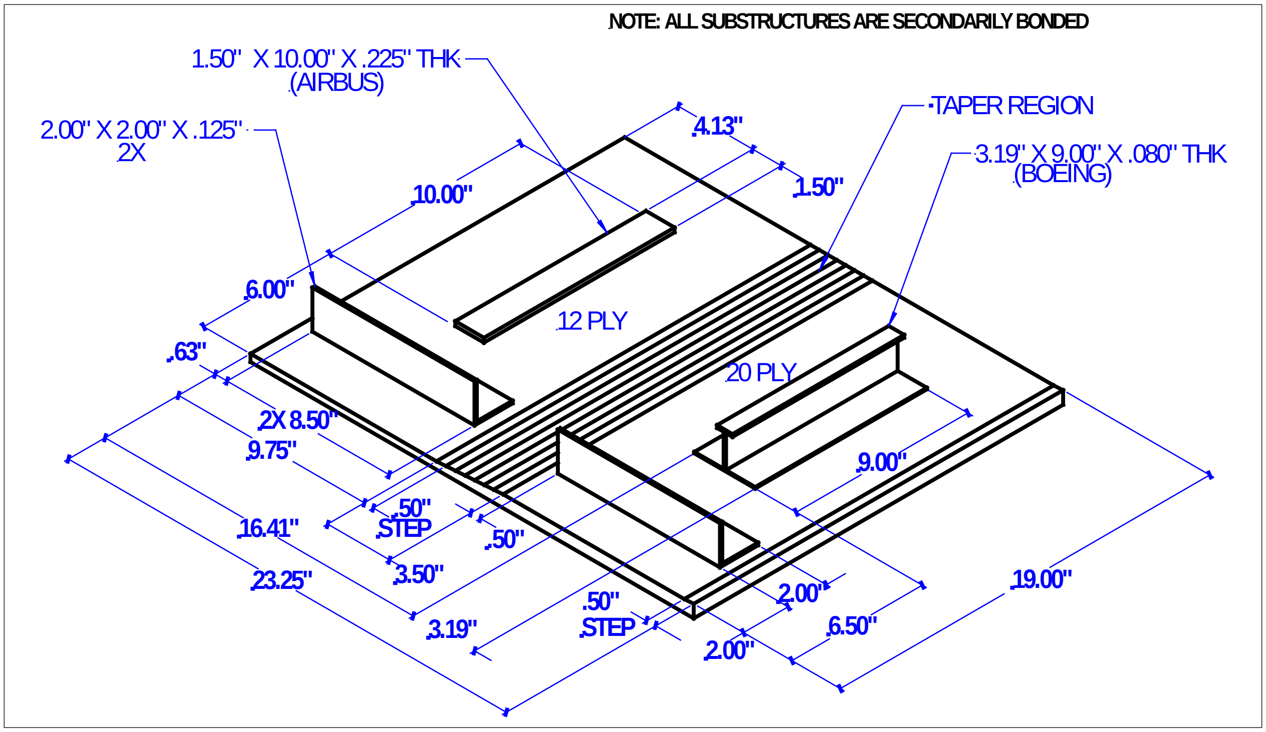

Figure 43. Simple taper lower test specimen drawing (12–20 plies)

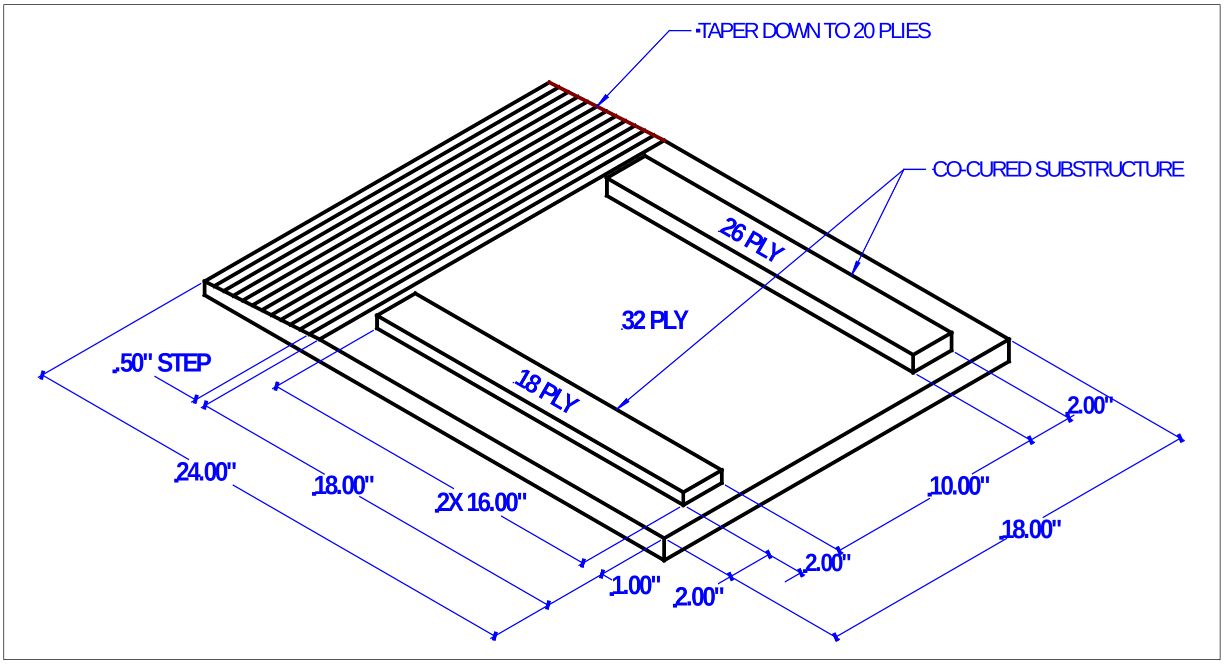

Figure 44. Simple taper 32 ply test specimen drawing (20–32 plies)

- Use of Specimen Drawings—drawings were provided to all inspectors taking part in this experiment. To simulate the level of information that an inspector might obtain from the OEM manuals, some basic schematics with a few dimensions and ply listings were produced. The inspector could then determine if signal changes were caused by the presence of a flaw or by geometry changes in the specimen.

- Specimen Area by Geometry Type—the total inspection area for each panel type is listed in tables 2–4. The inspection areas consisting of CG and CT are also calculated. Table 2 lists the total inspection area for the 12–20 ply specimen set, broken down by area of each panel type and geometry type. Table 3 shows the same information for the 20–32 ply specimen set. Table 4 shows the combined area calculations for the 12–20 ply and 20–32 ply specimen sets. Notice the inspection areas for both the CG and CT regions are almost equal.

Table 2. Thin 12–20 ply total inspection area table

Thin (12–20 ply)—Total Area = 34.1 ft^2				
Panel Type	ft^2	# Panels	Total ft^2	Geometry
BNs	5.6	3	16.8	Combined
	4.663	3	13.989	CG
	0.937	3	2.811	CT
CTs	1.319	4	5.276	Combined
	0.424	4	1.696	CG
	0.895	4	3.58	CT
STU/STLs	3.002	4	12.008	Combined
	0.977	4	3.908	CG
	2.025	4	8.1	CT

Table 3. Thick 20–32 ply total inspection area table

Thick (20–32 ply)—Total Area = 12 ft^2				
Panel Type	ft^2	# Panels	Total ft^2	Geometry
ST32s	3	4	12	Combined
	1.194	4	4.776	CG
	1.806	4	7.224	CT

Table 4. Combined 12–20 ply and 20–32 ply total inspection area table

Combined 12–20 ply and 20–32 ply Total Area = 46.1 ft^2		
	Total ft^2	% Area
CG	24.4	53%
CT	21.7	47%
Total	46.1	100%

4.3 FLAW MANUFACTURE OPTIONS

A key aspect of the production of the test specimens was the determination of the methods to engineer realistic flaws. To evaluate several different methods for engineering flaws into a composite laminate, a number of thick, composite laminate trial specimens were produced with different laminate thicknesses, as well as ply taper regions. Figure 45 shows one example of the trial specimens. It contains a matrix of six possible ways to produce delaminations. Flaws of different sizes were placed at different depths. Subsequent inspections produced S/N data (PE UT and low-frequency bond test) and attenuation data (through transmission ultrasonics). The goal was to determine methods for producing both “loose” delaminations (high attenuation and

S/N values) and “tight” delaminations (relatively low S/N values and attenuation levels in the range of the 12 dB accept-reject threshold). Test results showed that the 4-ply pillow inserts produced the more gross flaws whereas the GFI better simulated the tighter flaws. As a result, the experiment included both flaw scenarios. Figure 46 shows a C-scan image produced by PE UT inspections along with the S/N values associated with each flaw type and size. The goal was to use only flaws that produced an S/N level of 3 or greater. The pull tab and flat-bottom hole flaw engineering methods were also adopted into this experiment.

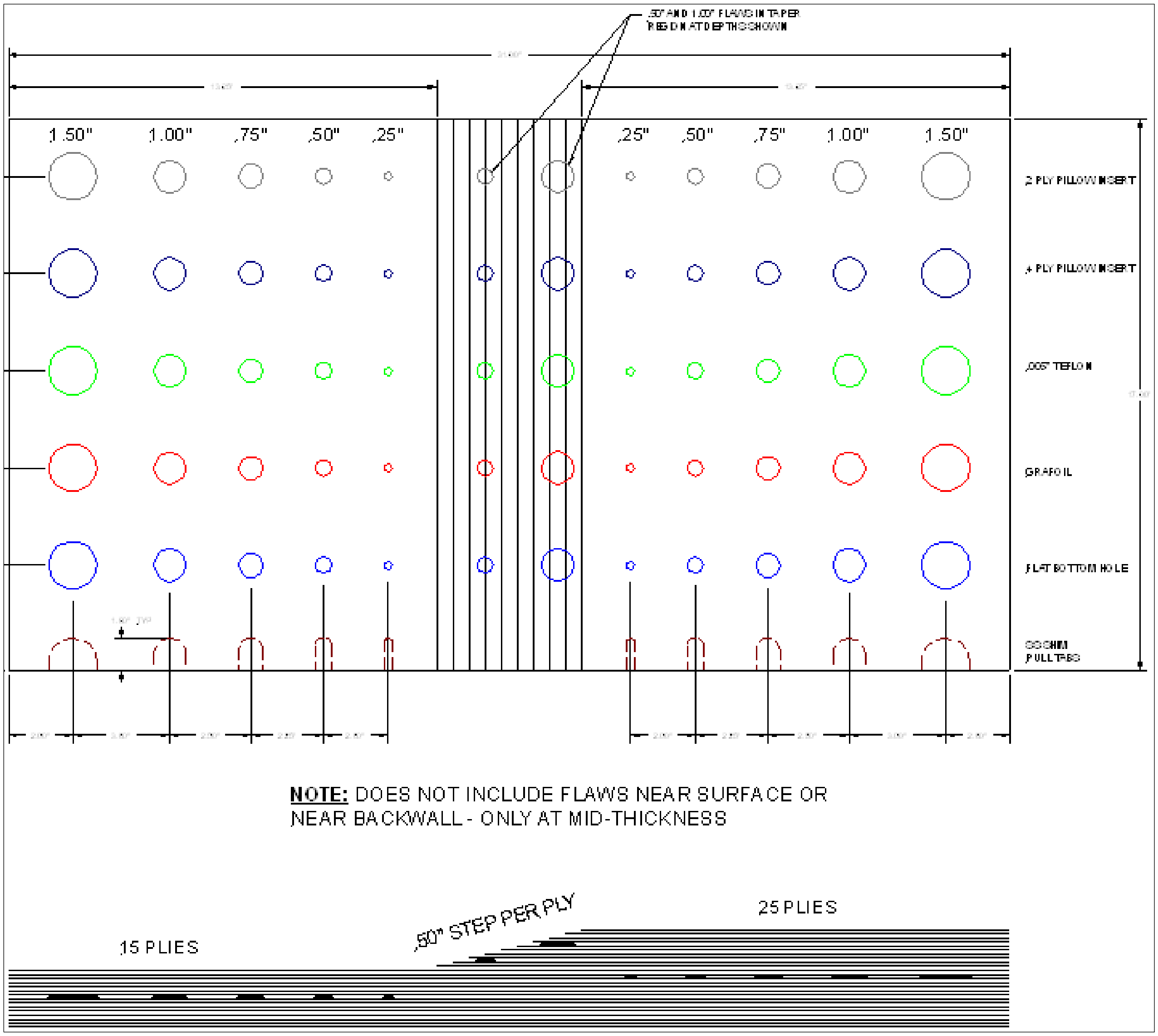

Figure 45. Trial S/N solid laminate specimen for preliminary testing of methods for producing engineered flaws

Figures 47 and 48 show some of the test specimens being fabricated. Figure 47 shows the Mylar templates that were used to ensure the proper placement of the flaws in each of the specimens while figure 48 shows the vacuum bagging/autoclave production process, some of the ply taper regions, secondary bonding of some substructure elements, and some of the post-production flaws that were added to the back side of the test specimens.

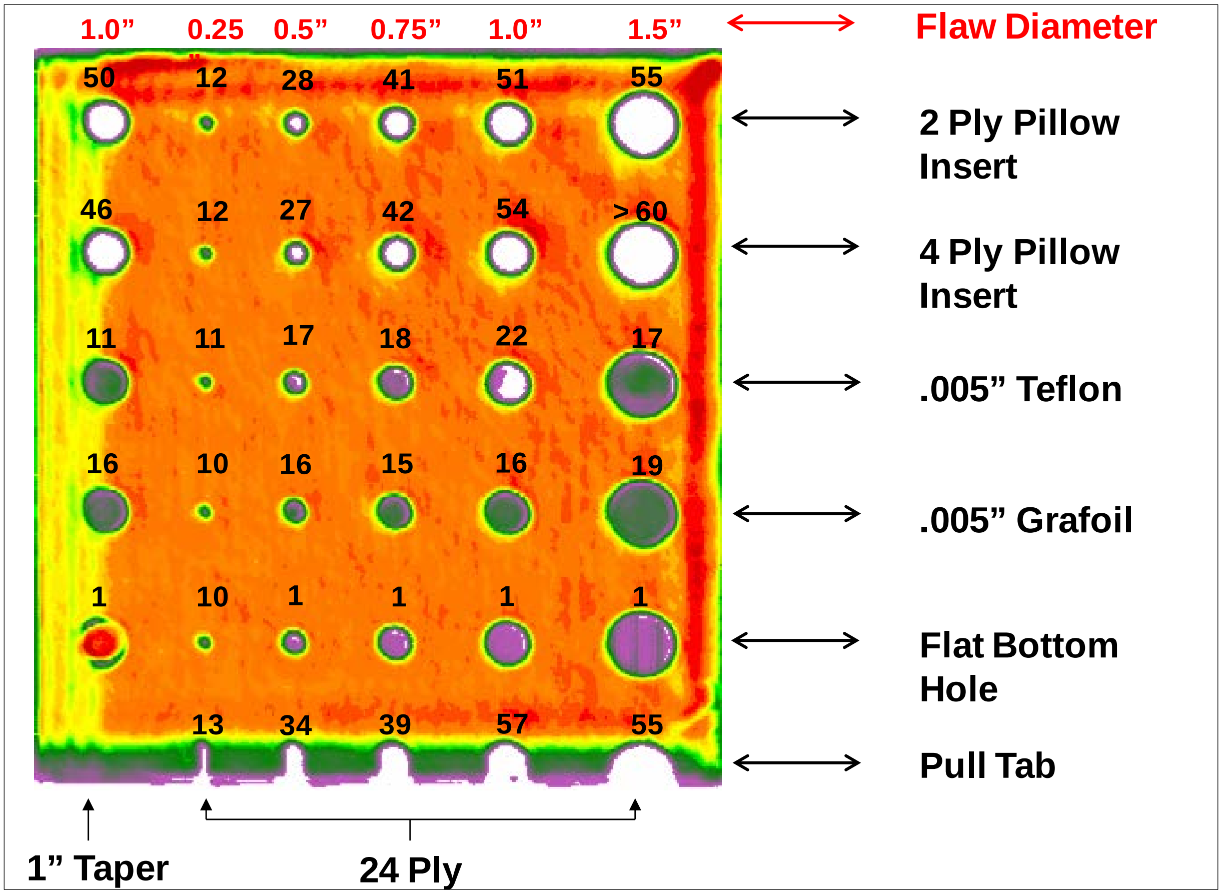

Figure 46. Ultrasonic scan of trial solid laminate specimen showing attenuation levels to establish viability of flaw engineering methods

Figure 47. Solid composite laminate flaw detection experiment—test specimen fabrication

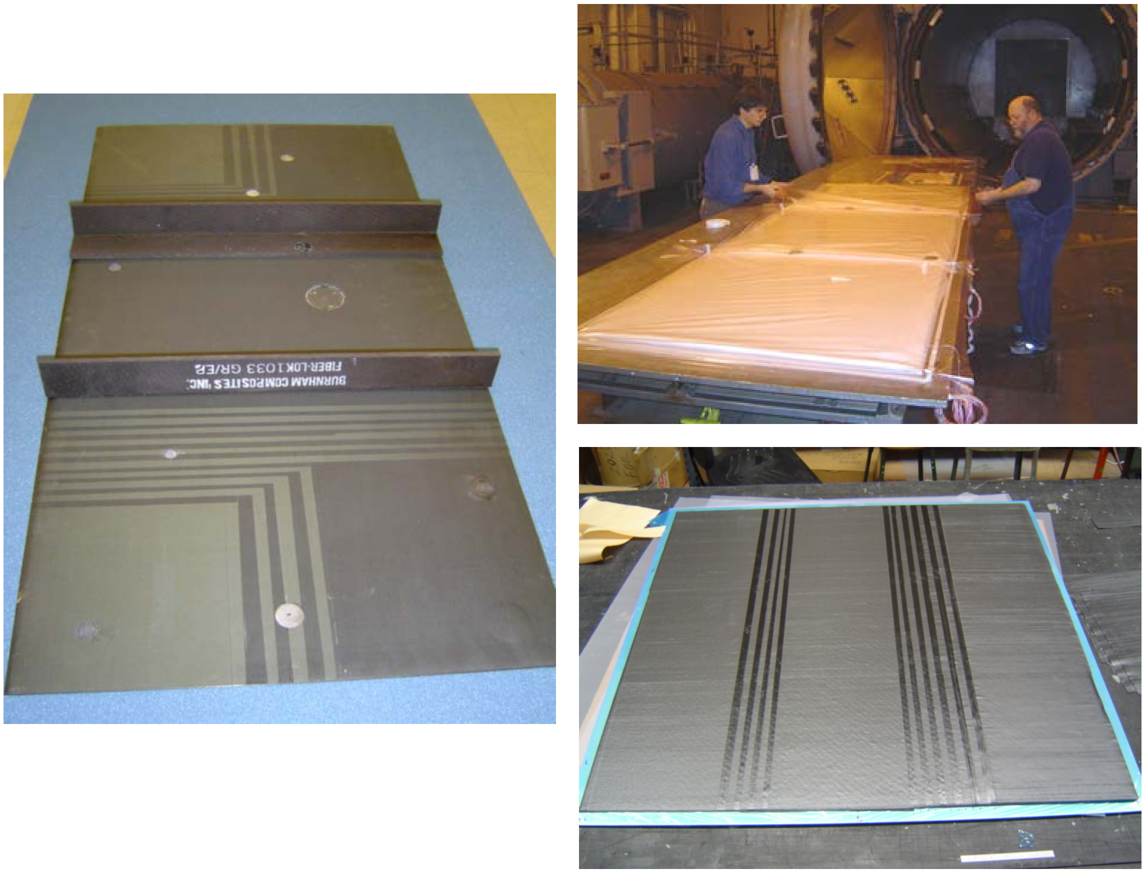

Figure 48. Layup of composite laminates with simple taper and complex taper and bonding of substructure elements

4.3.1 Flaw Characterization

To make a quantitative assessment of the viability of each engineered flaw in the SLE test specimens, the S/N of each defect versus the surrounding good structure was determined. The S/N was calculated using the amplitudes of the A-scan signals in the test specimens. The noise level was determined by examining the output variation corresponding to inspections along adjacent sections of good structure. This was compared to the signal obtained during inspections of the flawed areas:

$$S/N = \frac{FS - BS}{NS} \tag{1}$$

Where:

BS = base signal; peak signal at unflawed area
NS = noise signal; (max-min)/2 over range of unflawed area in each quadrant
FS = flaw signal; peak signal at each flaw site
S/N = signal-to-noise ratio

In general, an S/N ratio of at least 3 is desired to infer the presence of a flaw. Thus, all flaws in the SLE database were checked to ensure that the S/N was 3 or larger. Testing using this scheme did not require calibration on a median or neutral reference standard. The key measurement for each case was the difference between unflawed areas of the test panel and the defect area. The S/N can be calculated based on the flaw signal (FS) decrease in the back wall signal or the FS presence (amplitude) of a new intermediate signal between the front and back wall, which also indicates an anomaly. Table 5 shows sample results from the series of S/N calculations for a BN and CT specimen. If the drop in the back wall signal was used as the FS basis for the calculations, it is seen that the S/N values ranged from 29–89. If the new intermediate peak is used as the FS basis for the calculations, it is seen that the S/N values ranged from 8–69. With both calculations, all flaws were deemed viable for this study as they provided sufficient signal variation to be readily detectable.

Table 5. Sample S/N calculations for flaws in the BN and CT test specimens

Pulse Echo UT Amplitude Measurements								
Flaw No.	Panel Location	Laminate Thickness	Flaw Identification (Type/Size, Loc.)	Viability of Flaws—Attenuation	Backwall Response (% FSH)	S/N Ratio (Backwall Signal)	Flaw Response (% FSH)	S/N Ratio (Flaw Signal)
1	BN1	12–24	4PL-PI, 0.50″, b/t 4&5	17.6	21.1	87.1	80	44
3	BN1	12–24	GR-I, 1.0″, b/t 4&5	23.3	11.0	93.4	120	69
5	BN1	12	4PL-PI, 1.0″, b/t 4&5	18.7	18.7	88.6	120	69
6	BN1	12–24	GR-I, 0.75″, b/t 4&5	22.7	12.1	31.4	120	22
8	BN1	12–24	4PL-PI, 1.5″, b/t 8&9	21.4	14.1	31.0	125	8
10	BN1	12	GR-I, 1.0″, b/t 6&7	19.5	17.6	30.3	120	22
68	CT1	12–32 T	4PL-PI, 0.25″, b/t 16&17	23.4	6.3	32.3	31	10
69	CT1	20–32 T	GR-I, 2.0″, b/t 16&17	21.6	7.8	31.7	101	36
70	CT1	12–32 T	GR-I, 0.75″, b/t 22&23	26.0	4.7	32.9	117	42
71	CT1	12–32 T	4PL-PI, 1.5″, b/t 16&17	23.0	6.6	32.2	117	42
72	CT1	20–32 T	GR-I, 0.75″, b/t 16&17	20.7	8.6	31.4	109	39
75	CT1	12	4PL-PI, 0.25″, b/t 6&7	20.6	11.7	29.1	78	17

4.4 EXPERIMENT TIMING

Based on the FAA-AANC's experience with the similar composite honeycomb flaw detection experiment, the experiment was designed to not take more than 3–3½ days of an inspector's time. The planned inspections for all 15 test specimens were deemed to be more time-consuming than those deployed on the honeycomb suite of specimens, so it was important to determine the amount of surface area that an airline inspector could be expected to realistically cover in a 3-day test. Trial experiments were conducted with the simulated vertical stabilizer specimen shown in figure 49. This allowed for a quantitative assessment of the possible surface area that could be inspected in a 3-day span. To acquire some timing data, an A330 vertical stabilizer test specimen with engineered flaws was sent to United Airlines. Inspection results from two inspectors at United Airlines showed that almost all the flaws were detected. The two inspections took 2 hours and 35 minutes, and 3 hours and 30 minutes for the 10 ft^2 panel. This timing data indicated an expected coverage of 2.9–3.9 ft^2 per hour using handheld PE UT methods. Overall, these results indicated that a 3–3½ day experiment (18–22 hours of inspection time) could include approximately 60 ft^2 of inspection area. This experiment contains a total of 46 ft^2 (34.1 ft^2 thin laminate and 12.0 ft^2 thick laminate) of inspection area. For comparison purposes, inspection results from several different A-scan and C-scan NDI methods are shown in figure 50.

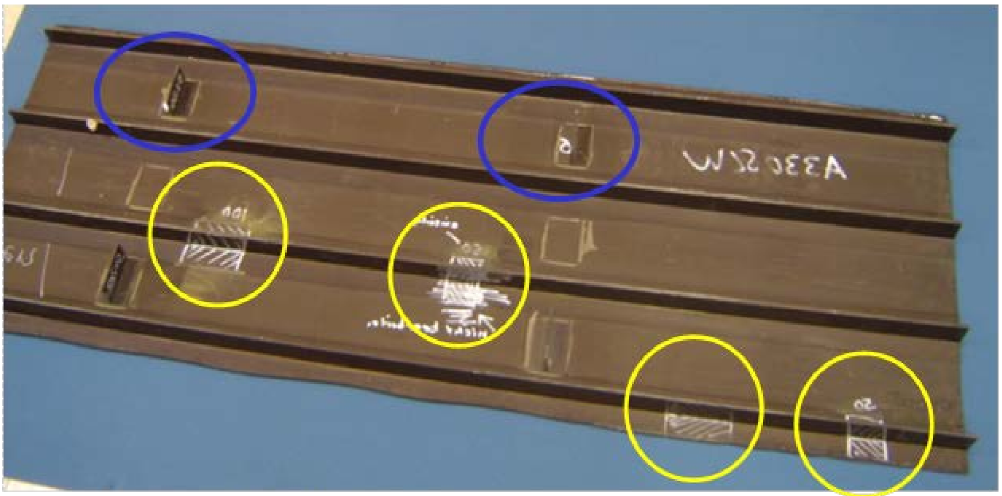

Simulated Vertical Stabilizer with Stringers, Rib Sections, and Engineered Flaws
Four stringer-to-skin disbonds (yellow)
Two rib-to-skin partial disbonds (blue)

Figure 49. Composite laminate vertical stabilizer test specimen used to obtain preliminary timing information for handheld PE UT inspections

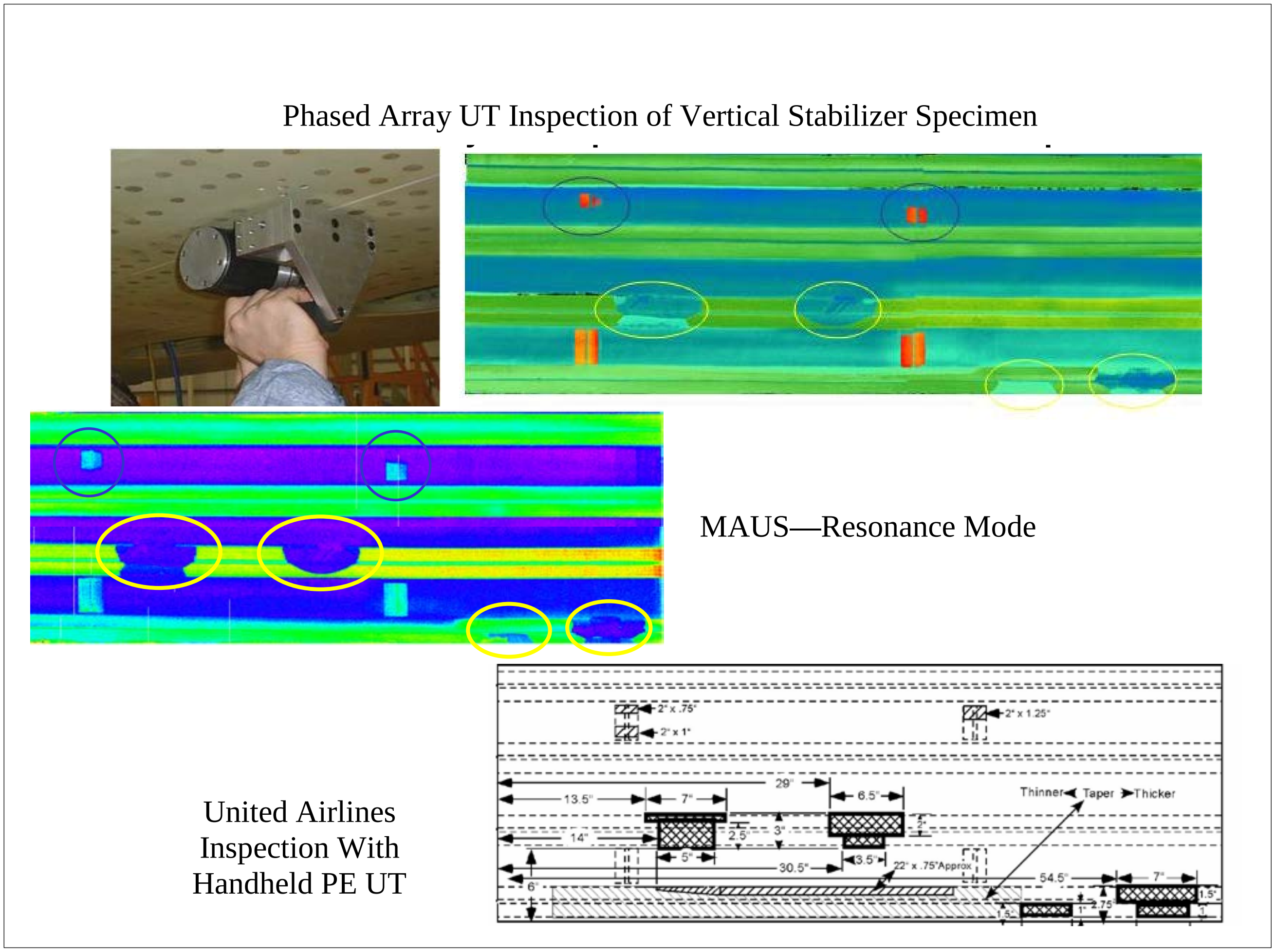

Figure 50. Inspection results showing detection of all stabilizer flaws by phased array UT, resonance scans, and handheld PE UT

4.5 RAMP DAMAGE CHECK EXPERIMENT

Several OEMs and airlines requested that the FAA-AANC adapt the SLE to conduct a blind evaluation of the viability of the Bondtracer™ and the Ramp Damage Checker. As a result, a customized POD experiment was produced from the SLE and is called the Ramp Damage Check Experiment (RDCE). The purpose of the RDCE is to assess new, ultrasonic-based go/no go equipment that OEMs plan to allow airlines to deploy at airports and other nonscheduled maintenance depots using non-NDI personnel (e.g., airframe and powerplant [A&P] mechanics). These go/no go devices are described in section 3. The equipment can be deployed when visual clues or other events occur that warrant closer scrutiny of a composite laminate structure. Ground personnel, with appropriate training on such equipment, will set up the equipment in accordance with OEM-supplied procedures and then make an assessment of the region in question. It is important to note that such go/no go UT equipment is intended to be used to assess local indications or regions only. They are not intended for wide-area inspections that cover areas of several square feet. Thus, equipment operators must be directed to very distinct locations. This was a key consideration in the design of the RDCE.

4.5.1 RDCE Design

- Selected locations and shapes were identified on the SLE specimens so that personnel participating in the RDCE were aware of: (1) exactly which regions to check and (2) which region to use for equipment calibration prior to inspection

- Selected locations, while a subset of the SLE, include all types of flaws and construction scenarios including substructure elements

- Selected locations averaged 8.62 in^2 (0.06 ft^2) in area over 140 locations for a total inspection area of 8.38 ft^2. These locations were divided into those having flaws (53%) and those having no flaws (47%). The inspection area to flaw ratio was greater than 20:1, meaning that for every 1 in^2 of flaw area, there were more than 20 in^2 of unflawed area in the overall RDCE

- Flaw sizes are the same as those deployed in the SLE—0.25″, 0.5″, 0.75″, 1″, 1.5″, and 2″

- 80 flaws were included in the RDCE design

- The RDCE was designed to allow for calculating PODs based on each individual participant's results

- The GE® Bondtracer™ and Olympus Ramp Damage Checker were used by an equal number of participants

- Both NDI inspectors and non-NDI personnel (all A&P qualified) were tested to determine if any difference in performance was observed

4.5.2 RDCE Implementation

- NDI feedback specimens, along with equipment setup procedures and overview training (see appendix E), were provided to all participants in the RDCE. Experiment participants were allowed to work with the NDI feedback specimens to increase their proficiency with either the Bondtracer™ or the Ramp Damage Checker before proceeding on to the blind POD experiment

- Each blank experiment panel (see figure 51) from the SLE was prepared for the focused inspections that were specifically selected for the RDCE

- An inspection region was consistently marked on each composite test specimen using a series of templates. Inspection locations and calibration locations were marked on each specimen by the experiment monitors using the RDCE design templates shown in figure 52. The template was placed on each specimen and the inspection regions on each panel were then clearly marked using this template. Each section was marked using a Vis-à-Vis® white board marker that can be erased without leaving any residue markings on the panel. In addition, the proper calibration regions were also provided so that the equipment was calibrated on an unflawed location of matching thickness

- Panels marked with inspection locations (boxes) were provided to each RDCE participant

- Specialized drawings, as shown in figure 53, were provided to each participant for guidance. The drawings showed the inspection regions to be covered along with the panel design (e.g., laminate thicknesses, substructure regions and thicknesses, taper regions) so that the inspectors were aware of the composite ply arrangement in each region

- Inspectors made their flaw indications directly on the test panel as shown in figure 54. Grading templates were then placed on top of the inspector's flaw calls to determine flaw hits, misses, false calls, and ability to correctly size each detected flaw

Figure 51. Test panel from the SLE

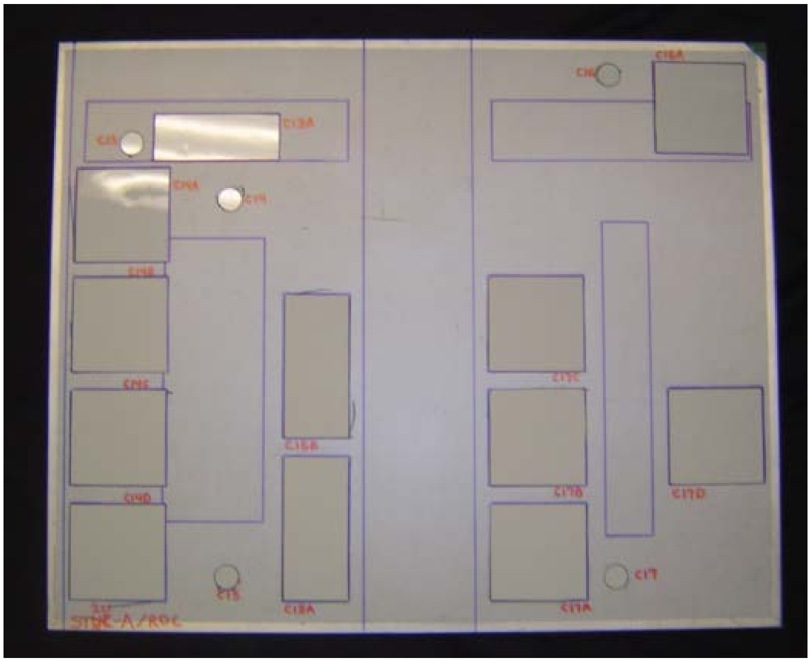

Figure 52. Use of template to mark the series of small inspection regions and the appropriate calibration point for the Bondtracer™ or ramp damage checker equipment

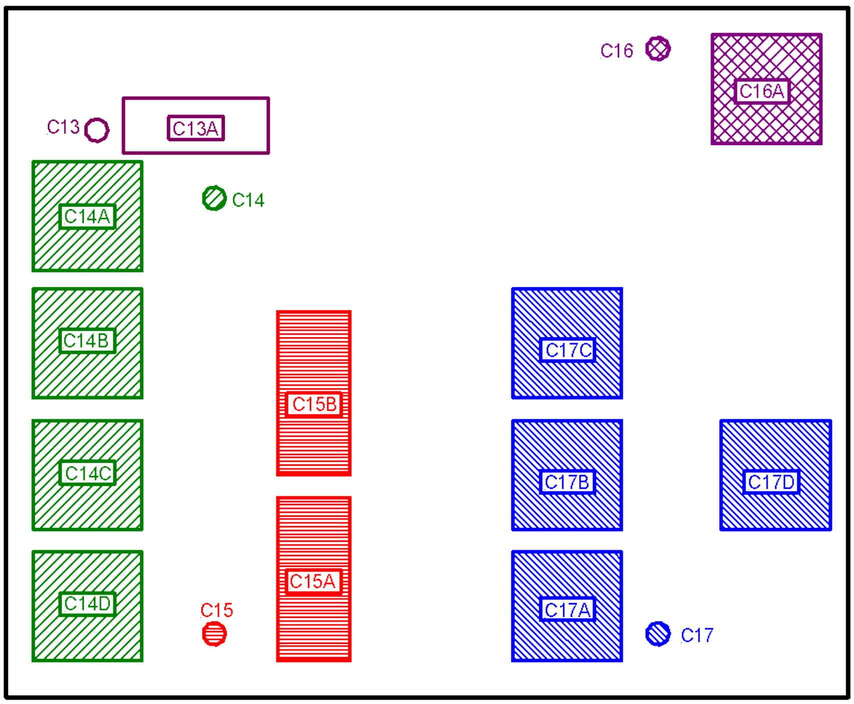

Figure 53. Drawings provided to inspectors for guidance show the inspection regions to be covered, the appropriate calibration points (note color coding), and the panel design features

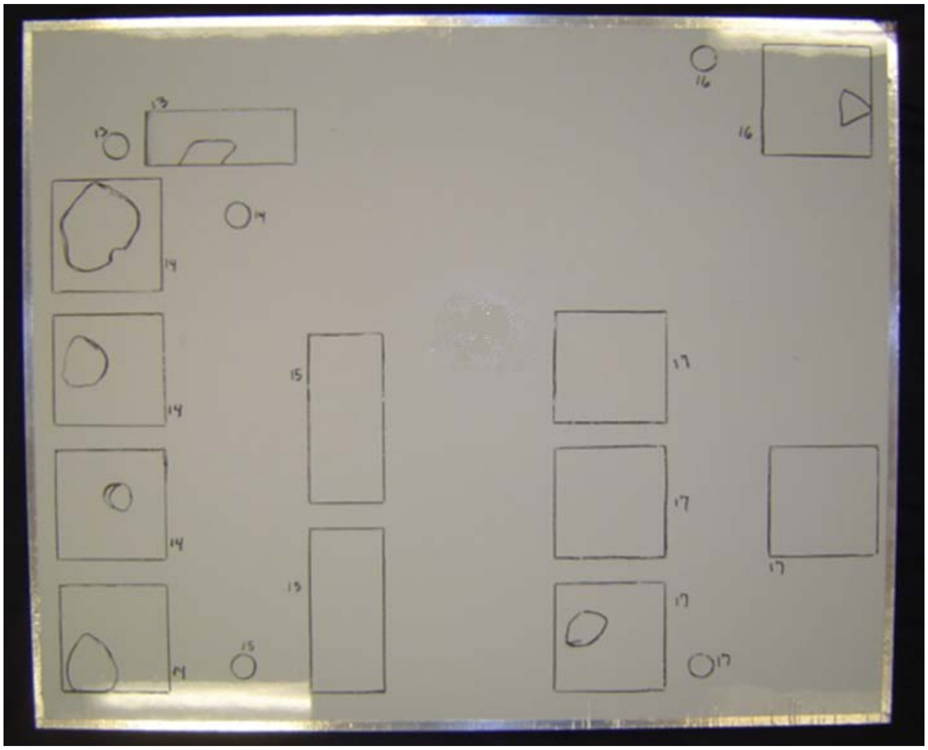

Figure 54. Test panel showing an inspector's flaw markings within the directed inspection regions

5. IMPLEMENTATION OF THE SLE

A set of experiment protocols was written to guide every aspect of the SLE implementation. The experiment protocols ensured that the information provided to all experiment participants was consistent and comprehensive so that all participants received similar guidance and inspection aids. The experiment protocols also provided step-by-step guidance to the experiment monitors so that all data and observations associated with the SLE were acquired in a consistent manner. A thorough Experiment Briefing Package was sent out in advance of every airline visit. The Experiment Briefing Package is included in appendix A and was provided to experiment participants at least one week in advance of the SLE blind testing. The set of NDI feedback specimens, with flaw locations clearly marked, was also sent out in advance so that experiment participants could conduct PE UT inspections to familiarize themselves with the composite structure and flaw detection requirements.

The first day of each experiment started with the presentation of the Experimenter Briefing included in appendix B. Figure 55 shows one of the briefings being provided to inspectors. This briefing explains the purpose of the experiment and the process the inspectors will use to indicate their flaw findings. The briefing was used at each facility to ensure a consistent presentation on the experiment goals and a thorough explanation of how the experiment will proceed. It also allowed the inspectors to ask questions. At this time, the inspectors were introduced to the inspection transducers, UT devices, and aids (e.g., delay lines) that they could optionally use. Inspectors could also decide to use their own PE UT equipment and transducers. Composite laminate inspection procedures were provided to the FAA-AANC by Boeing and Airbus for use in the SLE. These sample composite laminate NDI procedures were presented to the inspectors for their use. During the course of the NDI tests, the experiment monitors logged various observations along with the exact flaw calls provided by the inspectors. Appendix C contains the Experiment Monitor Data Acquisition Sheets that were used to guide the data logging.

Once the briefing was completed, each blind inspection process was preceded by inspections of appropriate NDI feedback specimens supplied by the experiment monitors. The inspector was provided with information on the manufactured flaws present in the NDI feedback specimens and was allowed to use the specimens for the checkout and setup of their inspection equipment. The NDI feedback specimens had a similar construction to the blind test specimens and included similar flaws. Thus, they were also used to allow inspectors to become familiar with an inspection device and learn about a specific equipment's response to various composite structures and flaws within those structures. Figures 44–47 show the flaw profiles of all the NDI feedback specimens.

Additional ultrasonic transducers were also provided by the experiment monitors so that the inspectors could experiment with different frequencies, probe diameters, and types (contact or delay). Once the inspectors were comfortable with their setup on the NDI feedback specimens, experiment monitors distributed the blind specimens to them for inspection. Inspectors were asked to locate and properly size the flaws they found by marking directly on the specimens using standard grease pencils. These data were then recorded and graded to determine their POD level and number of false calls and the inspectors' accuracy in sizing the flaws. Other secondary data were collected, such as timing (inspection time on each panel), inspector experience, NDI training level, inspection frequency, probe type, and equipment used for inspection. Figures 56 and 57 show the typical setup for the experiment deployment, in which each inspector has a workstation to set up their equipment and test specimens.

The participants included over 70 inspectors from 18 aircraft maintenance facilities, including 14 different airlines and two MROs. All of the maintenance facility inspectors used handheld PE UT inspection devices. The maintenance facilities included: All Nippon Airways®, American Airlines®, Cathay Pacific Airlines, China Airlines™, Continental Airlines® (pre-merger with United), Delta Air Lines (two facilities), Federal Express® (two facilities), Goodrich Aerospace, Japan Airlines, Northwest Airlines (pre-merger with Delta), Singapore Airlines, Taikoo Aircraft, Thai Airways, United Airlines, and US Airways.

As a separate, complementary activity, the SLE was also completed using a wide array of advanced NDI methods. The advanced NDI methods evaluated with the SLE included phased array ultrasonics (the Boeing MAUS® system, Olympus OmniScan®, Toshiba Matrixeye™, GE Phasor™), rolling wheel phased array ultrasonics (Sonatest Rapidscan, GE RotoArray™), laser ultrasonics (iPhoton), digital acousto-video (Imperium Acoustocam™), shearography (Dantec Dynamics, Laser Technology Inc.), flash thermography (Thermal Wave Imaging), line thermography (Mistras Group, Inc.), transient thermography (MoviTHERM), lock-in thermography (MoviTHERM), ultrasonic video (DolphiTech's DolphiCam), and microwave (Evisive). A forthcoming report will describe the POD results from the advanced NDI methods, with comparisons to the conventional PE UT method discussed in this report.

Figure 55. Experiment instructions being provided to supplement the written experimenter briefing and information packet

Figure 56. Typical experiment setup with separate inspector workstations

Figure 57. Inspector completing inspection using specimen drawing for reference of structural details

Figure 58. Inspector completing inspection and marking flaw detection on the test specimen

Figure 59. Participants in the SLE

6. RESULTS FROM THE SLE

Each inspection technique that was applied in this blind flaw detection experiment was evaluated using the following performance attributes: (1) accuracy and sensitivity, (2) data analysis capabilities, (3) versatility, (4) portability, (5) complexity, (6) human factors, and (7) inspection time. The most important of these parameters were the quantitative metrics because they are objective standards that can be numerically counted or quantified. Accuracy is the ability to detect flaws reliably and correctly in composite structures and repairs without false calls. Sensitivity is the extent to which the inspection system responds to flaws as a function of size, type, and location in the structure (e.g., proximity to edges, taper regions, underlying or adjacent structural elements).

The set of graphs in this section present all of the detailed results for all aspects of the SLE. These include the POD curves for each inspector, as well as the resulting cumulative POD curve for both the thin (12–20 ply) laminate experiment and thick (20–32 ply) laminate experiment. The curves show the variation within the group of inspectors that completed each experiment. In the thin (12–20 ply) laminate experiment, the best performing inspector produced a $POD_{[90/95]}$ = 0.53″ diameter flaw, the worst performing inspector produced a $POD_{[90/95]}$ = >3.00″ diameter flaw, and the overall cumulative result was a $POD_{[90/95]}$ = 1.29″ diameter flaw. For the thick (20–32 ply) laminate experiment, the best performing inspector produced a $POD_{[90/95]}$ = 0.54″ diameter flaw, the worst performing inspector produced a $POD_{[90/95]}$ = >3.00″ diameter flaw, and the cumulative result was a $POD_{[90/95]}$ = 0.82″ diameter flaw. Tabulated results are also provided to summarize various aspects of the experiments. The tables present the percentage of flaws detected for each flaw size in the different inspection categories of: (1) CT geometry, (2) CG, and (3) all flaws. The CT geometry is defined as the inspection regions where the number of plies remain constant. The CG regions are defined as those areas containing tapered skins (i.e., changing thickness), substructure, curved portions, fasteners, and laminate bonded to honeycomb. The CT geometry comprised 53% of the total 46.1 ft^2 of inspection area and the CG comprised 47% of the total 46.1 ft^2 in the total SLE. The tables also show the inspector's ability to properly size each flaw they detected. For example, of all the flaws they found in the CT category, 21% were correctly sized (100% coverage). Additional tables show the false calls for each inspector completing the thin and thick laminate experiments, as well as an average false call rate broken down into the different geometry categories and sizes.

Overall, with the exception of a few outliers, the POD results were consistent, which is fairly common for human performance assessment experiments. To represent the range of construction found on aircraft, the substructure on the thick laminate was co-cured and the substructure on the thin laminate was secondarily bonded. Secondarily bonded structures can be more difficult to inspect. The thickness of the substructure can also be a major factor in flaw detection. A large number of variables were studied and isolated to determine their impact on POD values. Overall, the false call rates were low.

6.1 INSPECTION PERFORMANCE RESULTS FOR THE 12–20 PLY THIN LAMINATE EXPERIMENT

6.1.1 Overall Results

Figure 60 shows the spread of all the individual inspector $POD_{[90]}$ curves (dashed lines) compared to the cumulative $POD_{[90]}$ curve (solid line) for all 27 inspectors. These results were produced by considering all flaws in the CT and CG regions. The spread shows 15 inspectors with a $POD_{[90]}$ value less than the cumulative $POD_{[90]}$ = 1.20″ diameter flaw ($POD_{[90/95]}$ = 1.29″) and 12 inspectors with a $POD_{[90]}$ value higher than the cumulative $POD_{[90]}$ value. The variation within the experiment ranges from a $POD_{[90]}$ = 0.53″ diameter flaw for the best performing inspector to a $POD_{[90]}$ = 2.17″ diameter flaw for the worst performing inspector. The standard deviation for the inspector $POD_{[90]}$ dataset was a 0.417″ diameter flaw. Figure 61 compares the maximum likelihood estimate ($POD_{[90]}$) to the POD curve that is calculated when a 90% flaw detection is combined with a 95% confidence bound ($POD_{[90/95]}$). This solid line in figure 62 provides the performance curve that the industry normally uses to measure the performance of NDI methods as used by representative inspectors. For these experiments, POD values were calculated using a pass/fail analysis with a log normal model. It can be seen in figure 61 that the overall cumulative $POD_{[90/95]}$ for all flaws in the thin laminate experiment (i.e., 12-20 ply skins plus substructure elements) was $POD_{[90/95]}$ = 1.29″ diameter flaw. Figure 62 shows a modified calculation of the $POD_{[90/95]}$ curve after the two highest (worst performing) and two lowest (best performing) inspector POD values were removed from the dataset. The difference between the two $POD_{[90/95]}$ values is less than 1%, which shows the consistency of the results for this specimen set and the robustness of the statistics in this experiment.

The use of performance brackets to assess POD are shown in figures 63–66. Performance brackets were used to place inspectors into groups and then calculate the resulting $POD_{[90/95]}$ for each performance bracket. These performance brackets used the inspectors that fell into the 30, 70, and 90 percentile categories. The inspectors that fell into the 30 percentile group (eight inspectors, each having a $POD_{[90]}$ less than 1.0″) produced a 39% improvement to $POD_{[90/95]}$ = 0.79″ diameter flaw value compared to the overall cumulative $POD_{[90/95]}$ = 1.29″ diameter flaw. The 50 percentile group (19 inspectors, each having a $POD_{[90]}$ less than 1.35″) produced an 18% improvement with a $POD_{[90/95]}$ = 1.06″ diameter flaw. The 90 percentile group (24 inspectors, each having a $POD_{[90]}$ less than 1.7″) shows only an 8% improvement with a $POD_{[90/95]}$ = 1.19″ diameter flaw. These performance brackets might be useful to airlines and MROs, which can judge where their inspectors fall within the brackets and the resulting performances they will obtain from their inspectors. The results in figures 63–66 also reveal the degree of inspection improvements that are possible when inspectors shift their performance from the higher (worse) performance brackets to the lower (better) performance brackets. This shift in performance can be brought about by improved or more extensive composite inspection training or through a number of other measures that are described in detail in section 7.

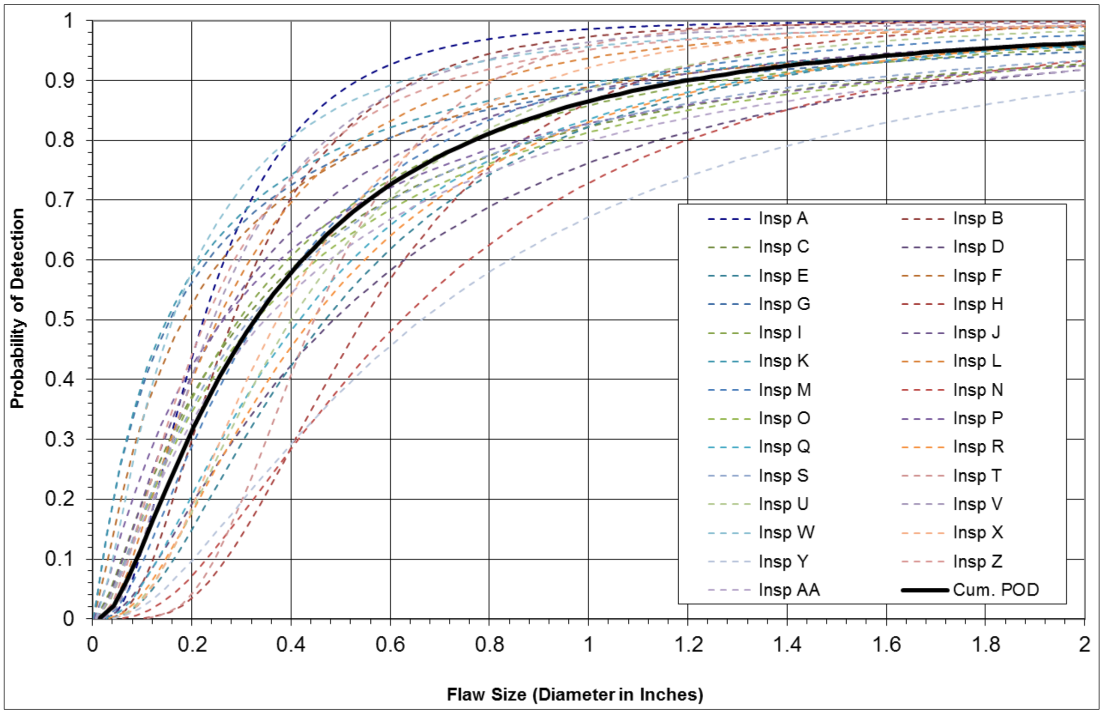

Figure 60. Individual and cumulative POD curve comparison for the 12–20 ply specimen set for all flaws in the CT and CG regions; all inspectors (27)—PE UT method

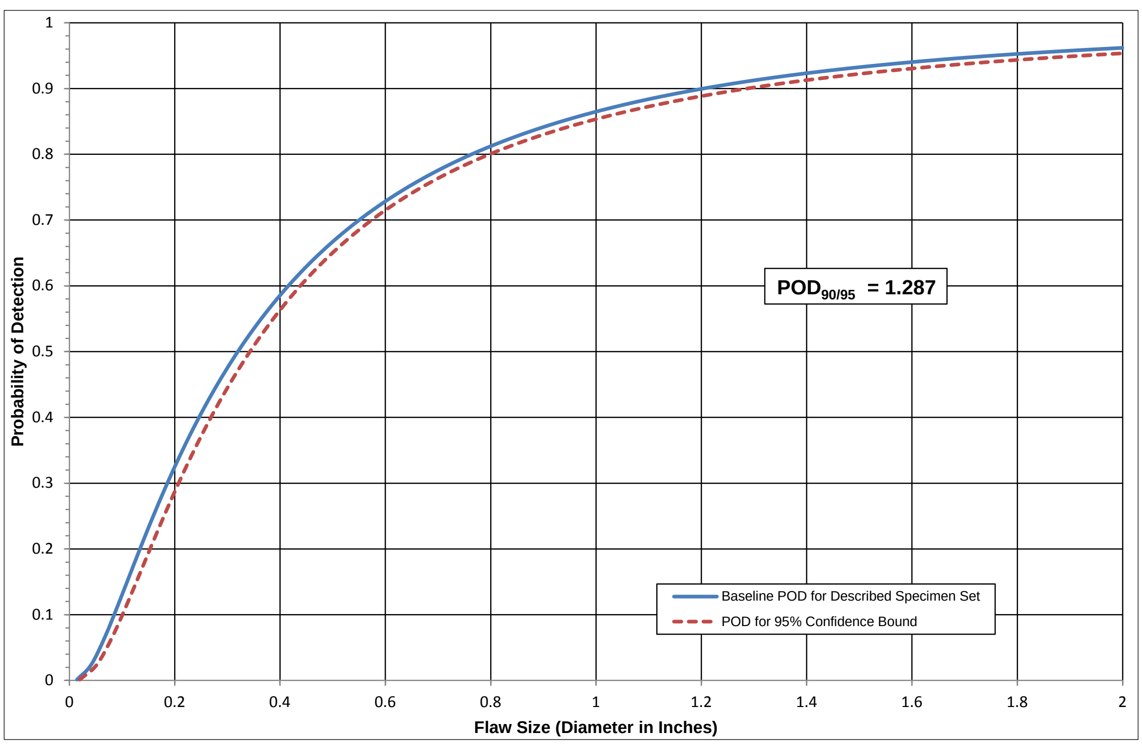

Figure 61. Cumulative POD curve for the 12–20 ply specimen set for all flaws in the CT and CG regions; all inspectors (27)—PE UT method

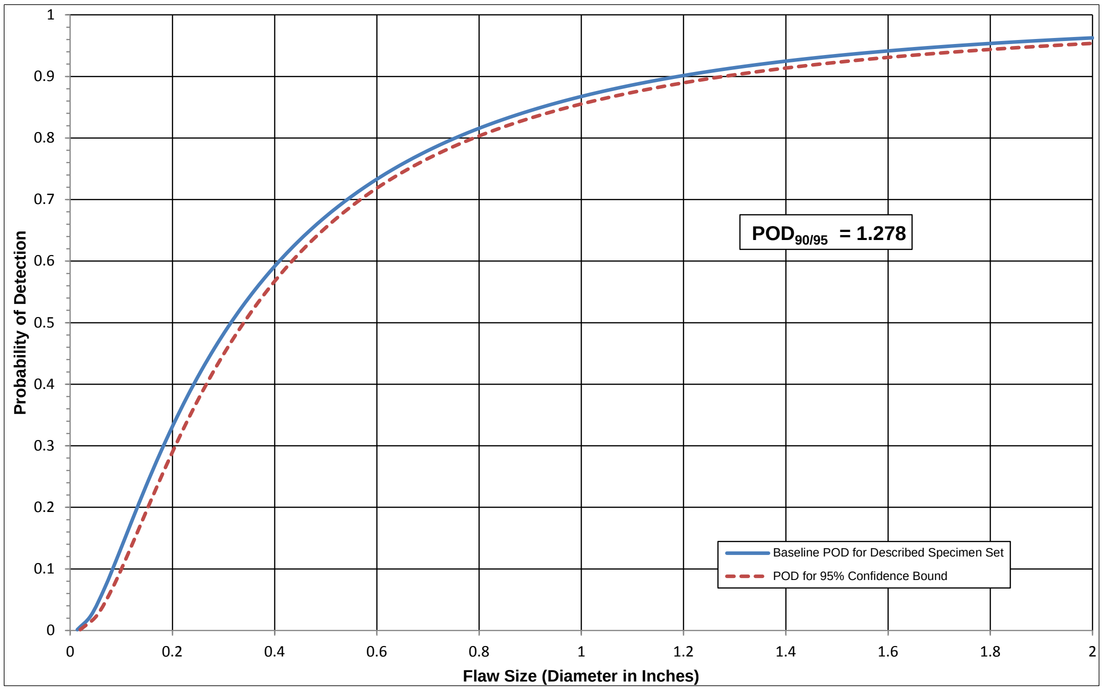

Figure 62. Cumulative POD curve with the two highest and two lowest inspector POD values removed for the 12–20 ply specimen set for all flaws in the CT and CG regions; 23 inspectors—PE UT method

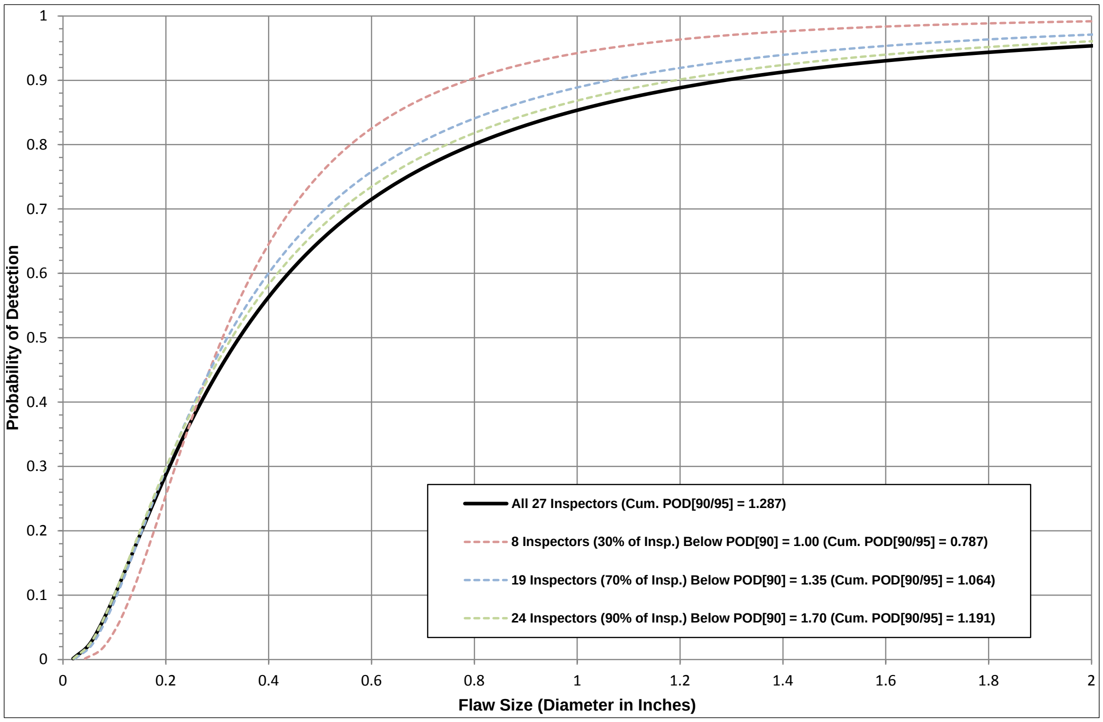

Figure 63. Cumulative POD curve comparison of the performance brackets for the 12–20 ply specimen set for all flaws in the CT and CG regions—PE UT method

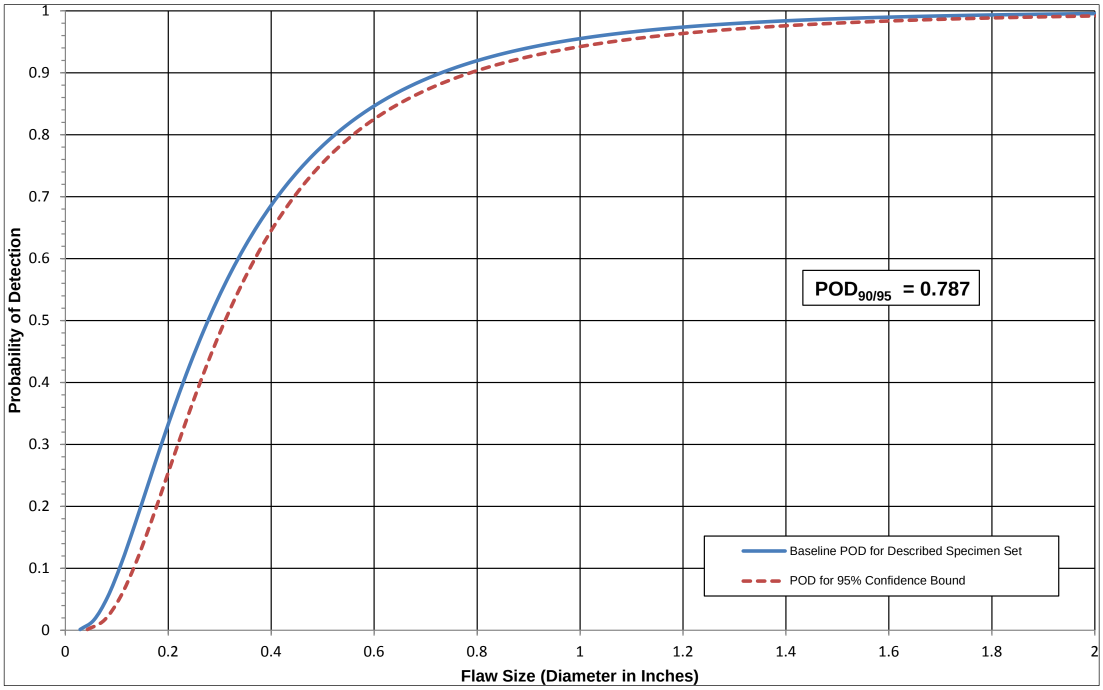

Figure 64. Cumulative POD curve for all inspectors in performance bracket below POD_{90}=1.00 (8 inspectors: 30 percentile) for the 12–20 ply specimen set for all flaws in the CT and CG regions—PE UT method

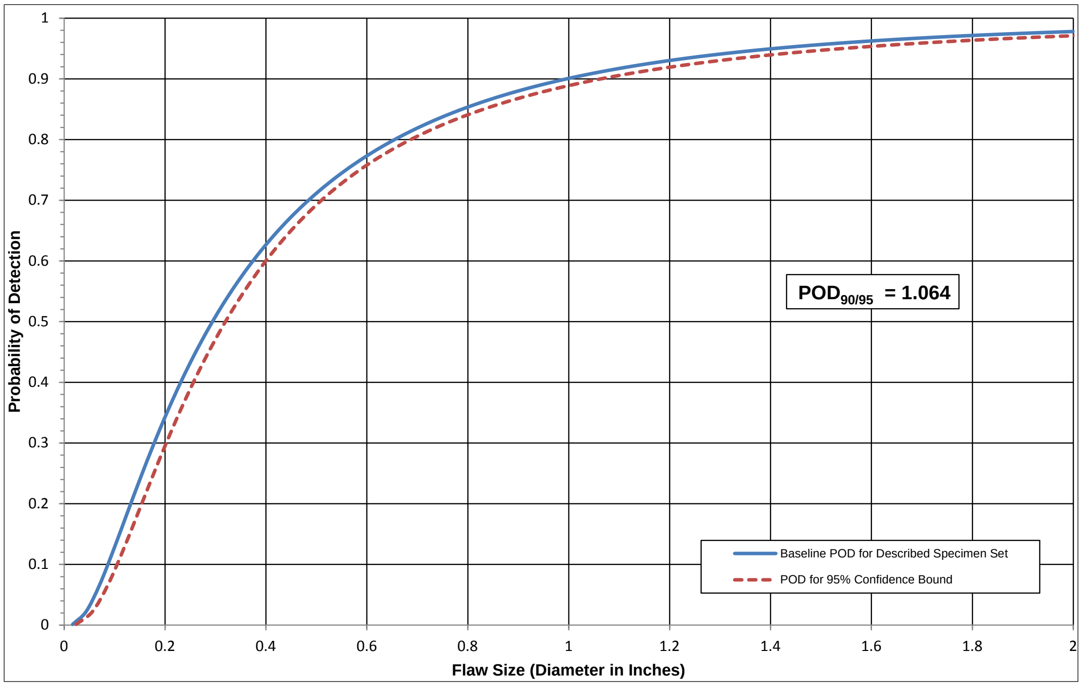

Figure 65. Cumulative POD curve for all inspectors in performance bracket below POD_{90}=1.35 (19 inspectors: 70 percentile) for the 12–20 ply specimen set for all flaws in the CT and CG regions—PE UT method

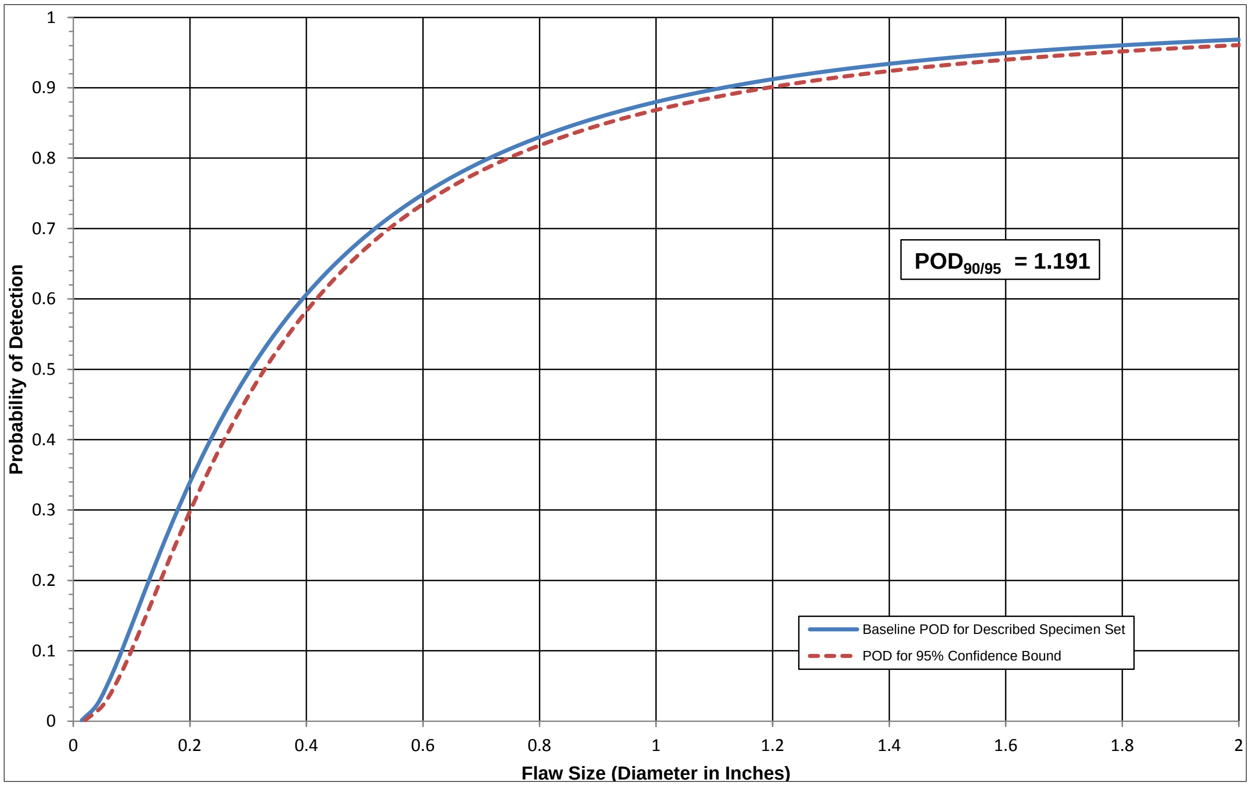

Figure 66. Cumulative POD curve for all inspectors in performance bracket below POD_{90}=1.70 (24 inspectors: 89 percentile) for the 12–20 ply specimen set for all flaws in the CT and CG regions—PE UT method

6.1.2 Effects of CG

The overall POD values were analyzed further to study the flaw detection performance within specific composite construction regions in the test specimen set. Figure 67 shows the POD curve representing inspectors' performance in the CT regions only. The CT regions are defined as regions that have no taper and no substructure, so they maintain a constant laminate thickness. The $POD_{[90/95]}$ = 0.80″ for CT geometry regions indicates a better performance compared to the overall cumulative $POD_{[90/95]}$ = 1.29″ when the CG regions are also included in the calculation. This result clearly shows the inspection challenge associated with the CG regions. Figures 68 and 69 show the CT results and the corresponding $POD_{[90/95]}$ values for skin thickness regions of 12-ply and 20-ply, respectively. Both of these plots show improvements over the overall cumulative POD value that also includes CG regions. Figure 70 considers a special structural configuration in this experiment. It addresses the spar region in the BN specimens only. The 38-ply CT regions are only found on the spar component (channel) in the BN specimens. Although this spar is a CT region (38 plies thick), it does contain some unique inspection challenges in that it is fabricated from carbon weave material versus the uniaxial material used in all other structures. The spar structures (only three in total) contained a relatively few number of flaws (eight), were more attenuative than the other laminates, and contained accessibility challenges associated with the shape and presence of adjacent fasteners (see specimen drawings in appendix D). The inspection areas were somewhat tight, with lockbolts protruding from both sides of the channel. These items accounted for the higher POD values in the special case of the 38-ply spar inspection ($POD_{[90/95]}$ = 1.28″). For comparison purposes, the 32-ply CT region in the thick laminate experiment produced a $POD_{[90/95]}$ = 0.74″, as will be discussed further in section 6.2.

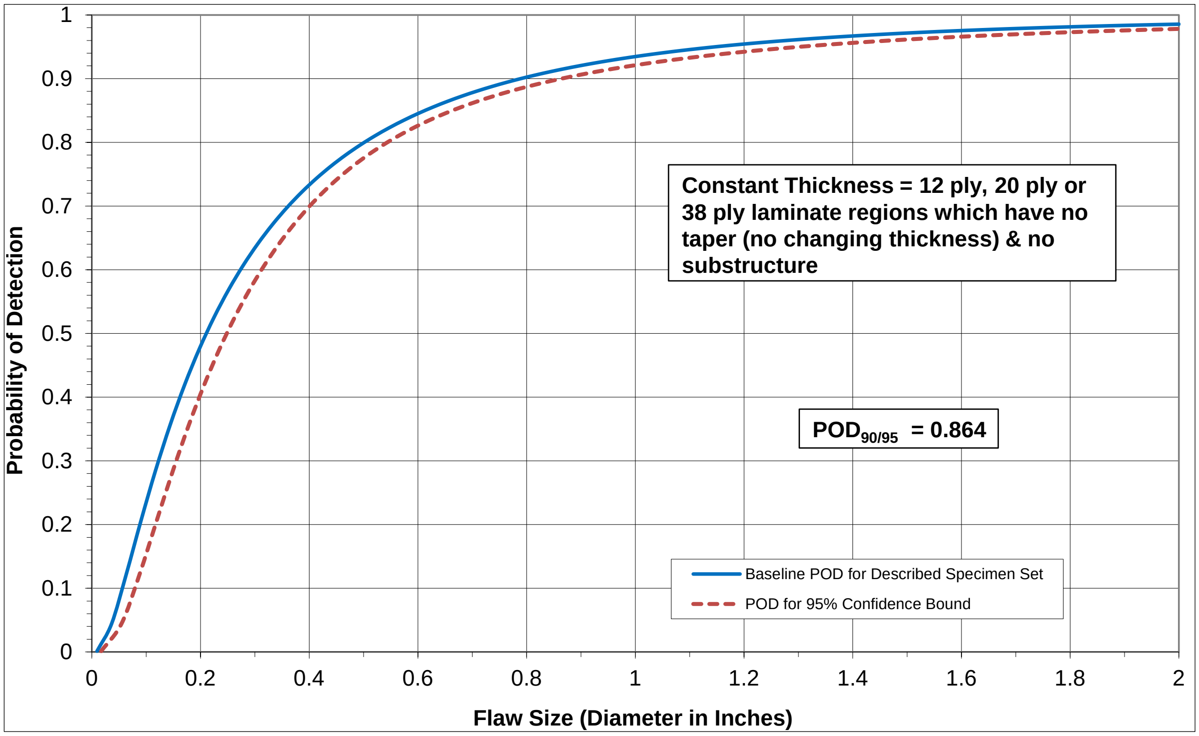

Figure 67. Cumulative POD curve for the 12–20 ply specimen set for flaws in the CT region only; all inspectors—PE UT method

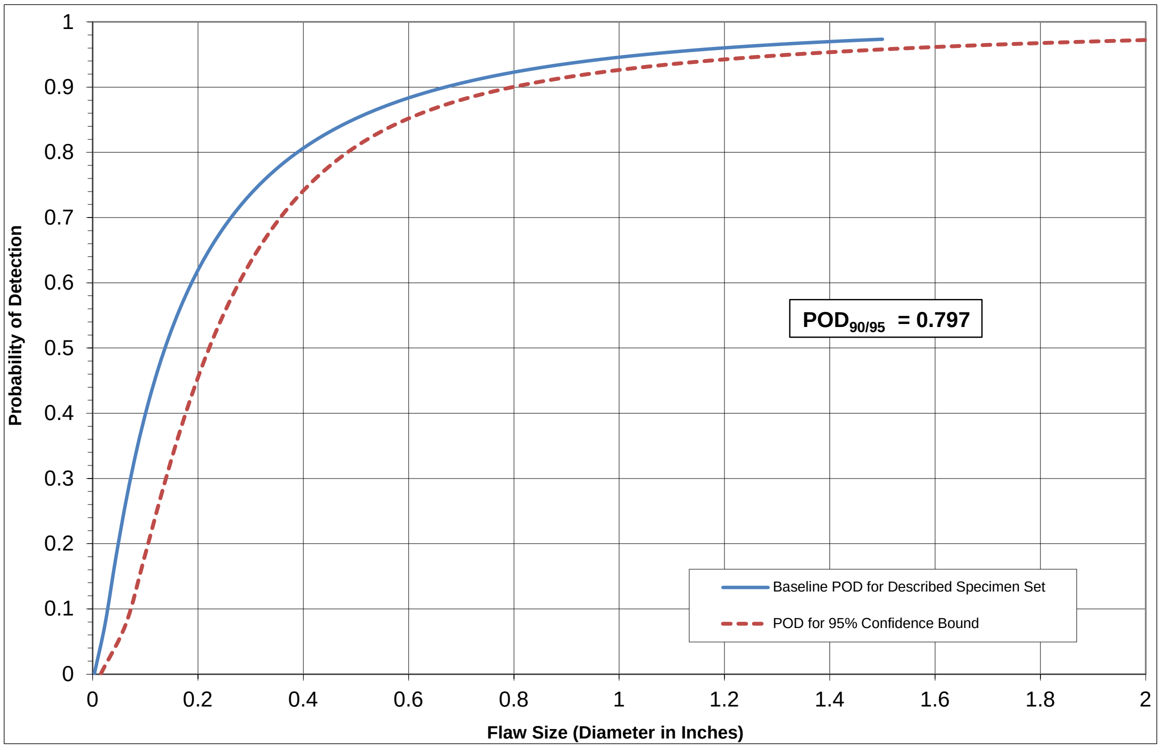

Figure 68. Cumulative POD curve for the 12–20 ply specimen set for flaws in the 12-ply CT regions only; all inspectors—PE UT method

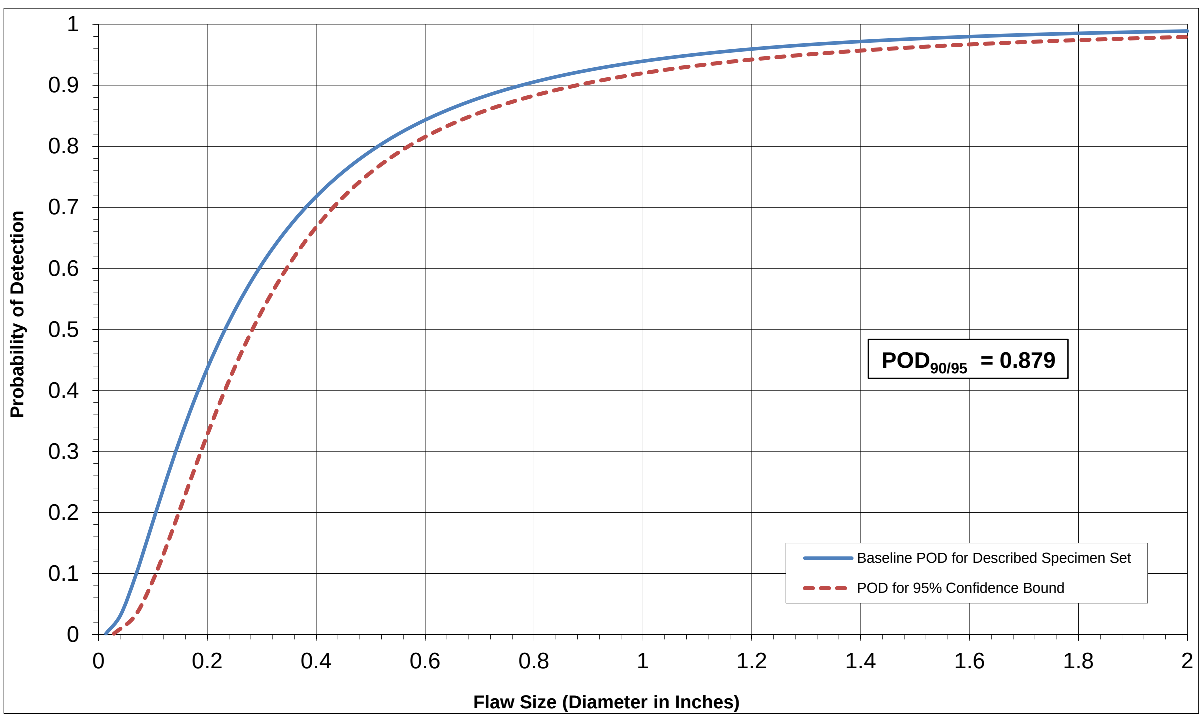

Figure 69. Cumulative POD curve for the 12-20 ply specimen set for flaws in the 20-ply CT regions only; all inspectors—PE UT method

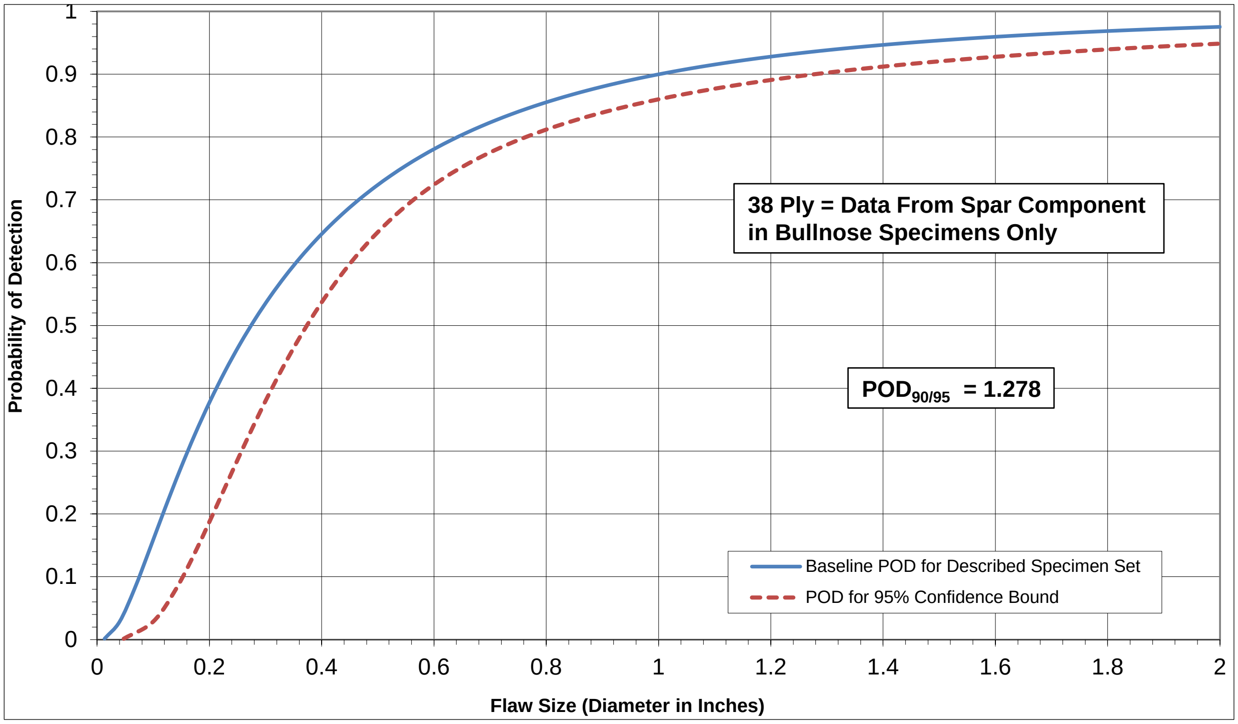

Figure 70. Cumulative POD curve for the 12–20 ply specimen set for flaws in the 38-ply CT regions only; all inspectors—PE UT method

A complementary set of results were determined using the inspection results from only the CG construction scenarios. Figure 71 shows the POD curve representing inspectors' performance in the CG regions only. The CG regions are defined as regions containing a taper, substructure (secondarily bonded), curved portion, fasteners, or laminate over honeycomb. The $POD_{[90/95]}$ = 1.493″ for the CG regions is a poorer performance than the cumulative $POD_{[90/95]}$ = 1.29″ when the CT regions are also included in the calculation. This shows that the CG regions are a major factor in driving up the overall cumulative 12–20 ply POD value. Figures 72–74 show the CG results broken down further into specific attributes: tapered regions only, curved surface regions only, and laminate over honeycomb regions only. The $POD_{[90/95]}$ values for each of these scenarios are lower than the overall cumulative 12–20 ply POD. Thus, these construction attributes are not deemed to be major inspection impediments. However, the overall CG POD, which includes the tapered, curved surface, and laminate over honeycomb regions, is higher than the cumulative 12–20 ply POD. This indicates that the final two components of the CG set—flaws in fastener regions and flaws in substructure regions—are the factors that caused the POD for CG inspections to be high. It should be noted that POD convergence could not be obtained for the fastener regions or the substructure regions because of low flaw detection levels in these regions. Thus, the presence of substructures and fasteners in the composite construction were determined to be major inspection impediments.

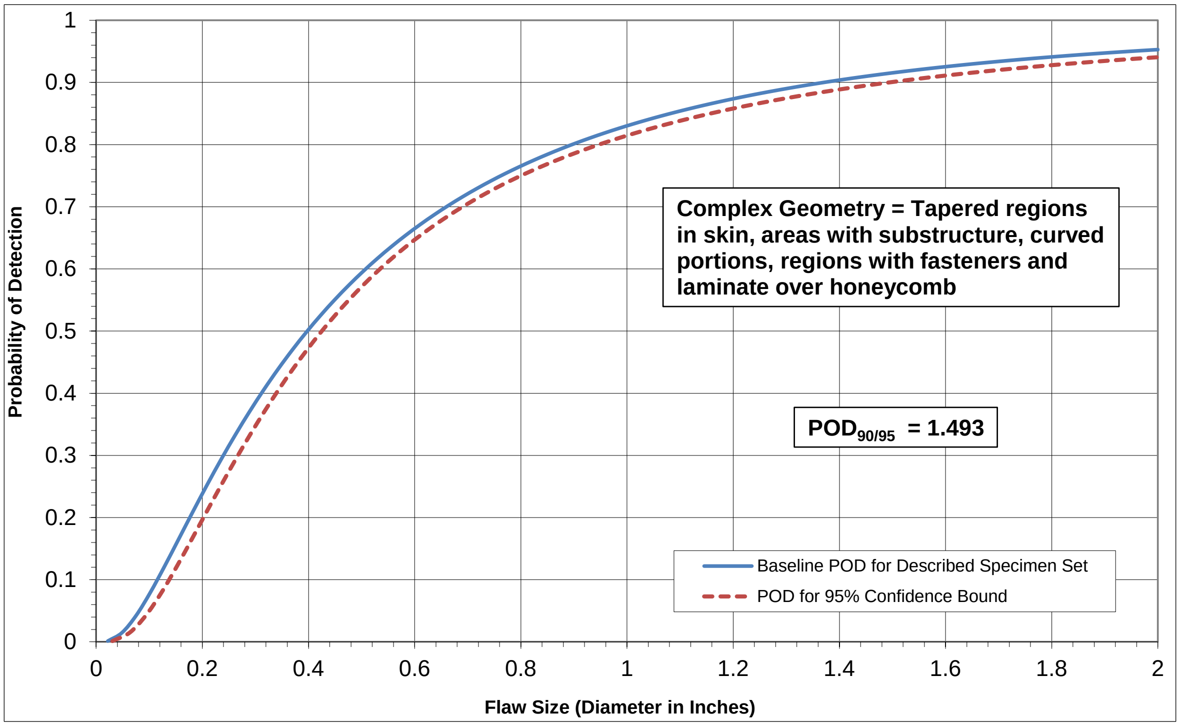

Figure 71. Cumulative POD curve for the 12–20 ply specimen set for flaws in the CG regions only; all inspectors—PE UT method

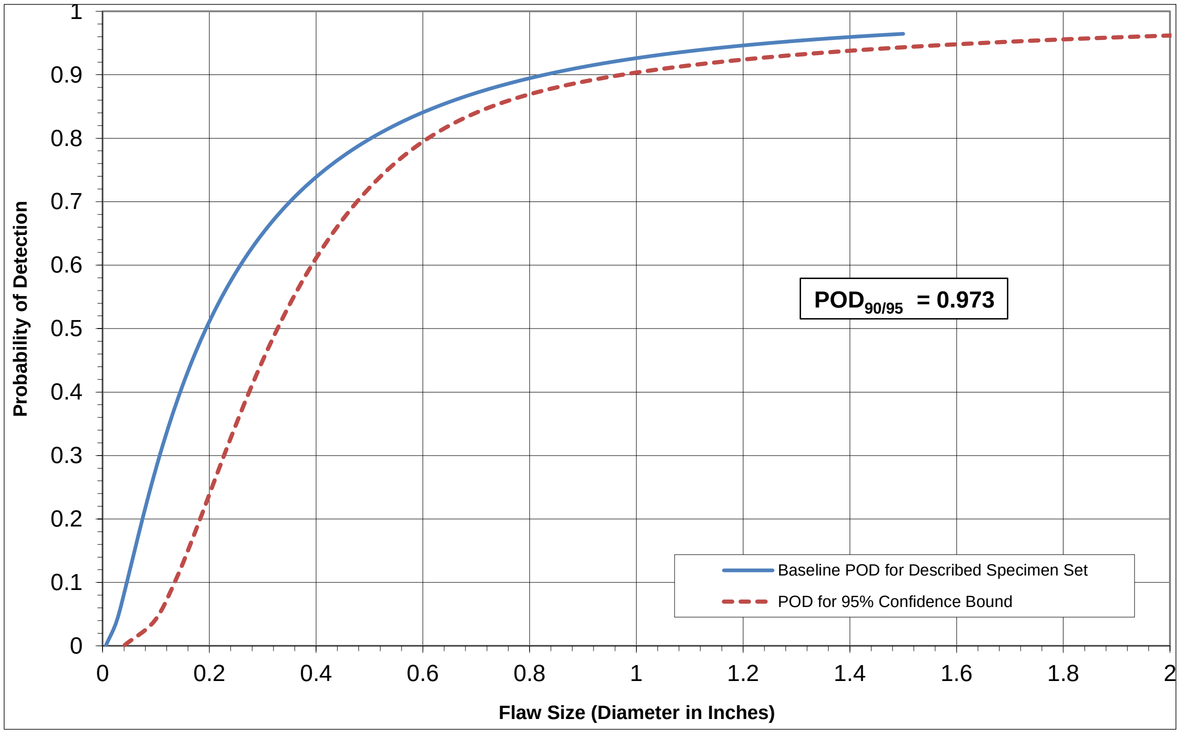

Figure 72. Cumulative POD curve for the 12–20 ply specimen set for flaws in the tapered regions only; all inspectors—PE UT method

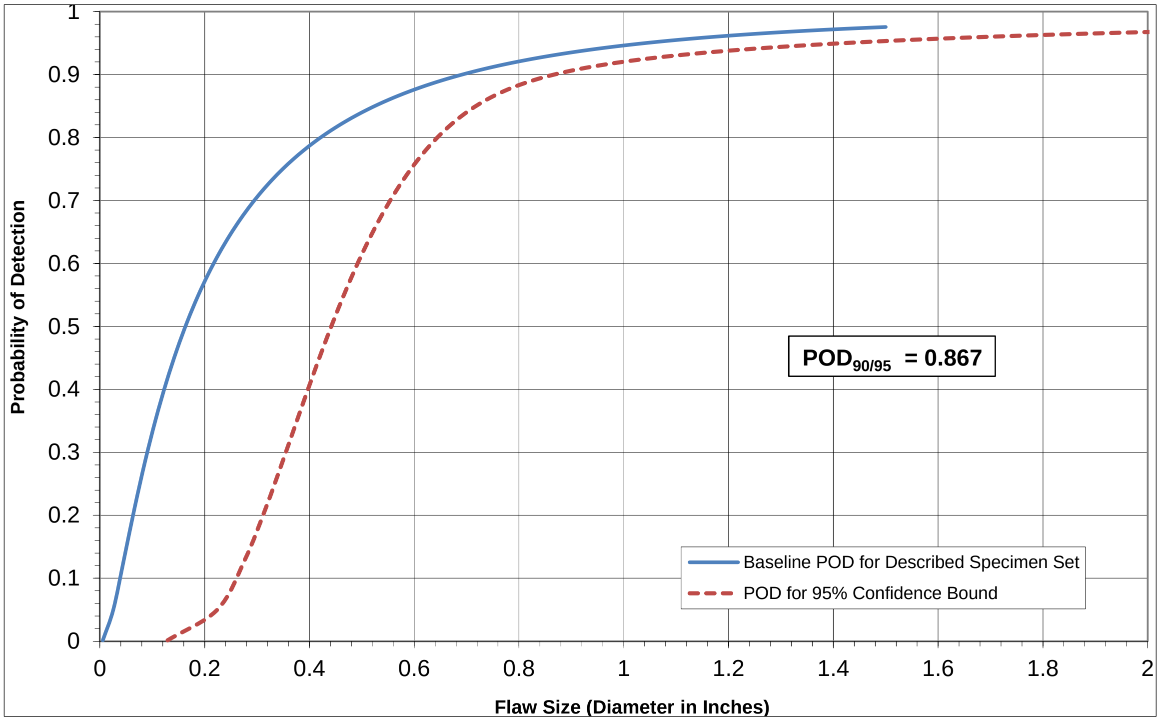

Figure 73. Cumulative POD curve for the 12–20 ply specimen set for flaws in the curved surface regions only; all inspectors—PE UT method

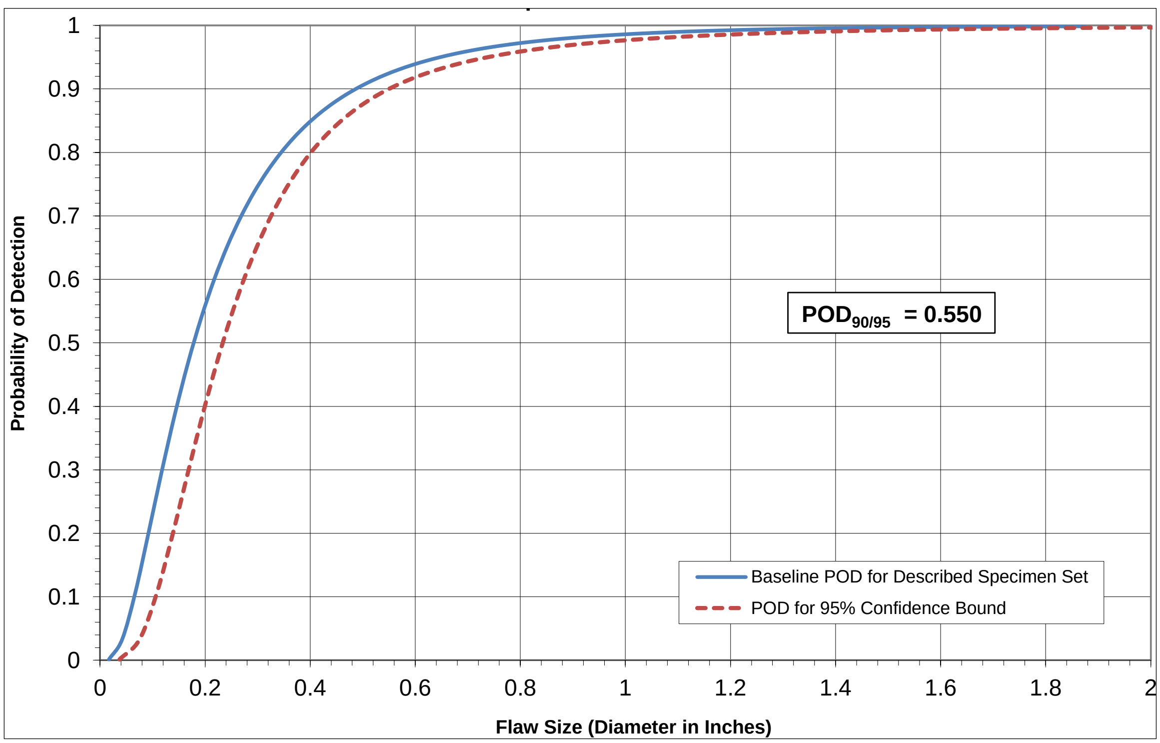

Figure 74. Cumulative POD curve for the 12–20 ply specimen set for flaws in the laminate over honeycomb regions only; all inspectors—PE UT method

Cumulative flaw detection percentages in the substructure and fastener regions are summarized in figures 75 and 76. Only 25% of the flaws in the fastener regions were detected and only 51% of the flaws were detected in the substructure regions. The fact that 43% of all the flaws in the CG dataset are in the substructure and fastener regions should be considered; it can then be seen how poor performance in these two construction areas will greatly affect the overall flaw-detection performance in the CG set. The substructure and fastener regions pinpoint the largest contributing factor in the CG POD value as well as the overall cumulative POD value. Improved flaw detection in these areas, through the use of better inspection techniques and possibly specialized training, could significantly reduce the overall cumulative POD value. One consideration for low detection in the fastener regions could be the large impedance mismatch between the carbon laminate and the sealant used in the fastener regions. A consideration in the substructure regions is that all of the substructure elements were secondarily bonded in the 12–20 ply specimen set. This made it more difficult to penetrate into the substructure—through the adhesive bond—with PE UT and correctly interpret the UT signals.

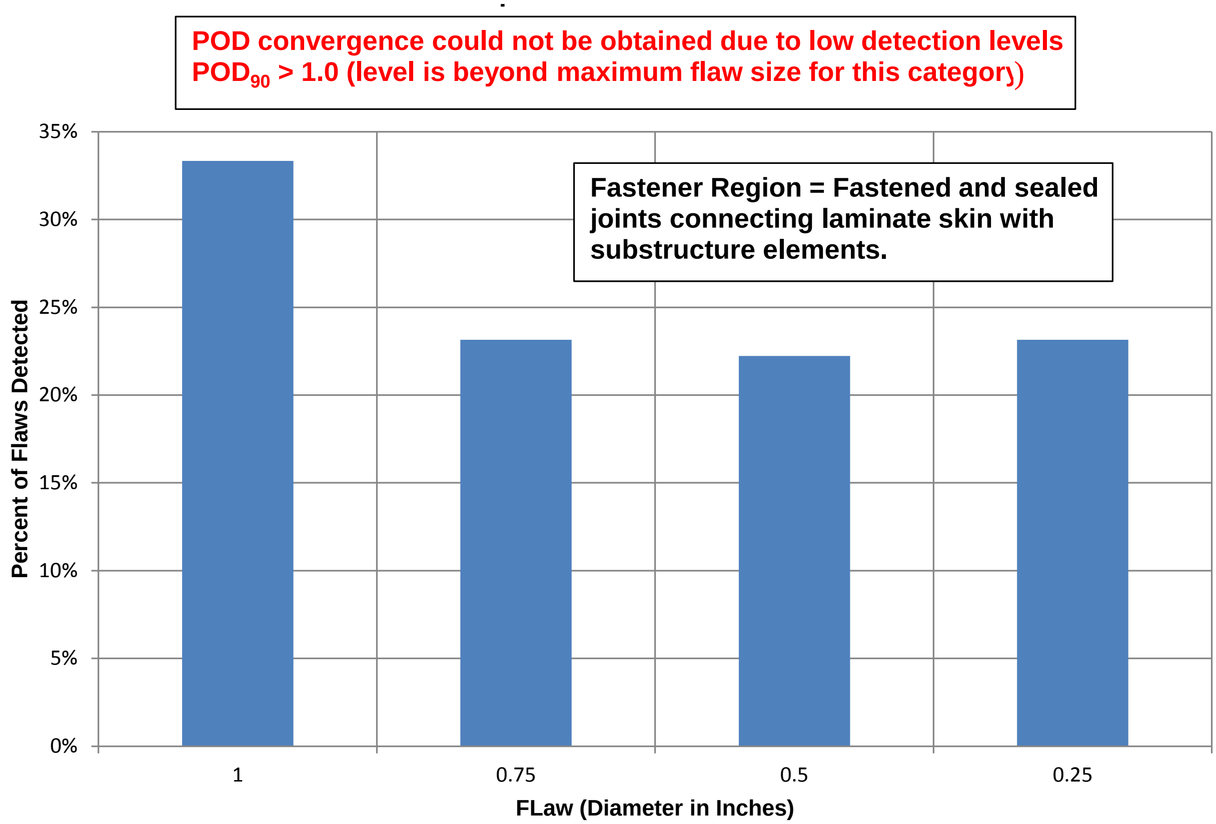

Flaws in Regions with Fasteners Only	
Percent of All Flaws Detected (297 Total Flaws)	24.92%
Percent of All 1.00" Flaws Detected	33.33%
Percent of All 0.75" Flaws Detected	23.15%
Percent of All 0.50" Flaws Detected	22.22%
Percent of All 0.25" Flaws Detected	23.15%

Figure 75. Cumulative flaw detection chart along with tabulated values for the 12–20 ply specimen set for flaws in regions with fasteners only (297 total flaws); all inspectors—PE UT method

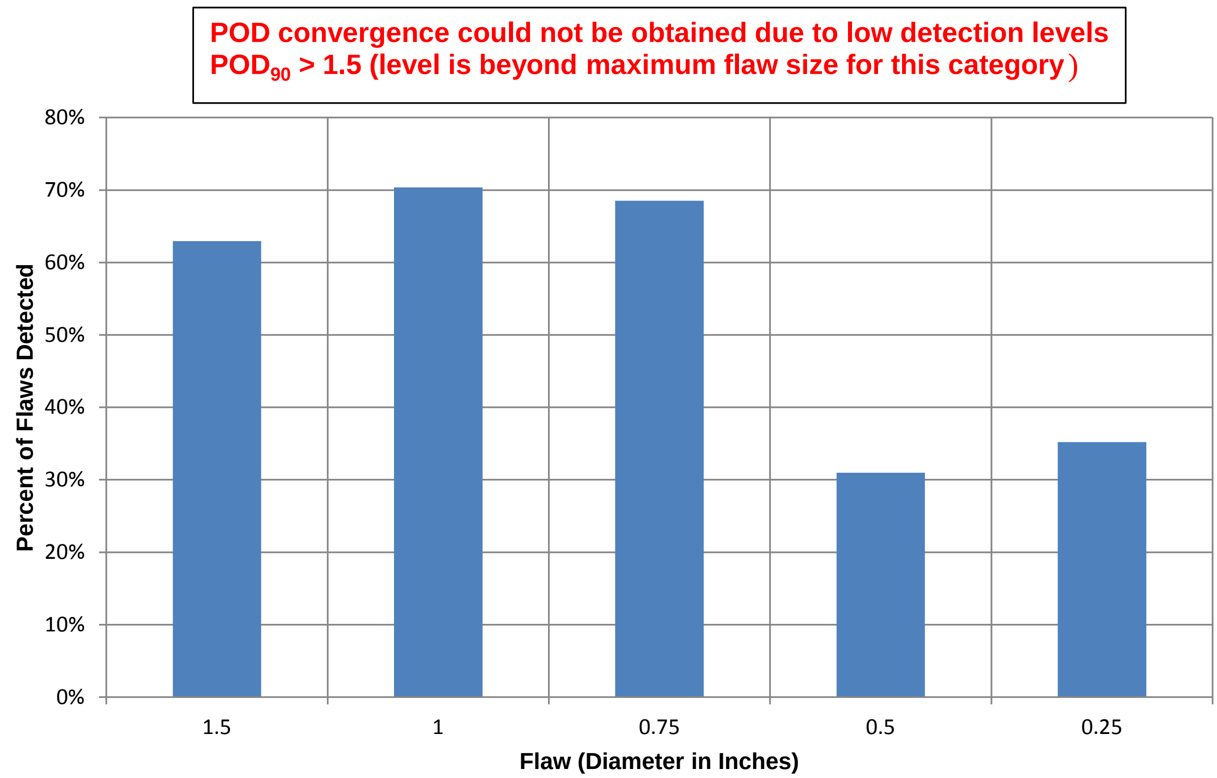

Flaws in Substructure Regions Only	
Percent of All Flaws Detected (729 Total Flaws)	51.03%
Percent of All 1.50" Flaws Detected	62.96%
Percent of All 1.00" Flaws Detected	70.37%
Percent of All 0.75" Flaws Detected	68.52%
Percent of All 0.50" Flaws Detected	30.98%
Percent of All 0.25" Flaws Detected	35.19%

Figure 76. Cumulative flaw detection chart along with tabulated values for the 12–20 ply specimen set for flaws in substructure regions only (729 total flaws); all inspectors—PE UT method

The experiment monitors recorded the various methods that inspectors used to ensure the inspection area was covered Monitors noted whether 100% surface coverage was achieved. Some inspectors covered the inspection area with their UT transducers using a pure freehand approach (i.e., no guides or markings on the panels). Some inspectors divided the inspection surface into quadrants to reduce freehand coverage errors. Some inspectors used a series of tick marks, often placed at 0.5″ or 1″ intervals, to divide the inspection surface into a number of rows and columns. Some inspectors used flexible straight edges to guide their transducer movement. The different surface coverage techniques that were observed fall into four categories. The POD results produced by each of these inspection coverage methods were calculated separately and are shown in figure 77 along with the corresponding $POD_{[90/95]}$ values. Figures 78–81 show the individual POD curves for each coverage technique. The method that produced the lowest (best) POD level was that for which inspectors made tick marks for spacing and used a straight edge on all panels throughout the experiment (seven inspectors). This produced a $POD_{[90/95]}$ = 1.055″, which is an 18% improvement compared to the overall cumulative 12–20 ply $POD_{[90/95]}$ value of 1.29″. The second-best performing coverage method was that in which inspectors used a straight edge on all panels throughout the experiment (seven inspectors), achieving a $POD_{[90/95]}$ = 1.101″ diameter flaw. This produced a 14% improvement compared to the overall cumulative 12–20 ply $POD_{[90/95]}$ value. The third-best performing coverage method was that in which inspectors started the experiment using a straight edge, but, at some point during the experiment, switched to freehand (eight inspectors). This method produced a $POD_{[90/95]}$ = 1.421″, which is a 10% decrease in performance compared to the overall cumulative 12–20 ply $POD_{[90/95]}$ value. The point at which an inspector switched to freehand was not documented, but it was observed and noted during the experiment that the inspector switched to freehand coverage after having started the experiment using a straight edge. The poorest performing coverage method was that in which inspectors used the freehand method on all panels throughout the experiment (five inspectors). This produced a $POD_{[90/95]}$ = 2.390″, which is an 86% decrease in performance compared to the overall cumulative 12–20 ply $POD_{[90/95]}$ value. The purpose for showing the data in this manner is to highlight the importance of proper scanning techniques and the effect that it can have on the overall inspection results. It can be seen that the effect is dramatic and often it has nothing to do with the capability of the NDI equipment.

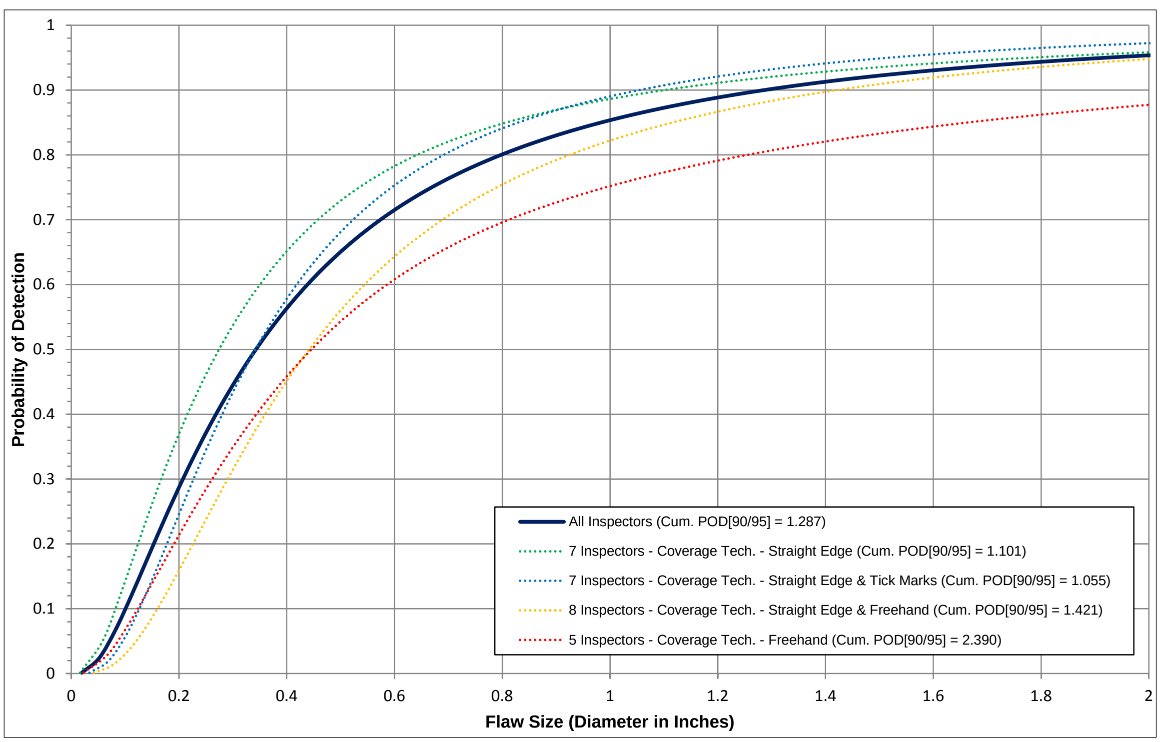

Figure 77. Cumulative POD curve comparison of different surface coverage techniques for the 12–20 ply specimen set for all flaws in the CT and CG regions; all inspectors (27)—PE UT method

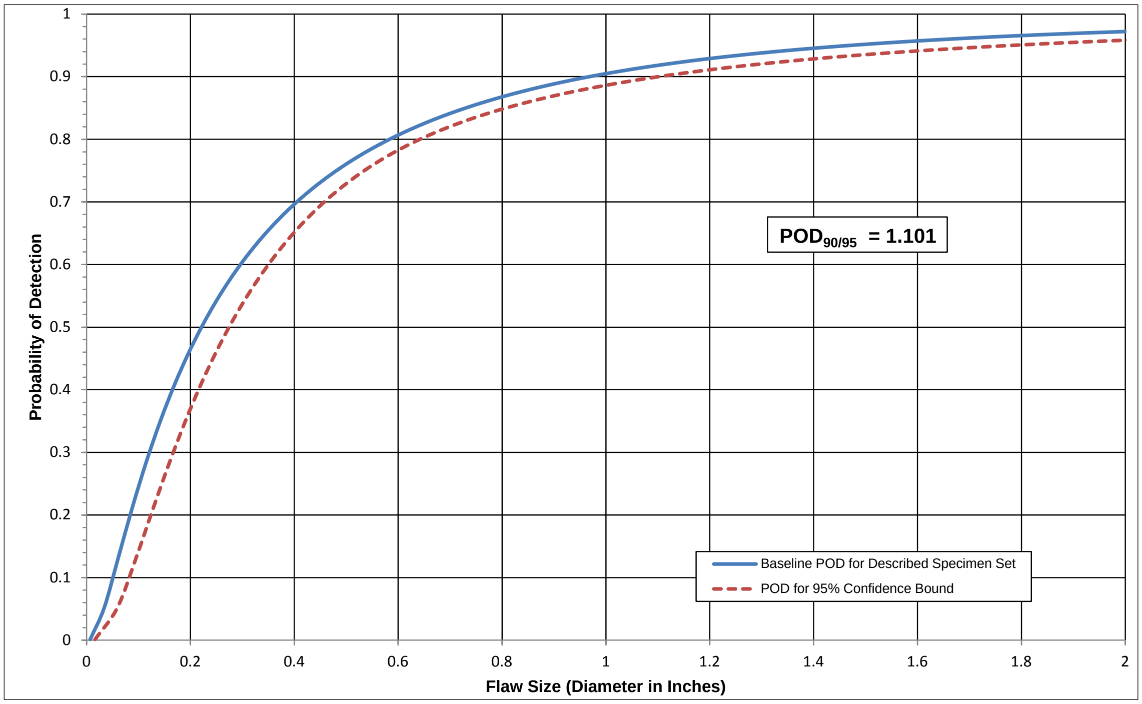

Figure 78. Cumulative POD curve for the straight edge coverage technique (seven inspectors) for the 12–20 ply specimen set for all flaws in the CT and CG regions—PE UT method

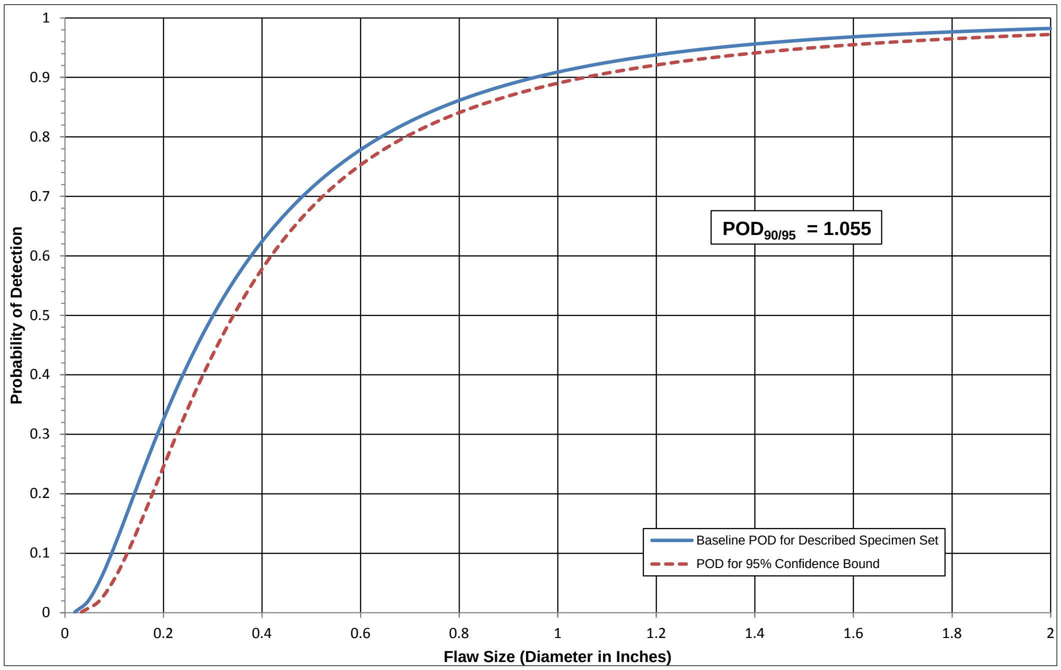

Figure 79. Cumulative POD curve for the straight edge and tick marks (indexing) coverage technique (seven inspectors) for the 12–20 ply specimen set for all flaws in the CT and CG regions—PE UT method

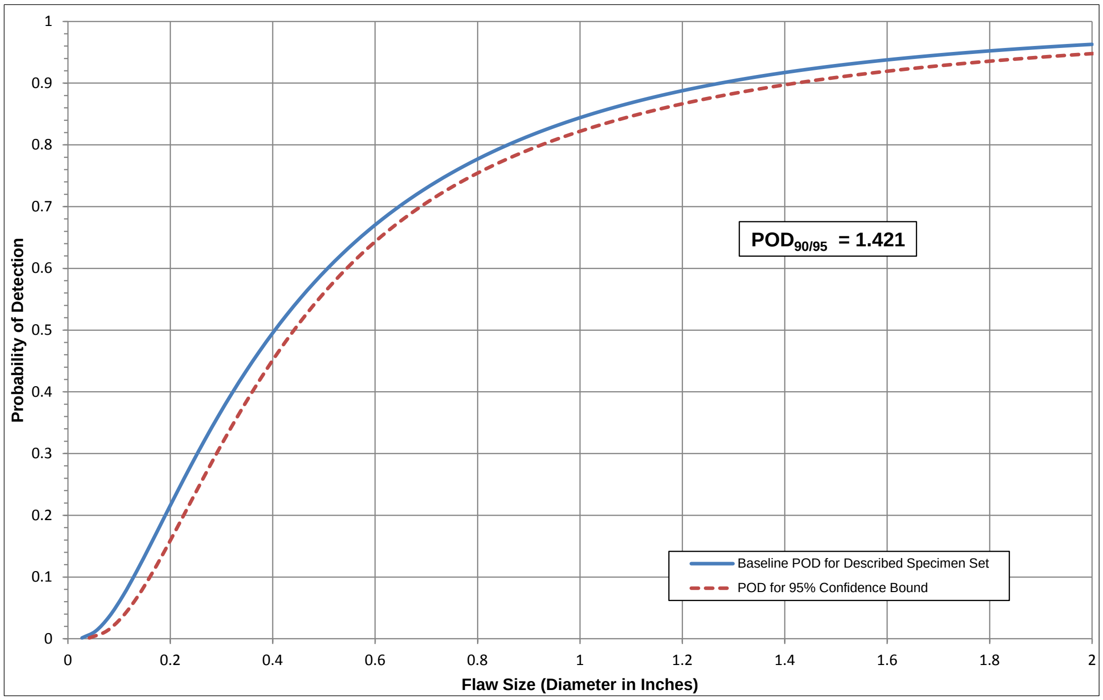

Figure 80. Cumulative POD curve for the straight edge and freehand coverage technique (eight inspectors) for the 12–20 ply specimen set for all flaws in the CT and CG regions—PE UT method

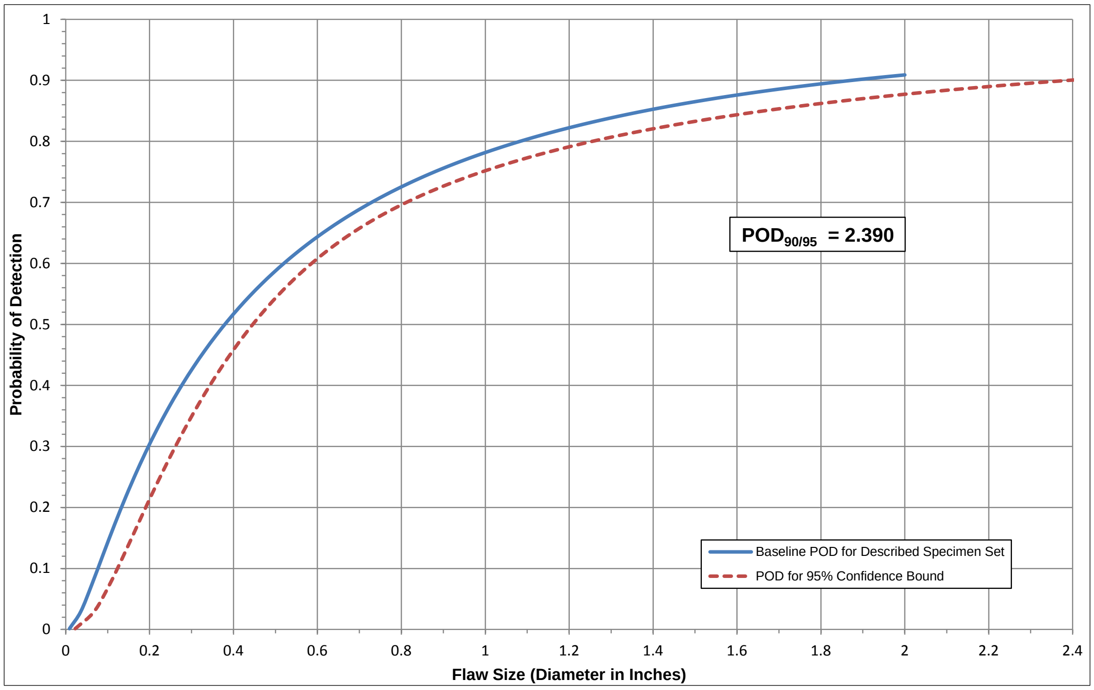

Figure 81. Cumulative POD curve for the freehand coverage technique (five inspectors) for the 12–20 ply specimen set for all flaws in the CT and CG regions—PE UT method

The summary of all $POD_{[90/95]}$ values for the 12–20 ply thin laminate experiment is presented in table 6.

Table 6. Cumulative POD results table for the 12–20 ply specimen set

Cumulative POD Results Table, 12–20 Ply Specimen Set	
Condition	POD[90/95]
All Flaws – All Regions – All 27 Inspectors	1.287
All Flaws – All Regions – 23 Inspectors, 2 High & 2 Low Removed	1.278
All Flaws – All Regions – 8 Inspectors Below POD[90] = 1.00 (30% of Inspectors)	0.787
All Flaws – All Regions – 19 Inspectors Below POD[90] = 1.35 (70% of Inspectors)	1.064
All Flaws – All Regions – 24 Inspectors Below POD[90] = 1.70 (89% of Inspectors)	1.191
All Flaws – All Regions – 7 Inspectors – Coverage Technique – Straight Edge	1.101
All Flaws – All Regions – 7 Inspectors – Coverage Technique – Straight Edge & Tick Marks	1.055
All Flaws – All Regions – 8 Inspectors – Coverage Technique – Straight Edge & Freehand	1.421
All Flaws – All Regions – 5 Inspectors – Coverage Technique – Freehand	2.390
Only Flaws in Constant Thickness Regions – All Inspectors	0.864
Only Flaws in 12-Ply Constant Thickness Regions – All Inspectors	0.797
Only Flaws in 20-Ply Constant Thickness Regions – All Inspectors	0.879
Only Flaws in 36-Ply Constant Thickness Regions – All Inspectors	1.278
Only Flaws in Complex Geometry Regions – All Inspectors	1.493
Only Flaws in Tapered Regions – All Inspectors	0.973
Only Flaws in Curved Surface Regions – All Inspectors	0.867
Only Flaws in Laminate Skin Over Honeycomb Regions – All Inspectors	0.550

In the Experimenter Information Packet (see appendix A) and during the Experiment Briefing (see appendix B), it was stated that “inspectors should use any positive indications to find flaws as small as 1/4″ in diameter.” A false call is defined as an inspector flaw indication in an area in which no flaw actually existed. However, there are manufacturing flaws that are not associated with the POD study, such as porosity. If an inspector made a call that correlated to an area of porosity, it was ignored and not deemed to be a false call.

6.1.3 False Calls

Table 7 summarizes the number of false calls made by each inspector for the 12–20 ply specimen set and lists the sizing category that incorporates each false call. The average number of false calls made was determined to be 4.4 false calls per inspector (34 ft^2 inspection area), with an average of one false call per 7.73 ft^2 of inspection area. Notice that the majority of false calls were made in the CG regions. Table 8 shows the false call data when false calls of less than 0.25 in^2 (i.e., very small items) were removed from the calculations. This table shows that the resulting average number of false calls was reduced to 2.4 false calls per inspector (34 $ft.^2$ inspection area) with an average of one false call per 14.17 ft^2 of inspection area. Thus, the overall false call rate was determined to be very low.

Table 7. Inspection false call table for the 12–20 ply specimen set; all inspectors—PE method

Inspection False Calls for 12-20 Ply Specimen Set – All Inspectors – Pulse Echo UT																													
Configuration/Sizing (in.^{2})	Insp. A	Insp. B	Insp. C	Insp. D	Insp. E	Insp. F	Insp. G	Insp. H	Insp. I	Insp. J	Insp. K	Insp. L	Insp. M	Insp. N	Insp. O	Insp. P	Insp. Q	Insp. R	Insp. S	Insp. T	Insp. U	Insp. V	Insp. W	Insp. X	Insp. Y	Insp. Z	Insp. AA	Total	Avg.
Constant Thickness (CT)																													
0–.25in^2	1	1	0	0	0	0	0	0	0	0	0	0	0	0	0	0	4	0	1	0	0	0	1	0	0	0	0	8	0.3
.26in^2–75in^2	0	0	0	0	0	0	0	0	0	1	0	0	0	0	0	0	0	0	0	0	0	0	0	0	0	0	0	1	0.0
76in^2–1.25in^2	0	0	0	0	0	0	0	0	0	0	0	0	0	0	0	0	0	0	0	0	0	0	0	1	0	0	0	1	0.0
1.26in^2–2.00in^2	0	0	0	0	0	0	0	0	0	0	0	0	0	0	0	0	0	0	0	0	0	0	0	0	0	0	0	0	0.0
>2.00in^2	0	0	0	0	0	0	0	0	0	0	0	0	0	0	1	0	0	0	0	0	0	0	0	0	0	0	0	1	0.0
CT Total	1	1	0	0	0	0	0	0	0	1	0	0	0	0	1	0	4	0	1	0	0	0	1	1	0	0	0	11	0.4
Complex Geometry (CG)																													
0–.25in^2	3	9	0	0	1	1	0	0	1	2	6	0	0	1	2	3	7	2	1	0	0	0	1	4	4	0	0	48	1.8
.26in^2–.75 in^2	3	1	0	1	0	0	0	0	1	3	0	0	0	5	1	0	2	3	5	3	0	0	2	0	1	0	0	31	1.1
.76 in^2–1.25 in^2	0	1	0	1	0	0	2	0	0	0	0	0	0	5	3	0	0	0	1	0	0	0	0	1	1	0	0	15	0.6
1.26 in^2–2.00 in^2	1	1	0	0	0	0	1	0	0	1	0	0	0	1	0	0	0	1	0	0	0	0	0	0	0	0	0	6	0.2
>2.00 in^2	0	0	0	0	0	2	3	0	0	0	0	0	0	1	3	0	0	0	0	0	0	0	0	0	0	0	0	9	0.3
CG Total	7	12	0	2	1	3	6	0	2	6	6	0	0	13	9	3	9	6	7	3	0	0	3	5	6	0	0	109	4.0
Total (All Flaws)	8	13	0	2	1	3	6	0	2	7	6	0	0	13	10	3	13	6	8	3	0	0	4	6	6	0	0	33	4.4
1 False Call on Average Per 7.73 ft^2 of Inspection Area																													

Table 8. Inspection false call table with false calls that were below 0.25 in^2 in size removed for the 12–20 ply specimen set; all inspectors—PE method

Inspection False Calls for 12-20 Ply Specimen Set – All Inspectors – Pulse Echo UT (False Calls that are below 0.25 in^2 in size have been removed)																													
Configuration/Sizing (in.^{2})	Insp. A	Insp. B	Insp. C	Insp. D	Insp. E	Insp. F	Insp. G	Insp. H	Insp. I	Insp. J	Insp. K	Insp. L	Insp. M	Insp. N	Insp. O	Insp. P	Insp. Q	Insp. R	Insp. S	Insp. T	Insp. U	Insp. V	Insp. W	Insp. X	Insp. Y	Insp. Z	Insp. AA	Total	Avg.
Constant Thickness (CT)																													
.26in^2–75in^2	0	0	0	0	0	0	0	0	0	1	0	0	0	0	0	0	0	0	0	0	0	0	0	0	0	0	0	1	0.0
76in^2–1.25in^2	0	0	0	0	0	0	0	0	0	0	0	0	0	0	0	0	0	0	0	0	0	0	0	1	0	0	0	1	0.0
1.26in^2–2.00in^2	0	0	0	0	0	0	0	0	0	0	0	0	0	0	0	0	0	0	0	0	0	0	0	0	0	0	0	0	0.0
>2.00in^2	0	0	0	0	0	0	0	0	0	0	0	0	0	0	1	0	0	0	0	0	0	0	0	0	0	0	0	0	0.0
CT Total	0	0	0	0	0	0	0	0	0	1	0	0	0	0	1	0	0	0	0	0	0	0	0	1	0	0	0	3	0.1
Complex Geometry (CG)																													
.26in^2–.75 in^2	3	1	0	1	0	0	0	0	1	3	0	0	0	5	1	0	2	3	5	3	0	0	2	0	1	0	0	31	1.1
.76 in^2–1.25 in^2	0	1	0	1	0	0	2	0	0	0	0	0	0	5	3	0	0	0	1	0	0	0	0	1	1	0	0	15	0.6
1.26 in^2–2.00 in^2	1	1	0	0	0	0	1	0	0	1	0	0	0	1	0	0	0	1	0	0	0	0	0	0	0	0	0	6	0.2
>2.00 in^2	0	0	0	0	0	2	3	0	0	0	0	0	0	1	3	0	0	0	0	0	0	0	0	0	0	0	0	9	0.3
CG Total	4	3	0	2	0	2	6	0	1	4	0	0	0	12	7	0	2	4	6	3	0	0	2	1	2	0	0	61	2.3
Total (All Flaws)	4	3	0	2	0	2	6	0	1	5	0	0	0	12	8	0	2	4	6	3	0	0	2	2	2	0	0	17	2.4
1 False Call on Average Per 14.17 ft^2 of Inspection Area																													

6.1.4 Inspection Time

Another critical part of the inspection process is how long it takes an inspector to scan a defined area. Table 9 shows the time it took for each inspector to scan each panel and their total inspection time. The average total inspection time for the 12–20 ply specimen set was just under 15 hours, which produced an average inspection coverage rate of 2.27 ft^2/hr. The lowest (quickest) total inspection time was under 10 hours, with an average inspection coverage rate of 3.48 ft^2/hr. The highest (slowest) total inspection time was just under 22 hours, with an average inspection coverage rate of 1.55 ft^2/hr.

Figure 82 shows the effect of total inspector time on the resulting inspector's $POD_{[90]}$ value. Even though there were a few inspectors with very quick inspection times and low POD values, the trend line in this scatter diagram indicates that a fast inspection time leads to a higher POD value and that longer inspection times can lead to slight improvements in POD. The scatter diagram in figure 83 shows the effect of total inspector time on the false call rate. The trend line here suggests that the faster inspection times lead to fewer false calls. However, the false call rate in this experiment was so low that this change only represents a very small shift in the total false calls. Figure 84 is a scatter diagram showing the effect of inspector $POD_{[90]}$ values on the inspector false calls made. The trend line in this diagram shows essentially no change in false calls over the range of POD values obtained.

Table 9. Experiment timing summary table for the 12–20 ply specimen set; all inspectors—PE UT method

Experiment Timing Summary 12-20 Ply specimen Set – All Inspectors – Pulse Echo UT												
	Specimen CT1-A	Specimen CT1-B	Specimen CT2-A	Specimen CT2-B	Specimen ST1U-A	Specimen ST1L-A	Specimen ST2U-A	Specimen ST2L-A	Specimen BN 1	Specimen BN 2	Specimen BN 3	Total Insp. Time (hr:min)
Inspector A	1:15	0:44	0:35	1:03	1:09	1:53	1:03	1:39	4:13	2:23	3:14	19:11
Inspector B	0:37	0:29	0:44	0:54	2:49	1:14	1:29	0:56	2:59	3:26	3:14	18:51
Inspector C	0:38	0:43	0:54	0:54	1:07	1:02	1:09	0:53	1:58	2:29	2:37	14:24
Inspector D	1:21	0:44	0:26	1:09	1:37	1:58	1:57	1:56	2:37	2:19	1:53	17:57
Inspector E	1:04	1:10	0:57	1:11	1:03	0:23	2:16	1:06	3:02	0:59	1:11	14:22
Inspector F	0:50	1:20	1:15	1:05	3:05	1:40	2:20	1:50	2:40	1:35	1:50	19:30
Inspector G	1:20	0:51	0:54	1:20	1:41	1:25	1:09	1:12	3:35	1:51	2:14	17:32
Inspector H	0:41	0:30	0:36	0:25	1:54	0:59	0:55	1:17	1:27	2:06	1:21	12:11
Inspector I	0:50	0:34	0:35	0:45	0:54	1:06	1:34	1:11	2:45	1:12	2:06	13:32
Inspector J	1:01	0:52	0:58	0:50	2:05	1:39	1:41	1:51	2:52	2:07	2:08	18:04
Inspector K	1:11	1:12	0:42	1:02	2:36	2:05	2:10	3:04	3:13	2:22	2:22	21:59
Inspector L	1:18	0:41	0:41	0:55	2:33	1:28	1:21	1:29	1:28	1:52	1:36	15:22
Inspector M	0:36	0:24	0:26	0:31	1:08	1:12	1:35	1:38	2:05	1:53	1:39	13:07
Inspector N	1:13	1:00	0:45	0:34	1:47	1:21	1:45	1:17	1:44	1:41	2:34	15:41
Inspector O	0:40	1:05	0:35	0:38	0:57	1:34	1:02	2:15	1:32	1:54	1:30	13:42
Inspector P	0:31	0:22	0:36	0:36	1:45	0:46	0:59	1:04	1:50	1:45	2:16	12:30
Inspector Q	0:58	0:40	1:07	0:43	1:08	1:14	0:50	1:16	1:32	2:13	1:50	13:31
Inspector R	1:30	1:28	1:14	0:51	1:40	1:22	1:31	1:24	1:09	1:34	2:05	15:48
Inspector S	0:31	0:23	0:16	0:22	0:42	0:38	0:42	1:14	1:18	1:33	2:07	9:46
Inspector T	0:47	0:31	0:33	0:21	1:15	0:59	1:13	0:54	1:43	1:21	0:54	10:31
Inspector U	0:52	0:34	0:34	0:35	1:13	0:55	1:35	1:23	1:22	1:38	1:20	12:01
Inspector V	0:29	0:26	0:31	0:28	1:05	1:01	1:07	1:04	2:47	1:33	1:49	12:20
Inspector W	0:44	0:46	0:39	0:36	0:43	1:00	0:52	0:47	3:08	2:31	3:56	15:42
Inspector X	0:38	0:30	0:31	0:35	1:46	1:42	2:10	1:48	2:30	1:37	2:00	15:47
Inspector Y	0:34	0:26	0:21	0:44	1:00	1:19	1:13	1:29	1:09	1:24	2:21	12:00
Inspector Z	1:22	0:25	0:48	0:34	1:19	1:17	3:34	1:35	1:31	1:13	1:31	15:09
Inspector AA	0:49	0:52	0:54	0:52	1:19	1:01	0:53	1:19	2:09	1:22	1:43	13:13
Ave. Insp. Time (hr:min)	0:54	0:43	0:42	0:45	1:31	1:16	1:29	1:26	2:14	1:50	2:03	14:57
Average Inspection Coverage Rate = 2.27 ft^2/hr												

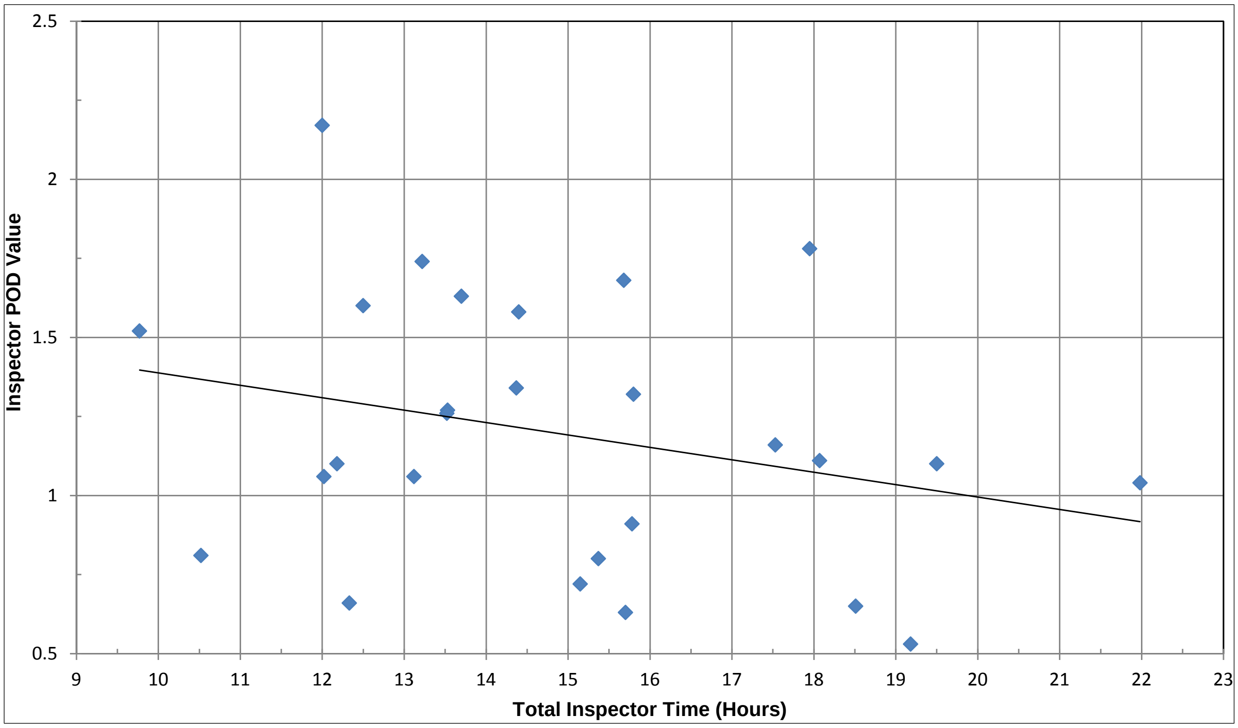

Figure 82. Scatter diagram showing effect of total inspector time on inspector POD_{90} values for the 12–20 ply specimen set; all inspectors—PE UT method

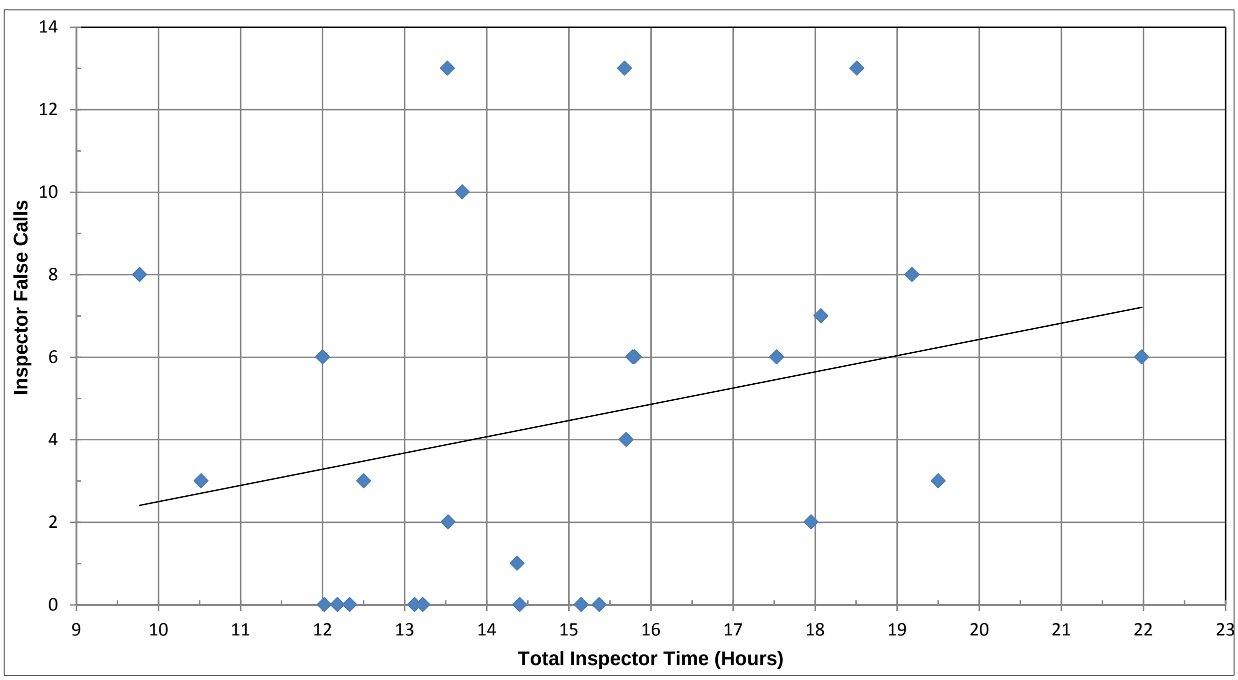

Figure 83. Scatter diagram showing effect of total inspector time on inspector false calls for the 12–20 ply specimen set; all inspectors—PE UT method

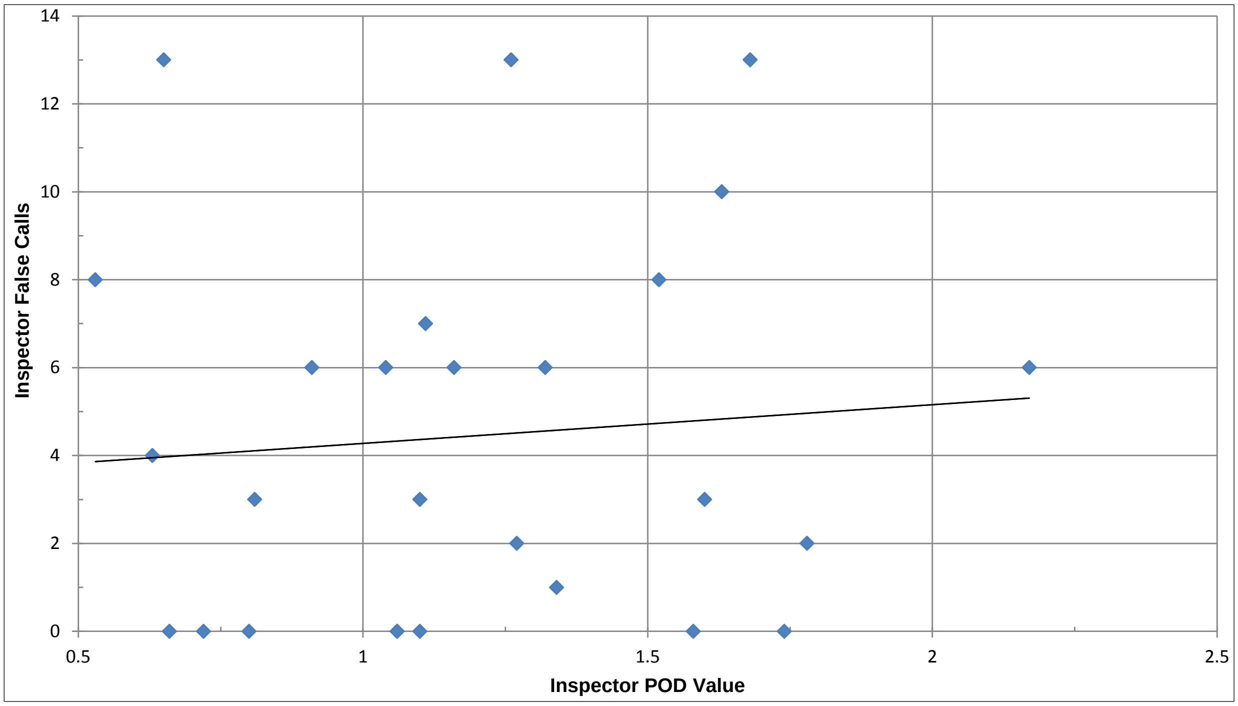

Figure 84. Scatter diagram showing effect of inspector POD_{90} values on inspector false calls for the 12–20 ply specimen set; all inspectors—PE UT method

6.1.5 Damage Sizing and Flaw Detection Percentage

Inspector flaw calls were also graded to evaluate the accuracy of each inspector's flaw sizing. The overall test results identified hits (calls with any amount of overlap between the call and the actual flaw location), misses (no call for an area of a known flaw), false calls (call with no overlap of a flaw), and the degree of overlap between experimenter calls and actual flaw areas (sizing performance). Figure 85 is a grading parameter drawing that shows how the accuracy of flaw coverage (overlap or sizing performance) was graded.

Table 10 summarizes the results for the overall flaw detection percentage and the associated accuracy in determining flaw size for the 12–20 ply specimen set (thin laminate experiment). This table includes combined data for all inspectors and all flaws in both the CT and CG regions. It should be noted that, for the 12–20 ply specimen set, 76% of all flaws were detected—or 2,766 of the total 3,645 flaws were detected. The flaw sizing performance shows that 38% of the detected flaws were sized properly (five categories for 100% coverage). Twenty-four percent of the flaws were sized in the 76–99% coverage category and 16% of the flaws were sized in the 51–75% coverage category. Thus, 78% of the detected flaws were sized with 51–100% accuracy. This table also shows a breakdown of percent detection based on flaw size. For example, 100% of the 2″ flaws were detected, meaning all 27 inspectors found every 2″ flaw in the 12–20 ply specimen set. On the smaller side, only 47% of the 0.25″ flaws were detected. Figure 86 shows the detection percentage based on flaw size in chart form.

Table 11 summarizes the results for the overall flaw detection percentage and the associated accuracy in determining flaw size for the CT regions only. In this case, 86% of all flaws were detected—or 1,109 of the 1,296 total flaws in the CT regions were detected. The flaw sizing performance shows that 34% of the detected flaws were sized properly (five categories for 100% coverage). The chart in figure 87 shows the detection percentage based on flaw size for the CT regions.

Table 12 summarizes the results for the overall flaw detection percentage and the associated accuracy in determining flaw size for the CG regions only. In this case, 76% of all flaws were detected—or 1,657 of the 2,349 total flaws in the CG regions were detected. The flaw sizing performance shows that 41% of the detected flaws were sized properly (five categories for 100% coverage). The chart in figure 88 shows the detection percentage based on flaw size.

Figures 89–91 show the individual inspector's flaw detection percentages broken down by all flaws in all regions, all flaws in the CT regions, and all flaws in the CG regions. These plots highlight the variation in performance over the full set of inspectors tested. This should be very representative of the aviation industry.

6.1.6 Profile of Inspectors Who Participated in the SLE

For all inspectors who participated in the 12–20 ply experiment, a breakdown of their NDI experience in years, PE UT NDI level, and NDI experience with composites can be seen in tables 13–15. Again, this shows that an adequate cross-section of inspectors was obtained so that these results provide an accurate view of the overall aviation industry.

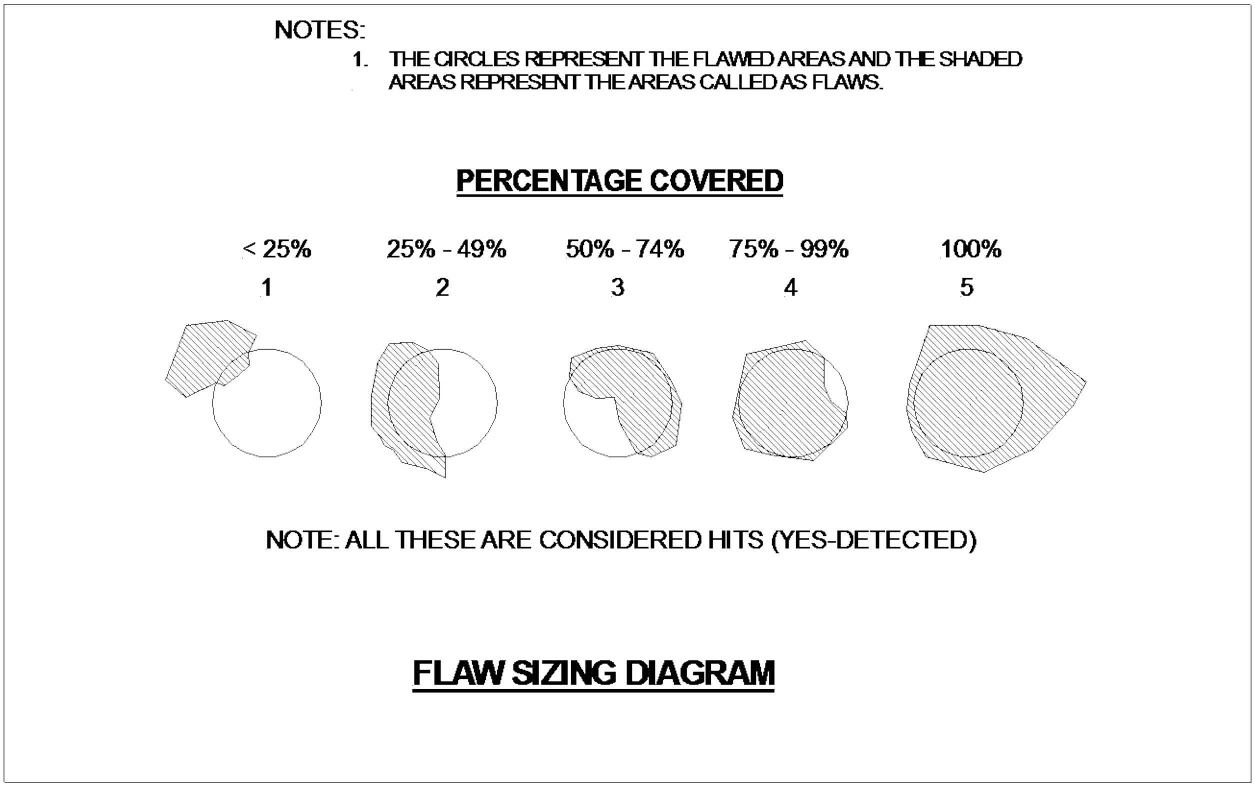

Figure 85. Flaw sizing diagram showing the sizing categories used for experimenter flaw calls with actual flaw information

Table 10. Tabulated results showing overall flaw detection percentage and accuracy in determining flaw size for the 12–20 ply specimen set for all flaws in the CT and CG regions; all inspectors—PE UT method

Overall Flaw Detection Percentage & Accuracy in Determining Flaw Size 12-20 Ply Specimen Set – All Inspectors – All Flaws (CT & CG)							
Accuracy in Sizing the Flaws That Were Detected (2766 Total Flaws Detected)						Flaw Detection Percentage (3645 Total Flaws)	
Flaw Size	5 (100%)	4 (76%-99%)	3 (51%-75%)	2 (25%-50%)	1 (< 25%)	Flaw Size	Percent Detected
0.25	57%	9%	7%	10%	16%	0.25	47%
0.50	40%	16%	12%	18%	15%	0.50	63%
0.75	42%	23%	16%	14%	5%	0.75	78%
1.00	35%	26%	19%	13%	6%	1.00	87%
1.50	29%	33%	23%	10%	6%	1.50	95%
2.00	40%	46%	11%	1%	2%	2.00	100%
Overall Sizing Performance	38%	24%	16%	13%	8%	Overall Flaw Detection	76%

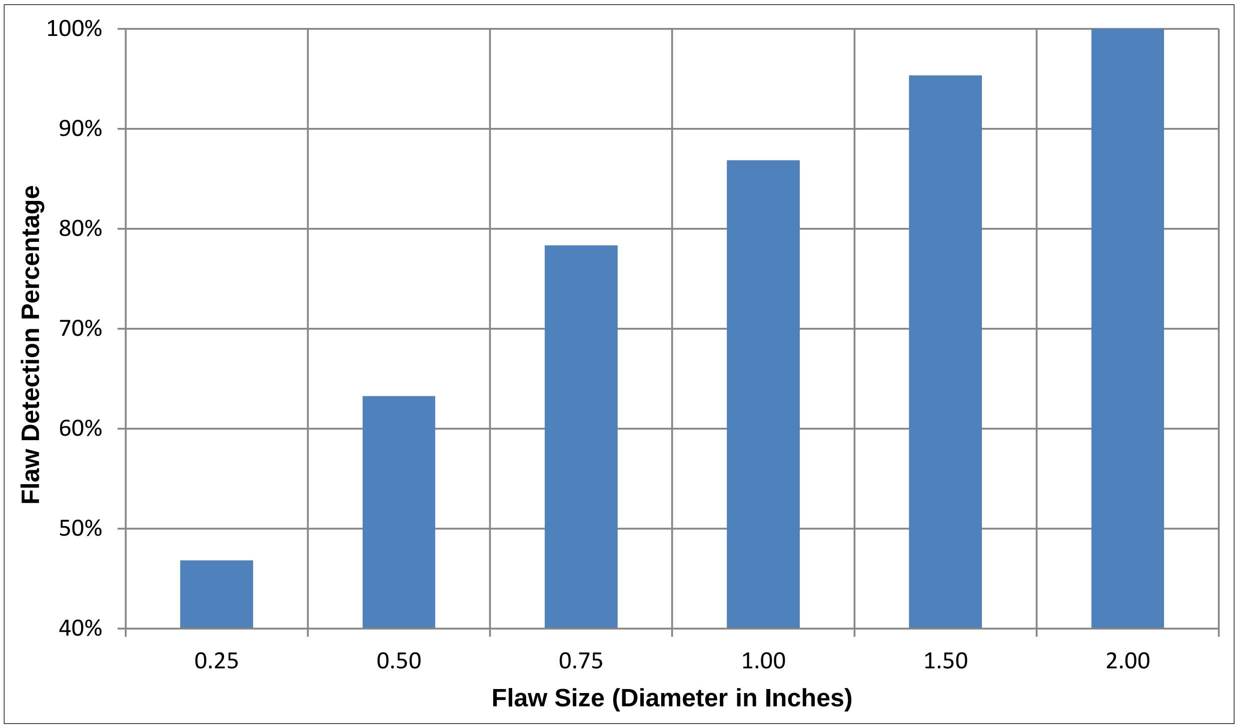

Figure 86. Overall flaw detection percentage chart for the 12–20 ply specimen set for all flaws in the CT and CG regions; all inspectors—PE UT method

Table 11. Tabulated results showing overall flaw detection percentage and accuracy in determining flaw size for the 12–20 ply specimen set for all flaws in the CT regions; all inspectors—PE UT method

Overall Flaw Detection Percentage & Accuracy in Determining Flaw Size 12-20 Ply Specimen Set – All Inspectors – All Constant Thickness (CT) Flaws							
Accuracy in Sizing the Flaws That Were Detected (1109 Total Flaws Detected)						Flaw Detection Percentage (1296 Total Flaws)	
Flaw Size	5 (100%)	4 (76%-99%)	3 (51%-75%)	2 (25%-50%)	1 (< 25%)	Flaw Size	Percent Detected
0.25	58%	6%	3%	15%	18%	0.25	60%
0.50	38%	17%	12%	19%	15%	0.50	78%
0.75	34%	23%	21%	16%	6%	0.75	87%
1.00	31%	29%	23%	11%	5%	1.00	94%
1.50	25%	38%	25%	9%	3%	1.50	98%
2.00	30%	54%	13%	2%	2%	2.00	100%
Overall Sizing Performance	34%	26%	18%	13%	8%	Overall Flaw Detection	86%

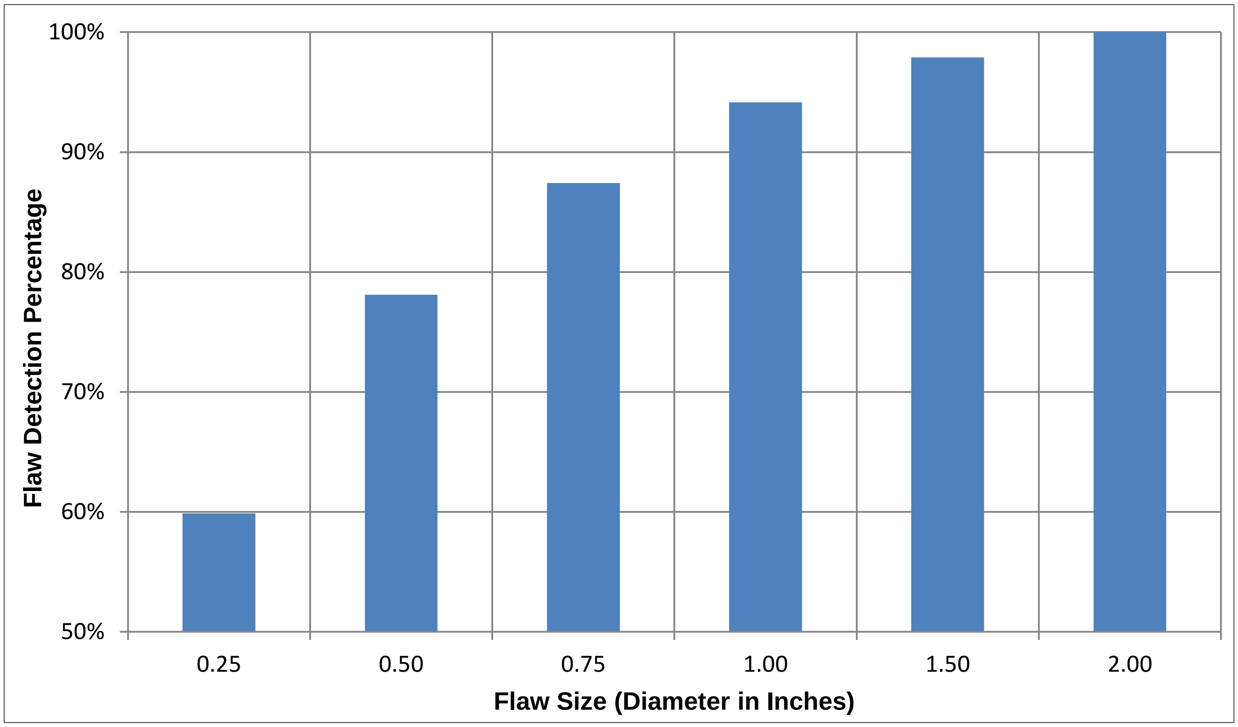

Figure 87. Overall flaw detection percentage chart for the 12–20 ply specimen set for all flaws in the CT regions; all inspectors—PE UT method

Table 12. Tabulated results showing overall flaw detection percentage and accuracy in determining flaw size for the 12–20 ply specimen set for all flaws in the CG regions; all inspectors—PE UT method

Overall Flaw Detection Percentage & Accuracy in Determining Flaw Size 12-20 Ply Specimen Set – All Inspectors – All Complex Geometry (CG) Flaws							
Accuracy in Sizing the Flaws That Were Detected (1657 Total Flaws Detected)						Flaw Detection Percentage (2349 Total Flaws)	
Flaw Size	5 (100%)	4 (76%-99%)	3 (51%-75%)	2 (25%-50%)	1 (< 25%)	Flaw Size	Percent Detected
0.25	56%	13%	13%	4%	15%	0.25	37%
0.50	42%	15%	11%	17%	15%	0.50	56%
0.75	46%	23%	14%	12%	5%	0.75	74%
1.00	37%	25%	16%	14%	7%	1.00	83%
1.50	33%	28%	21%	10%	8%	1.50	93%
2.00	59%	30%	7%	0%	4%	2.00	100%
Overall Sizing Performance	41%	22%	15%	13%	9%	Overall Flaw Detection	71%

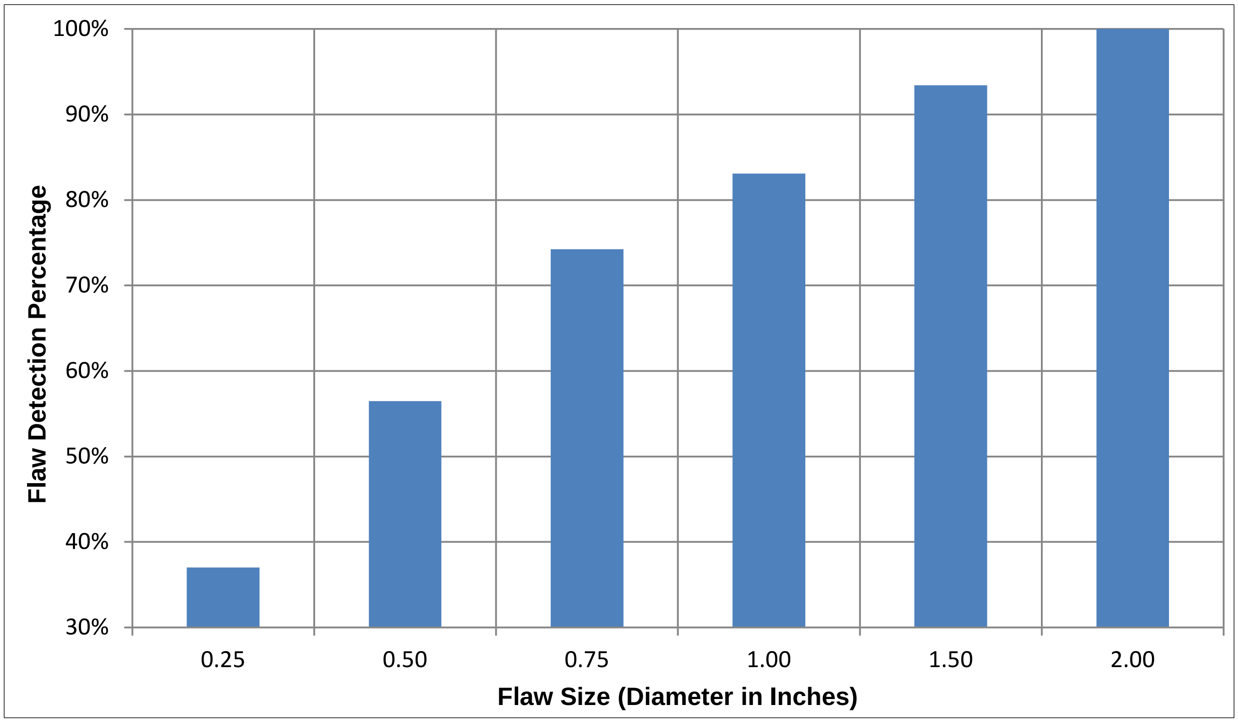

Figure 88. Overall flaw detection percentage chart for the 12–20 ply specimen set for all flaws in CG regions; all inspectors—PE UT method

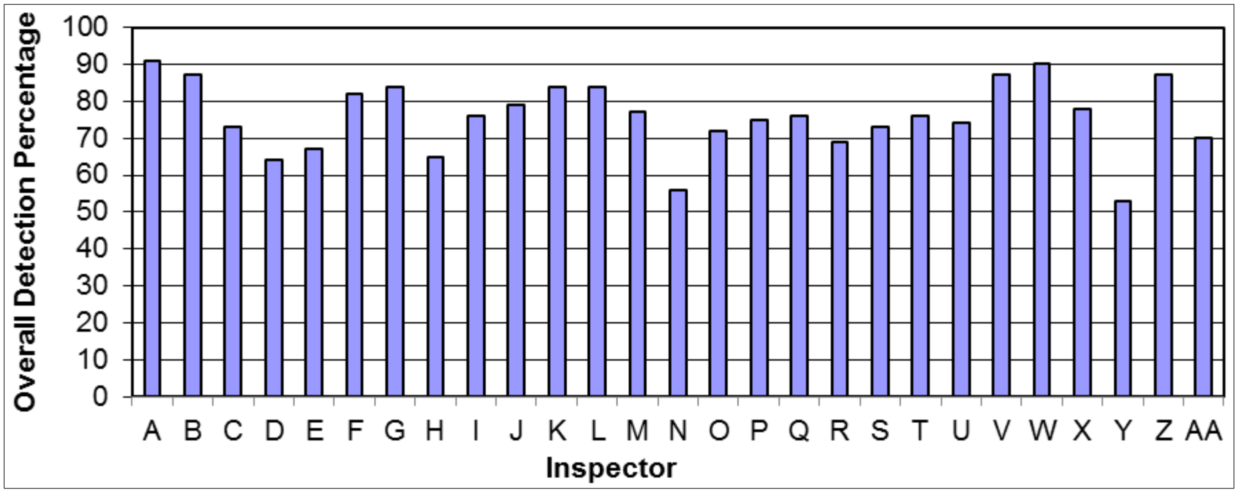

Figure 89. Inspector flaw detection percentage chart for the 12–20 ply specimen set for all flaws in the CT and CG regions—PE UT method

Figure 90. Inspector flaw detection percentage chart for the 12–20 ply specimen set for all flaws in the CT regions only—PE UT method

Figure 91. Inspector flaw detection percentage chart for the 12–20 ply specimen set for all flaws in the CG regions only—PE UT method

Table 13. Table showing inspector's reported NDI experience level in years (12–20 ply specimen set—PE UT method)

12-20 Inspector Reported Experience Level – Pulse Echo UT	
Years of NDI Experience	No. of Inspectors
1-3	2
4-8	8
9-12	4
13-16	3
17-20	4
21-24	1
25 or Greater	5

Table 14. Table showing inspector's reported PE UT NDI level (12–20 ply specimen set—PE UT method)

12-20 Inspector Reported NDI Level Pulse Echo UT	
NDI Level	No. of Inspectors
I	4
II	18
III	5

Table 15. Table showing inspector's reported experience with composites in years (12–20 ply specimen set—PE UT method)

12-20 Inspector Reported Experience Level – Composites	
Years of NDI Experience	No. of Inspectors
Trained, No Exp.	4
0	4
1-3	6
4-8	5
9-12	3
13-16	4
17-20	1

6.2 INSPECTION PERFORMANCE RESULTS FOR THE 20–32 PLY THICK LAMINATE EXPERIMENT

6.2.1 Overall Results

Figure 92 shows the spread of all the individual inspector $POD_{[90]}$ curves (dashed lines), compared to the cumulative $POD_{[90]}$ curve (solid line), for all 30 inspectors who participated in the 20–32 ply thick laminate experiment. These results were produced by considering all flaws in the CT and CG regions. The spread shows 19 inspectors with a $POD_{[90]}$ value less than the overall cumulative $POD_{[90]}$ = 0.77″ diameter flaw ($POD_{[90/95]}$ = 0.82″) and 11 inspectors with a $POD_{[90]}$ value higher than the overall cumulative $POD_{[90]}$ value. The variation within the experiment ranges from a $POD_{[90]}$ = 0.20″ diameter flaw for the best performing inspector to a $POD_{[90]}$ = 1.70″ diameter flaw for the worst performing inspector. The standard deviation for the inspector $POD_{[90]}$ dataset is 0.420″ diameter flaw. Figure 93 compares the maximum likelihood estimate ($POD_{[90]}$) to the POD curve that is calculated when a 90% flaw detection is combined with a 95% confidence bound ($POD_{[90/95]}$). This solid line in figure 93 provides the performance curve that the industry normally uses to measure the performance of NDI methods as used by representative inspectors. It can be seen in figure 93 that the overall cumulative $POD_{[90/95]}$ for all flaws in the thick laminate experiment (i.e., 20–32 ply skins plus substructure elements) was $POD_{[90/95]}$ = 0.82″ diameter flaw. When compared to the 12–20 ply thin laminate experiment, the $POD_{[90/95]}$ value for the 20–32 ply thick laminate experiment was better (lower). This was mainly because of the construction method used for this set of test panels, which involved a co-cured substructure bond line that is less attenuative, and includes less “noise” in the signals, than the secondarily bonded substructure (film adhesive bonding) that was used in most of the thin laminate experiment test specimens. Also, the test specimens for the thick laminate experiment did not contain curvature, fasteners, sealed joints, or skin over honeycomb substructure. This eliminated some of the deployment, human factor, and signal interpretation challenges that were present in the thin laminate experiment. Finally, it should be noted that the 20–32 ply specimen set includes 12 ft^2 of inspection area, whereas the 12–20 ply specimen set includes 34 ft^2 of inspection area. Thus, inspector fatigue is less of an issue in the thick laminate experiment.

Figure 94 shows a modified calculation of the $POD_{[90/95]}$ curve after the two highest (worst performing) and two lowest (best performing) inspector POD values were removed from the dataset. The difference between the two $POD_{[90/95]}$ values is less than 4%, which shows the consistency of the results for this specimen set and the robustness of the statistics in this experiment. The use of other performance brackets to assess POD are shown in figures 95–98. Performance brackets were used to place inspectors into groups and then calculate the resulting $POD_{[90/95]}$ for each performance bracket. These performance brackets used the inspectors who fell into the 40, 60, and 80 percentile categories. The inspectors who fell into the 40 percentile group (12 inspectors, each having a $POD_{[90]}$ less than 0.55″) produced a 42% improvement to $POD_{[90/95]}$ = 0.48″ diameter flaw value compared to the overall cumulative $POD_{[90/95]}$ = 0.82″ diameter flaw. The 60 percentile group (18 inspectors, each having a $POD_{[90]}$ less than 0.75″) produced a 34% improvement with a $POD_{[90/95]}$ = 0.54″ diameter flaw. The 80 percentile group (24 inspectors, each having a $POD_{[90]}$ less than 1.00″) shows a 20% improvement with a $POD_{[90/95]}$ = 0.66″ diameter flaw. These performance brackets might be useful to airlines and MROs that can judge where their inspectors fall within the brackets and the resulting performance they will obtain from their inspectors. The results in figures 95–98 also reveal the degree of inspection improvements that are possible if inspectors can shift their performance from the higher (worse) performance brackets to the lower (better) performance brackets. This shift in performance can be brought about by improved or more extensive composite inspection training or through a number of other measures that are described in detail in section 7.

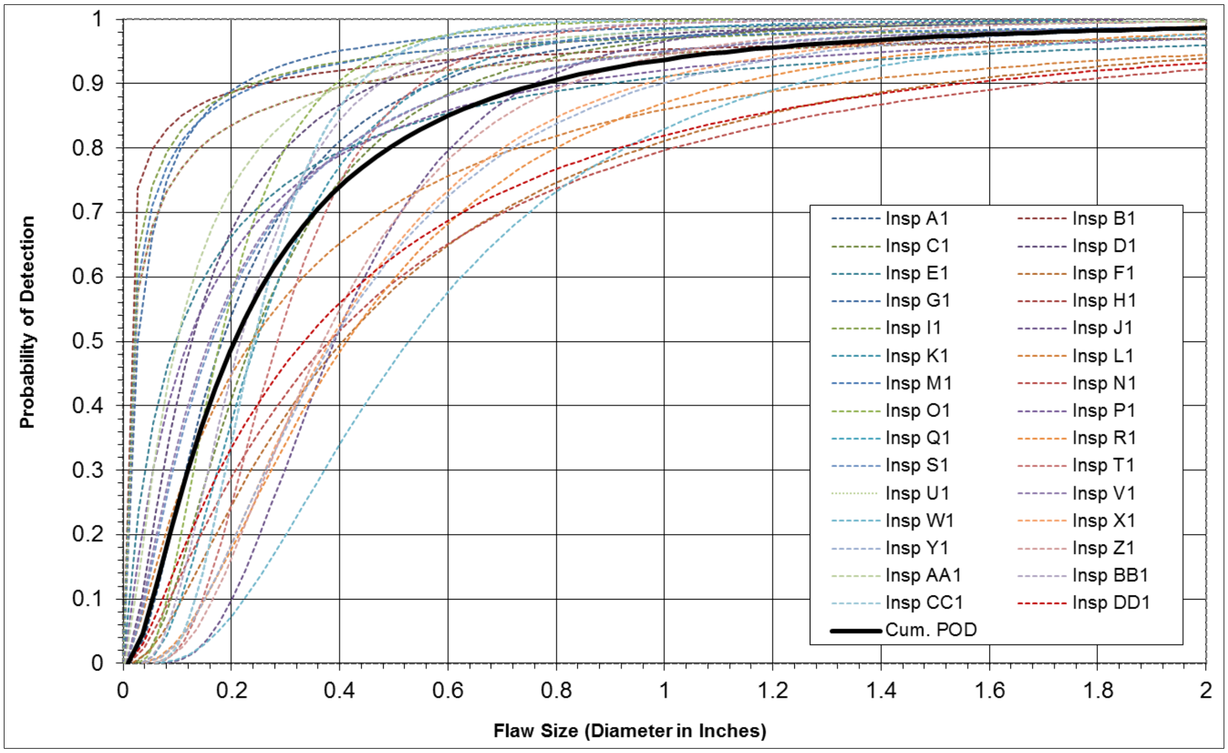

Figure 92. Individual and cumulative POD curve comparison for the 20–32 ply specimen set for all flaws in the CT and CG regions; all inspectors—PE UT method

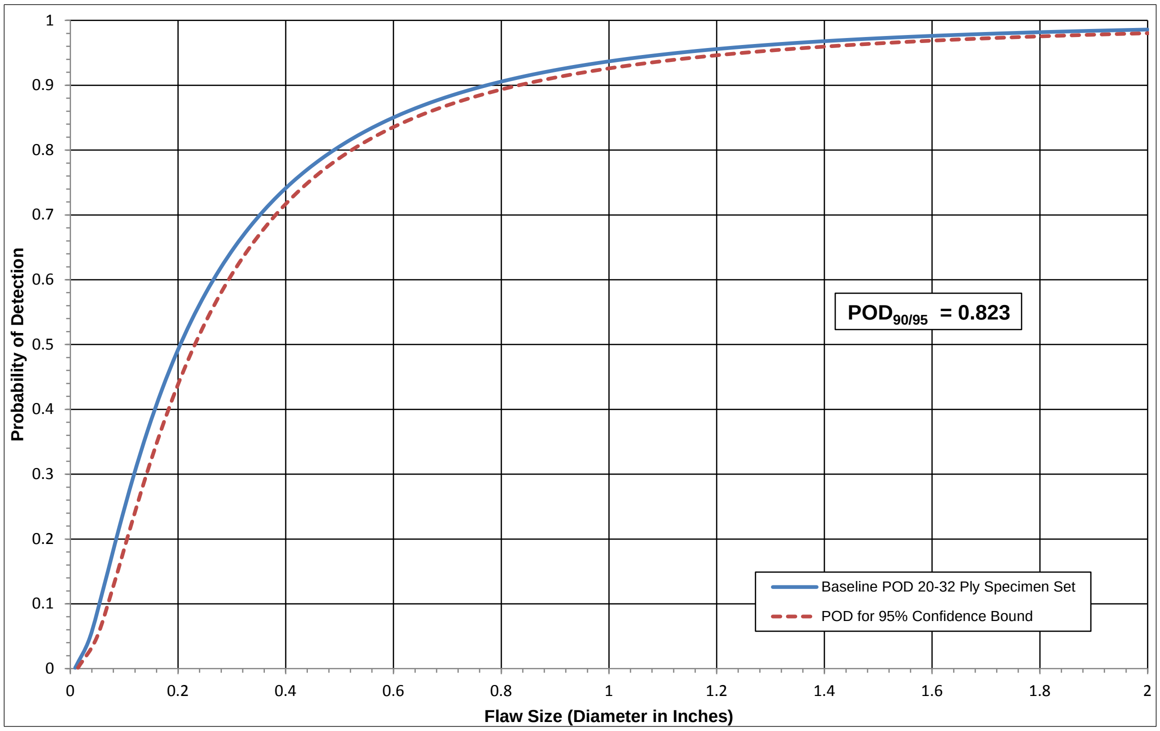

Figure 93. Cumulative POD curve for the 20–32 ply specimen set for all flaws in the CT and CG regions; all inspectors (30)—PE UT method

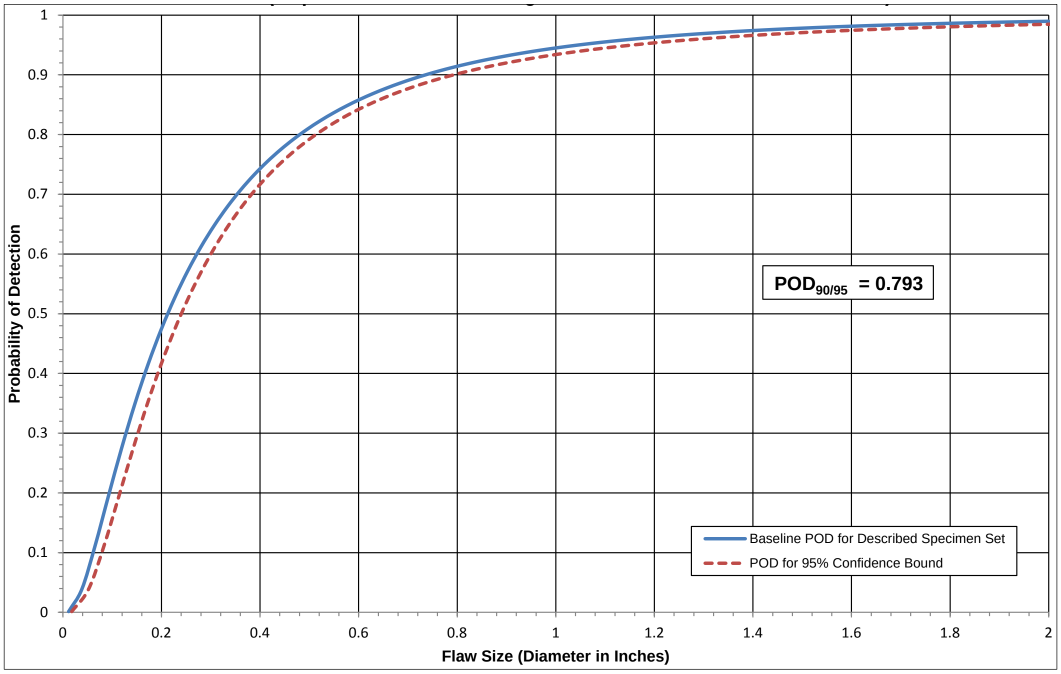

Figure 94. Cumulative POD curve with the two highest and two lowest inspector POD values removed for the 20–32 ply specimen set for all flaws in the CT and CG regions; 26 inspectors—PE UT method

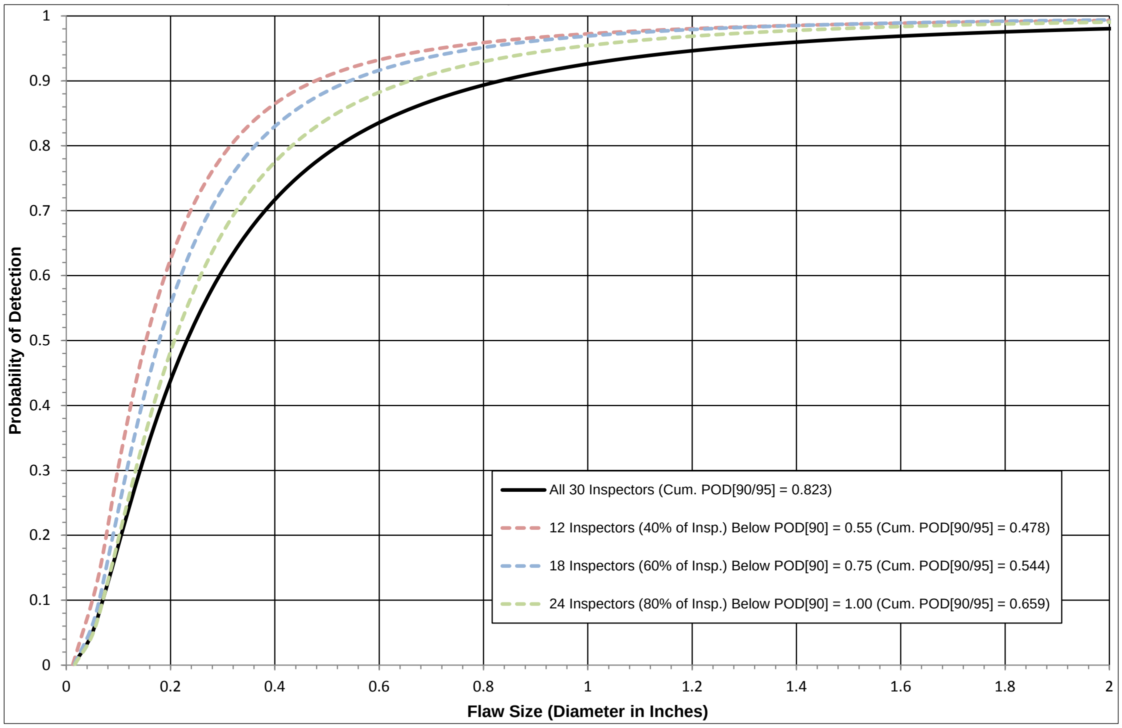

Figure 95. Cumulative POD curve performance brackets for the 20–32 ply specimen set for all flaws in the CT and CG regions—PE UT method

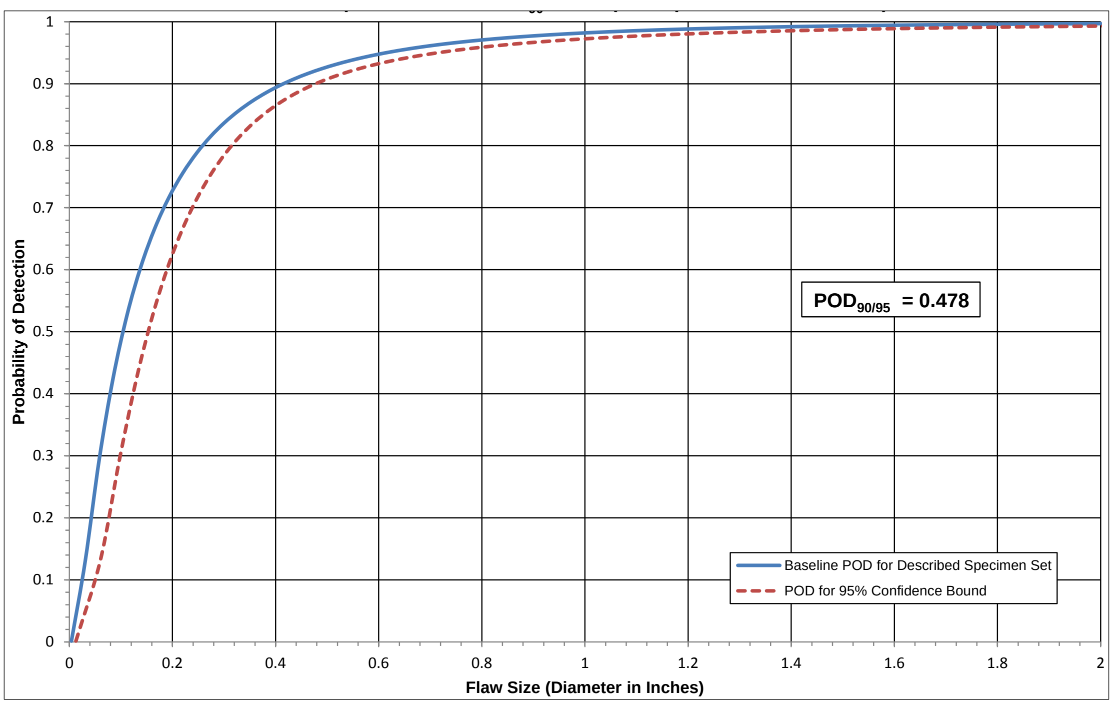

Figure 96. Cumulative POD curve for all inspectors in performance bracket below POD_{90} = 0.55 (12 inspectors: 40 percentile) for the 20–32 ply specimen set for all flaws in the CT and CG regions—PE UT method

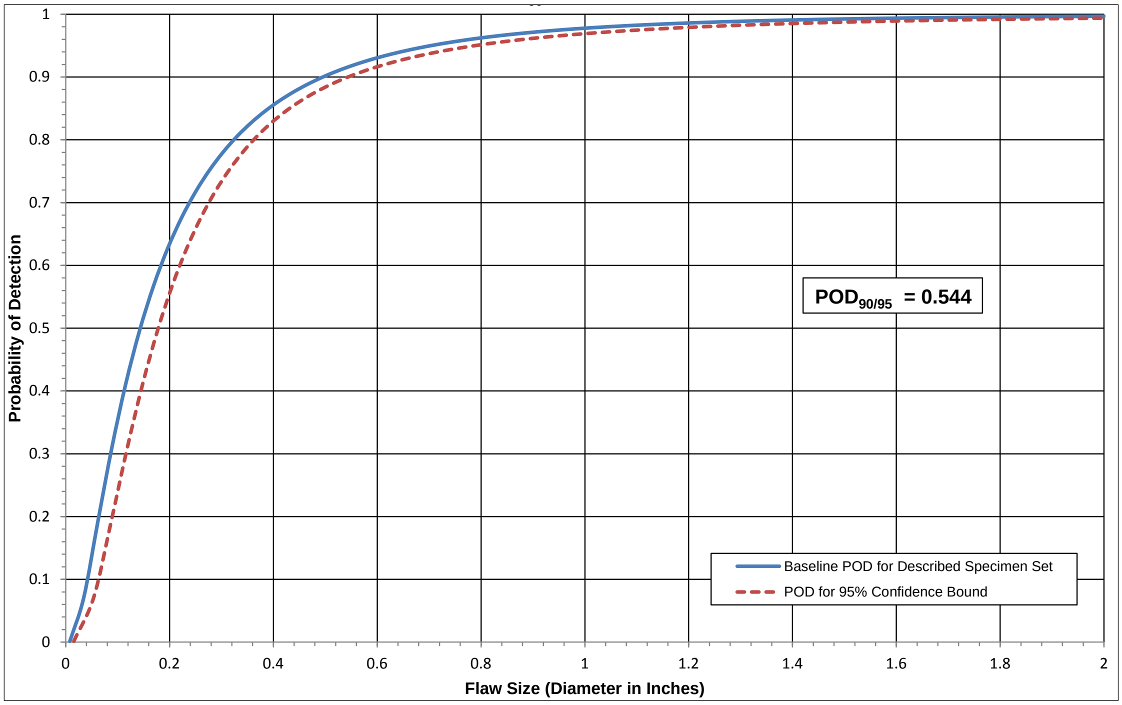

Figure 97. Cumulative POD curve for all inspectors in performance bracket below POD_{90} = 0.75 (18 inspectors: 60 percentile) for the 20–32 ply specimen set for all flaws in the CT and CG regions—PE UT method

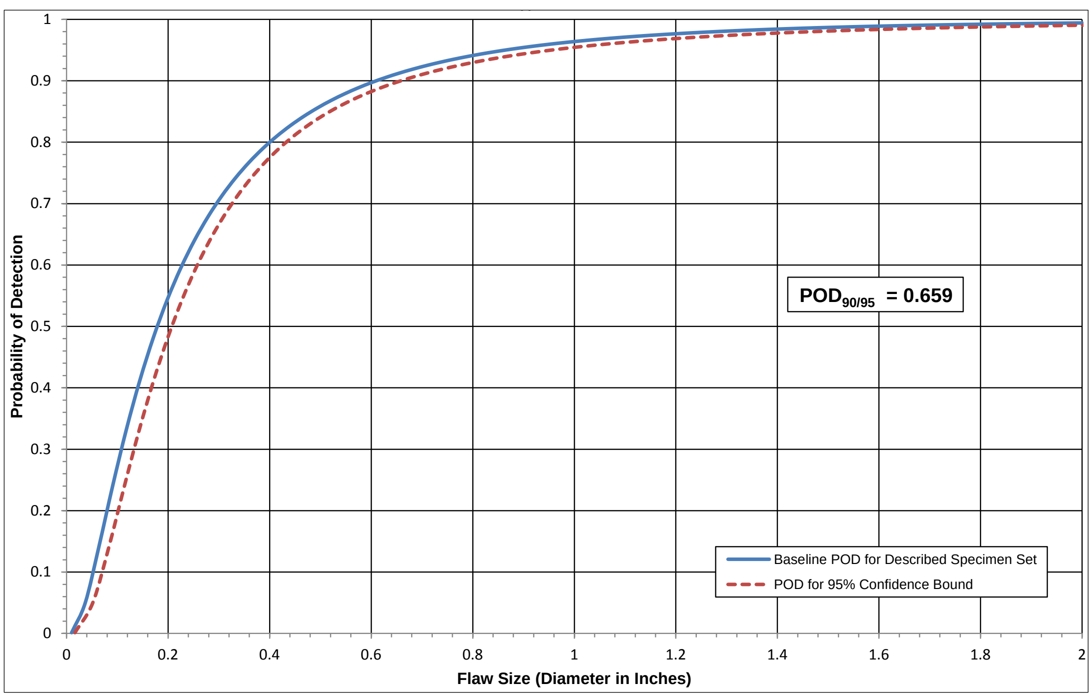

Figure 98. Cumulative POD curve for all inspectors in performance bracket below POD_{90} = 1.00 (24 inspectors: 80 percentile) for the 20–32 ply specimen set for all flaws in the CT and CG regions—PE UT method

6.2.2 Effects of CG

The overall POD values were analyzed further to study the flaw detection performance within specific composite construction regions in the test specimen set. Figure 99 shows the POD curve representing inspectors' performance in the CT regions, representing only 32-ply CT. The CT regions for this specimen set are defined as regions that have no taper and no substructure, so they maintain a constant laminate thickness. The $POD_{[90/95]}$ = 0.74″ for CT geometry regions indicates a better performance compared to the overall $POD_{[90/95]}$ = 0.82″ when the CG regions are also included in the calculation. A complementary set of results was determined using the inspection results from only the CG construction scenarios. Figure 100 shows the POD curve representing inspectors' performance in the CG regions only. The CG regions for this specimen set are defined as regions containing a taper or substructure (no curved portions, fasteners, or laminate over honeycomb are included in this specimen set). The $POD_{[90/95]}$ = 0.93″ for the CG regions is a slightly poorer performance than the overall $POD_{[90/95]}$ = 0.82″ when the CT regions are also included in the calculation. This shows that the CG regions are a factor in driving up the overall cumulative 20–32 ply POD value. Figures 101 and 102 show the CG results broken down further into specific attributes: tapered regions only and substructure regions only. The $POD_{[90/95]}$ = 0.70″ for the tapered regions is lower than the overall $POD_{[90/95]}$ value. For the substructure regions only, the $POD_{[90/95]}$ = 1.50″ is much higher, indicating that the substructure is the primary factor in reducing inspector performance in the CG regions and in driving up the cumulative 20–32 ply POD values. Substructure inspections appear to be the most challenging aspect of thick laminate inspections.

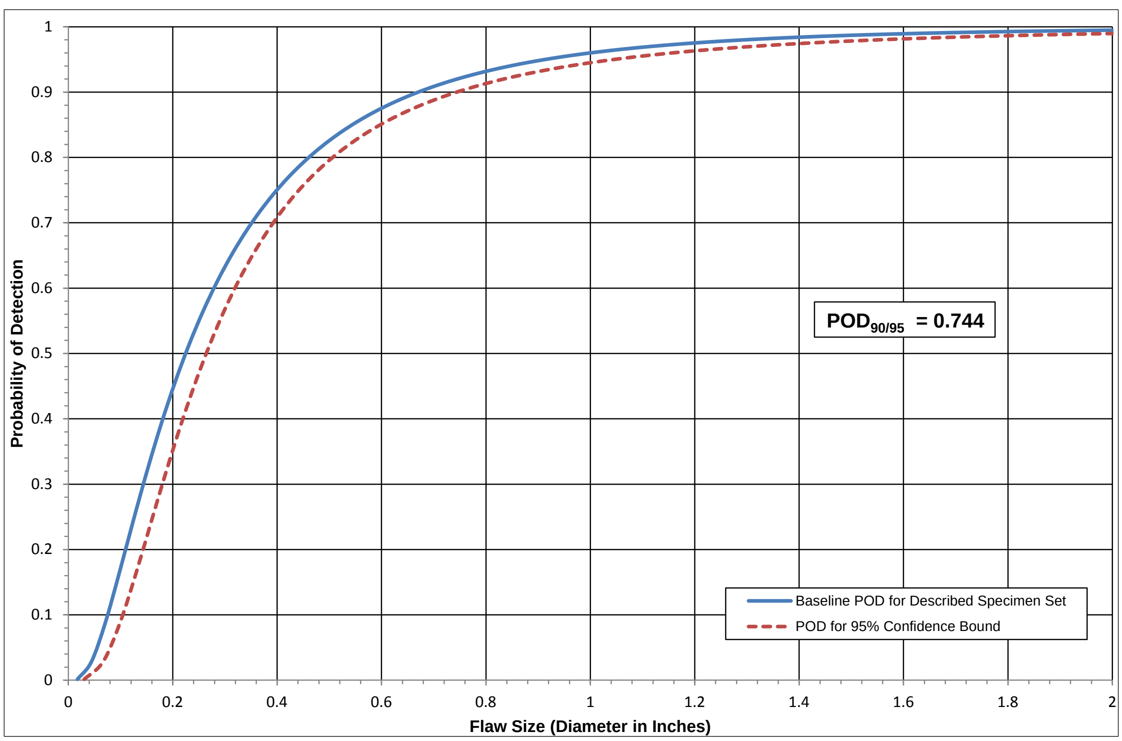

Figure 99. Cumulative POD curve for the 20–32 ply specimen set for flaws in the CT regions only (32 ply); all inspectors—PE UT method

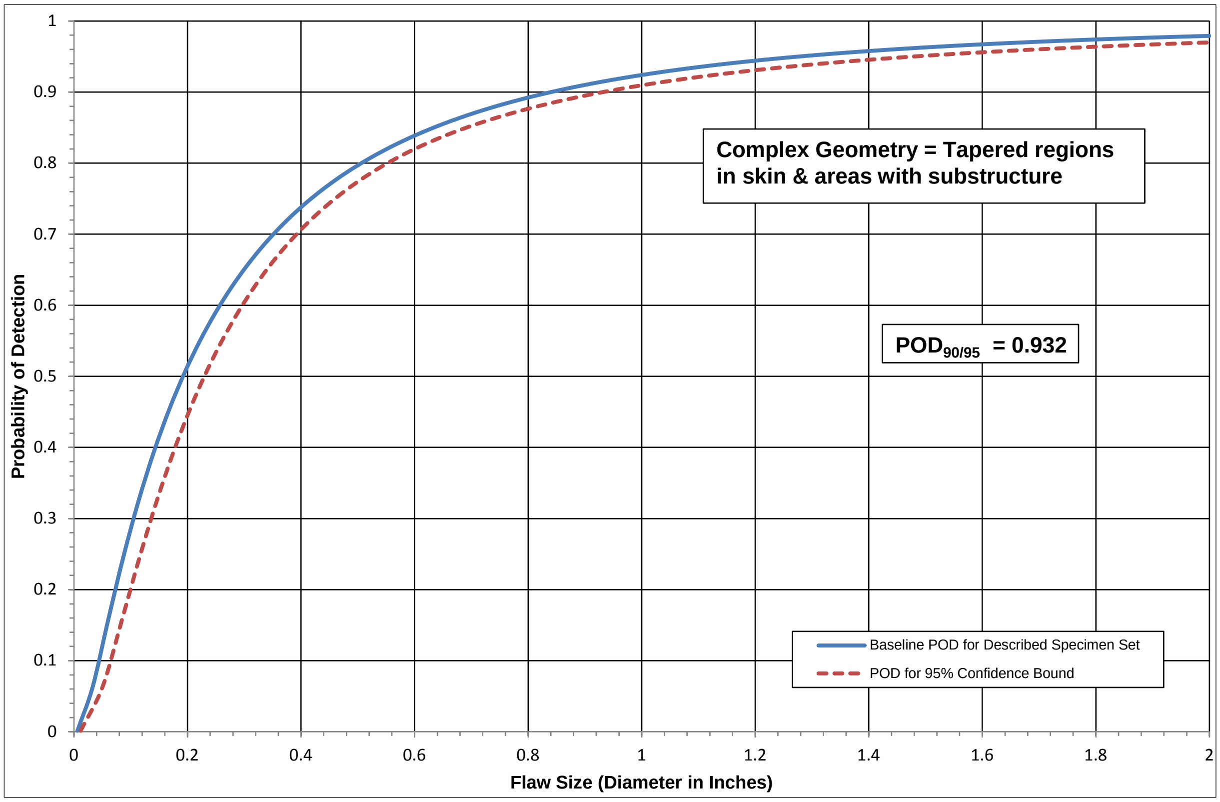

Figure 100. Cumulative POD curve for the 20–32 ply specimen set for flaws in the CG regions only; all inspectors—PE UT method

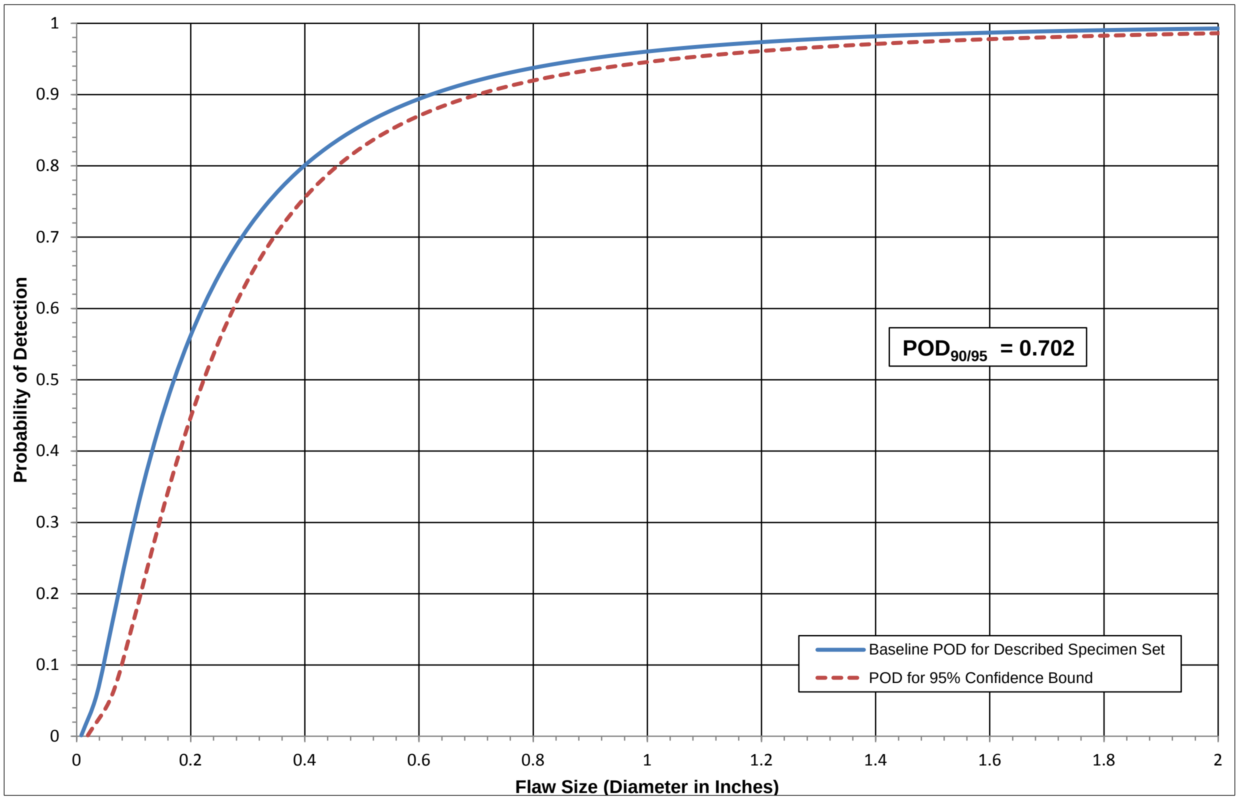

Figure 101. Cumulative POD curve for the 20–32 ply specimen set for flaws in the tapered regions only; all inspectors—PE UT method

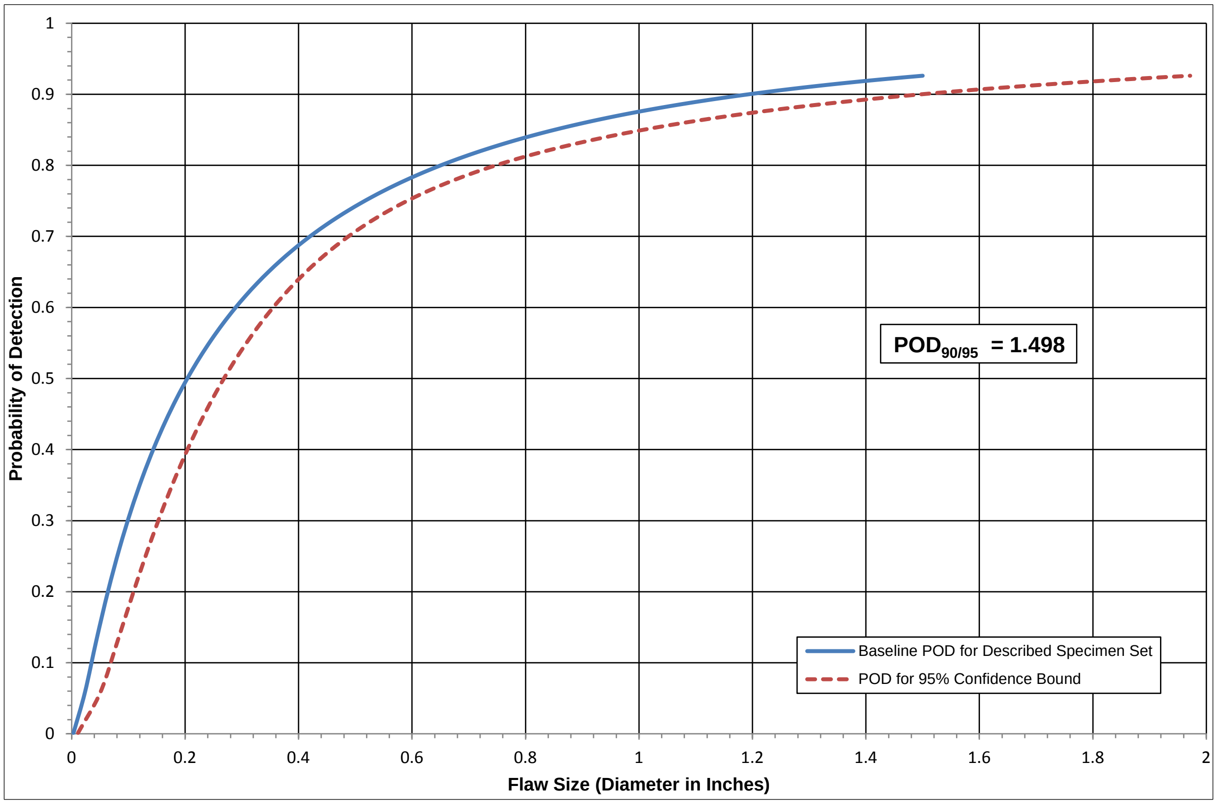

Figure 102. Cumulative POD curve for the 20–32 ply specimen set for flaws in the substructure regions only; all inspectors—PE UT method

The experiment monitors also recorded the various methods that inspectors used to ensure inspection area coverage for the 20–32 ply thick laminate experiment. Some inspectors covered the inspection area with their UT transducers using a pure freehand approach (i.e., no guides or markings on the panels). Some inspectors divided the inspection surface into quadrants to reduce freehand coverage errors. Some inspectors used a series of tick marks, often placed at 0.5″ or 1″ intervals, to divide the inspection surface into a number of rows and columns. Some inspectors used flexible straight edges to guide their transducer movement. The different surface coverage techniques that were observed fall into four categories. The POD results produced by each of these inspection coverage methods were calculated separately and are shown in figure 103 along with the corresponding $POD_{[90/95]}$ values. Figures 102–105 show the individual POD curves for each coverage technique. The method that produced the lowest (best) POD level was where inspectors used a straight edge on all panels throughout the experiment (11 inspectors), achieving a $POD_{[90/95]}$ = 0.62″ diameter flaw. This produced a 26% improvement compared to the overall cumulative 20–32 ply $POD_{[90/95]}$ value of 0.83″. The second-best performing coverage method was that in which inspectors made tick marks for spacing and used a straight edge on all panels throughout the experiment (six inspectors), achieving a $POD_{[90/95]}$ = 0.64″ diameter flaw. This produced a 23% improvement compared to the overall cumulative 20–32 ply $POD_{[90/95]}$ value. The third-best performing coverage method was that in which inspectors started the experiment using a straight edge, but, at some point during the experiment, switched to freehand (five inspectors). This method produced a $POD_{[90/95]}$ = 0.98″, which is actually a decrease in performance of 17% compared to the overall cumulative 20–32 ply $POD_{[90/95]}$ value of 0.82″.

The point at which an inspector switched to freehand was not documented, but it was observed and noted during the experiment that the inspector switched to freehand coverage after starting the experiment using a straight edge. The poorest performing coverage method was that in which inspectors used the freehand method on all panels throughout the experiment (eight inspectors). This produced a $POD_{[90/95]}$ = 1.35″, which is a 62% decrease in performance compared to the overall cumulative 20–32 ply $POD_{[90/95]}$ value. The freehand method has been shown in both the 12–20 ply and 20–32 ply experiments to be the worst performing method to use for ensuring proper inspection area coverage. The purpose for showing the data in this manner is to highlight the importance of proper scanning techniques and the effect that it can have on the overall inspection results. It can be seen in both experiments that the effect is dramatic and not related to the capability of the NDI equipment.

The summary of all $POD_{[90/95]}$ values for the 20–32 ply thick laminate experiment is presented in table 16.

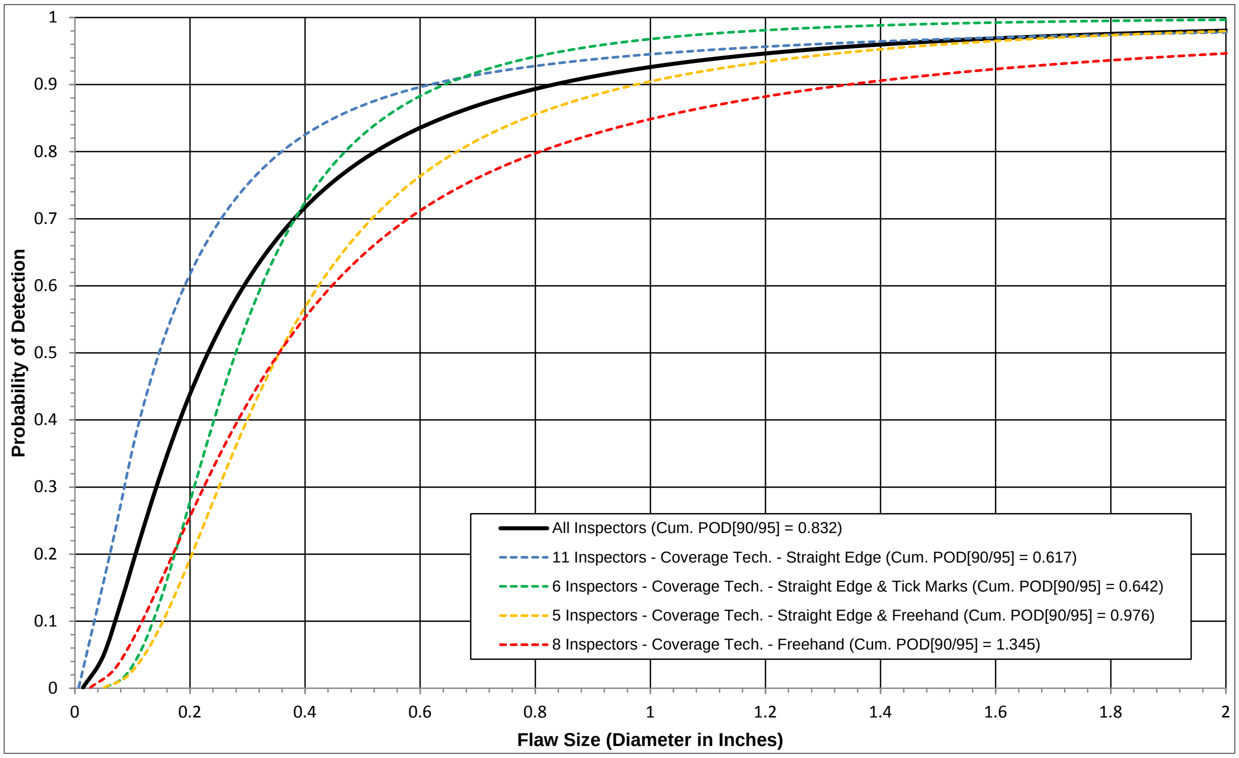

Figure 103. Cumulative POD curve comparison of different surface coverage techniques for the 20–32 ply specimen set for all flaws in the CT and CG regions; all inspectors (30)—PE UT method

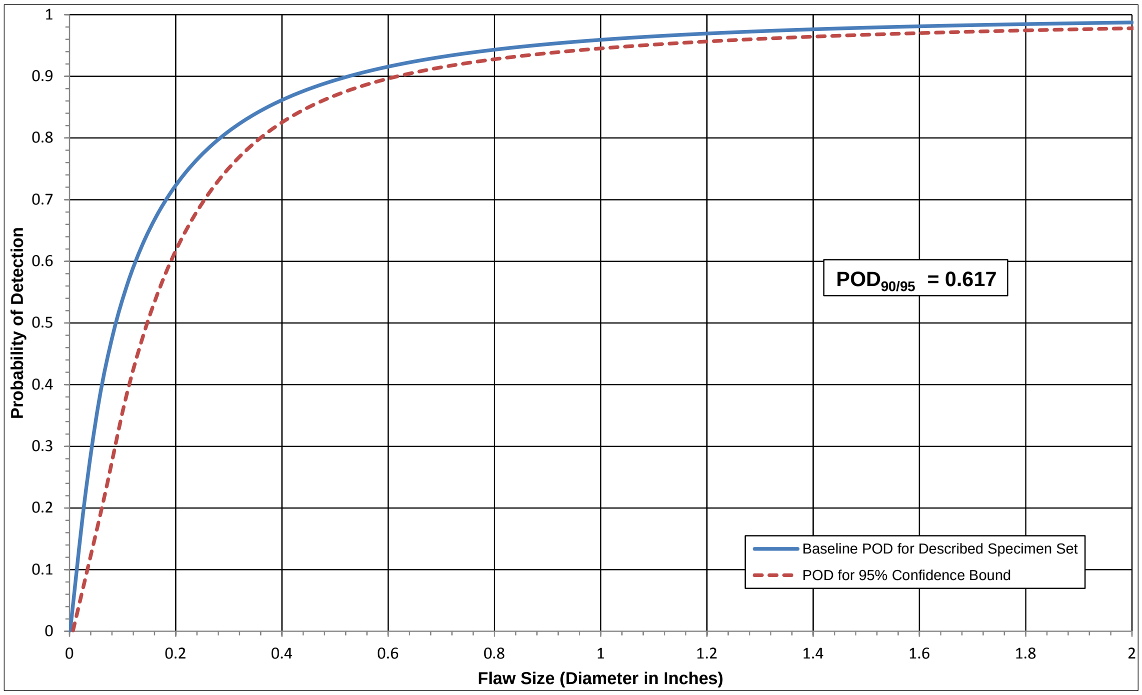

Figure 104. Cumulative POD curve for the straight edge coverage technique (11 inspectors) for the 20–32 ply specimen set for all flaws in the CT and CG regions—PE UT method

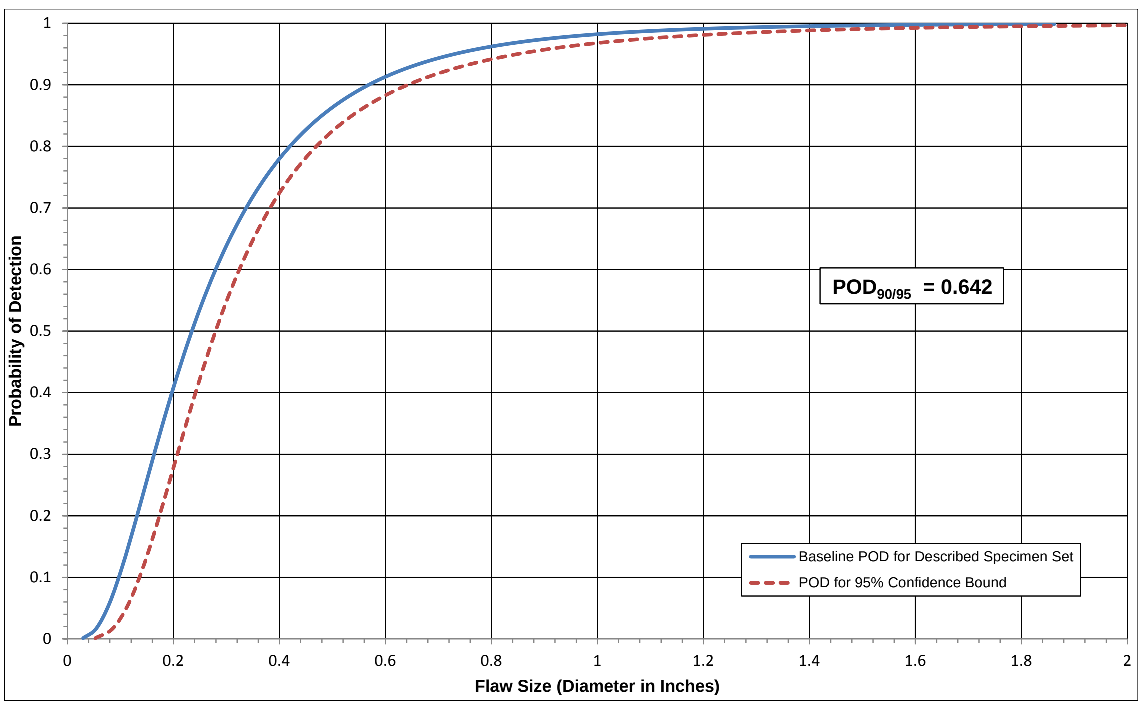

Figure 105. Cumulative POD curve for the straight edge and tick marks (indexing) coverage technique (six inspectors) for the 20–32 ply specimen set for all flaws in the CT and CG regions—PE UT method

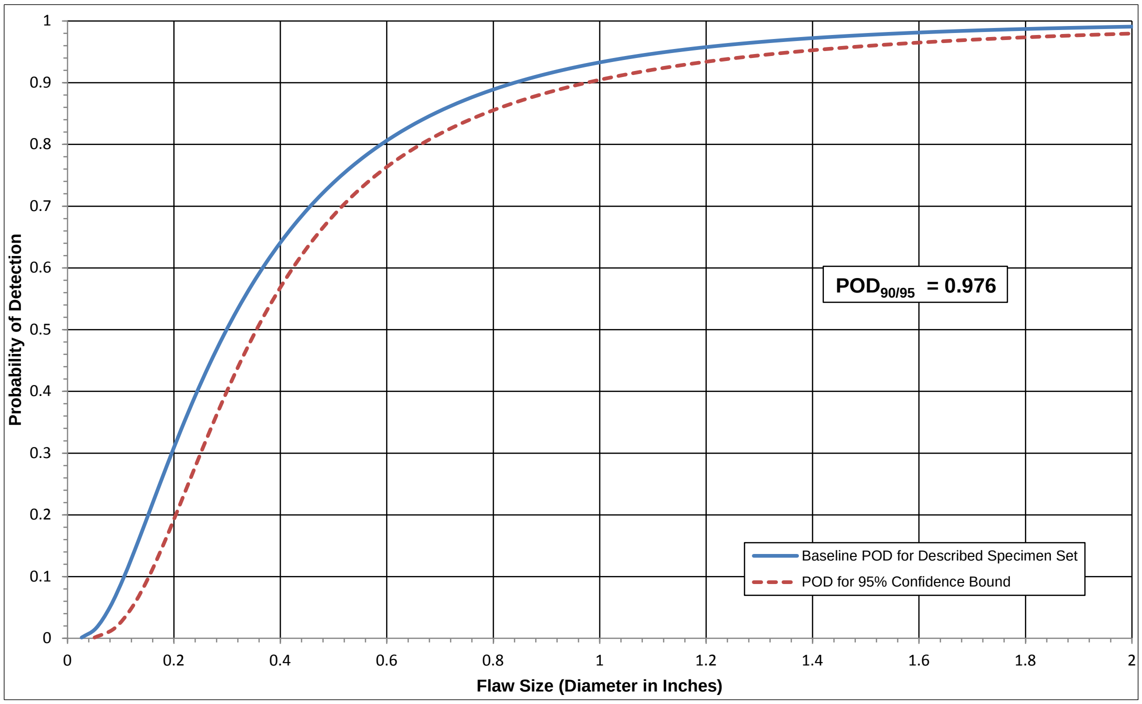

Figure 106. Cumulative POD curve for the straight edge and freehand coverage technique (five inspectors) for the 20–32 ply specimen set for all flaws in the CT and CG regions—PE UT method

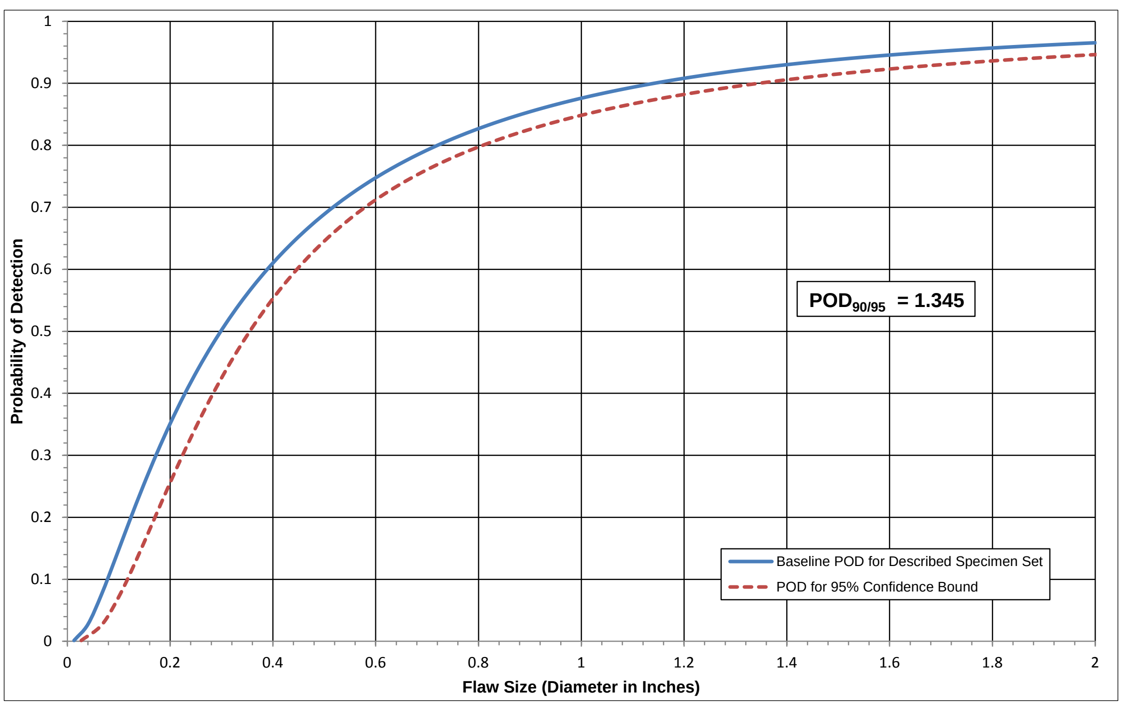

Figure 107. Cumulative POD curve for the freehand coverage technique (eight inspectors) for the 20–32 ply specimen set for all flaws in CT and CG regions—PE UT method

Table 16. Cumulative POD results table for the 20–32 ply specimen set

Cumulative POD Results Table, 20-32 Ply Specimen Set	
Condition	$POD_{90/95}$
All Flaws – All Regions – All 30 Inspectors	0.823
All Flaws – All Regions – 26 Inspectors, 2 High & 2 Low Removed	0.793
All Flaws – All Regions – 12 Inspectors Below POD_{90} = 0.55 (40% of Inspectors)	0.478
All Flaws – All Regions – 18 Inspectors Below POD_{90} = 0.75 (60% of Inspectors)	0.544
All Flaws – All Regions – 24 Inspectors Below POD_{90} = 1.00 (80% of Inspectors)	0.659
All Flaws – All Regions – 11 Inspectors – Coverage Technique – Straight Edge	0.617
All Flaws – All Regions – 6 Inspectors – Coverage Technique – Straight Edge & Tick Marks	0.642
All Flaws – All Regions – 5 Inspectors – Coverage Technique – Straight Edge & Freehand	0.976
All Flaws – All Regions – 8 Inspectors – Coverage Technique – Freehand	1.345
Only Flaws in 32 Ply Constant Thickness – All Inspectors	0.744
Only Flaws in Complex Geometry Regions – All Inspectors	0.932
Only Flaws in Tapered Regions – All Inspectors	0.702
Only Flaws in Substructure Regions – All Inspectors	1.498

6.2.3 False Calls

The Experimenter Information Packet (see appendix A) and face-to-face Experiment Briefing (see appendix B) both state that "inspectors should use any positive indications to find flaws as small as 1/4″ in diameter." A false call is defined as an inspector flaw indication in an area where no flaw actually exists. However, there are unintentional manufacturing flaws, such as porosity, that are not associated with the POD study. If an inspector made a call that correlated to an area of porosity, it was ignored and not deemed to be a false call.

Table 17 summarizes the number of false calls made by each inspector. This table shows the number of false calls made by each inspector for the 20–32 ply specimen set and lists the sizing category that incorporates each false call. The average number of false calls made was determined to be 1.1 false calls per inspector (12 ft^2 inspection area), with an average of one false call per 10.91 ft^2 of inspection area. It should be noted that the majority of false calls were made in the CG regions. Table 18 shows the false call data when false calls of less than 0.25 in^2 (i.e., very small items) were removed from the calculations. This table shows the resulting average number of false calls were reduced to 0.3 false calls per inspector (12 ft^2 inspection area), with an average of one false call per 40 ft^2 of inspection area. Thus, the overall false call rate was determined to be very low.

Table 17. Inspection false call table for the 20–32 ply specimen set all inspectors—PE method

Inspection False Calls for 20-32 Ply Specimen Set – All Inspectors – Pulse Echo UT																																
Configuration/Sizing ($in.^2$)	Insp. A1	Insp. B1	Insp. C1	Insp. D1	Insp. E1	Insp. F1	Insp. G1	Insp. H1	Insp. I1	Insp. J1	Insp. K1	Insp. L1	Insp. M1	Insp. N1	Insp. O1	Insp. P1	Insp. Q1	Insp. R1	Insp. S1	Insp. T1	Insp. U1	Insp. V1	Insp. W1	Insp. X1	Insp. Y1	Insp. Z1	Insp. AA1	Insp. BB1	Insp. CC1	Insp. DD1	Total	Avg.
Constant Thickness (CT)																																
0–.25in^2	2	0	0	0	1	1	0	0	1	0	0	0	0	0	1	0	0	0	1	0	1	0	1	9	0	0	0	0	0	1	19	0.6
.26in^2–75in^2	0	0	0	0	1	0	0	0	0	0	0	0	0	0	0	0	0	0	2	0	0	0	0	0	0	0	1	0	0	0	4	0.1
76in^2–1.25in^2	0	0	0	0	0	0	0	0	0	0	0	0	0	0	0	2	0	0	0	0	0	0	0	0	0	0	0	0	0	0	2	0.1
1.26in^2–2.00in^2	0	0	0	0	0	0	0	0	0	0	0	0	0	0	0	0	0	0	0	0	0	0	0	0	0	0	0	0	0	0	0	0.0
>2.00in^2	0	0	0	0	0	0	0	0	0	0	0	0	0	0	0	0	0	0	0	0	0	0	0	0	0	0	0	0	0	0	0	0.0
CT Total	2	0	0	0	2	1	0	0	1	0	0	0	0	0	1	2	0	0	3	0	1	0	1	9	0	0	1	0	0	1	25	0.8
Complex Geometry (CG)																																
0–.25in^2	0	0	0	0	0	0	0	0	0	0	0	0	0	0	0	0	0	0	1	0	0	0	0	2	2	0	0	0	0	0	5	0.2
.26in^2–.75 in^2	0	0	0	0	0	0	0	0	0	0	0	0	0	0	0	0	0	0	1	0	0	0	0	1	0	0	0	0	0	0	2	0.1
.76 in^2–1.25 in^2	0	0	0	0	0	0	0	0	0	0	0	0	0	0	0	0	0	0	0	0	0	0	0	0	0	0	0	0	0	0	0	0.0
1.26 in^2–2.00 in^2	0	0	0	0	0	0	0	0	0	0	0	0	0	0	0	0	0	0	0	0	0	0	0	0	0	0	0	0	0	0	0	0.0
>2.00 in^2	0	0	0	0	0	0	0	0	0	0	0	0	0	0	0	0	0	0	1	0	0	0	0	0	0	0	0	0	0	0	1	0.0
CG Total	0	0	0	0	0	0	0	0	0	0	0	0	0	0	0	0	0	0	3	0	0	0	0	3	2	0	0	0	0	0	8	0.3
Total (All Flaws)	2	0	0	0	2	1	0	0	1	0	0	0	0	0	1	2	0	0	6	0	1	0	1	12	2	0	1	0	0	1	33	1.1
1 False Call on Average Per 10.91 ft^2 of Inspection Area																																

Table 18. Inspection false call table with false calls that are below 0.25 in^2 in size removed for the 20–32 ply specimen set; all inspectors—PE method

Inspection False Calls for 20-32 Ply Specimen Set – All Inspectors – Pulse Echo UT
(False Calls that are below 0.25 in^2 in size have been removed)

Configuration/Sizing (in.^{2})	Insp. A1	Insp. B1	Insp. C1	Insp. D1	Insp. E1	Insp. F1	Insp. G1	Insp. H1	Insp. I1	Insp. J1	Insp. K1	Insp. L1	Insp. M1	Insp. N1	Insp. O1	Insp. P1	Insp. Q1	Insp. R1	Insp. S1	Insp. T1	Insp. U1	Insp. V1	Insp. W1	Insp. X1	Insp. Y1	Insp. Z1	Insp. AA1	Insp. BB1	Insp. CC1	Insp. DD1	Total	Avg.
Constant Thickness (CT)																																
.26in^2–75in^2	0	0	0	0	1	0	0	0	0	0	0	0	0	0	0	0	0	0	2	0	0	0	0	0	0	0	1	0	0	0	4	0.1
76in^2–1.25in^2	0	0	0	0	0	0	0	0	0	0	0	0	0	0	0	2	0	0	0	0	0	0	0	1	0	0	0	0	0	0	2	0.1
1.26in^2–2.00in^2	0	0	0	0	0	0	0	0	0	0	0	0	0	0	0	0	0	0	0	0	0	0	0	0	0	0	0	0	0	0	0	0.0
>2.00in^2	0	0	0	0	0	0	0	0	0	0	0	0	0	0	0	0	0	0	0	0	0	0	0	0	0	0	0	0	0	0	0	0.0
CT Total	0	0	0	0	1	0	0	0	0	0	0	0	0	0	0	2	0	0	2	0	0	0	0	0	0	0	1	0	0	0	6	0.2
Complex Geometry (CG)																																
.26in^2–.75 in^2	0	0	0	0	0	0	0	0	0	0	0	0	0	0	0	0	0	0	1	0	0	0	0	1	0	0	0	0	0	0	2	0.1
.76 in^2–1.25 in^2	0	0	0	0	0	0	0	0	0	0	0	0	0	0	0	0	0	0	0	0	0	0	0	0	0	0	0	0	0	0	0	0.0
1.26 in^2–2.00 in^2	0	0	0	0	0	0	0	0	0	0	0	0	0	0	0	0	0	0	0	0	0	0	0	0	0	0	0	0	0	0	0	0.0
>2.00 in^2	0	0	0	0	0	0	0	0	0	0	0	0	0	0	0	0	0	0	1	0	0	0	0	0	0	0	0	0	0	0	1	0.0
CG Total	0	0	0	0	0	0	0	0	0	0	0	0	0	0	0	0	0	0	2	0	0	0	0	1	0	0	0	0	0	0	3	0.1
Total (All Flaws)	0	0	0	0	1	0	0	0	0	0	0	0	0	0	0	2	0	0	4	0	0	0	0	1	0	0	1	0	0	0	9	0.3

1 False Call on Average Per 40 ft^2 of Inspection Area

6.2.4 Inspection Time

Another critical part of the inspection process is how long it takes an inspector to scan a defined area. Table 19 shows the time it took for each inspector to scan each panel and their total inspection time. The average total inspection time for the 20–32 ply specimen set was just over 6.25 hours, which produced an average inspection coverage rate of 1.91 ft^2/hr. The lowest (quickest) total inspection time was just over two hours, with an average inspection coverage rate of 5.76 ft^2/hr. The highest (slowest) total inspection time was just over 9.75 hours, with an average inspection coverage rate of 1.22 ft^2/hr.

Figure 108 shows the effect of total inspector time on the resulting inspector's $POD_{[90]}$ value. The trend line in this scatter diagram indicates that a lower inspection time leads to a higher POD value and longer inspection times can lead to improvements in POD. The scatter diagram in Figure 109 shows the effect of total inspector time on the false call rate. The trend line here suggests that the faster inspection times lead to fewer false calls. However, the false call rate in this experiment was so low that this change only represents a very small shift in the total false calls and may be affected by the two inspectors with a high number of false calls when compared to the average. Thus, this result is deemed insignificant. Figure 110 is a scatter diagram showing the effect of inspector $POD_{[90]}$ values on the inspector false calls made. The trend line in this diagram shows essentially little change in false calls over the range of POD values obtained, taking the two inspectors with high false calls into account. Once again, this result is negligible, primarily because of the very low false call rate in this experiment.

Table 19. Experiment timing summary table for the 20–32 ply specimen set; all inspectors—PE UT method

Experiment Timing Summary 20-32 Ply Specimen Set All Inspectors – Pulse Echo UT					
	Specimen ST32-1	Specimen ST32-2	Specimen ST32-3	Specimen ST32-4	Total Insp. Time (hr:min)
Inspector A1	1:01	1:08	1:05	1:02	4:16
Inspector B1	1:13	1:35	1:53	2:32	7:13
Inspector C1	1:28	1:51	1:03	1:20	5:42
Inspector D1	2:26	2:44	2:41	1:57	9:48
Inspector E1	1:56	1:59	2:54	1:44	8:33
Inspector F1	1:31	2:18	0:50	1:11	5:50
Inspector G1	1:35	1:43	2:30	2:10	7:58
Inspector H1	1:30	2:09	2:29	2:33	8:41
Inspector I1	0:43	1:30	1:55	0:51	4:59
Inspector J1	1:43	1:18	2:31	1:32	7:04
Inspector K1	1:02	1:08	0:53	2:10	5:13
Inspector L1	2:31	1:53	2:41	1:51	8:56
Inspector M1	1:17	3:36	2:42	2:04	9:39
Inspector N1	1:54	1:09	1:57	1:42	6:42
Inspector O1	2:02	2:17	2:50	1:57	9:06
Inspector P1	0:23	0:18	0:55	0:29	2:05
Inspector Q1	0:56	3:13	1:52	1:21	7:22
Inspector R1	1:51	1:19	1:03	1:01	5:14
Inspector S1	0:51	0:39	1:37	0:58	4:05
Inspector T1	1:17	0:53	1:12	1:31	4:53
Inspector U1	1:46	1:18	1:26	2:05	6:35
Inspector V1	0:39	1:43	1:10	1:18	4:50
Inspector W1	0:47	1:19	0:32	0:28	3:06
Inspector X1	1:21	0:34	2:26	0:49	5:10
Inspector Y1	0:39	0:35	0:55	0:42	2:51
Inspector Z1	1:11	1:44	3:08	1:28	7:31
Inspector AA1	1:03	1:21	1:48	1:40	5:52
Inspector BB1	1:39	1:45	1:19	1:32	6:15
Inspector CC1	0:53	1:51	1:50	1:15	5:49
Inspector DD1	1:33	2:05	1:33	1:40	6:51
Ave. Insp. Time (hr:min)	1:21	1:37	1:47	1:29	6:16
Average Inspection coverage Rate = 1.91 ft^2/hr					

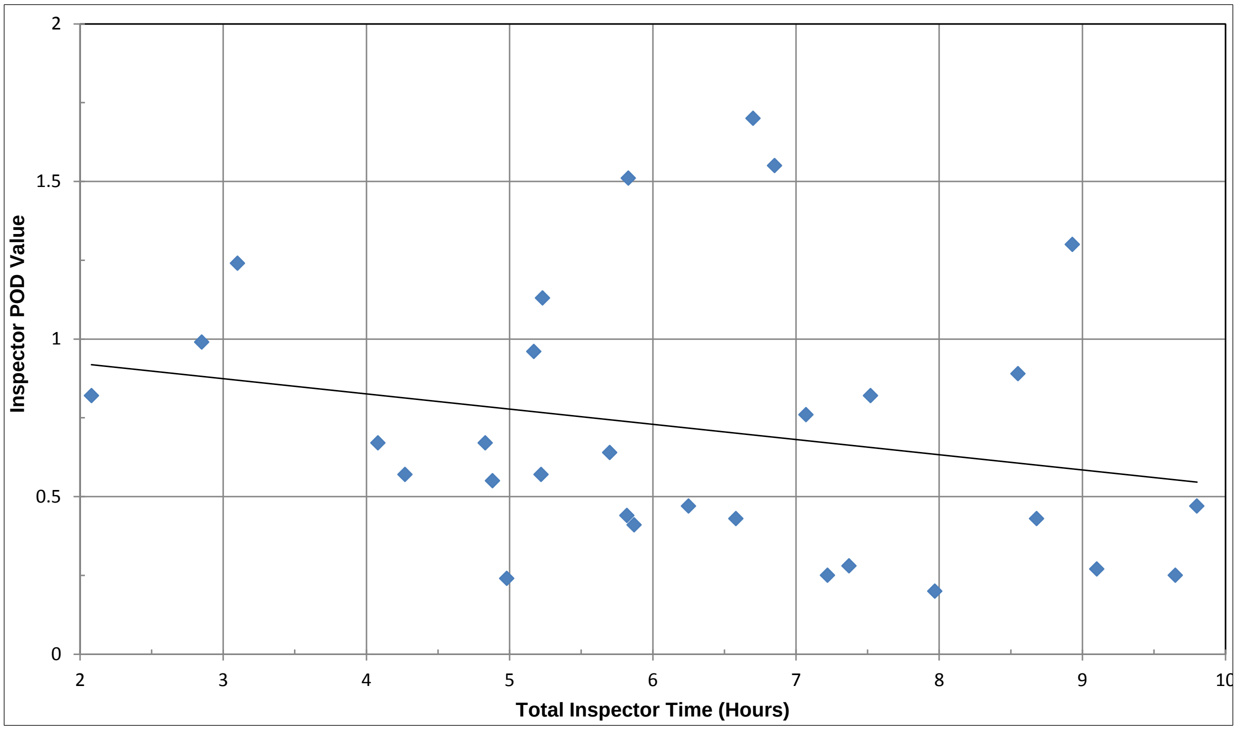

Figure 108. Scatter diagram showing effect of total inspector time on inspector pod values for the 20–32 ply specimen set; all inspectors—PE UT method

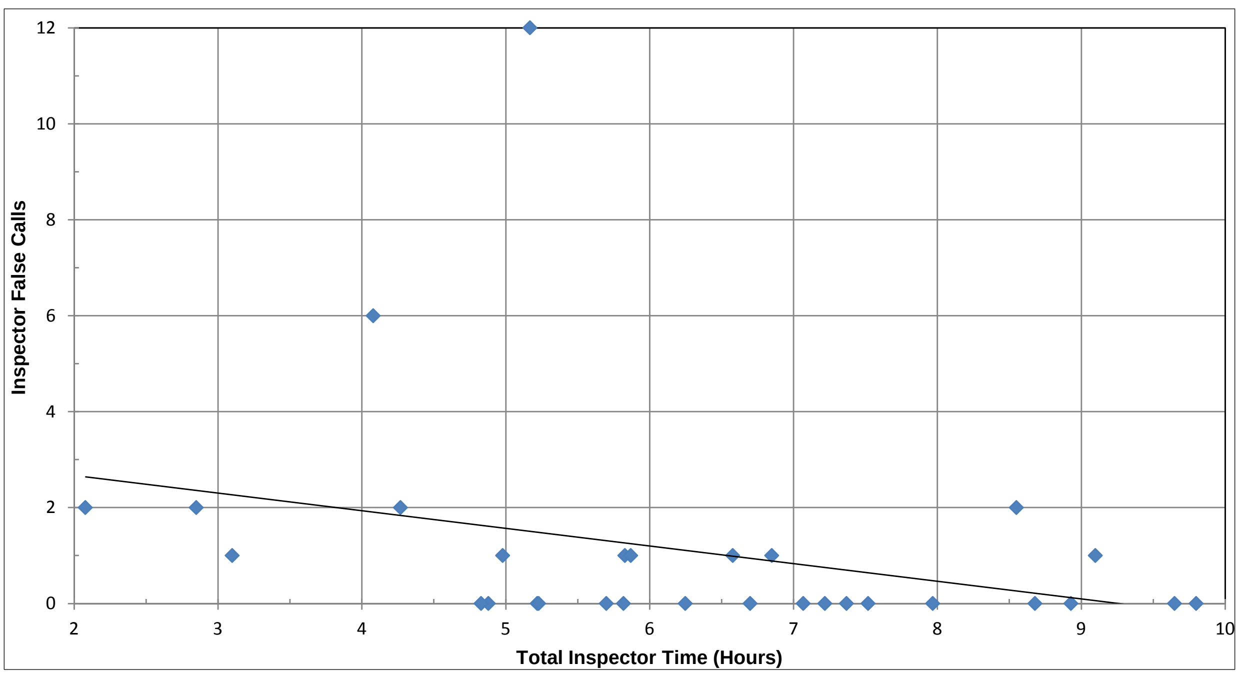

Figure 109. Scatter diagram showing effect of total inspector time on inspector false calls for the 20–32 ply specimen set; all inspectors—PE UT method

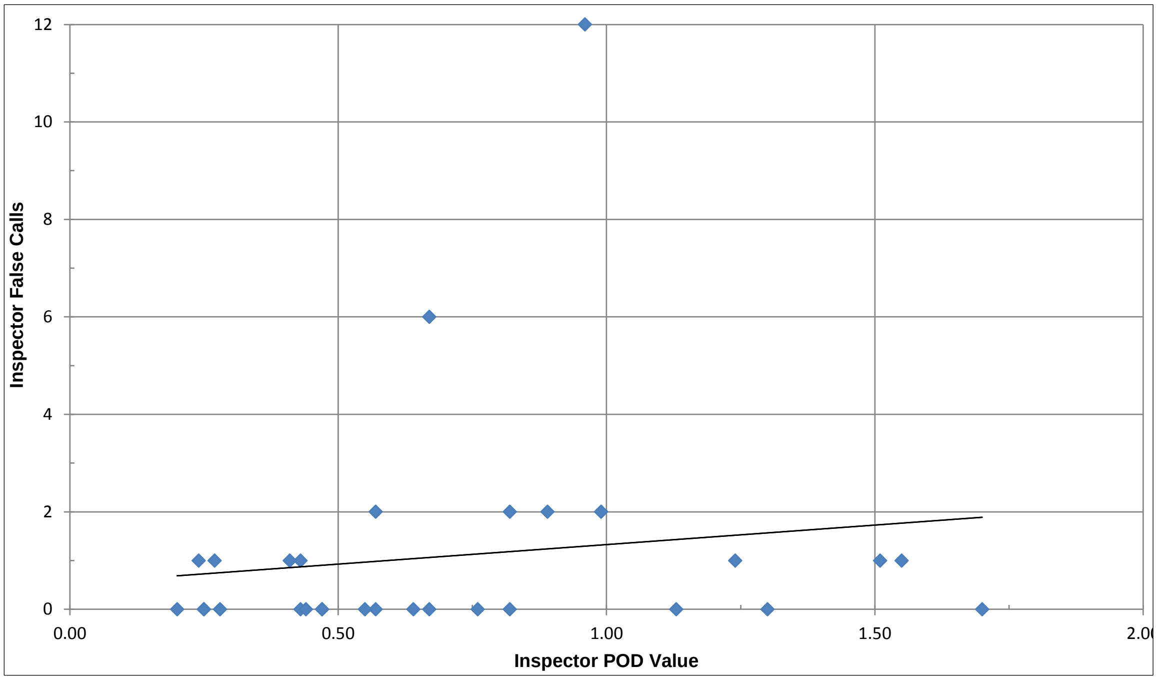

Figure 110. Scatter diagram showing effect of inspector POD values on inspector false calls for the 20–32 ply specimen set; all inspectors—PE UT method

6.2.5 Damage Sizing and Flaw Detection Percentage

Inspector flaw calls were also graded to evaluate the accuracy of each inspector's flaw sizing. The overall test results identified hits (calls with any amount of overlap between the call and the actual flaw location), misses (no call for an area of a known flaw), false calls (call with no overlap of a flaw), and the degree of overlap between experimenter calls and actual flaw areas (sizing performance). The grading parameter drawing that shows how the accuracy of flaw coverage (overlap or sizing performance) was determined is shown in figure 85.

Table 20 summarizes the results for the overall flaw detection percentage and the associated accuracy in determining flaw size for the 20–32 ply specimen set (thick laminate experiment). This table includes combined data for all inspectors and all flaws in both the CT and CG regions. Notice that for the 20–32 ply specimen set, 85% of all flaws were detected—or 1,709 of the total 2,010 flaws were detected. The flaw sizing performance shows that 31% of the detected flaws were sized properly (five categories for 100% coverage), 27% of the flaws were sized in the 76–99% coverage category, and 18% of the flaws were sized in the 51–75% coverage category. Thus, 76% of the detected flaws were sized with 51–100% accuracy. This table also shows a breakdown of percent detection based on flaw size. For example, 99% of the 2″ flaws were detected. In this case, that represents 29 of the 30 inspectors finding every 2″ flaw in the 20–32 ply specimen set (only one 2″ flaw was missed by an inspector). On the smaller side, 56% of the 0.25″ flaws were detected. Figure 111 shows the detection percentage based on flaw size in chart form.

Table 21 summarizes the results for the overall flaw detection percentage and the associated accuracy in determining flaw size for the CT regions only. In this case, 87% of all flaws (623 of the 720 total flaws) were detected in the CT regions. The flaw sizing performance shows that 34% of the detected flaws were sized properly (five categories for 100% coverage). The chart in figure 112 shows the detection percentage based on flaw size for the CT regions.

Table 22 summarizes the results for the overall flaw detection percentage and the associated accuracy in determining flaw size for the CG regions only. In this case, 84% of all flaws (1,086 of the 1,290 total flaws) were detected in the CG regions. The flaw sizing performance shows that 29% of the detected flaws were sized properly (five categories for 100% coverage). The chart in figure 113 shows the detection percentage based on flaw size.

Figures 114–116 show the individual inspector's flaw detection percentages categorized by all flaws in all regions, all flaws in the CT regions, and all flaws in the CG regions. These plots highlight the variation in performance over the full set of inspectors tested. This should be very representative of the aviation industry.

6.2.6 Profile of Inspectors Who Participated in the SLE

Tables 23–25 show a categorization of all inspectors who participated in the 20–32 ply experiment in terms of their NDI experience in years, PE UT NDI level, and NDI experience with composites. Again, this shows that an adequate cross-section of inspectors was obtained and that these results provide an accurate view of the overall aviation industry.

Table 20. Tabulated results showing overall flaw detection percentage and accuracy in determining flaw size for the 20–32 ply specimen set for all flaws in the CT and CG regions; all inspectors—PE UT method

Overall Flaw Detection Percentage & Accuracy in Determining Flaw Size 20–32 Ply Specimen Set – All Inspectors – All Flaws (CT & CG)							
Accuracy in Sizing the Flaws That Were Detected (1,709 Total Flaws Detected)						Flaw Detection Percentage (2,010 Total Flaws)	
Flaw Size	5 (100%)	4 (76%–99%)	3 (51%–75%)	2 (25%–50%)	1 (< 25%)	Flaw Size	Percent Detected
0.25	47%	11%	6%	7%	28%	0.25	56%
0.50	31%	21%	16%	16%	16%	.050	84%
0.75	26%	28%	20%	20%	6%	0.75	89%
1.00	30%	30%	20%	15%	5%	1.00	91%
1.50	25%	34%	26%	11%	5%	1.50	99%
2.00	32%	45%	18%	3%	2%	2.00	99%
Overall Sizing Performance	31%	27%	18%	14%	10%	Overall Flaw Detection	85%

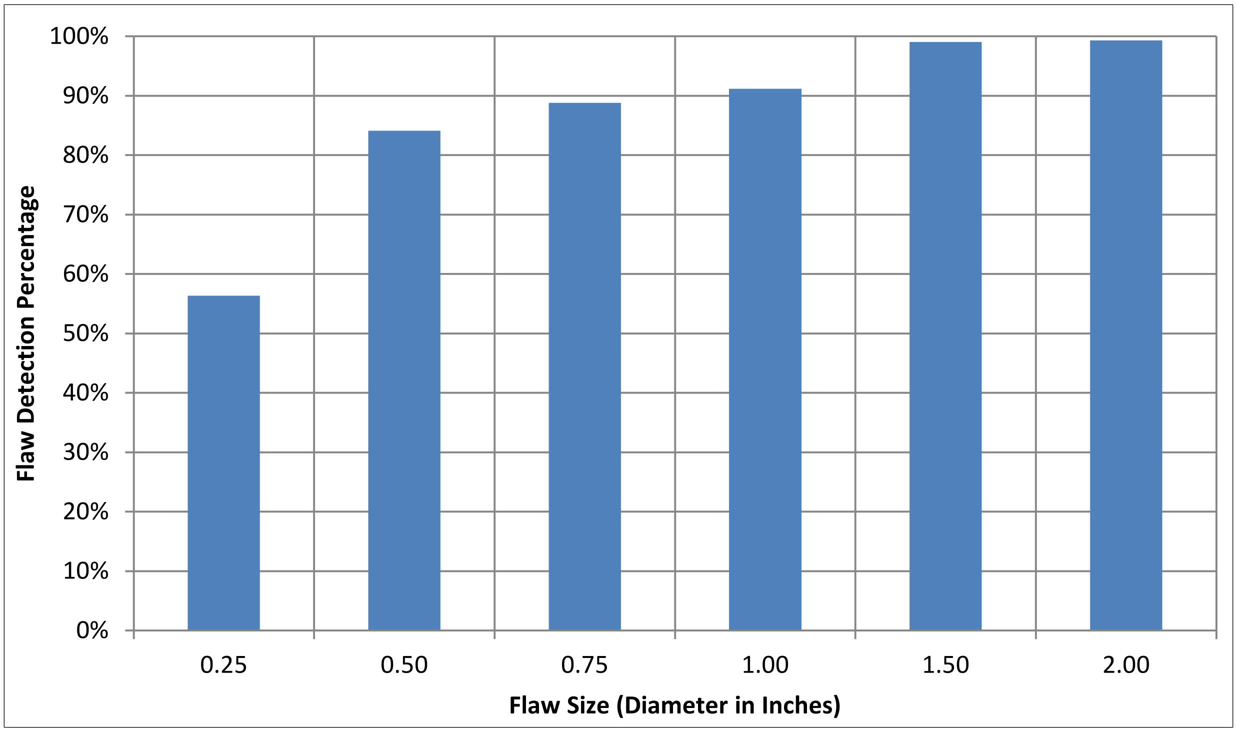

Figure 111. Overall flaw detection percentage chart for the 20–32 ply specimen set for all flaws in the CT and CG regions; all inspectors—PE UT method

Table 21. Tabulated results showing overall flaw detection percentage and accuracy in determining flaw size for the 20–32 ply specimen set for all flaws in the CT regions; all inspectors—PE UT method

Overall Flaw Detection Percentage & Accuracy in Determining Flaw Size 20-32 Ply Specimen Set – All Inspectors – All Constant Thickness (CT) Flaws							
Accuracy in Sizing the Flaws That Were Detected (623 Total Flaws Detected)						Flaw Detection Percentage (720 Total Flaws)	
Flaw Size	5 (100%)	4 (96%-99%)	3 (51%-75%)	2 (25%-50%)	1 (< 25%)	Flaw Size	Percent Detected
0.25	50%	13%	13%	3%	22%	0.25	53%
0.50	35%	18%	15%	14%	18%	0.50	86%
0.75	25%	29%	19%	22%	5%	0.75	91%
1.00	38%	29%	19%	12%	2%	1.00	96%
1.50	17%	27%	33%	20%	3%	1.50	100%
2.00	36%	44%	19%	0%	1%	2.00	99%
Overall Sizing Performance	34%	28%	18%	13%	8%	Overall Flaw Detection	87%

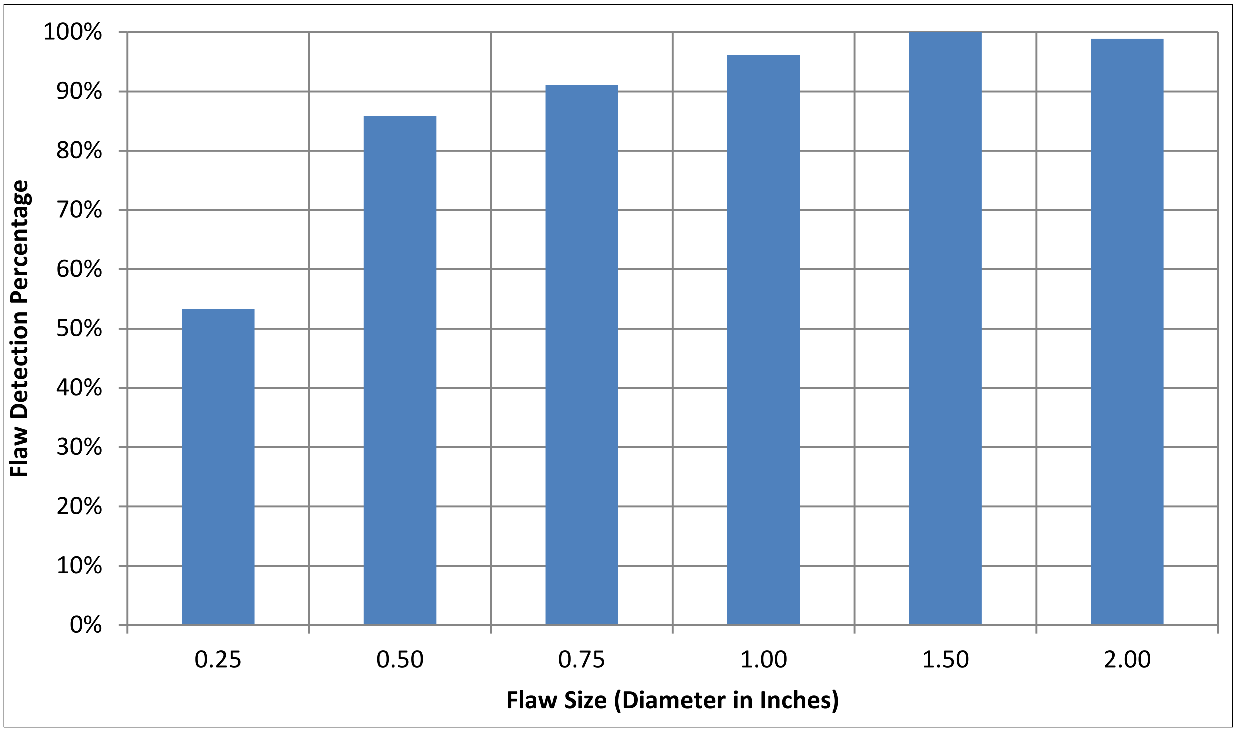

Figure 112. Overall flaw detection percentage chart for the 20–32 ply specimen set for all flaws in CT regions; all inspectors—PE UT method

Table 22. Tabulated results showing overall flaw detection percentage and accuracy in determining flaw size for the 20–32 ply specimen set for all flaws in the CG regions; all inspectors—PE UT method

Overall Flaw Detection Percentage & Accuracy in Determining Flaw Size 20-32 Ply Specimen Set – All Inspectors – All Complex Geometry (CG) Flaws							
Accuracy in Sizing the Flaws That Were Detected (1086 Total Flaws Detected)						Flaw Detection Percentage (1290 Total Flaws)	
Flaw Size	5 (100%)	4 (96%-99%)	3 (51%-75%)	2 (25%-50%)	1 (< 25%)	Flaw Size	Percent Detected
0.25	46%	10%	3%	9%	32%	0.25	58%
0.50	30%	22%	16%	17%	15%	0.50	83%
0.75	27%	27%	20%	18%	8%	0.75	87%
1.00	26%	30%	21%	17%	7%	1.00	88%
1.50	26%	35%	25%	10%	5%	1.50	99%
2.00	27%	47%	17%	7%	3%	2.00	100%
Overall Sizing Performance	29%	27%	18%	14%	11%	Overall Flaw Detection	84%

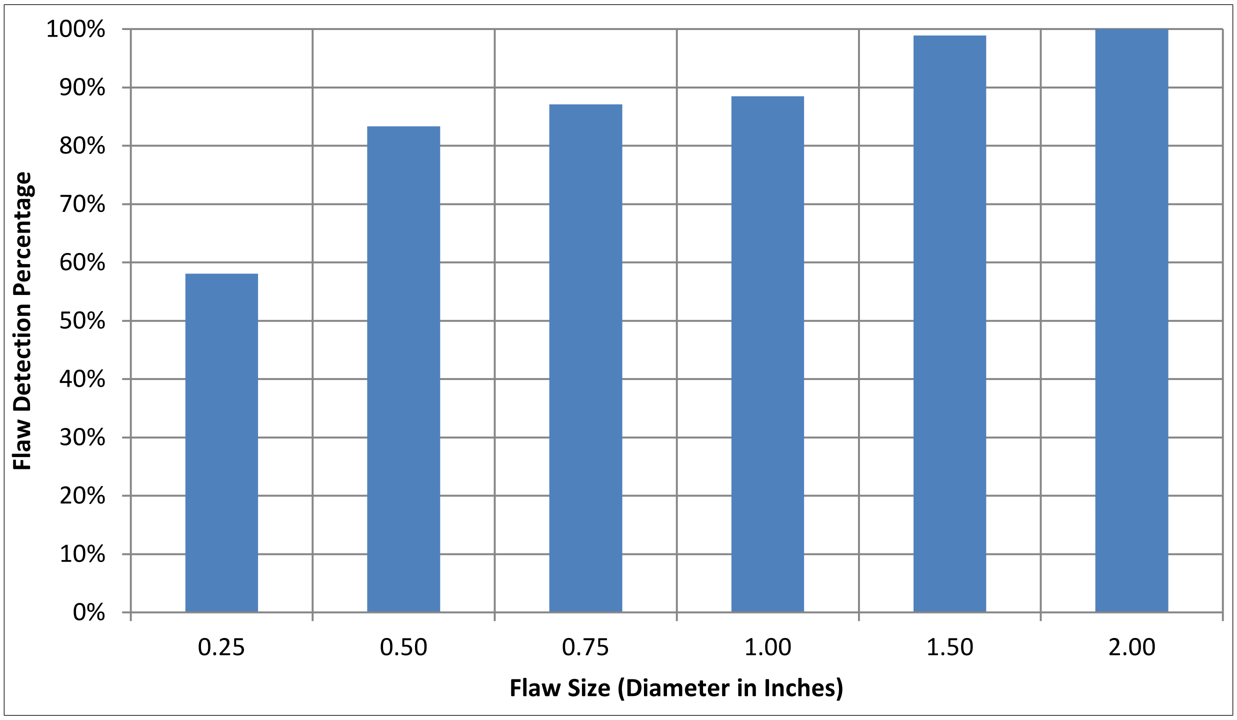

Figure 113. Overall flaw detection percentage chart for the 20–32 ply specimen set for all flaws in CG regions; all inspectors—PE UT method

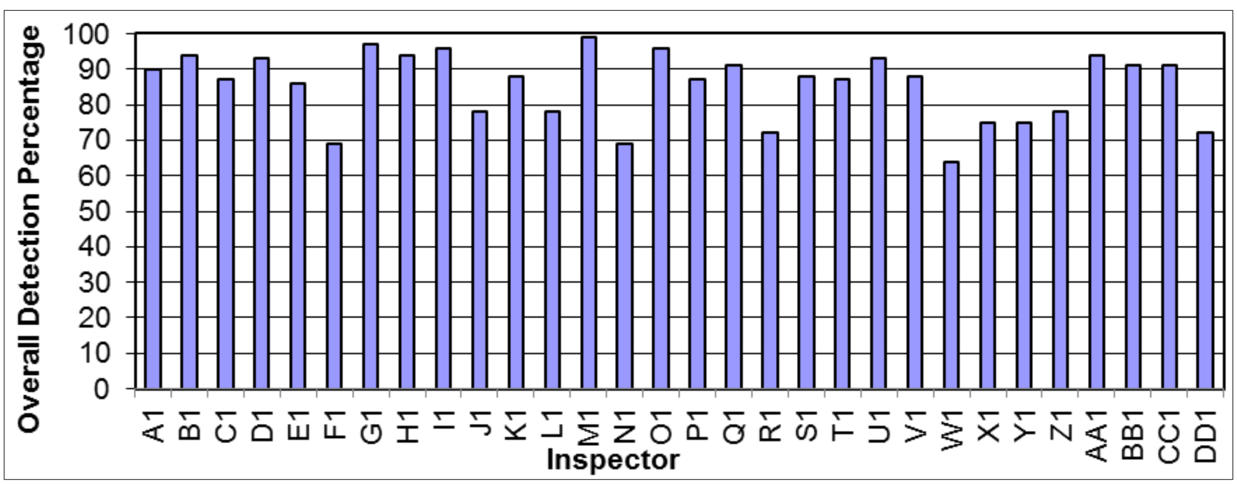

Figure 114. Inspector flaw detection percentage chart for the 20–32 ply specimen set for all flaws in the CT and CG regions—PE UT method

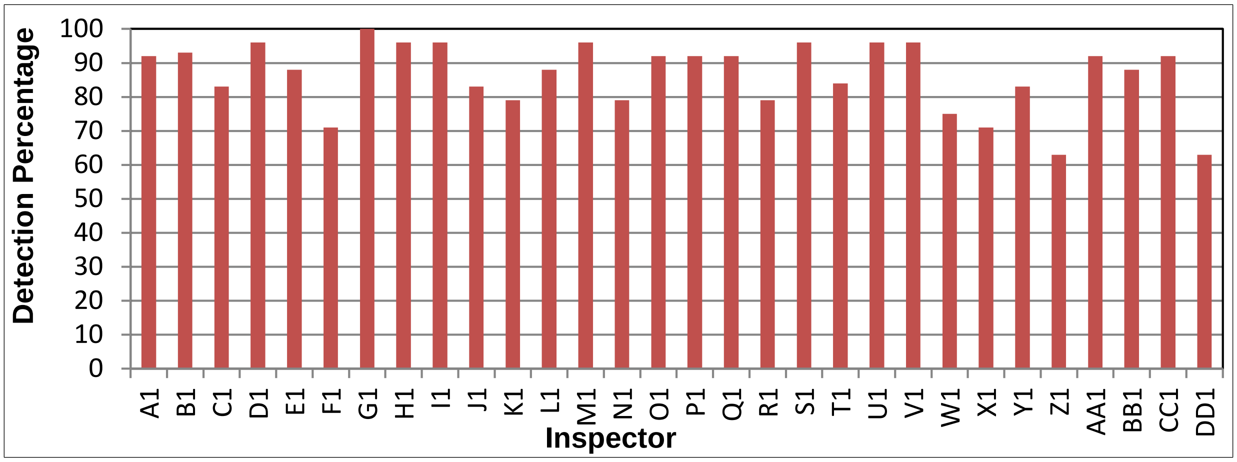

Figure 115. Inspector flaw detection percentage chart for the 20–32 ply specimen set for all flaws in the CT regions only—PE UT method

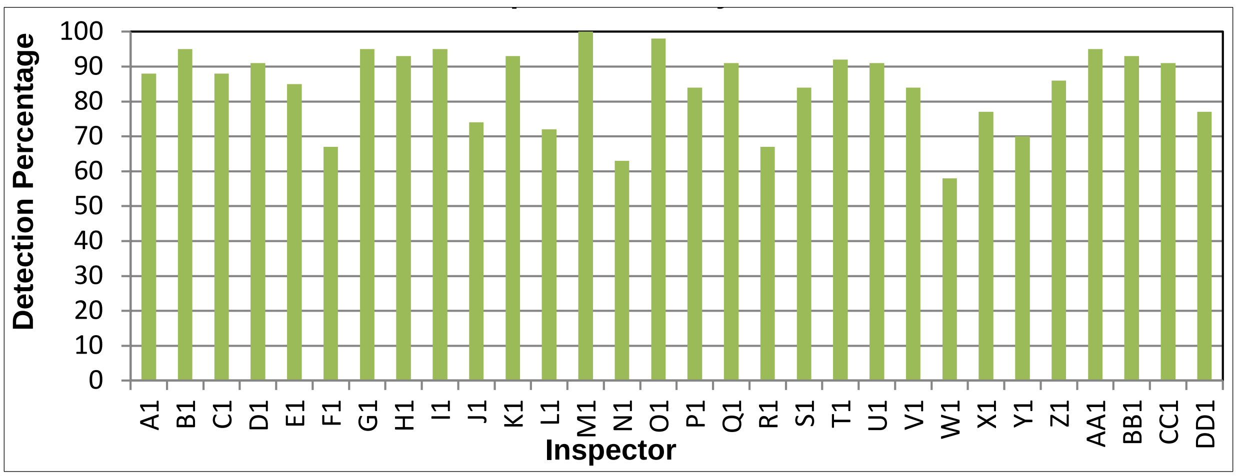

Figure 116. Inspector flaw detection percentage chart for the 20–32 ply specimen set for all flaws in the CG regions only—PE UT method

Table 23. Inspector's reported NDI experience level in years for the 20–32 ply specimen set—PE UT method

20-32 Inspector Reported Experience Level – Pulse Echo UT	
Years of NDI Experience	No. of Inspectors
1-3	4
4-8	8
9-12	8
13-16	2
17-20	3
21-24	3
25 or Greater	2

Table 24. Inspector's reported PE UT NDI level for the 20–32 ply specimen set—PE UT method

20-32 Inspector Reported NDI Level Pulse Echo UT	
NDI Level	No. of Inspectors
I	3
II	22
III	5

Table 25. Inspector's reported experience with composites in years for the 20–32 ply specimen set—PE UT method

20-32 Inspector Reported Experience Level – Composites	
Years of NDI Experience	No. of Inspectors
Trained, No Exp.	3
< 1	2
1-3	9
4-8	7
9-12	4
13-16	1
17-20	4

6.3 INSPECTION PERFORMANCE RESULTS FOR THE OVERALL COMBINED SOLID LAMINATE INSPECTION EXPERIMENT—COMBINED 12–20 PLY THIN LAMINATE EXPERIMENT AND 20–32 PLY THICK LAMINATE EXPERIMENT

6.3.1 Overall Results

Figure 117 shows the POD curve representing the performance of all 57 inspectors for the cumulative, combined 12–20 and 20–32 ply specimen sets. The overall POD for solid laminate composite structures is $POD_{[90/95]}$ = 1.13″ diameter flaw ($POD_{[90]}$ = 1.07″). This represents a POD value that is consistent with the desired OEM minimum detectable flaw size as discussed in section 4. Figure 118 shows a modified calculation of the $POD_{[90/95]}$ curve after the two highest (worst performing) and two lowest (best performing) inspector POD values from each specimen set were removed from the combined dataset. The difference between the two $POD_{[90/95]}$ values is less than 3%, again showing consistency of the results for the combined specimen set and the robustness of the statistics in this entire experiment. The cumulative POD curve comparison for the 12–20 ply thin laminate experiment ($POD_{[90/95]}$ = 1.29″), the 20–32 ply thick laminate experiment ($POD_{[90/95]}$ = 0.82″) and the overall, combined specimen sets ($POD_{[90/95]}$ = 1.13″) are shown in figure 119.

6.3.2 Effects of CG

POD values were also analyzed for the combined specimen sets within the categorization of specific composite construction regions. Figure 120 shows the cumulative POD curve for the combined 12–20 and 20–32 ply specimen sets for all flaws in the CT regions. The overall POD for CT regions in solid laminate composite structures is $POD_{[90/95]}$ = 0.80″ diameter flaw. This represents a value calculated from inspection data for all flaws in the 12-ply, 20-ply, 32-ply, and 38-ply (spar component) CT regions. Figure 121 compares the CT region POD curves for the 12–20 ply and 20–32 ply experiments and the overall, combined specimen sets. All of the $POD_{[90/95]}$ values are quite similar and are in the range of 0.75″–0.85″ diameter flaw. Figure 122 shows the resulting cumulative POD curve for the combined 12–20 and 20–32 ply specimen sets for all flaws in the CG regions. The overall POD for CG regions in solid laminate composite structures is $POD_{[90/95]}$ = 1.34″ diameter flaw. This represents a value calculated from inspection data for all flaws in regions containing a ply taper, substructure (co-cured and secondarily bonded), curved portions, fasteners, or laminate over honeycomb. Figure 123 compares the CG region POD curves for the 12–20 ply thin laminate experiment, 20–32 ply thick laminate experiment, and overall, combined specimen sets. In this case, the $POD_{[90/95]}$ values range from 0.93″–1.49″ diameter flaw. The last type of geometry that could be combined for analysis is the tapered regions. Figure 124 shows the cumulative POD curve for the combined 12–20 and 20–32 ply specimen sets for all flaws in the tapered regions, with a resulting overall $POD_{[90/95]}$ = 0.78″ diameter flaw. Figure 125 compares the tapered region POD curves for the 12–20, 20–32, and combined specimen sets.

The experiment monitors also recorded the various methods that inspectors used to ensure inspection area coverage for the composite laminate POD experiment. Some inspectors covered the inspection area with their UT transducers using a pure freehand approach (i.e., no guides or markings on the panels). Some inspectors divided the inspection surface into quadrants to reduce freehand coverage errors. Some inspectors used a series of tick marks, often placed at 0.5″ or 1″

intervals, to divide the inspection surface into a number of rows and columns; some inspectors used flexible straight edges to guide their transducer movement. The different surface coverage techniques that were observed fall into four categories. The POD results achieved by each of these inspection coverage methods were calculated separately and compared to quantify the benefits of using specific inspection coverage methods.

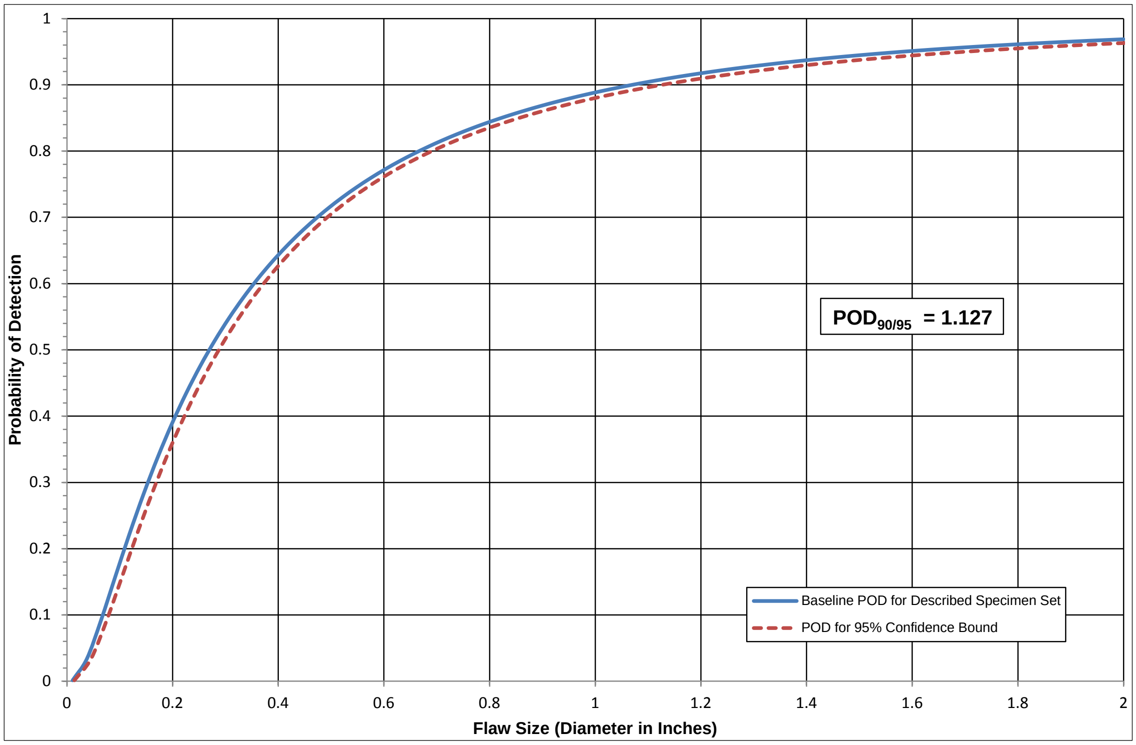

Figure 117. Cumulative POD curve for the 12–20 and 20–32 ply combined specimen sets for all flaws in the CT and CG regions; all inspectors (57)—PE UT method

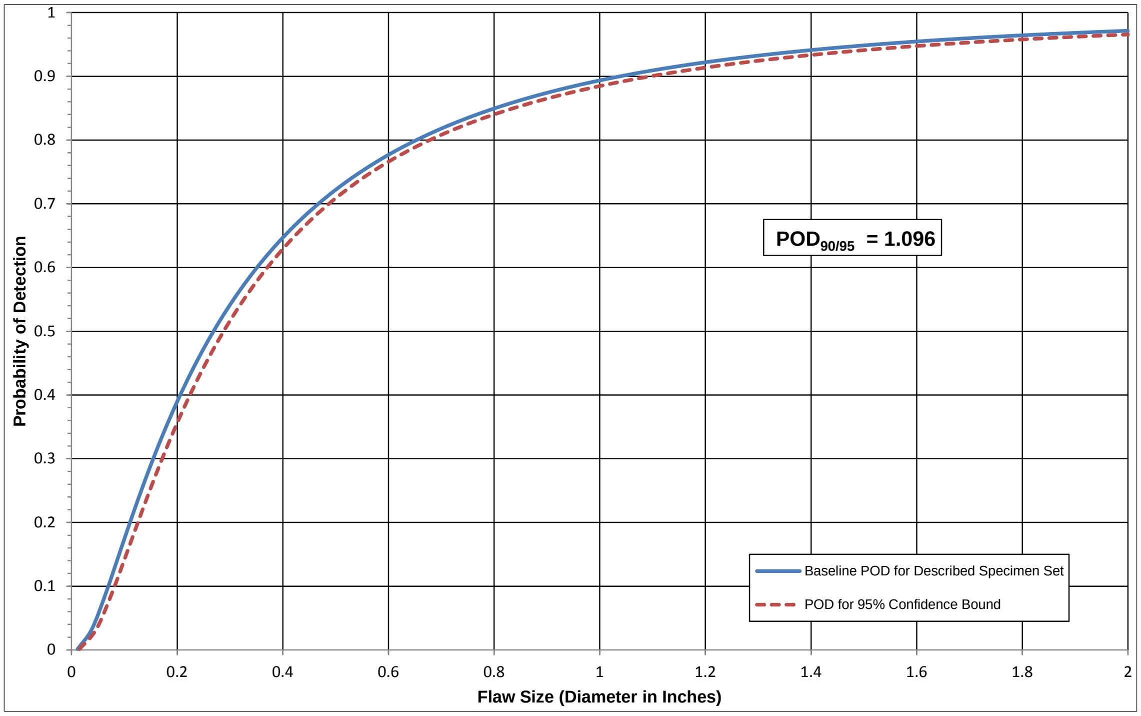

Figure 118. Cumulative POD curve with the two highest and two lowest inspector POD values removed from each specimen set for the 12–20 and 20–32 ply combined specimen sets for all flaws in the CT and CG regions; 49 inspectors—PE UT method

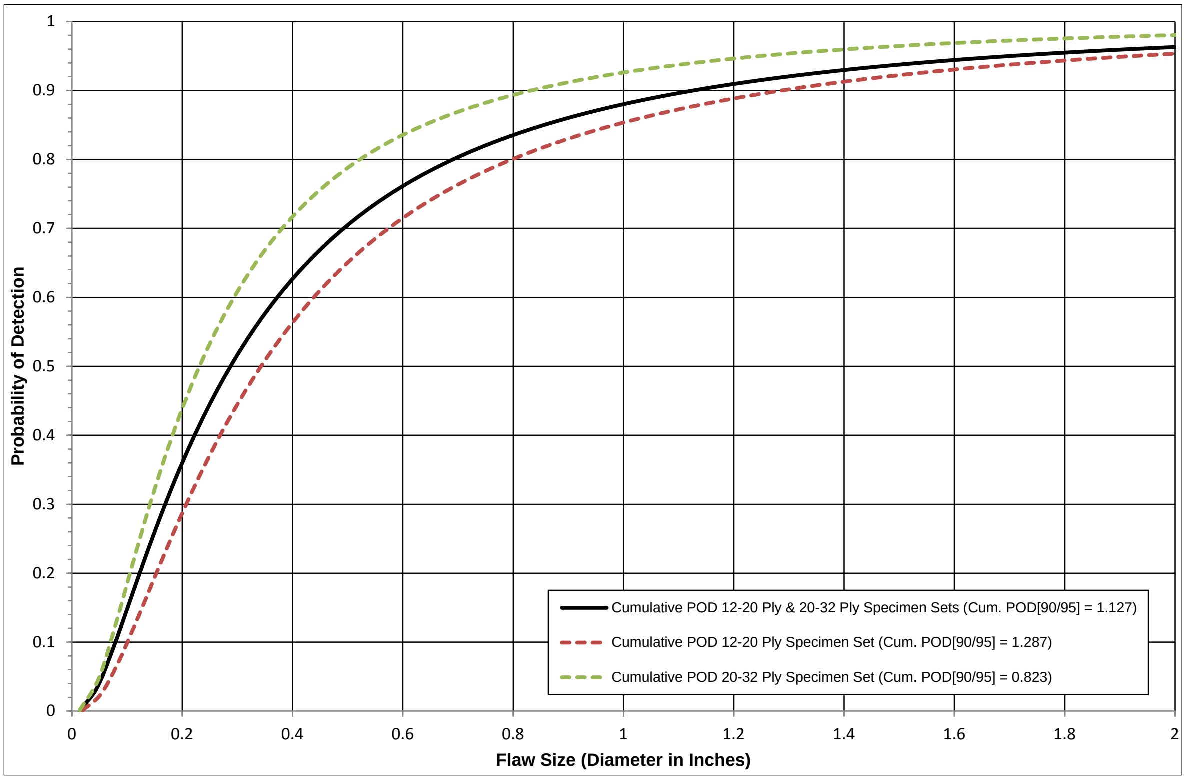

Figure 119. Cumulative POD curve comparison for the 12–20 and 20–32 ply specimen sets for all flaws in CT and CG regions; all inspectors (57)—PE UT method

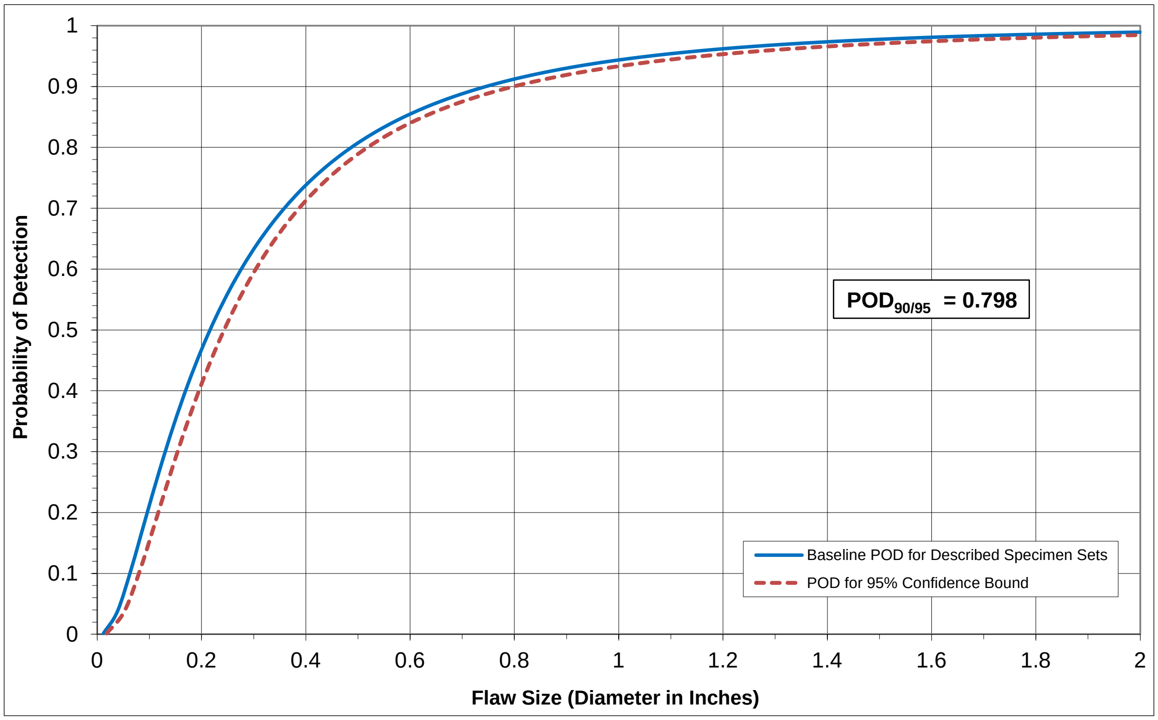

Figure 120. Cumulative POD curve for the 12–20 and 20–32 ply combined specimen sets for all flaws in the CT regions only; all inspectors (57)—PE UT method

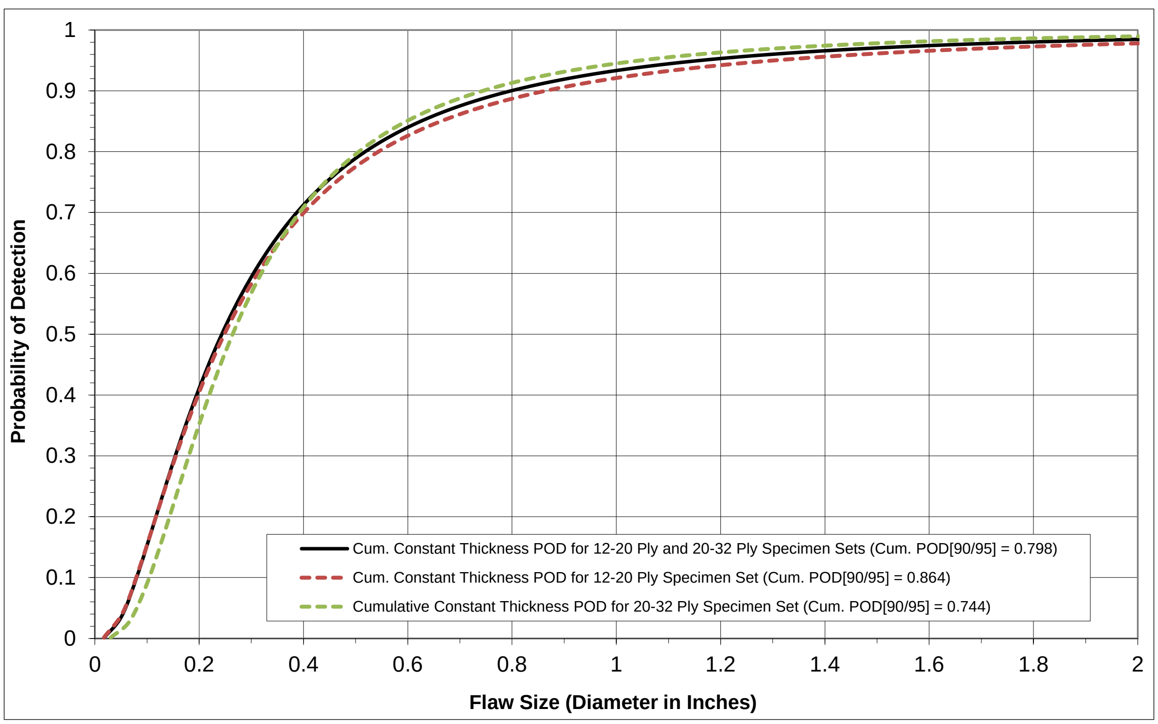

Figure 121. Cumulative POD curve comparison for the 12–20 and 20–32 ply specimen sets for all flaws in the CT regions only; all inspectors (57)—PE UT method

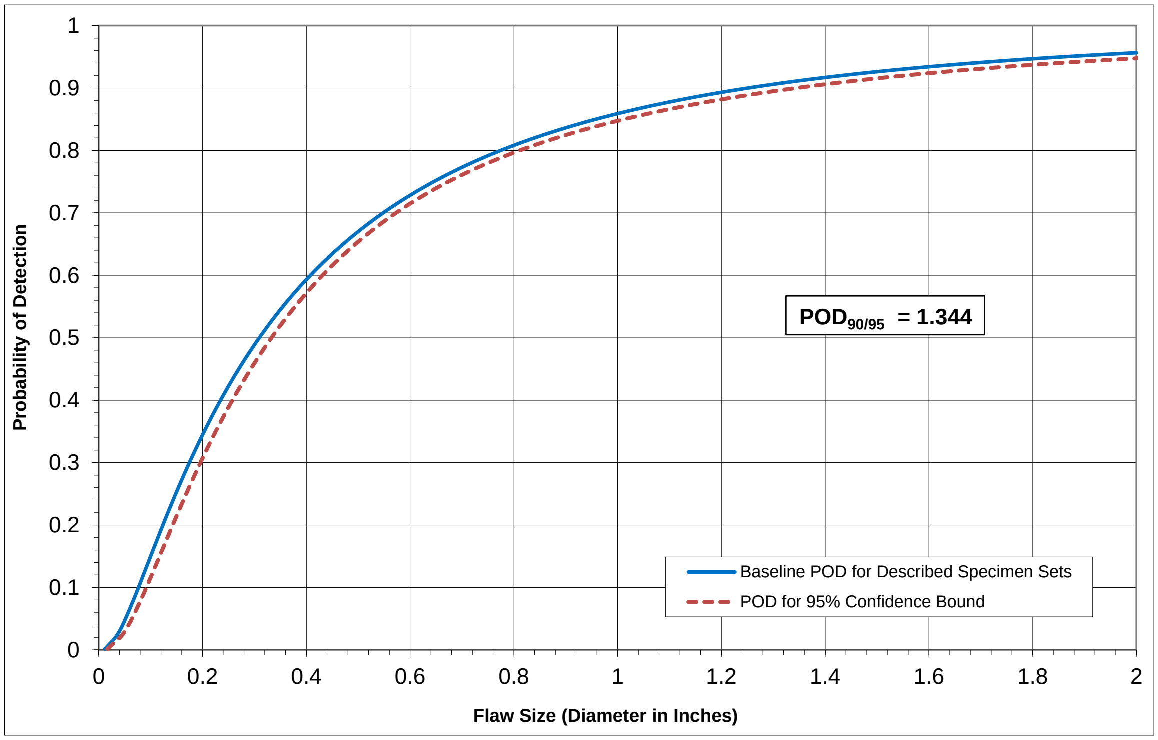

Figure 122. Cumulative POD curve for the 12–20 and 20–32 ply combined specimen sets for all flaws in the CG regions only; all inspectors (57)—PE UT method

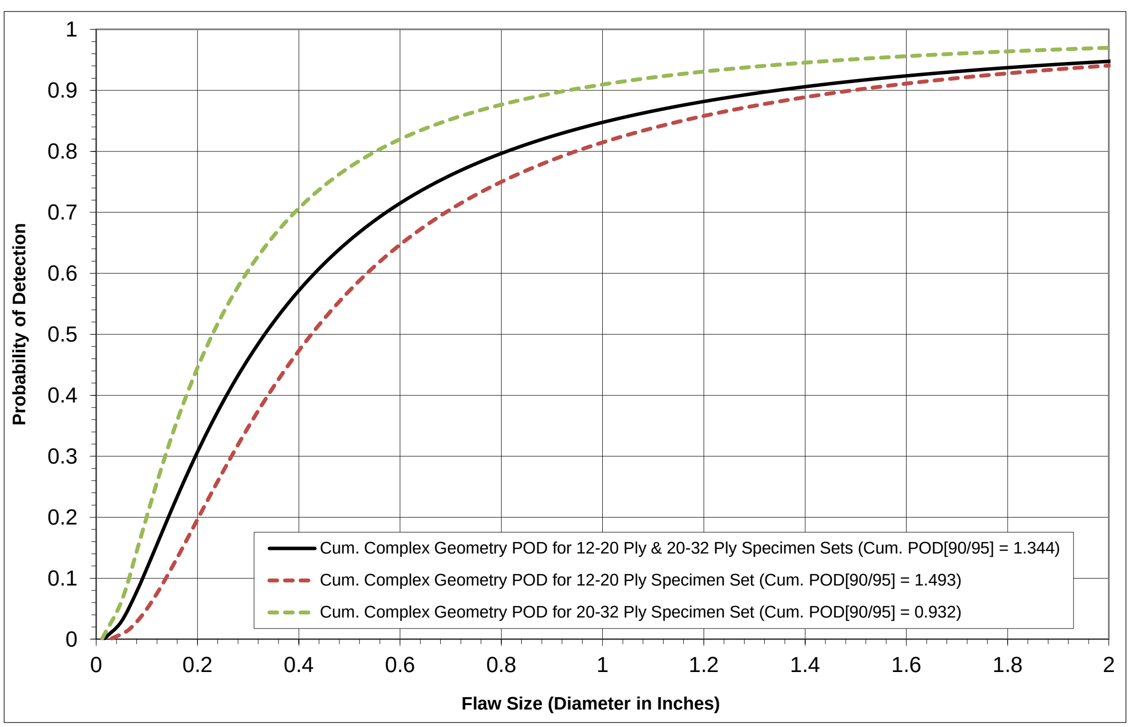

Figure 123. Cumulative POD curve comparison for the 12–20 and 20–32 ply specimen sets for all flaws in the CG regions only; all inspectors (57)—PE UT method

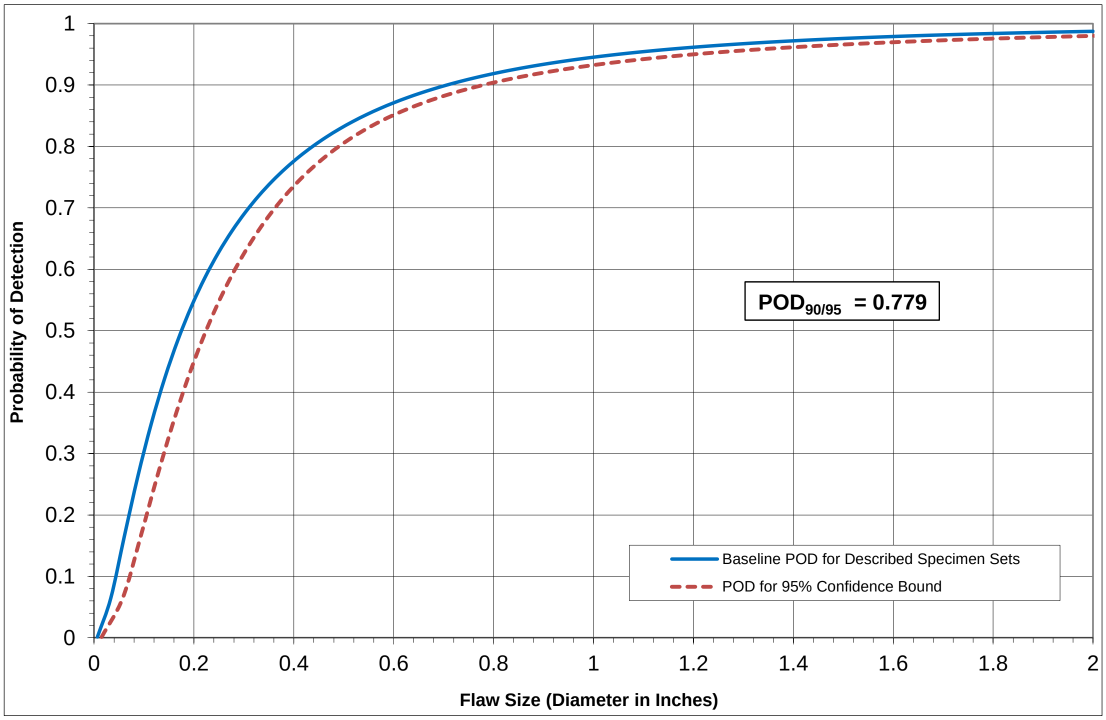

Figure 124. Cumulative POD curve for the 12–20 and 20–32 ply combined specimen sets for all flaws in tapered regions only; all inspectors (57)—PE UT method

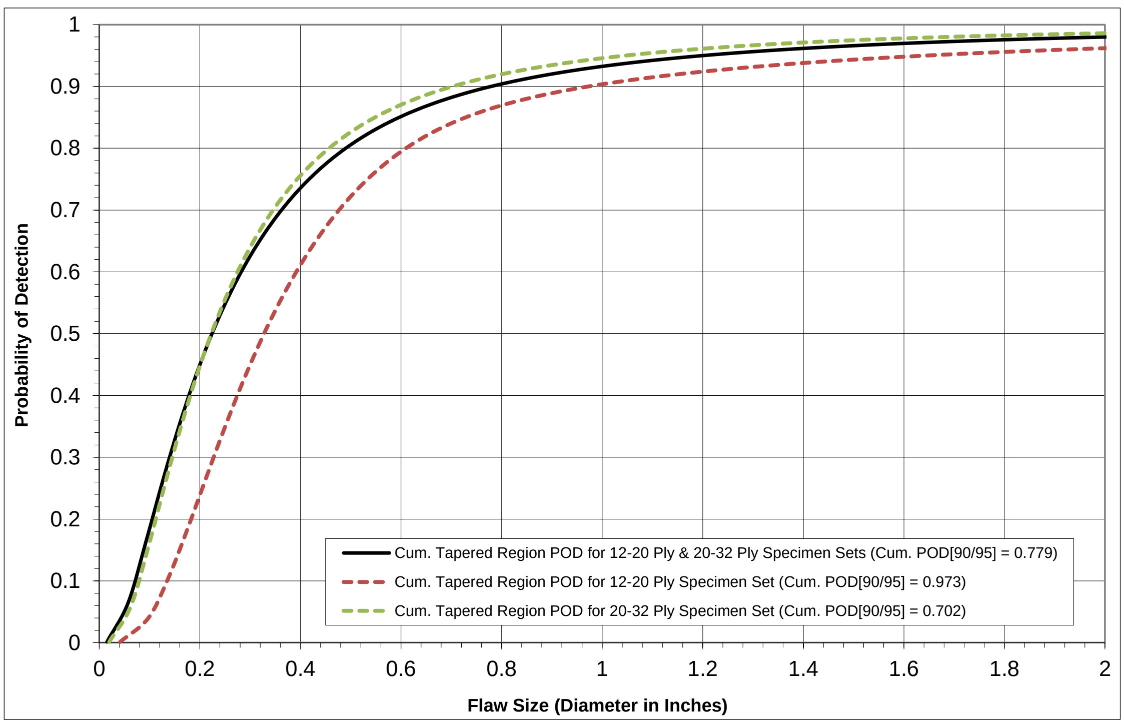

Figure 125. Cumulative POD curve comparison for the 12–20 and 20–32 ply specimen sets for all flaws in tapered regions only; all inspectors (57)—PE UT method

The results from the four different surface coverage methods were combined and analyzed for the overall solid laminate POD experiment. The POD results produced by each of these inspection coverage methods for the 12–20 ply and 20–32 ply specimen sets were combined and calculated separately. These are plotted in figure 126 along with the corresponding $POD_{[90/95]}$ values. Figures 127–130 show the individual POD curves for each combined coverage technique (maximum likelihood estimate baseline POD and the 90/95 POD). The method that produced the lowest (best) combined POD level was that in which inspectors used a straight edge on all panels throughout both experiments (18 inspectors). This produced a $POD_{[90/95]}$ = 0.89″, which is a 21% improvement compared to the overall, cumulative combined 12–20 ply and 20–32 ply $POD_{[90/95]}$ value of 1.13″ diameter flaw. The second-best performing coverage method was that in which inspectors made tick marks for spacing and used a straight edge on all panels throughout both experiments (13 inspectors), achieving a $POD_{[90/95]}$ = 0.91″ diameter flaw. This produced a 19% improvement compared to the overall cumulative combined 12–20 ply and 20–32 ply $POD_{[90/95]}$ value. The third-best performing coverage method was that in which inspectors started the experiments using a straight edge but at some point during the experiments switched to freehand (13 inspectors). This method produced a $POD_{[90/95]}$ = 1.29″, which is actually a decrease in performance of 15% compared to the overall cumulative combined 12–20 ply and 20–32 ply $POD_{[90/95]}$ value. The point at which an inspector switched to freehand was not documented, but it was observed and noted during the experiment that the inspector switched to freehand coverage after starting the experiment using a straight edge. The poorest performing coverage method was that in which inspectors used the freehand method on all panels throughout both experiments (13 inspectors). This produced a $POD_{[90/95]}$ = 1.75″, which is a 55% decrease in performance compared to the overall cumulative combined 12–20 ply and 20–32 ply $POD_{[90/95]}$ value. The summary of all $POD_{[90/95]}$ values for the overall solid laminate POD experiment (combined 12–20 ply and 20–32 ply specimen sets) is shown in table 26.

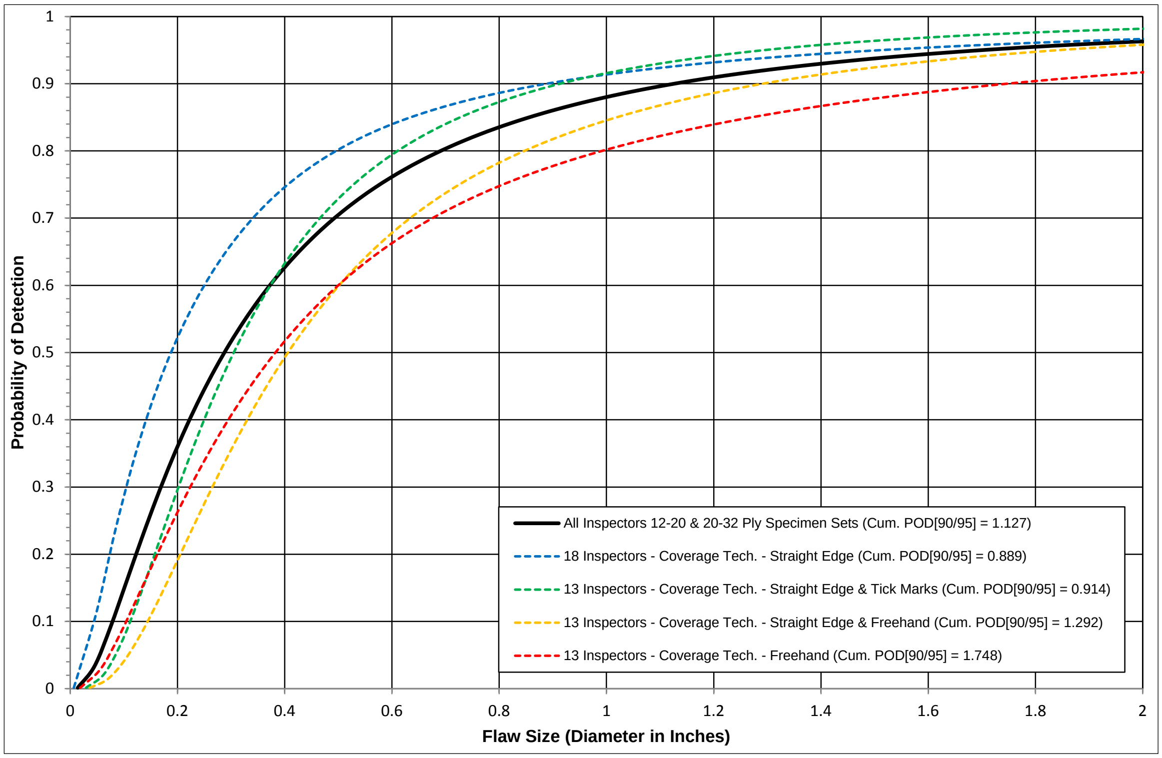

Figure 126. Cumulative POD curve comparison of different surface coverage techniques for the 12–20 and 20–32 ply specimen sets for all flaws in the CT and CG regions; all inspectors (57)—PE UT method

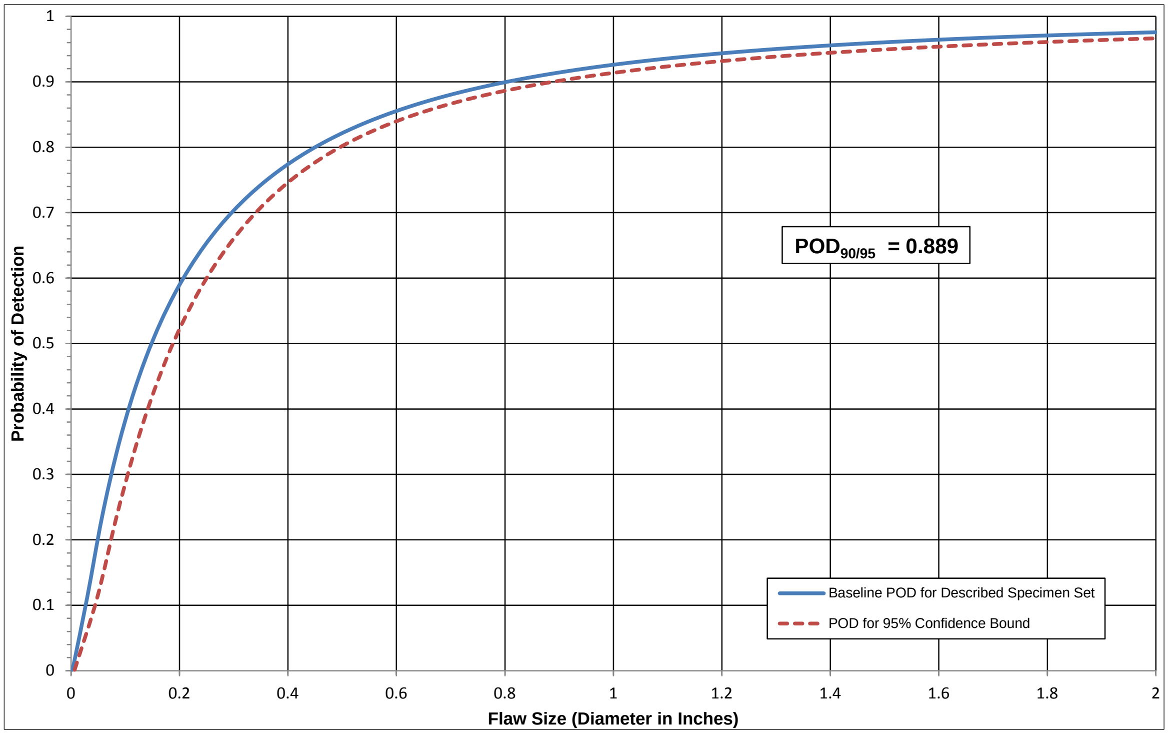

Figure 127. Cumulative POD curve for the straight edge coverage technique (7 inspectors [12–20 ply] and 11 inspectors [20–32 ply]) for the 12–20 and 20–32 ply combined specimen sets for all flaws in the CT and CG regions—PE UT method

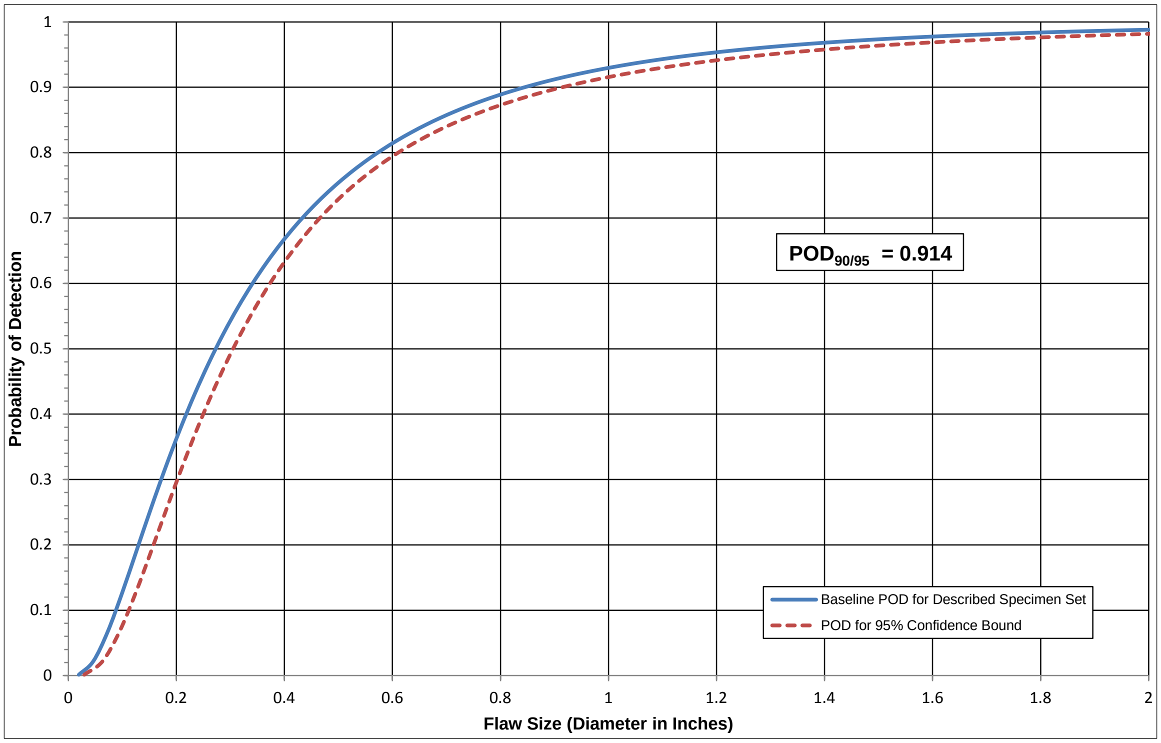

Figure 128. Cumulative POD curve for the straight edge and tick marks (indexing) coverage technique (7 inspectors [12–20] and 6 inspectors [20–32]) for the 12–20 and 20–32 ply combined specimen sets for all flaws in the CT and CG regions—PE UT method

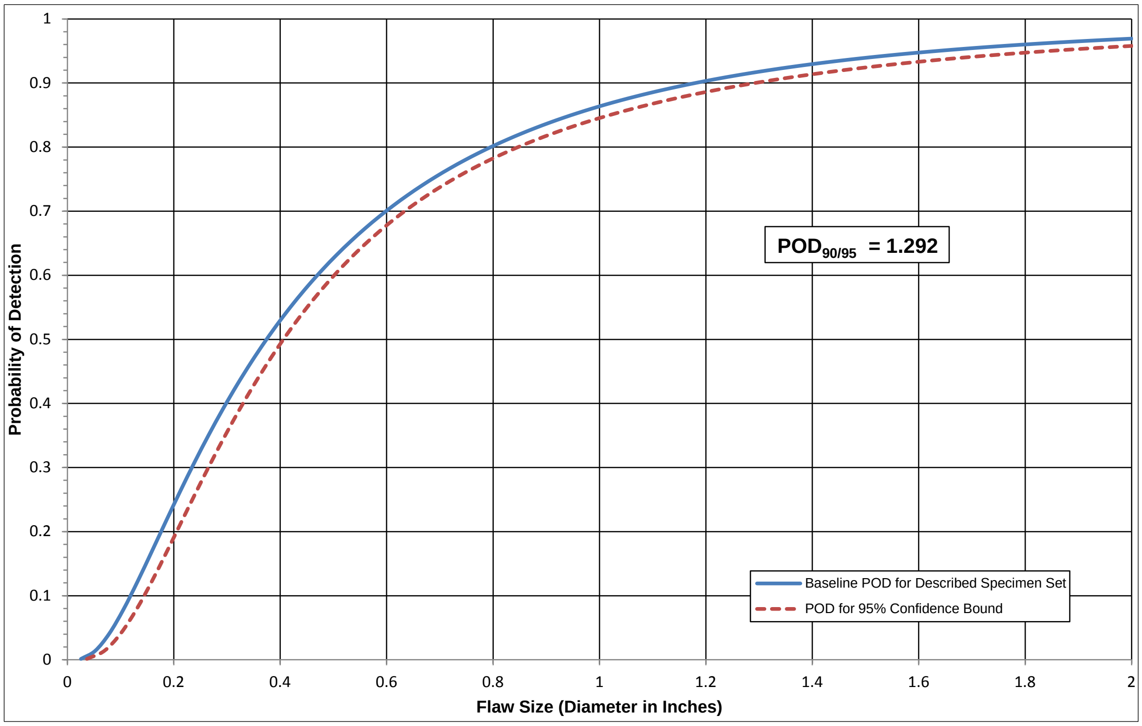

Figure 129. Cumulative POD curve for the straight edge and freehand coverage technique for the 12-20 ply (eight inspectors) and 20–32 ply (five inspectors) combined specimen sets for all flaws in the CT and CG regions—PE UT method

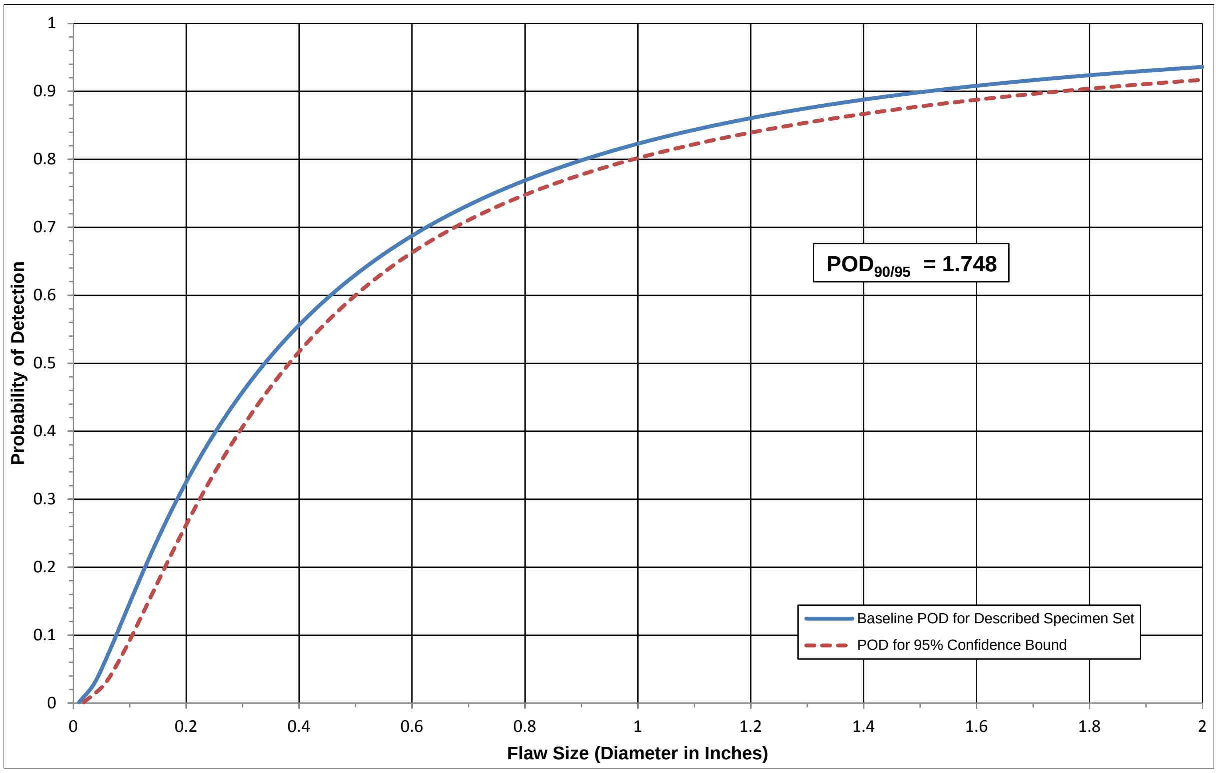

Figure 130. Cumulative POD curve for the freehand coverage technique (five inspectors [12–20 ply] and eight inspectors [20–32 ply]) for the 12–20 and 20–32 ply combined specimen sets for all flaws in the CT and CG regions—PE UT method

Table 26. Cumulative POD results table for the 12–20 and 20–32 ply combined specimen sets

Cumulative POD Results Table, 12-20 Ply & 20-32 Ply Specimen Sets	
Condition	$POD_{90/95}$
All Flaws – All Regions – All 57 Inspectors	1.127
All Flaws – All Regions – 49 Inspectors, 2 High & 2 Low Removed From Each Set	1.096
Only Flaws in Constant Thickness – All 57 Inspectors	0.798
Only Flaws in Complex Geometry Regions – All 57 Inspectors	1.344
Only Flaws in Tapered Regions – All 57 Inspectors	0.779
All Flaws – All Regions – 18 Inspectors – Coverage Technique – Straight Edge	0.889
All Flaws – All Regions – 13 Inspectors – Coverage Technique – Straight Edge & Tick Marks	0.914
All Flaws – All Regions – 13 Inspectors – Coverage Technique – Straight Edge & Freehand	1.292
All Flaws – All Regions – 13 Inspectors – Coverage Technique – Freehand	1.748

6.4 INSPECTION PERFORMANCE RESULTS FOR THE RDCE

6.4.1 Overall Results

The solid laminate POD experiment was also used to evaluate two similar devices that are being considered for use in local, focused inspections: the RDC and BT devices. The following POD curves compare the performance of individual participants, which included both inspectors and A&P mechanics, for the deployment of the RDC and BT in the SLE. This experiment was customized, as described in section 4, to accommodate the evaluation of the RDC and BT devices. For the inspection approach that accompanies the use of either the RDC or the BT device, specific, small regions were designated as focused inspection regions. These devices are not intended for wide-area inspections. Thus, specific regions on each test specimen—some containing flaws and some containing only pristine, undamaged structure—were identified with surface markers and the experiment was completed using only the subset of inspection regions. In total, there were 140 separate inspection regions for a total, combined inspection area of 8.4 ft^2 (average of 0.06 ft^2 per individual region). The RDCE is the customized presentation of the SLE. All of the specimens (both thin and thick laminate) were used in the RDCE, so the results provided in this section are the overall results for the entire range of specimen thicknesses. Prior to conducting the RDCE, each inspector was provided with a brief training package on the RDC and BT devices. The inspectors were also allowed to familiarize themselves with the inspection devices through the use of the feedback specimens.

Figure 131 shows the spread of all individual inspector $POD_{[90]}$ curves (dashed lines) compared to the cumulative $POD_{[90]}$ curve (solid line) for all 20 participants in the RDCE. The participants included 10 A&P mechanics, 9 NDI inspectors, and 1 student intern (to represent an untrained person). These results were produced by considering all flaws in the RDCE, including those in the CT and CG regions. The spread shows 11 participants with a $POD_{[90]}$ value less than the cumulative $POD_{[90]}$ = 0.75″ diameter flaw and 9 participants with a $POD_{[90]}$ value higher than the cumulative $POD_{[90]}$ value. Overall, the result from the RDCE for all participants combined was $POD_{[90/95]}$ = 0.78″ diameter flaw. The variation of results ranged from a $POD_{[90]}$ = 0.44″ diameter flaw for the best performing participant to a $POD_{[90]}$ = 1.38″ diameter flaw for the worst performing participant. A total of 19 of the 20 participants performed better than (below) a $POD_{[90]}$ = 0.90″ diameter flaw. The standard deviation in the $POD_{[90]}$ for the entire set of participants is 0.20″ diameter flaw. The variation among the inspectors who participated in the RDCE ranged from a $POD_{[90]}$ = 0.44″ diameter flaw for the best performing inspector to a $POD_{[90]}$ = 1.38″ diameter flaw for the worst performing inspector. It was noted by the experiment monitors that the worst performing inspector, whose results were quite a bit above the tight cluster of other inspectors' results, was not looking at the device when scanning. This inspector also kept the device far away from the probe and only occasionally looked at the screen while scanning. It was noted that flaws were missed by the inspector using this scanning method, meaning that the device indicated flaws that the inspector did not notice. Additional procedural guidance concerning the placement of the device relative to the inspection surface could minimize this reduction in performance caused by poor equipment monitoring. The variation among the A&P mechanics who participated in the RDCE ranged from a $POD_{[90]}$ = 0.65″ diameter flaw for the best performing A&P mechanic to a $POD_{[90]}$ = 0.87″ diameter flaw for the worst performing A&P mechanic. It should be noted that the student intern performed well with a $POD_{[90]}$ = 0.48″ diameter flaw. The student intern represented a data point for someone with no

NDI or A&P experience. This allowed us to study the deployment of a pass/fail device by someone with minimal training.

Figure 132 compares the maximum likelihood estimate ($POD_{[90]}$) to the POD curve that is calculated when a 90% flaw detection level is combined with a 95% confidence bound ($POD_{[90/95]}$). The solid line in figure 132 provides the performance curve that the industry normally uses to measure the performance of NDI methods as deployed by representative inspectors. It can be seen in figure 132 that the cumulative $POD_{[90/95]}$ for all flaws and all participants in the RDCE was $POD_{[90/95]}$ = 0.78″ diameter flaw.

The POD values were analyzed further to compare the flaw detection performance between the participant groups. Figure 133 compares the $POD_{[90/95]}$ cumulative curves for all inspectors and A&P mechanics. Both participant groups performed well with the 9 inspectors producing a cumulative $POD_{[90/95]}$ = 0.77″ diameter flaw and the 10 A&P mechanics producing a cumulative $POD_{[90/95]}$ = 0.84″ diameter flaw. The difference between the two POD values is less than 10%. Figures 132–134 compare the maximum likelihood estimate ($POD_{[90]}$) to the POD curve that is calculated when a 90% flaw detection is combined with a 95% confidence bound ($POD_{[90/95]}$). Figure 134 shows the cumulative $POD_{[90]}$ and $POD_{[90/95]}$ curves for the 9 inspectors who participated in the RDCE. Figure 135 shows the cumulative $POD_{[90/95]}$ performance improvement after the worst inspector (outlier curve shown in figure 129) was removed from the dataset. Removing the worst inspector resulted in a 12% lower (better) cumulative $POD_{[90/95]}$ = 0.68″ diameter flaw when compared to the cumulative $POD_{[90/95]}$ = 0.77″ for all inspectors. Figure 136 shows the cumulative $POD_{[90]}$ and $POD_{[90/95]}$ curves for the 10 A&P mechanics who participated in the experiment, achieving a cumulative $POD_{[90/95]}$ = 0.84″ diameter flaw. The summary of all $POD_{[90/95]}$ values for the RDCE is presented in table 27.

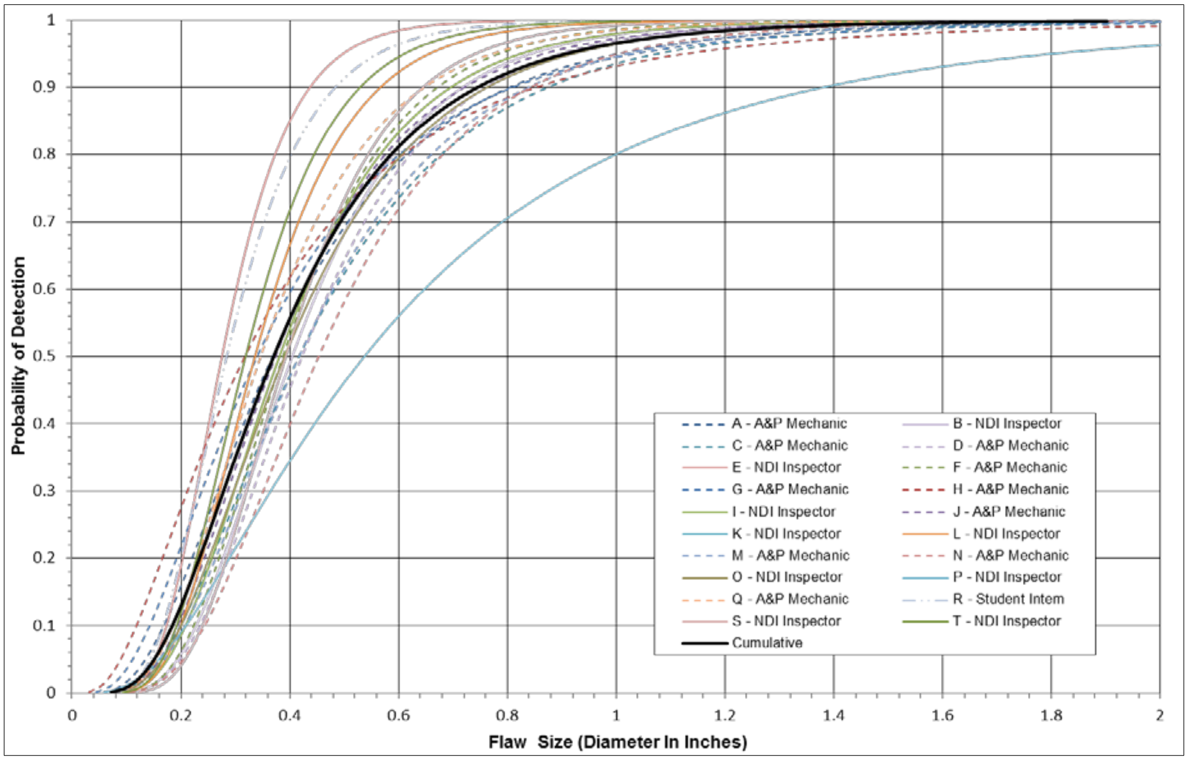

Figure 131. Individual and cumulative POD curve comparison for the RDCE specimen set for all flaws; all participants (10 A&P mechanics, 9 NDI inspectors, and 1 student intern)—BT and RDC

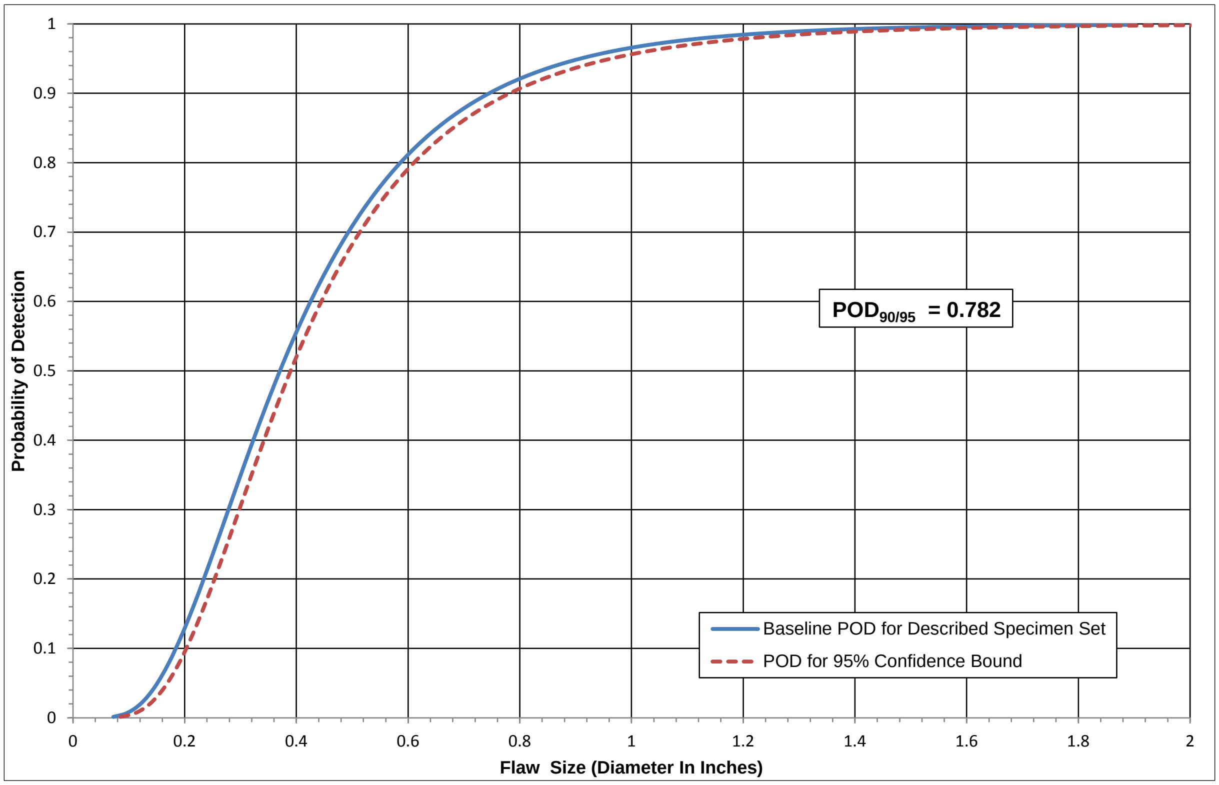

Figure 132. Cumulative POD curve for the RDCE specimen set for all flaws; all participants—BT and RDC

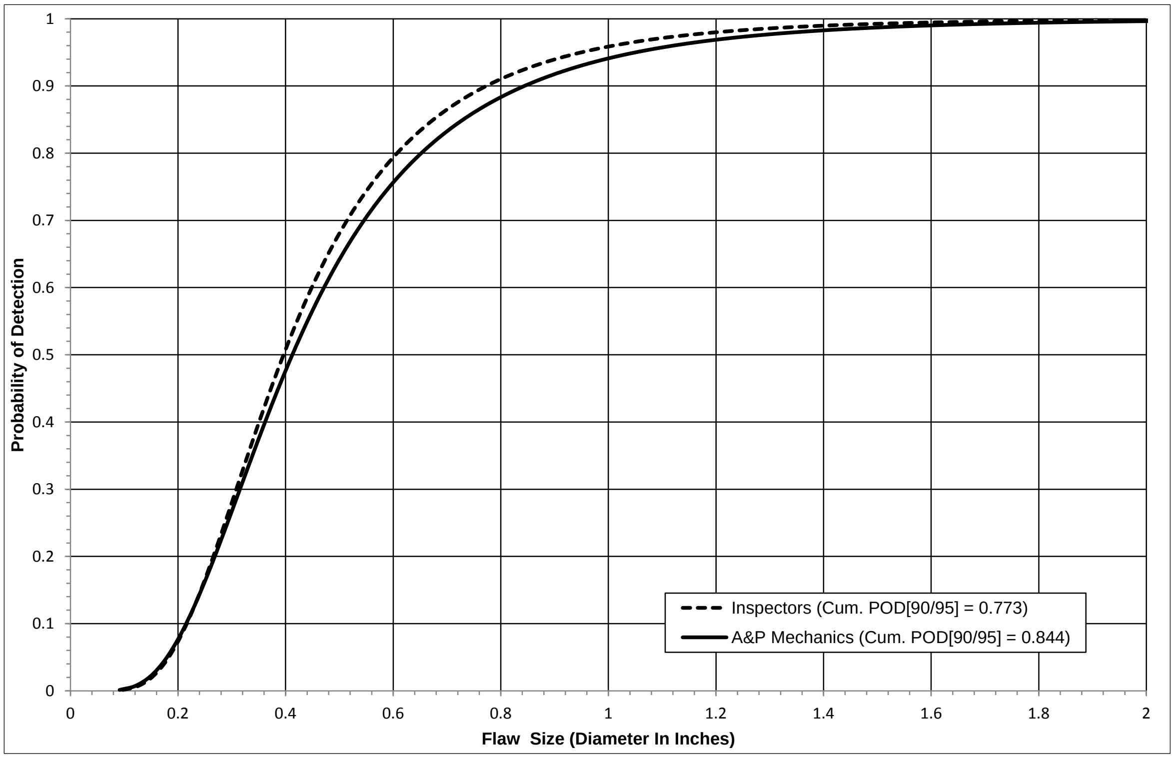

Figure 133. Cumulative POD curve comparison of all NDI inspectors and A&P mechanics for the RDCE specimen set for all flaws—BT and RDC

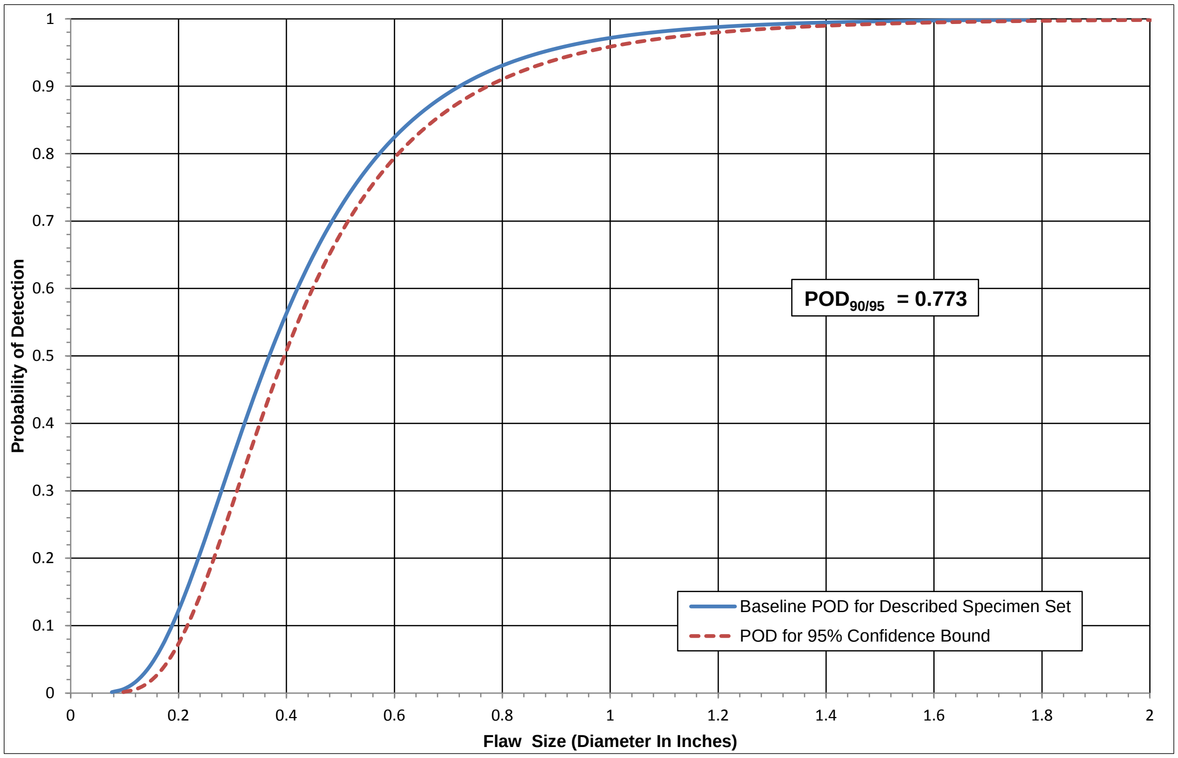

Figure 134. Cumulative POD curve for all NDI inspectors for the RDCE specimen set for all flaws—BT and RDC

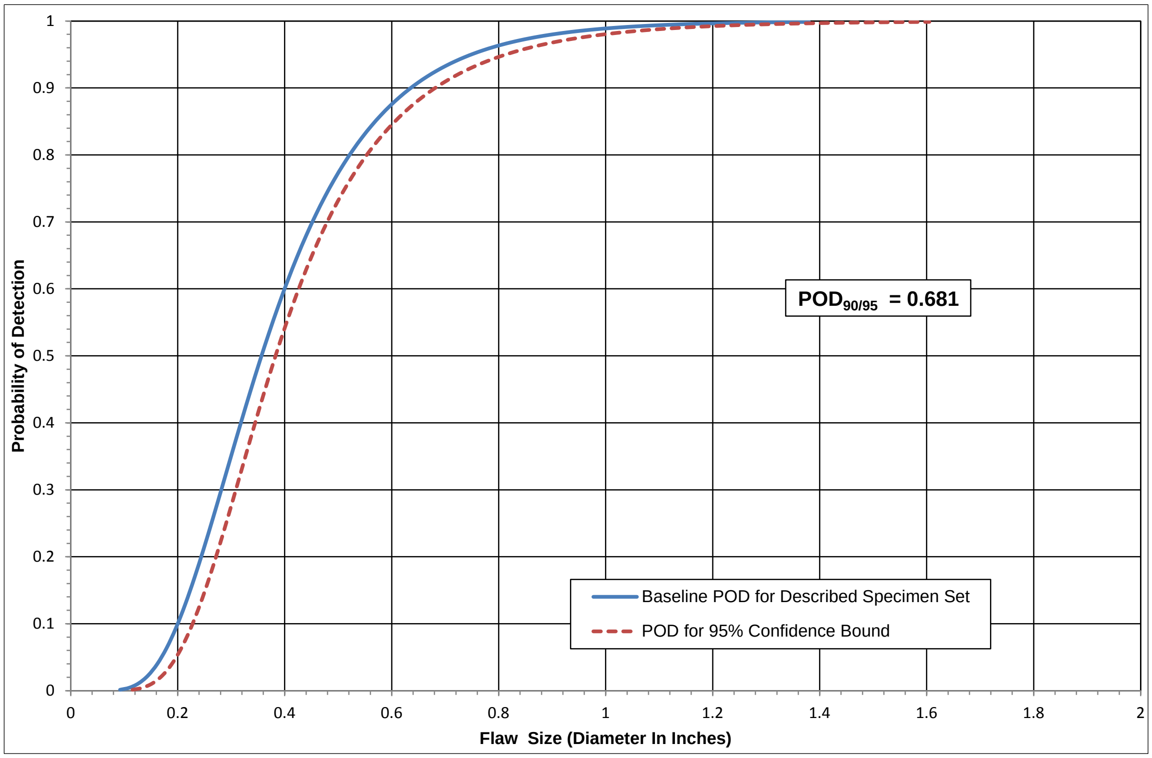

Figure 135. Cumulative POD curve for NDI inspectors (8) with worst performing inspector removed for the RDCE specimen set for all flaws—BT and RDC

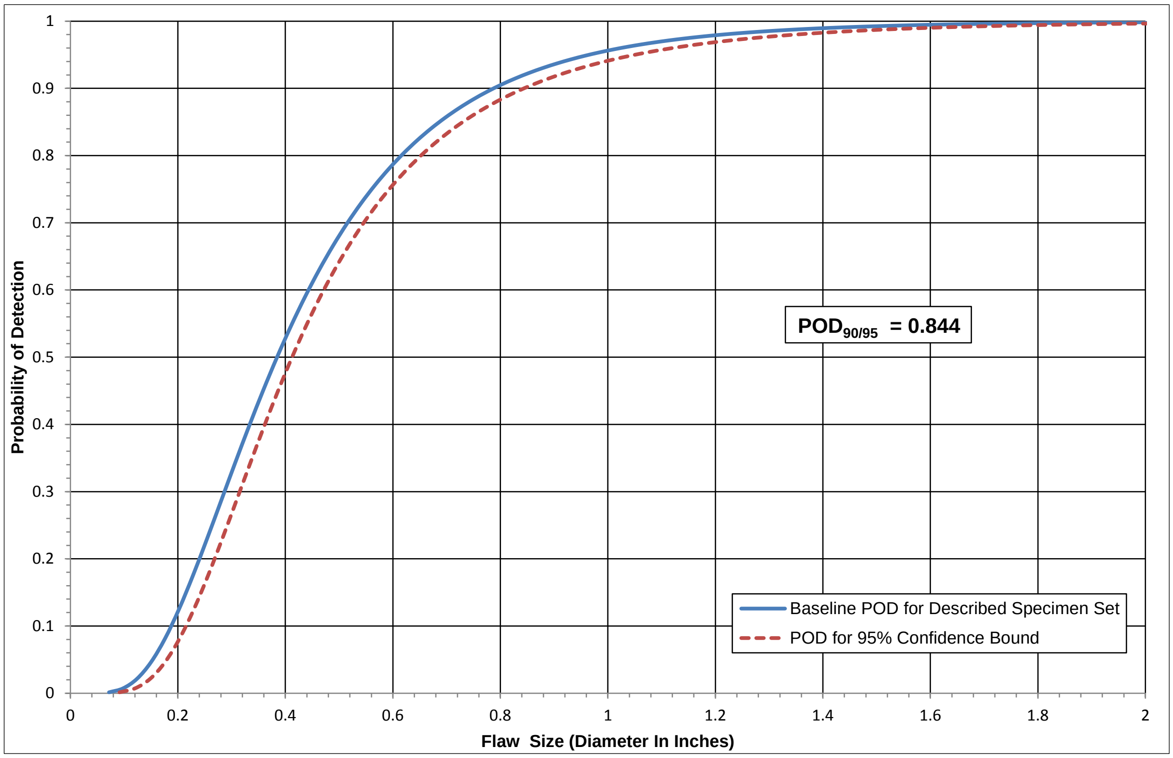

Figure 136. Cumulative POD curve for all A&P mechanics (10) for the RDCE specimen set for all flaws—BT and RDC

Table 27. Cumulative POD results table for the RDCE specimen set

Cumulative POD Results Table RDCE Specimen Sets	
Condition	$POD_{90/95}$
All Flaws – All Participants (Inspectors & A&P Mechanics, 1 Intern)	0.782
All Flaws – All NDI Inspectors (9)	0.773
All Flaws – NDI Inspectors (8) With Worst Performing Inspector Removed	0.681
All Flaws – All A&P Mechanics (10)	0.844

6.4.2 False Calls

A false call is defined as an inspector flaw indication in an area where no flaw actually exists. However, there are manufacturing flaws that are not associated with the POD study, such as porosity. If an inspector made a call that correlated to an area of unintentionally high porosity, it was ignored and not deemed to be a false call. Table 28 summarizes the number of false calls made by each participant during the RDCE. This table shows the number of false calls made by each participant for the RDCE specimen set and lists the sizing category that incorporates each false call. The average number of false calls made was determined to be 0.6 false calls per inspector (8.38 ft^2 inspection area), with an average of one false call per 13.97 ft^2 of inspection area. Thus, the overall false call rate was determined to be very low.

Table 28. Inspection false call table for the ramp damage check experiment specimen set; all participants—BT and RDC

Inspection False Calls for RDCE Specimen Set – All Participants – GE Bondtracer & Olympus NDT 35RDC																						
Configuration/Sizing (in.^{2})	A&P A	Insp. B	A&P C	A&P D	Insp. E	A&P F	A&P G	A&P H	Insp. I	A&P J	Insp. K	Insp. L	A&P M	A&P N	Insp. O	Insp. P	A&P Q	Intern R	Insp. S	Insp. T	Total	Avg.
RDCE Specimen Set																						
0-.25in^2	0	0	0	0	0	1	1	0	0	0	0	0	1	0	0	0	0	0	0	0	3	0.2
.26in^2–75in^2	0	0	0	1	1	0	1	0	0	1	0	0	0	0	1	0	1	0	0	0	6	0.3
76in^2–1.25in^2	0	0	0	2	0	0	0	0	0	0	0	0	0	0	0	0	0	0	0	0	2	0.1
1.26in^2–2.00in^2	0	0	0	0	0	0	0	0	0	0	0	0	0	0	0	0	0	0	0	0	0	0.0
>2.00in^2	0	0	0	0	0	0	0	0	0	0	0	0	0	0	1	0	0	0	0	0	1	0.1
Total (All Flaws)	0	0	0	3	1	1	2	0	0	1	0	0	1	0	2	0	1	0	0	0	12	0.6
1 False Call on Average Per 13.97 ft^2 of Inspection Area																						

6.4.3 Inspection Time

As with the other experiments, a critical part of the inspection process was how long it took for a participant to scan a defined area. Table 29 shows the time it took for each participant to scan the inspection regions on each panel along with their total inspection time. The average total inspection time for the RDCE specimen set was just over 6.5 hours, which produced an average inspection coverage rate of 1.29 ft^2/hr. The lowest (quickest) total inspection time was 3.5 hours, with an average inspection coverage rate of 2.39 ft^2/hr. The highest (slowest) total inspection time was just under 10.5 hours, with an average inspection coverage rate of 0.80 ft^2/hr.

Table 29. Experiment timing summary table for the RDCE specimen set; all participants—BT and RDC

Experiment Timing Summary 12-20 Ply specimen Set – All Inspectors – Pulse Echo UT																
	Specimen CT1-A	Specimen CT1-B	Specimen CT2-A	Specimen CT2-B	Specimen ST32-1	Specimen ST32-2	Specimen ST32-3	Specimen ST32-4	Specimen BN 1	Specimen BN 2	Specimen BN 3	Specimen ST1U-A	Specimen ST1L-A	Specimen ST2U-A	Specimen ST2L-A	Total Insp. Time (hr.min)
A&P Mech. A	0:17	0:17	0:25	0:22	0:37	1:09	0:39	0:37	0:53	0:34	0:57	0:52	0:50	0:41	0:47	9:57
Inspector B	0:07	0:12	0:10	0:10	0:39	0:35	0:43	0:28	0:31	0:31	0:33	0:26	0:19	0:19	0:22	6:05
A&P Mech. C	0:13	0:17	0:12	0:10	0:24	0:14	0:17	0:16	0:27	0:22	0:21	0:54	0:35	0:32	0:15	5:29
A&P Mech. D	0:12	0:12	0:16	0:21	0:32	0:41	0:38	0:29	0:23	0:22	0:34	0:29	0:34	0:27	0:28	6:38
Inspector E	0:16	0:09	0:26	0:23	0:48	0:46	0:45	0:58	0:29	0:21	0:29	0:54	1:00	0:44	0:32	9:00
A&P Mech. F	0:13	0:16	0:15	0:09	0:17	0:18	0:22	0:11	0:26	0:20	0:36	0:27	0:24	0:29	0:37	5:20
A&P Mech. G	0:10	0:14	0:16	0:11	0:35	0:30	0:39	0:28	0:29	0:27	0:30	0:52	0:47	0:35	0:32	7:15
A&P Mech. H	0:15	0:12	0:25	0:12	0:22	0:24	0:29	0:21	0:22	0:27	0:21	0:26	0:24	0:28	0:43	5:51
Inspector I	0:20	0:25	0:24	0:20	0:38	0:54	0:45	0:47	0:45	0:52	0:45	0:57	0:37	0:31	1:18	10:18
A&P Mech. J	0:19	0:26	0:30	0:37	0:37	0:28	2:09	0:32	0:39	0:35	0:28	0:52	1:00	0:43	0:30	10:25
Inspector K	0:12	0:14	0:21	0:17	0:25	0:28	0:25	0:16	0:40	0:32	0:28	0:44	0:48	0:21	0:21	6:32
Inspector L	0:25	0:24	0:47	0:40	0:15	0:28	0:25	0:22	0:34	0:27	0:49	0:27	0:26	1:06	0:24	7:59
A&P Mech. M	0:07	0:08	0:10	0:10	0:11	0:15	0:20	0:11	0:23	0:28	0:17	0:16	0:17	0:14	0:13	3:40
A&P Mech. N	0:04	0:07	0:06	0:06	0:30	0:23	0:50	0:33	0:38	0:53	0:15	0:15	0:14	0:12	0:30	5:36
Inspector O	0:04	0:05	0:06	0:08	0:10	0:18	0:15	0:12	0:14	0:15	0:15	0:20	0:20	0:30	0:17	3:29
Inspector P	0:12	0:05	0:11	0:07	0:13	0:26	0:22	0:24	0:26	0:29	0:18	0:33	0:17	0:37	0:16	4:56
A&P Mech Q.	0:05	0:07	0:08	0:22	0:21	0:29	0:52	0:16	0:26	0:23	0:14	0:19	0:24	0:42	0:34	5:42
Intern R	0:06	0:10	0:16	0:15	0:25	0:40	0:24	0:24	0:21	0:20	0:19	0:25	0:33	0:20	0:26	5:24
Inspector S	0:05	0:19	0:07	0:07	0:28	0:31	0:23	0:16	0:12	0:20	0:32	0:23	0:26	0:28	0:23	5:00
Inspector T	0:08	0:11	0:31	0:10	0:13	0:28	1:03	0:28	0:40	0:29	0:26	0:25	0:33	0:42	0:59	7:26
Ave. Insp. Time (hr:min)	0:11	0:13	0:18	0:15	0:26	0:31	0:38	0:25	0:29	0:28	0:28	0:33	0:32	0:32	0:31	6:36

6.4.4 Damage Sizing and Flaw Detection Percentage

Participant flaw calls were also graded to evaluate the accuracy of each participant's flaw sizing. The overall test results identified hits (calls with any amount of overlap between the call and the actual flaw location), misses (no call for an area of a known flaw), false calls (calls with no overlap of a flaw), and the degree of overlap between experimenter calls and actual flaw areas (sizing performance). The same grading parameter drawing shown in figure 85 was used to determine the accuracy of flaw coverage (overlap or sizing performance).

Table 30 summarizes the results for the overall flaw detection percentage and the associated accuracy in determining flaw size for the RDCE specimen set. This table includes combined data for all participants and all flaws. It should be noted that, for the RDCE specimen set, 81% of all flaws were detected—or 1,294 of the total 1,600 flaws. The flaw sizing performance shows that 13% of the detected flaws were sized properly (five categories for 100% coverage). A total of 32% of the flaws were sized in the 76–99% coverage category and 30% of the flaws were sized in the 51–75% coverage category. Thus, 75% of the detected flaws were sized with 51–100% accuracy. This table also shows a breakdown of percent detection based on flaw size. For example, 98% of the 2″ flaws were detected. On the smaller side, only 23% of the 0.25″ flaws were detected. Figure 136 shows a chart for the detection percentage for all participants based on flaw size. Table 31 summarizes the results for the overall flaw detection percentage and the associated accuracy in determining flaw size for the 10 A&P mechanics only. In this case, 79% of all flaws (or 635 of the 800 total flaws) were detected. The flaw sizing performance shows that 10% of the detected flaws were sized properly (five categories for 100% coverage). This table also shows a breakdown of percent detection based on flaw size. For example, 95% of the 2″ flaws were detected by the A&P mechanics. Figure 137 shows a chart for the detection percentage for all A&P mechanics based on flaw size. Table 32 summarizes the results for the overall flaw detection percentage and the associated accuracy in determining flaw size for the nine inspectors only. In this case, 82% of all flaws (or 587 of the 720 total flaws) were detected. The flaw sizing performance shows that 18% of the detected flaws were sized properly (five categories for 100% coverage). This table also shows a breakdown of percent detection based on flaw size. For example, 100% of the 2″ flaws were detected by the inspectors. The chart in figure 138 shows the inspectors' detection percentage based on flaw size.

Table 30. Tabulated results showing overall flaw detection percentage and accuracy in determining flaw size for the RDCE specimen set for all flaws; all participants—BT and RDC

Overall Flaw Detection Percentage & Accuracy in Determining Flaw Size Ramp Damage Check Experiment – All Flaws – All Participants							
Accuracy in Sizing the Flaws That Were Detected (1294 Total Flaws Detected)						Flaw Detection Percentage (1600 Total Flaws)	
Flaw Size	5 (100%)	4 (76%–99%)	3 (51%–75%)	2 (25%–50%)	1 (< 25%)	Flaw Size	Percent Detected
0.25	31%	22%	7%	7%	33%	0.25	23%
0.50	18%	19%	24%	24%	15%	0.50	68%
0.75	17%	26%	28%	22%	7%	0.75	95%
1.00	8%	37%	31%	19%	4%	1.00	97%
1.50	7%	36%	45%	11%	1%	1.50	98%
2.00	12%	59%	27%	3%	0%	2.00	98%
Overall Sizing Performance	13%	32%	30%	18%	7%	Overall Flaw Detection	81%

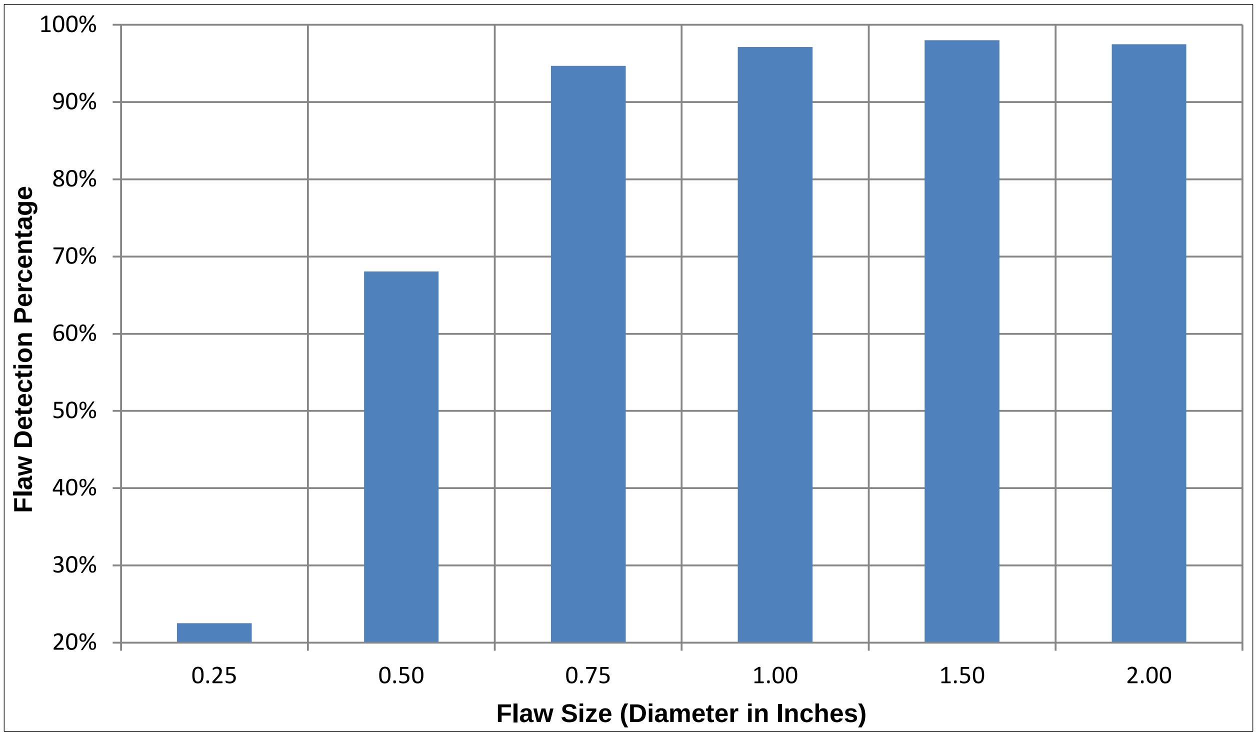

Figure 137. Overall flaw detection percentage chart for the RDCE specimen set for all flaws; all participants—BT and RDC

Table 31. Tabulated results showing overall flaw detection percentage and accuracy in determining flaw size for the RDCE specimen set for all flaws; all A&P mechanics—BT and RDC

Overall Flaw Detection Percentage & Accuracy in Determining Flaw Size Ramp Damage Check Experiment – All Flaws – All A&P Mechanics (10)							
Accuracy in Sizing the Flaws That Were Detected (635 Total Flaws Detected)						Flaw Detection Percentage (800 Total Flaws)	
Flaw Size	5 (100%)	4 (76%–99%)	3 (51%–75%)	2 (25%–50%)	1 (< 25%)	Flaw Size	Percent Detected
0.25	18%	27%	14%	9%	32%	0.25	22%
0.50	14%	19%	26%	19%	23%	.050	62%
0.75	15%	27%	28%	23%	7%	0.75	95%
1.00	6%	30%	35%	23%	5%	1.00	98%
1.50	4%	34%	43%	16%	2%	1.50	97%
2.00	3%	58%	34%	5%	0%	2.00	95%
Overall Sizing Performance	10%	29%	32%	20%	9%	Overall Flaw Detection	79%

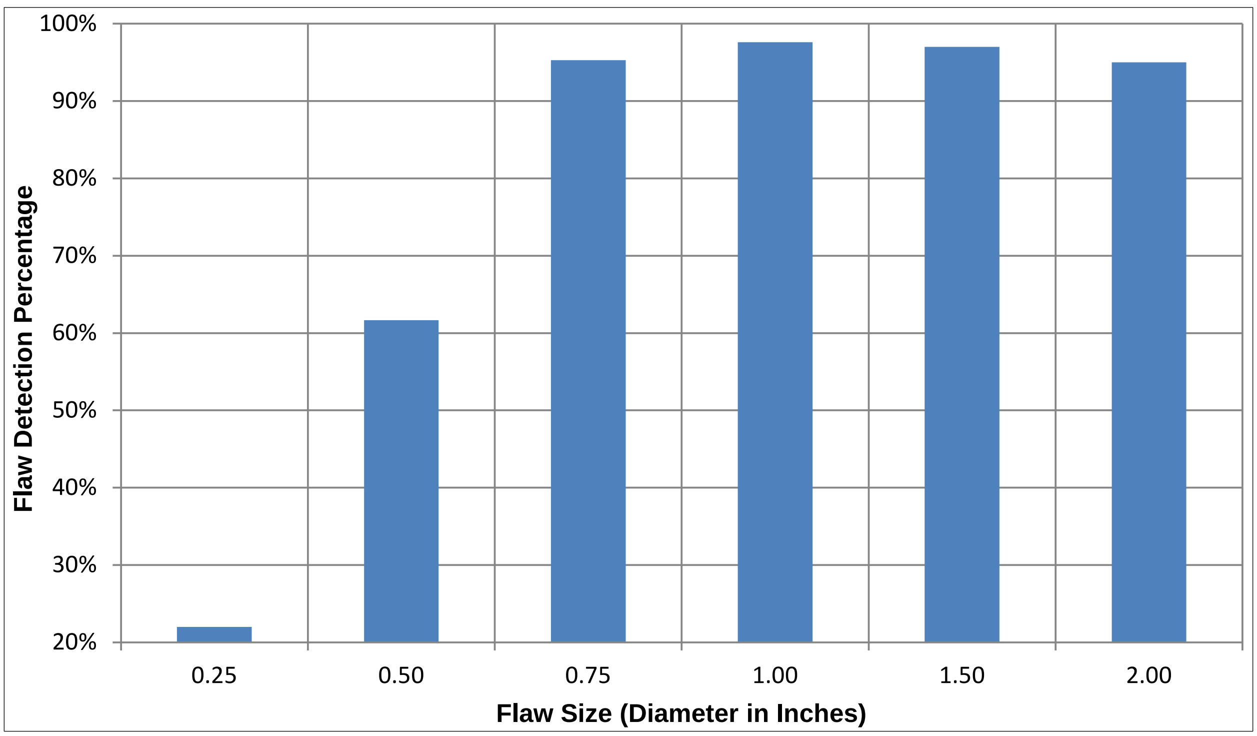

Figure 138. Overall flaw detection percentage chart for the RDCE specimen set for all flaws; all A&P mechanics—BT and RDC

Table 32. Tabulated results showing overall flaw detection percentage and accuracy in determining flaw size for the RDCE specimen set for all flaws; all NDI inspectors—BT and RDC

Overall Flaw Detection Percentage & Accuracy in Determining Flaw Size Ramp Damage Check Experiment – All Flaws – All NDI Inspectors (9)							
Accuracy in Sizing the Flaws That Were Detected (587 Total Flaws Detected)						Flaw Detection Percentage (720 Total Flaws)	
Flaw Size	5 (100%)	4 (76%–99%)	3 (51%–75%)	2 (25%–50%)	1 (< 25%)	Flaw Size	Percent Detected
0.25	42%	16%	0%	5%	37%	0.25	21%
0.50	23%	21%	20%	26%	9%	.050	73%
0.75	22%	27%	28%	19%	5%	0.75	93%
1.00	11%	47%	26%	13%	2%	1.00	96%
1.50	11%	42%	43%	4%	0%	1.50	99%
2.00	22%	58%	19%	0%	0%	2.00	100%
Overall Sizing Performance	18%	36%	27%	15%	5%	Overall Flaw Detection	82%

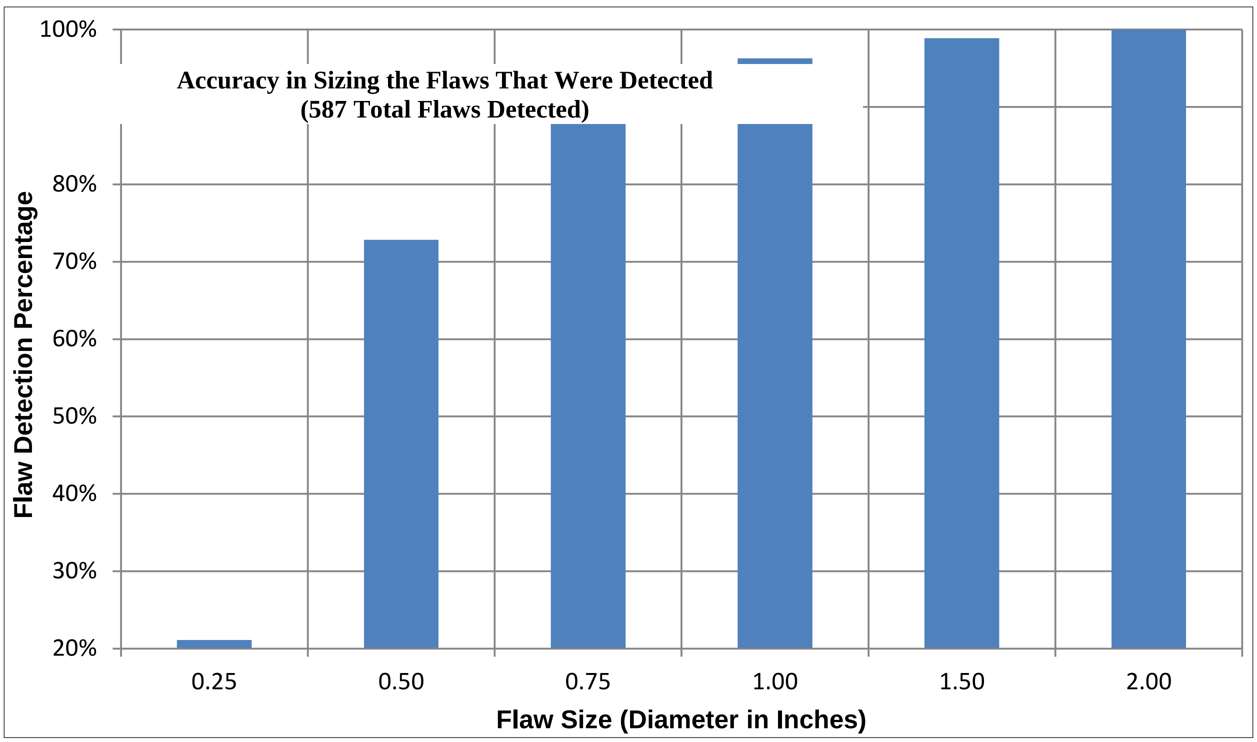

Figure 139. Overall flaw detection percentage chart for the RDCE specimen set for all flaws; all NDI inspectors—BT and RDC

6.5 AVIATION INDUSTRY SURVEY OF COMPOSITE NDI TRAINING

For an inspector deploying handheld PE ultrasonic inspection methods, the overall $POD_{[90/95]}$ levels for solid laminate composite structures occur when the flaw, or damage, is approximately 1.0″ in diameter ($POD_{[90/95]}$ = 1.0″). Although this is in alignment with the industry-desired flaw detection capabilities, it was also observed that the inspector performance varied for the same set of test specimens. Some inspection scenarios showed a larger spread in individual inspector results than others. These results generated an interest in understanding one of the key factors in inspector performance: NDI training.

It was observed multiple times during the deployment of this experiment, and referenced numerous times in this report, that inspector training unquestionably plays a key role in flaw detection performance. Specifically, it is postulated that inspection performance improvements can be achieved through the use of additional inspector training that focuses on the unique nature and challenges associated with composite inspections. In addition, it is believed that the spread in performance numbers observed across the spectrum of inspectors can be reduced if uniform and comprehensive composite NDI training classes were to be provided to aircraft inspectors. Toward that end, the FAA-AANC conducted a “Composite NDI Training Survey” to identify current practices, and potential needs, at the aircraft maintenance depots.

The main objectives of the Composite NDI Training Survey were to: (1) understand the general nature of the training available for NDI of composites, (2) identify the similarities and differences in training among the major aircraft maintenance depots and passenger and cargo airlines, (3) determine the needs with respect to composite NDI training, as defined by the aviation industry, (4) identify additional training and/or training aids that will help move inspectors from average to good, and outstanding, categories to improve composite NDI performance, and (5) translate these results into actions for aviation industry teams and airline training departments to facilitate improvements.

Successful efforts to transition inspectors from average to good or outstanding performance levels will have a significant effect on $POD_{[90/95]}$ levels. The survey discussed in this report was conducted in an effort to understand and define the NDI training practices currently being carried out to prepare inspectors for composite laminate inspections. With these results in hand, it is then possible to propose improvements in composite NDI training practices. It is believed that the results compiled from this survey will help formulate critical NDI training, whether developed in-house or by industry support groups such as the CACRC-ITG, that can improve inspector performance and, thus, improve the POD and reliability of composite laminate inspections.

One of the most important indicators of training needs comes from the aviation maintenance personnel. Twenty airline (passenger and cargo) and MRO companies were contacted by phone to participate in the Composite NDI Training Survey. Survey responses were obtained from personnel in charge of NDI training programs and managers of NDI shops. The respondents were asked about their view of additional composite NDI training via the following question: “In your opinion, do Level I, II, and III training/qualifications provide the necessary expertise for both metal and composite NDI or should additional training take place for composite inspections?” Figure 139 summarizes the industry opinion, in which over 80% of the respondents indicated that additional, focused training is needed to support composite inspections. It is important to link this request for additional training with another piece of survey information that revealed that only 25% of responders currently have special composite NDI training in place.

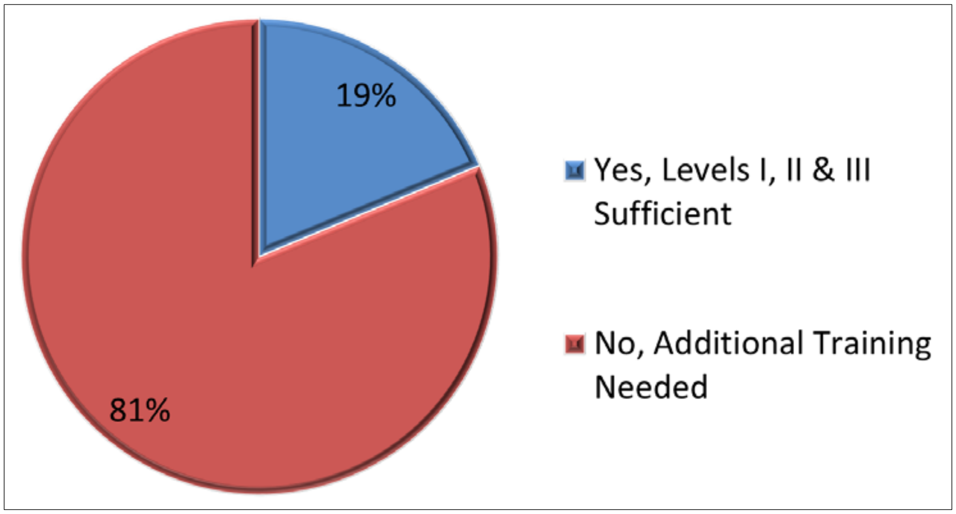

Figure 140. Chart showing percentage of the aviation industry that thinks level I, II, & III training/qualifications provide the necessary expertise for both metal and composite NDI (aviation industry—all respondents)

Another survey question solicited industry input on the type of guidance they would like to receive to help them establish the proper composite NDI training classes. The question asked was, "In what areas is additional guidance needed to help ensure comprehensive composite training programs for the aviation industry?" Figure 140 shows that an overwhelming majority (94%) of the respondents would like help in setting up composite inspection training. In addition, the respondents asked for guidance from all sources, including the FAA, OEMs, and industry groups such as the CACRC-ITG. Only 6% of the respondents felt no guidance was necessary.

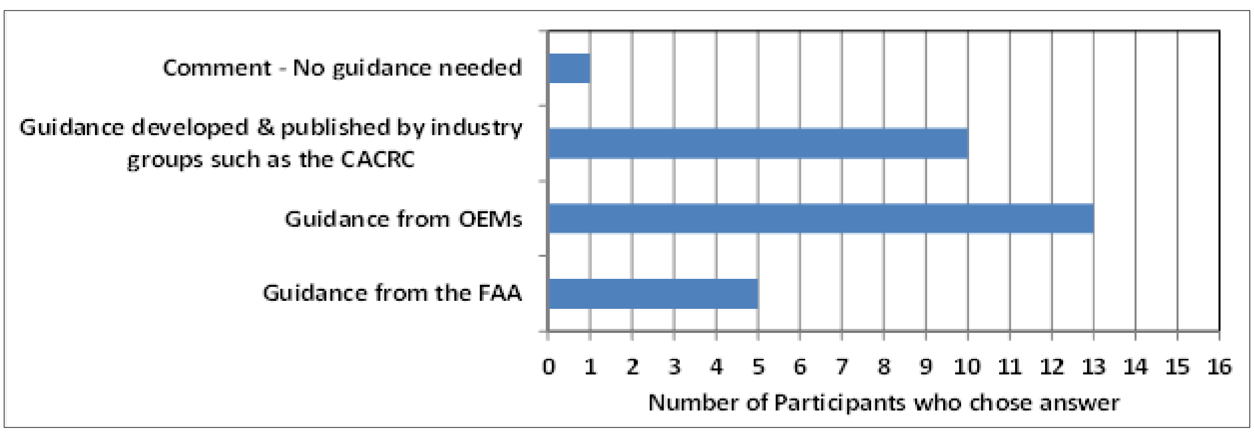

Figure 141. Chart showing the areas chosen by the aviation industry for additional guidance to help ensure comprehensive composite training programs (aviation industry—all respondents)

A complete description of the Composite NDI Training Survey and presentation of all results and conclusions is provided in appendix F. Recommendations resulting from the survey are listed in section 7.7.

7. CONCLUSIONS AND RECOMMENDATIONS

7.1 OVERVIEW

This section contains an overview of the thoughts on NDI for solid laminate composite structures.

- Engineering and economic benefits of composites will continue to expand its use

- Damage tolerance and durability is good but parts will sustain damage

- Maintenance and training issues are being addressed at airlines and Maintenance Repair Organizations (MRO) to accommodate the transition to increased inspection of composite structures

- This program assessed current industry capabilities by quantifying flaw detection performance in solid laminate composite structures

- This experiment provides overall probability of detection (POD) values versus flaw size for inspecting solid laminate composite structures so that the aviation industry can: (1) better understand what type of damage detection is possible for specific inspection scenarios, (2) adjust inspection procedures to optimize performance, and (3) intelligently enhance inspector preparation and training to generate the performance improvements possible via optimized nondestructive inspection (NDI) deployment, sufficient knowledge of the inspection idiosyncrasies, and increased exposure to realistic composite inspection demands.

- The Solid Laminate Flaw Detection Experiment (SLE) study showed that lower POD values are obtained in CT regions and higher POD values in more complex regions

- Overall, the results from the SLE will produce a capability baseline for current NDI techniques and will quantify improvements stemming from advanced NDI

- The field testing approach to this experiment provided insights into procedural and implementation issues

- While the size of flaw, or damage, that must be detected is affected by many parameters (structure type, location on aircraft, stress, and fatigue levels), the general goal for composite inspections is to detect flaws that are 1″ in diameter or larger. Many of the NDI reference standards in OEM nondestructive testing manuals use 1″ diameter flaws to guide equipment setup. In addition, the CACRC-ITG members generally concur that 1″ flaw detection provides a good center point for this SLE.

- The purpose of the SLE was to determine the minimum flaw size for which there is a 95% confidence that the POD is at least 90% (POD[90/95]). Therefore a range of flaw sizes from 0.25″ to 2″ was used. From the data collected, POD versus flaw size curves were generated and the intersect with the 95% threshold determined.

- NDI growth areas are focusing on features for large area, rapid scanning, improved data presentation, enhanced sensitivity, defect characterization, automated analysis, and advanced sensors/probes

- The viability of certain NDI methods, selected to meet specific application demands, and the quantification of performance must be continually pursued. Toward that end, this SLE is available for continued testing. All future testing will have the results from this pulse echo ultrasonic testing assessment to serve as the basis of comparison and help quantify NDI improvements

- An accompanying Advanced Solid Laminate POD Experiment is underway that is focusing on the application of advanced NDI methods. Once this experiment is complete, it will be able to show the degree of flaw detection improvements that are possible through the application of more sophisticated NDI. This experiment will also identify limitations and development needs in advanced NDI methods that may be proposed for future composite inspections

- The Solid Laminate POD Experiment will be available to continuously serve FAA programs to quantify the performance of NDI methods in a uniform and repeatable manner

7.2 POD COMPARISONS

7.2.1 Overall Inspector Performance

The overall results for the SLE, which includes all areas and all skin and substructure flaws, follow:

- Thin 12–20 ply skins $POD_{[90/95]}$ = 1.29″ in diameter (60–90% of flaws were detected depending on the inspector)

- Thick 20–32 ply skins $POD_{[90/95]}$ = 0.82″ in diameter (70–95% of flaws were detected depending on the inspector)

- Overall (combined 12–20 and 20–32 ply skins) $POD_{[90/95]}$ = 1.13″ in diameter

This indicates that a flaw of approximately 1.125″ in diameter could be reliably detected (within the industry standard of 90% POD with a 95% confidence) by an inspector using manually deployed, PE UT equipment to inspect a composite structure in the 12–32 ply-skin-thickness range (plus substructures that make the total layup a maximum of 64 plies).

7.2.2 Consistency of Results.

To check on the consistency of results and the spray in performance numbers, the two best (lowest POD) and two worst (highest POD) performing inspectors were removed from the dataset and the POD analysis was completed in their absence. The results showed no significant change in the overall POD numbers (less than 3%) when these inspectors were removed from the analysis. The overall results for all test specimens in the SLE (12–20 and 20–32 ply skin specimens) showed an overall $POD_{[90/95]}$ of 1.13″ and only a slight shift to 1.10″ when the outlying inspectors were removed from the dataset.

7.2.3 Performance Brackets

To determine the difference between outstanding, good, and average inspectors, the flaw detection data were adjusted to eliminate individual inspectors whose performance dropped below a specific level. Natural gaps in performance clusters were used to determine which inspectors to exclude from specific groups. The POD analyses were then completed on the remaining set of inspection data to calculate the resulting overall POD levels corresponding to inspector categories. The results from this analysis approach follow:

- 12–20 Ply Skins $POD_{[90/95]}$ = 1.29″ in diameter (all inspectors)
- 12–20 Ply Skins $POD_{[90/95]}$ = 1.19″ in diameter (top 90th percentile)—Average

- 12–20 Ply Skins $POD_{[90/95]}$ = 1.06″ in diameter (top 70th percentile)—Good
- 12–20 Ply Skins $POD_{[90/95]}$ = 0.79″ in diameter (top 30th percentile)—Outstanding
- 20–32 Ply Skins $POD_{[90/95]}$ = 0.82″ in diameter (all inspectors)
- 20–32 Ply Skins $POD_{[90/95]}$ = 0.70″ in diameter (top 80th percentile)—Average
- 20–32 Ply Skins $POD_{[90/95]}$ = 0.54″ in diameter (top 60th percentile)—Good
- 20–32 Ply Skins $POD_{[90/95]}$ = 0.48″ in diameter (top 40th percentile)—Outstanding

Inspectors in the upper bracket performed approximately 40% better than the overall results produced by all inspectors combined. The purpose of this exercise was to demonstrate the clear improvements that are possible if an inspector's skills reach the next performance level. Although this is not always achievable through increased oversight and experience, it is expected that some level of improvement can be gained. Methods that an airline might use to transition their inspectors toward the "outstanding" bracket include enhanced/increased training, apprenticeships, exposure to representative inspections, enhanced procedures along with reiteration of proper procedures, inspector teaming or other oversight, awareness training on inspection obstacles and suitable mitigation plans, and more frequent in-house testing to complement external testing and training, such as that provided by the American Society for Nondestructive Testing.

7.2.4 False Calls

Overall, false calls were not deemed to be a problem. In fact, depending on the tolerance of the airline or MRO to revisit sites to make final determinations on flaw calls, it seems that inspectors could possibly set their thresholds slightly lower to possibly improve flaw detection while only slightly increasing the number of false calls. This would mean that the number of false calls could increase above the current overall numbers of one false call per 8.4 ft^2 (or one false call per 17 ft^2 for false calls greater than 0.25 in^2 in size), but the POD could be improved. The false call rates follow:

- 12–20 ply = one false call per 7.7 ft^2
- 12–20 ply (using only false calls that were larger than 0.25″ in diameter) = one false call per 14 ft^2
- 20–32 ply = one false call per 10.9 ft^2
- 20–32 ply (using only false calls that were larger than 0.25″ in diameter) = one false call per 40 ft^2
- Overall (combined 12–20 and 20–32 ply) = one false call per 8.4 ft^2
- Overall (combined 12–20 and 20–32 ply and using only false calls that were larger than 0.25″ in diameter) = one false call per 17 ft^2

If the inspection regions are of CT with no underlying substructure, the false call rate drops even further. The overall false call rates in the CT regions for the 12–20 and 20–32 ply laminate experiments combined were one false call per 38.3 ft^2 (or one false call per 153 ft^2 for false calls greater than 0.25 in^2 in size).

7.2.5 Flaw Sizing

Inspectors were asked to provide the size and shape of the flaws they detected. Once the inspectors found a flaw, their ability to size the flaw using their UT equipment was very consistent. Approximately 60% of the flaws were sized between 75–100% of their actual size and approximately 80% were sized at 50–100% of their actual size. This was for all flaws, including surface skin and substructure regions. Such flaw-sizing capability can be important when damage tolerance is considered and when making decisions regarding repair options.

7.3 INSPECTION CHALLENGES

7.3.1 Flaw Detection in Substructure Regions

Detection of flaws in the presence of substructure elements, either in the bond line or substructure itself (e.g., stringer, frame), present the most challenging. The complexity of the PE UT waveform increases drastically in the areas of substructure elements. In addition, the added signal penetration requirement and associated porosity increase, coupled with reflections from dissimilar materials (resin or bond lines versus composite laminates) create lower amplitude signals. This decreases the S/Ns so that flaw signals are more difficult to discern. Further, intermediate signals, stemming from internal inclusions, disbonds, and delaminations are more difficult to clearly identify amidst an extensive set of internal reflection peaks and signal harmonics. As a result of these issues, additional NDI training and use of representative NDI reference standards (or specialized training test specimens) would probably improve flaw detection in the presence of substructure elements. The reduction in performance when inspecting CG regions can be summarized in the following results:

- 12–20 ply skins $POD_{[90/95]}$ = 1.29″ in diameter (all regions)
- 12–20 ply skins $POD_{[90/95]}$ = 0.86″ in diameter (CT regions)
- 12–20 ply skins $POD_{[90/95]}$ = 1.49″ in diameter (all CG regions)
- 12–20 ply skins $POD_{[90/95]}$ = 0.97″ in diameter (tapered geometry regions only)
- 12–20 ply skins $POD_{[90/95]}$ = 0.87″ in diameter (curved geometry regions only)
- 12–20 ply skins $POD_{[90/95]}$ = 0.55″ in diameter (honeycomb regions only)
- 12–20 ply skins $POD_{[90/95]}$ = NR, no result (substructure regions only)
- 20–32 ply skins $POD_{[90/95]}$ = 0.82″ in diameter (all regions)
- 20–32 ply skins $POD_{[90/95]}$ = 0.74″ in diameter (CT regions)
- 20–32 ply skins $POD_{[90/95]}$ = 0.93″ in diameter (all CG regions)
- 20–32 ply skins $POD_{[90/95]}$ = 0.70″ in diameter (tapered geometry regions only)
- 20–32 ply skins $POD_{[90/95]}$ = 1.50″ in diameter (substructure regions only)
- Overall (12–20 and 20–32 ply skins) $POD_{[90/95]}$ = 1.13″ in diameter (all regions)
- Overall (12–20 and 20–32 ply skins) $POD_{[90/95]}$ = 0.80″ in diameter (CT regions)
- Overall (12–20 and 20–32 ply skins) $POD_{[90/95]}$ = 1.34″ in diameter (all CG regions)

The “no result” above indicates that no POD results were obtained because of insufficient flaw detection in the substructure regions. For the 12–20 ply skin specimen set, only 51% of the flaws in the regions with substructure elements were detected. This includes flaws in the surface skin as well as flaws in the substructure elements or bond line beneath the surface skin. Only 65% of the flaws greater than 0.75″ in diameter were detected and only 30% of the flaws less than 0.75″ in diameter were detected. Thus, it was not possible to converge on a POD value for the substructure regions alone. Overall, in the 12–20 ply skin (thin laminate) experiment and comparing PODs from CT and CG regions, there was a 72% increase in POD (from 0.86″ to 1.49″) because of the presence of the confounding information arising from the CG. The data show that the tapered regions had a very minor effect on the performance and that curved surfaces did not impede inspection performance. Finally, the presence of honeycomb under the laminate did not adversely affect the inspection and excellent POD values were obtained from these regions.

Overall, comparing PODs from CT and CG regions in the 20–32 ply skin (thick laminate) experiment, there was a 26% increase in POD (from 0.74″–0.93″) because of the presence of the confounding information arising from the CG. The data show that the tapered regions had no effect on the performance. It should be noted that the drawings provided to the inspectors indicated the exact location and type of taper on each specimen, so the importance of this information in conducting accurate inspections should not be overlooked. Although it was possible to calculate a $POD_{[90/95]}$ value for the thick laminate experiment, it was determined that the inspection performance declined by 82% when compared with the overall POD and was twice the $POD_{[90/95]}$ value obtained in the CT region (0.74″ in CT versus 1.50″ in the substructure regions). This further emphasizes the point that flaw detection in the presence of substructures is a major challenge. Additional experience and use of very representative NDI reference standards could help improve the detection levels in substructure regions.

For all specimens combined into the overall SLE (12–20 and 20–32 ply skin specimens), the inspection performance declined in the CG regions. It was determined that the inspection performance in all substructure regions was 19% worse than the overall $POD_{[90/95]}$ and was 68% worse than the $POD_{[90/95]}$ value obtained in the CT region (0.80″ in CT versus 1.34″ in the substructure regions).

7.3.2 Confounding Effects of Signal Harmonics

Signal harmonics can appear in the range of interest when harmonics from thinner surface laminates fold into the same time frame as the actual signals of interest generated from the back wall of a substructure element. In these cases, it may be critical to infer that the appearance of new intermediate signals implies there is damage present. Substantial changes in the expected shape of the back wall signals could also indicate the presence of intermediate damage where such changes may not be below the normal accept-reject threshold.

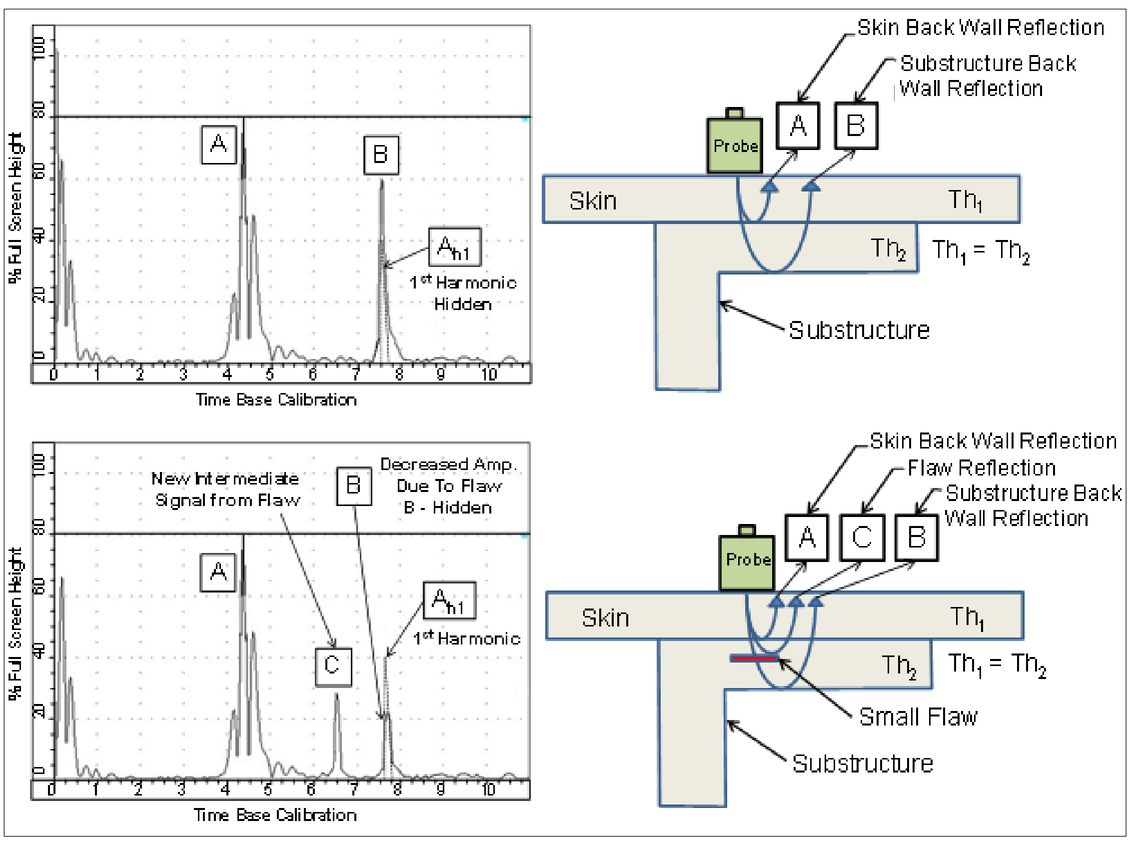

Figure 142. Inspection impediment where signal harmonics occur in the same time frame as the signals of interest

7.3.3 Effect of Laminate Thickness

Flaw detection performance was not affected by the thickness of the laminate. The selected probe frequencies for this experiment were normally 2.5 MHz or 5 MHz. Some inspectors also used a 1 MHz probe when inspecting the thicker regions, such as those with 32-ply laminates bonded to 32-ply substructure. These inspection frequencies provided a very nice depth of signal penetration, even in some of the more attenuative, bonded joints, so that the thickness of the part was not observed to cause a decrease in flaw detection performance. In fact, the overall POD results from the thick laminate experiment (20–32 plies; $POD_{90/95}$ = 0.82″ in diameter) actually exceeded those produced in the thin laminate experiment (12–20 plies; $POD_{90/95}$ = 1.29″ in diameter). The inspections in the presence of CG, which produces more interwoven and confusing signals, have the greatest effect on inspection performance.

7.3.4 Probe Size Versus Flaw Size

An important experiment design feature to keep in mind is that the inspectors were asked to detect flaws as small as 0.25″ in diameter. The ultrasonic transducers that were used to conduct the inspections, and transducers that are typically used in the 2.5–5 MHz range, were 0.5″ in diameter. This means that, even if the transducer was centered directly over 0.25″ flaws (i.e., flaws less than the diameter of the transducer), the transducer signal would be composed partly of information from a flaw region and partly of information from the unflawed region around the small flaws. Thus, the overall effect of the flaw on the transducer response would be lessened. In some instances, the 0.25″ flaws would only have a slight effect on the response and this signal change would be below the recommended “flaw call” threshold provided in the procedures. Figure 142 depicts this situation. An analysis of all flaws in the SLE revealed that all of the flaws were found by some experimenters. Thus, detection was possible. Such small flaws were necessary to the experiment design and the associated statistical POD analysis. However, if the objective is to detect flaws of 0.25″ in diameter, smaller diameter transducers, which might only be realistically applied in localized inspections, should be used.

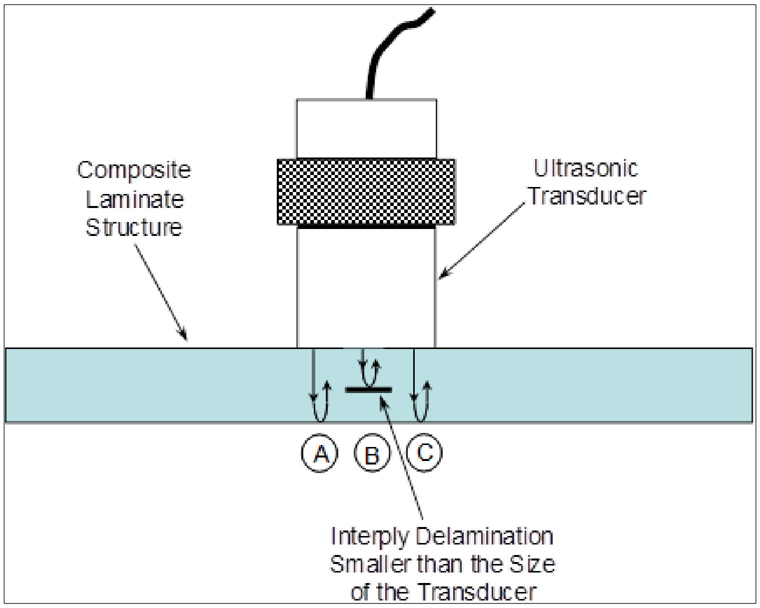

Figure 143. Schematic showing reflection of PE UT signals when the flaw is smaller than the diameter of the UT probe

7.3.5 Use of Curved Delay Line for BN Leading Edge Regions

Custom delay lines were manufactured to accommodate transducer placement on the curved region of the BN test specimens. Only some inspectors used this custom delay line that eliminated the rocking motion induced in the flat delay lines because of a non-exact fit to the inspection surface. This rocking motion in the transducer deployment could create spurious signals and changes in amplitude in the PE UT response. However, no discernible difference was noted between the inspectors that used the curved delay lines and those that did not. Inspection results on the curved laminate regions were essentially identical to those obtained from the flat CT regions ($POD_{90/95}$ = 0.87″ in diameter on curved surfaces).

7.4 HUMAN FACTORS ISSUES

7.4.1 Amount of Overall Time Spent Inspecting Composites

The duration of this experiment was longer, and, thus, more tedious than what would normally be expected of an inspector. The inspections lasted 2–3 days and involved up to 46 ft^2 of inspection region. The thin laminate experiment (12–20 ply skins) covered 34 ft^2 of inspection area and the thick laminate experiment (20–32 ply skins) included 12 ft^2 of inspection area. Some inspectors would complete both experiments in 3½ days. As demonstrated in the smaller, more focused RDCE experiment, inspectors performed much better when directed to specific regions (i.e., shorter, more focused inspections). When subjected to exceptionally long inspections, it is not unusual for the inspector’s attention to wane at times, which increases the possibility of missing a flaw. The BN specimens are a good example of this type of development. Each of the three BN specimens required approximately two hours to complete their inspection (compared to 1–1.5 hours for the other specimens). In addition, the BN specimens included honeycomb substructure, curved surfaces, sealed (not bonded) substructure, and the presence of fasteners. It was the most challenging test specimen and was one reason that the thin laminate (12–20 ply) experiment had higher POD levels than the thick laminate (20–32 ply) experiment. The recommendation is that wide-area inspections associated with large composite structures be divided into a series of smaller inspection regions to allow for the necessary inspection focus. In addition, some of the more demanding inspections that involve larger regions or complex structure should be inspected using a two-man team. Discussions on signal quality and interpretation between the two inspectors should improve the overall flaw detection performance. To gain some insight into how a two-man team, or a single inspection followed by another single inspection, might improve the POD results, the data from two different inspectors from the 12–20 thin laminate experiment were combined. Table 33 lists the results from various two-man combinations, such as the best performing inspector combined with the second-best inspector; the best inspector with the worst inspector; and a medium-performing inspector with the worst inspector. Median-1 and Median-2 were inspectors who performed near the midpoint of the $POD_{[90/95]}$ values for the set of 27 inspectors. The percentage decrease (improvement) in $POD_{[90/95]}$ is based on combining the hits and misses for each pair of inspectors, recalculating the $POD_{[90/95]}$, and then comparing this result with the better performer of the two inspectors being teamed together. This example does not reflect results from an actual two-man team conducting this experiment but does illustrate the potential for improvement as every pair of inspectors studied in the table showed a significant improvement in the combined $POD_{[90/95]}$ values.

Table 33. POD results when performance of two inspectors are combined, simulating a second inspection that follows the first

12-20 Ply – Two-Man Hit/Miss Combined – $POD_{90/95}$				
Individual Inspector Category	Individual Inspector $POD_{90/95}$	Combined Hit/Miss $POD_{90/95}$	Combined Flaw Hit/Miss Increase	Percent Decrease In $POD_{90/95}$
Best	0.654	0.537	5	17.89%
2nd Best	0.787			
2nd Best	0.787	0.537	11	31.77%
3rd Best	0.824			
Best	0.654	0.603	2	7.80%
Median-1	1.414			
Best	0.654	0.622	5	4.89%
Median-2	1.678			
Best	0.654	0.622	2	4.89%
Worst	3.366			
Median-1	1.414	0.997	15	29.49%
Median-2	1.678			
Median-1	1.414	1.151	7	18.60%
Worst	3.366			
Median-2	1.678	0.987	9	41.18%
Worst	3.366			
3rd Worst	2.733	2.174	19	20.45%
2nd Worst	2.951			
2nd Worst	2.951	1.734	12	41.24%
Worst	3.366			

7.4.2 Effect of Inspection Rate on POD

The average inspection rates for the SLE experiment follow:

- 12–20 ply average coverage rate = 2.3 ft^2/hour (max rate = 3.5 ft^2/hour; min rate = 1.5 ft^2/hour)

- 20–32 ply average coverage rate = 1.9 ft^2/hour (max rate = 4.2 ft^2/hour; min rate = 1.2 ft^2/hour)

It was noted that there was an improvement of approximately 10% in POD levels when comparing inspection rates of 2 ft^2/hour or less with those above 2 ft^2/hour. Thus, inspection rates faster than 2 ft^2/hour are not recommended. Previous studies by the FAA-AANC revealed that there are diminishing improvements to be obtained by slowing the inspection rate to very small numbers. Thus, rates below 1.5 ft^2/hour are not expected to yield better results except in cases in which structural complexities warrant slower inspection rates to properly understand the resulting UT signals.

7.4.3 Effect of Inspection Rate on False Calls

The false call rates are described in detail above. Overall, there was a slight observed effect of inspection rate on the occurrence of false calls. In one analysis, it was determined that a decrease in the inspection rate from 3.2 ft^2/hour to 1.8 ft^2/hour could reduce the overall false call rate from 2 to 1 per 12 ft^2. Ultimately, this decision is linked to an airline's tolerance for false calls and the need to revisit these sites for final determinations. In both cases where the effect of the inspection rate on POD and false call inspection performance was determined, the results indicate that an inspection rate of approximately 2 ft^2/hour would produce the best results.

7.4.4 Lack of Exposure to Composite Laminate Inspections

While all of the inspectors that participated in this experiment were trained and qualified to inspect composite laminate structures, they did not have extensive exposure to such inspections. This is due to the current commercial fleet profiles, which do not include a lot of solid laminate composite structure. Thus, the experiment monitors noted some variation in the inspectors' comfort level in conducting these inspections. Use of the NDI reference standards, or NDI feedback specimens, provided to the inspectors helped alleviate this issue. However, it does indicate that additional training and exposure to solid laminate inspections—and the unique challenges associated with inspecting complex, multilayered composite structures—could help improve these POD results even further. Section 7.7 expands on this training element discussion and indicates that inspectors would benefit from periodic refresher classes that would renew, or even improve, their level of expertise with respect to the PE UT method in general as well as with the unique aspects of composite laminate inspections.

7.5 PROPER EXECUTION OF PROCEDURES

7.5.1 Use of Aids to Ensure Proper Coverage

The inspection procedures discussed proper coverage of the inspection area and even suggested the use of grids or other methods to ensure that the UT transducer is moved over the entire surface area. In addition, conformable straight edges and rulers were provided to the inspectors. Some inspectors completed their work using a simple freehand (unguided) motion over the entire surface area of each specimen. Some inspectors divided the test specimens into quadrants, while still moving the transducer in a freehand motion, so that they could better monitor their coverage and transducer movement. Some inspectors used straight edges to guide their transducer movement while some inspectors also added tick marks to ensure that they moved their straight edge in 0.5″ increments along the test specimens. Finally, some inspectors used straight edges in some regions and freehand in other regions (the percentage of each was not logged, but this combined practice was noted). The inspection results showed a significant improvement in POD for inspectors who used straight edges. The following POD values compare inspectors who used freehand transducer deployment with inspectors who used straight edges with tick marks:

- 12–20 ply freehand $POD_{[90/95]}$ is extrapolated to be approximately 2.4″ in diameter
- 12–20 ply straight edge with tick marks $POD_{[90/95]}$ = 1.06″ in diameter
- 20–32 ply freehand $POD_{[90/95]}$ = 1.35″ in diameter
- 20–32 ply straight edge with tick marks $POD_{[90/95]}$ = 0.64″ in diameter
- Overall (combined 12–20 and 20–32 ply) freehand $POD_{[90/95]}$ = 1.75″ in diameter
- Overall (combined 12–20 and 20–32 ply) straight edge with tick marks $POD_{[90/95]}$ = 0.91″ in diameter

Thus, it can be seen that the inspection performance decreased by a factor of 100–125% when the inspectors attempted to accurately cover the entire inspection area using a freehand method. As the inspection regions become smaller, this effect will start to decrease; however, this does not diminish the value of the findings described here. When inspectors are inspecting large areas, as may be the case in composite aircraft structures, they should use some form of guides or grids to ensure proper coverage of the inspection area.

7.5.2 Inspection of Tapered Regions

It was noted that the inspections conducted in the regions with composite thickness taper produced flaw detection results that were almost as good as the best results in the CT regions. Overall, the $POD_{90/95}$ was 0.78″ in diameter for the tapered regions, whereas the $POD_{90/95}$ was 0.80″ in diameter for the simpler CT regions. There is essentially no difference in the inspection performance. This is probably because each test specimen was accompanied by a schematic that showed the inspectors the exact locations of the tapered regions. Thus, inspectors were better able to interpret the changing back wall peak that moved along the time axis as the UT transducer moved along the taper (changing laminate thickness). This result indicates that inspectors need clear drawings or schematics of the inspection region to properly set up and operate their equipment. Such schematics should clearly indicate where ply tapers, local laminate reinforcements, stringers, frames, shear ties, sealed interfaces, or other substructure members are located.

7.5.3 Training

The issues described above can also be addressed through additional personnel training. Some of the training could be in the form of composite awareness training to instruct inspectors on composite materials, composite structure fabrication, and typical aircraft composite construction designs. Other forms of training could emphasize procedural aspects of the inspections, such as the use of NDI deployment aids and the proper use of drawings to assist in signal interpretation.

7.6 APPLICATION OF RAMP CHECK DEVICES

7.6.1 Overall POD for Focused Inspection Regions

When participants were directed to particular inspection regions—simulating occasions when impact or other visible surface features indicated a need for a local inspection—they were able to improve their flaw detection well beyond that produced in an open, wide area inspection mode. As per the RDCE design, the inspection regions were kept small, with the largest region being 0.6 ft^2 and the smallest region being 0.03 ft^2. The overall results from all 140 inspection zones, containing 80 flaws and totaling 8.38 ft^2, were:

- Overall (12–20 and 20–32 ply) $POD_{[90/95]}$ = 0.78″ in diameter (all participants)
- Overall (12–20 and 20–32 ply) $POD_{[90/95]}$ = 0.77″ in diameter (inspector participants)
- Overall (12–20 and 20–32 ply) $POD_{[90/95]}$ = 0.84″ in diameter (A&P participants)

The results were tightly clustered for all participants, although the inspectors had a slightly (9%) better performance than the A&P mechanics. One of the best POD performance levels was achieved by a summer intern student who had no inspection experience and no previous knowledge of the equipment. Both of these results indicate the ability of untrained people to receive basic training and properly deploy the equipment if they are sufficiently attentive to detail. However, the user must properly set up the equipment for subsequent inspections to be effective. In the RDCE, participants were given the exact calibration points for each inspection region; otherwise, an improper equipment setup (calibration) could occur, which could lead to erroneous inspections . In direct comparisons of equipment performance, it was determined that the Olympus RDC and the GE® BT produced equivalent performance numbers.

7.6.2 Other Performance Measures: False Calls, Flaw Sizing, and Inspection Rate

The false call rate was approximately the same as the full SLE. The ratio of flawed to unflawed areas for the RDCE was greater than 20:1 and the number of unflawed regions was 74, out of a total of 140, directed inspection regions. The inspection rate was faster than the PE UT inspections on the full SLE as might be expected for directed inspections covering small regions. Flaw sizing was more difficult because of the “blind” nature of the equipment readout, which did not provide A-scans but simply “Green Light/Red Light” or “Good/Bad” indications.

7.6.3 Accurate Calibration Requirements

The inspection devices that operate in a go/no go mode, such as the RDC and the BT, performed well in the areas where there was no substructure. Typically, in non-substructure areas, the calibration is performed immediately adjacent to the desired inspection area, where it is assumed there is no damage. If the probe is then moved over a damaged region in a region of the same thickness, the message provided by the unit would state “Bad” and the damage would be found. However, if the calibration were conducted on a thick region, which is a region with some substructure element, and the subsequent inspection was performed on the thinner, undamaged skin alone, the unit would interpret this as a loss of back wall signal and provide a false call indication of “Bad” (i.e., equipment setup that is conducted on thicker regions will not accommodate inspections on regions of lesser thickness). In other words, if someone calibrates on a thicker laminate, then tests over a thinner laminate, the device would indicate a flaw when none exists. Figure 143 compares A-scan signals to show how calibration on a thick region will produce flaw indications when the device is subsequently applied to a thinner region. When using these go/no go devices, it is necessary for the inspector to know the exact layout of any substructure or ply taper areas in the test zone. This will allow for accurate and proper calibration on an area where the total thickness matches the inspection area of interest. Accurate drawings should be available for any locations that use these devices.

7.6.4 Use of Ramp Damage Check Equipment in Regions of Changing Geometry

Inspections performed using the RDC unit on full-scale composite fuselage panels proved to be difficult on impact locations over substructure because of the tapered geometry of the stringer and shear-tie co-bonded areas. In FAA-AANC trial inspections on known structures with known damage regions, it was determined that use of the unit was straightforward over mid-bay regions. However, the inspector must have significant knowledge of any tapered region, bonded substructure, and any thickness changes behind the skin. Because of the continuously changing thickness of the taper regions, it is very difficult to apply this equipment to tapered portions of the structure. Tracing out the substructure on the skin of the panel was necessary to perform initial calibration of the unit to ensure that the initial calibration measurement was taken at the same thickness section of the panel as the desired inspection region. If the probe was moved as little as 1/8″ perpendicular across a taper region, the message provided by the unit would state “out of calibration thickness” during subsequent inspections on stringer and shear-tie built-up sections (i.e., equipment setup that is conducted on thinner regions will not accommodate inspections on regions of greater thickness). This should not result in a false call but will be confusing to the user and probably end in a “no decision” for the area of interest. Figure 144 compares A-scan signals to show how calibration on a thin region will produce “out of calibration thickness” messages when the device is subsequently applied to a thicker region.

7.6.5 Maintaining Proper Instrument Orientation

It was noted that some inspectors did not place the readout screen directly within their line-of-sight. Rather, the unit was placed more in their peripheral view. When a flaw is detected, a “Bad” message is displayed on the screen or a red light on the unit is illuminated, depending on the device being used. In cases where the device is not placed in the direct line-of-sight, it was observed that, while the unit was indicating the presence of a flaw, the inspector was not observing this, which resulted in a missed call. The recommendation is that additional guidance be provided for people operating this equipment. The guidance should state that the unit should be placed in the direct line-of-sight of the operator. Even with proper device placement, it was observed that the black monochrome screen could sometimes be hard to see clearly.

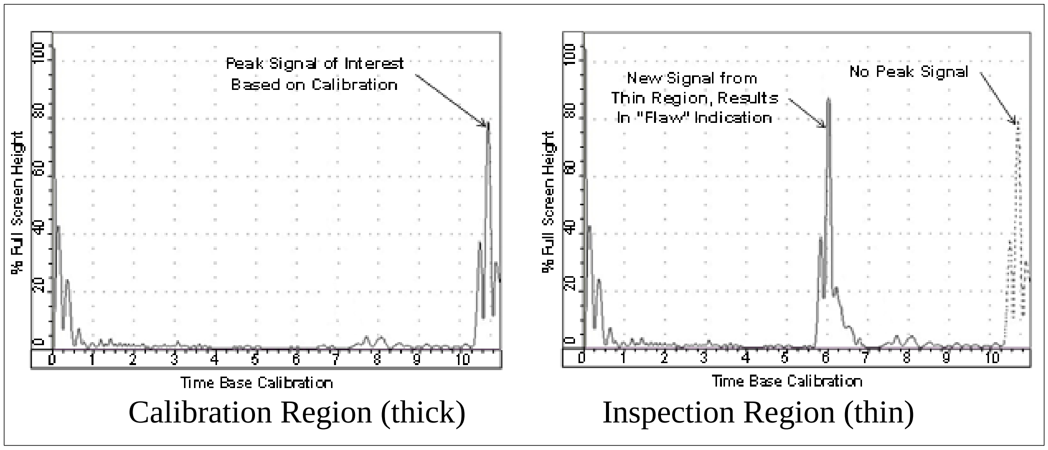

Figure 144. Comparison of A-scan signals from calibration on a thick region followed by an inspection on a thinner region

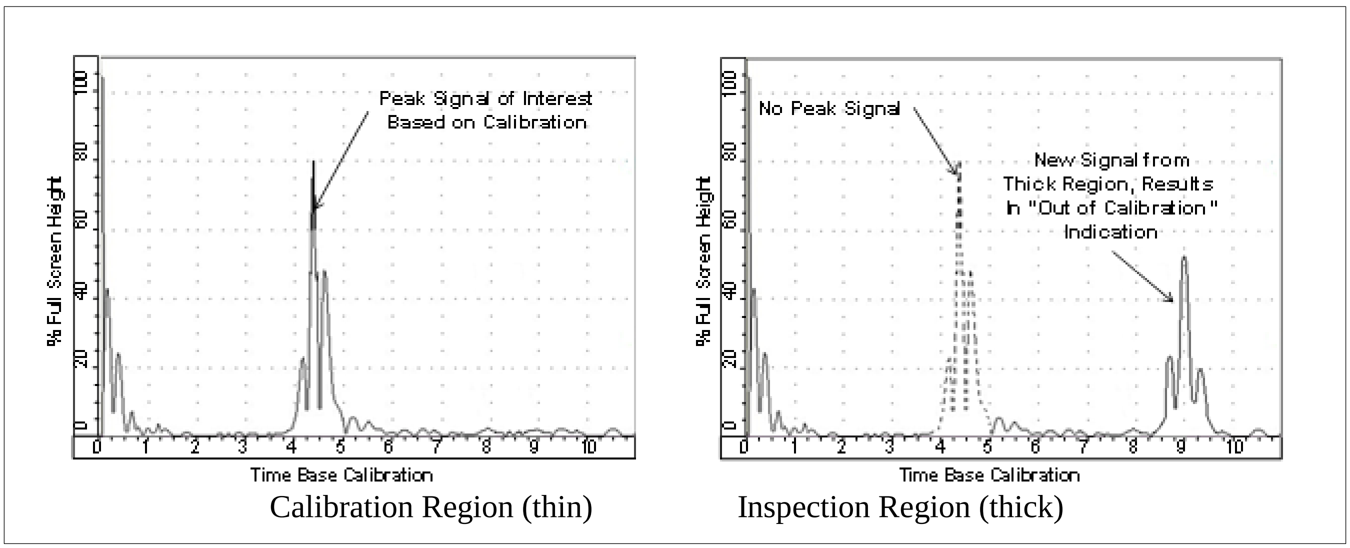

Figure 145. Comparison of A-scan signals from calibration on a thin region followed by an inspection on a thicker region

7.6.6 Minimizing the Effects of Poor Instrument Orientation

@The effects of poor instrument orientation could be overcome by placing an audible alarm on the device, adding an alarm light to the handheld probe, or taking both of these actions. This would prevent the operator from having to look at the device to read the display at all times. This would also eliminate the tedious and tiring eye motion back-and-forth between reading the device display and watching the probe to ensure it is being deployed properly (orientation and trace path). Another option is to use a two-man rule for deploying this equipment in which one person is attentive to the probe deployment while another watches the equipment display readout.

7.6.7 Training

Most of the issues described above pertain to proper equipment deployment along with a clear understanding of the limitations regarding equipment use. Specific training on the use of the go/no go devices is still evolving and is primarily driven by OEMs. This basic training and guidance on equipment deployment should be expanded to address the potential pitfalls described above. Additional composite awareness training that teaches inspectors about aircraft composite construction will help ensure proper calibration of the equipment.

7.7 COMPOSITE NDI TRAINING RECOMMENDATIONS

The Composite NDI Training Survey discussed in this report was conducted in an effort to understand and define the NDI training practices currently being carried out to prepare inspectors for composite structure inspections. Based on the information that this NDI Training Survey gathered from companies conducting aircraft maintenance, some valuable insights were obtained. The following are some recommendations to help translate these results into actions for aviation industry teams and airline training departments to facilitate inspection improvements.

- Overall, the identified, potential measures to improve inspectors' performance on composite inspections include increased training, apprenticeships, exposure to representative inspections, enhanced procedures, inspector teaming, and awareness training on inspection obstacles

- More specialized training, beyond Level I, II, and III certification, needs to be developed to specifically address composite inspections. It would help to have a class that focuses on the unique challenges and signal differences associated with composite inspections. Signal characteristics related to ply tapers, secondary bonds, and composite repairs, for example, could be discussed so that it would be easier for inspectors to distinguish flaw signals from those generated by pristine structure

- The majority (86%) of the industry does not have additional, special inspector qualification/certification to qualify personnel to conduct composite inspections. Most companies use the normal qualification program for general NDI inspection as qualification for composite inspection. Specialized certification for aircraft NDI professionals should be considered for those inspecting composite structures

- Respondents requested additional guidance related to composite NDI training from the OEMs, the FAA, and industry groups in the areas of specific instrument training, specific methods training, repair inspections, composite construction training, and reference standard fabrication and use. Programs supporting the evolution of such training should be initiated and pursued using an industry-wide approach

- Some of the specific composite NDI training needs can be addressed by more on-the-job training (OJT) and apprentice programs. Fewer than half of the respondents indicated they place inspectors in their composite shops. An apprentice program could rotate inspectors into composite shops so that they can learn about composite construction while exploring the effects of different construction scenarios on NDI. While 56% of the aviation industry indicates that they use an apprentice program to expose newer inspectors to certain types of composite inspections, the survey results indicate that this practice should be more widespread. The apprentice programs are not particularly formal nor uniformly applied

- There is a general concern that the lack of routine exposure to composite inspections makes it difficult for the inspectors to maintain the necessary level of expertise. Furthermore, exposure to available flaw specimens is viewed as a way to keep the inspectors ready for when an aircraft needs inspection because of damage. So, in addition to formal composite NDI training classes, aircraft inspectors should conduct routine practice inspections on representative composite structures that contain realistic damage. Such test specimens should be more complex and varied than the existing NDI reference standards and contain known, but nonuniformly-spaced, flaw profiles. Industry teams that allow for participation from OEMs, airlines, and MROs should carry out an initiative to develop such test specimens along with specifications for specimen acquisition and use

- Two-thirds of the industry reported that they provide general composite fabrication training to teach composite materials, plies, layups, scarfed repairs, composite design, and processing. However, only 25% of the industry provides additional, specialized training specifically for inspectors who perform composite inspections. The cross-training of inspectors should be pursued to provide them with a greater understanding of the structures they are inspecting

- Approximately 33% of the industry reported that a mechanic can use a simple go/no-go device to conduct composite inspections. Half of the respondents stated there would be labor issues associated with a mechanic performing inspector functions. It is recommended that mechanics who are allowed to use such devices for composite inspections receive training on how the device is used, along with recurrent training and possibly some composite training. The testing of such devices at the FAA-AANC showed that it can be confusing for an untrained mechanic/inspector to use a simple device for composite inspections when the user is unfamiliar with the composite substructure. For example, using a simple go/no-go device for inspections on tapered composite structures is very difficult

- Based on responses from the industry, the FAA, working with OEMs and industry groups, should consider publishing an Advisory Circular (AC) or produce a new Aerospace Recommended Practice (ARP) providing enhanced training guidelines specific to the inspection of composite structures. The overwhelming majority of respondents (81%) think additional training should take place for composite inspection, so an AC or ARP outlining enhanced training guidelines could be very useful to the industry. It will be necessary to determine an appropriate way for this to be referenced by existing training standards, such as ATA-105, NAS-410, SNT-TC-1A, and EN-4179

7.8 SUMMARY OF KEY POINTS AND BEST NDI PRACTICES

- Overall, the results from this study provide input and recommendations to the FAA regarding guidance (e.g., AC) that can enhance the composite inspection process. This study is driven by the goal of improving aircraft safety. Airlines and OEMs can use these results to guide NDI deployment and training, to define what flaws/damage can be reliably found by inspectors, and to reduce the human factors issues to produce improved NDI performance in the field

- For an inspector deploying handheld, PE UT methods, the overall $POD_{[90/95]}$ level for solid laminate composite structures occurs when the flaw, or damage, is approximately 1.0″ in diameter. Flaw detection in skins has a lower (better) $POD_{[90/95]}$, whereas flaw detection in substructure elements has a higher (worse) $POD_{[90/95]}$

- The inspection performance in all substructure regions was 19% worse than the overall $POD_{[90/95]}$ and was 68% worse than the $POD_{[90/95]}$ value obtained in the CT region ($POD_{[90/95]}$ = 0.80″ in CT versus 1.34″ in the substructure regions)

- Specific procedural improvements were identified for the deployment of both conventional PE UT and the RDC/BT devices. These can be readily integrated into NDI procedures in OEM NDT manuals

- When inspecting composites with substructure elements, additional signal penetration requirements—coupled with a more extensive set of complex reflections—results in a clear reduction in NDI performance in the region of substructure elements. Additional NDI training and the use of more representative NDI reference standards are recommended to improve flaw detection in the presence of substructure elements

- False call rates for composite laminate inspections using PE UT methods were extremely low, with one false call occurring per 8.5 ft^2 of inspection area (or one false call per 17 ft^2 of inspection area if only false calls greater than 0.25 ft^2 in area are considered)

- Signal harmonics and composite construction scenarios that result in a complex set of signal reflections were determined to be the major contributors in reducing NDI performance, whereas laminate thickness; tapered ply regions; and curved, or nonflat, surfaces were not significant factors on the NDI results

- From a human factors perspective, the inspection of large areas can reduce NDI performance and the recommendation is that any wide-area inspections be divided into a number of smaller regions to allow for the necessary inspection focus. The use of two-man teams is another recommendation for NDI improvement and this was supported by the analysis accompanying this experiment

- With respect to both POD and the generation of false calls, it was determined that the optimum inspection rate is approximately 2 ft^2 per hour. Furthermore, the SLE tests revealed that aircraft inspectors currently conduct their inspections with a coverage rate of approximately 2 ft^2 per hour

- The use of inspection coverage aids, such as straight edges/tick marks, is highly recommended. It was determined that inspectors who used such aids performed significantly better than inspectors who did not

- Successful efforts to transition inspectors from "average" to "good" or "outstanding" performance levels will have a significant effect on $POD_{[90/95]}$ levels. Possible measures to achieve this include increased training, apprenticeships, exposure to representative inspections, enhanced procedures, inspector teaming, and awareness training pertaining to inspection obstacles

- More specialized training, beyond Level I, II, and III certification, needs to be developed to specifically address composite inspections. It would help to have a class that focuses on the unique challenges and signal differences associated with composite inspections. Some of the specific composite NDI training needs can be addressed by more OJT and apprentice programs. An apprentice program could rotate inspectors into composite shops so that they can learn about composite construction while exploring the effects of different construction scenarios on NDI

- The RDCE revealed the ability of untrained people to receive basic training and properly deploy the go/no go NDI equipment if they are sufficiently attentive to detail. The key is that the user must properly set up the equipment for the subsequent inspections to be effective

- Limitations in the application of the go/no go devices were identified and user guidance with respect to equipment deployment in various composite constructions was developed. Equipment users must understand the exact layout of the composite structure (surface, subsurface, and taper regions) to complete an accurate calibration and understand the resulting indications from the equipment

- The inspection devices that operate in a go/no go mode, such as the RDC and BT, cannot be easily deployed in taper regions or other regions with rapidly changing configurations

- The use of an audible alarm on the go/no go devices, the addition of an alarm light to the handheld probe, or taking both of these actions is highly recommended. This would prevent the operator from having to look at the device to read the display at all times. It would also eliminate tedious eye motion, as well as the concern over proper equipment orientation relative to the user

- Based on responses from the industry, the FAA—working with OEMs and industry groups—should consider publishing an AC or produce a new ARP providing enhanced training guidelines specific to the inspection of composite structures

- In general, the lack of routine exposure to composite inspections makes it difficult for inspectors to maintain the necessary level of expertise. It is recommended that OEMs, or some other aviation agency, design a set of composite specimens—much like the NDI feedback specimens used in this experiment—for inclusion within aircraft NDI shops.

Added exposure to available flaw specimens is viewed as a strategy for keeping inspectors ready, well-trained, and current on composite inspections

8. REFERENCES

1. Roach, D.P., Dorrell, L.R., Kollgaard, J., and Dreher, T., "Improving Aircraft Composite Inspections Using Optimized Reference Standards," SAE Airframe Maintenance and Repair Conference, November 1998, SAE Technical Paper 98AEMR–34.

2. Roach, D. and Rackow, K., "Composite Honeycomb NDI Reference Standards," *SAE Aerospace Recommended Practice ARP5606*, in conjunction with CACRC Inspection Task Group, March 2001.

3. Roach, D. and Rackow, K., "Solid Composite Laminate NDI Reference Standards," *SAE Aerospace Recommended Practice ARP5606*, in conjunction with CACRC Inspection Task Group, March 2001.

4. Baker, A.A., "Fatigue Studies Related to Certification of Composite Crack Patching for Primary Metallic Aircraft Structure," FAA-NASA Symposium on Continued Airworthiness of Aircraft Structures, FAA report DOT/FAA/AR-97-2, Volume I, July 1997.

5. Fredell, R.S., "Damage Tolerant Repair Techniques for Pressurized Aircraft Fuselages," PhD Thesis, Delft University of Technology, 1994.

6. Rice, R., Francini, R., Rahman, S., et al., "Effects of Repair on Structural Integrity," FAA report DOT/FAA/CT-93/79, December 1993.

7. Jones, R., Chiu, C., and Paul, J., "Designing for Damage Tolerant Bonded Joints," *Composite Structures*, Vol. 25, 1993.

8. Chiu, W.K., Rees, D., Chalkley, P., and Jones, R., "Designing for Damage Tolerant Repairs," ARL Aircraft Structures Report 450, August 1992.

9. Roach, D.P., Moore, D., and Walkington, P., "Nondestructive Inspection of Bonded Composite Doublers for Aircraft," Proceedings of SPIE Conference on Nondestructive Evaluation of Aging Aircraft, December 1996.

10. Roach, D., Beattie, A., Dahlke, L., et al., "Emerging Nondestructive Inspection Methods for Aging Aircraft," Department of Energy SAND Report 92-2732, March 1994, FAA report DOT/FAA/CT-94/11, October 1994.

11. Palmer, D.D. and Wood, N.O., "Development of MAUS Enhancements for Large Area Wing Inspections," Air Force Structural Integrity Conference, December 1999.

12. Roach, D. and Rackow, K., “Development and Utilization of Composite Honeycomb and Solid Reference Standards for Aircraft Applications,” Department of Energy SAND Report 2003-2112, June 2004.

APPENDIX A—Solid Laminate Experiment—Experimenter Information Packet

(sent to host coordinators prior to experiment deployment)

Detection of Hidden Flaws in Aircraft Solid Laminate Composite Structure

EXPERIMENTER INFORMATION PACKET

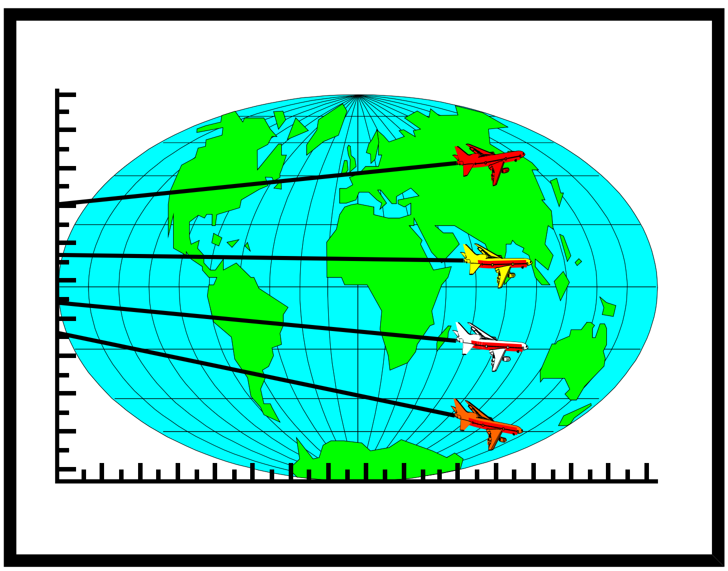

Experiment Coordinators: **D. Roach (505)844-6078**
T. Rice (505)844-7738

FAA Airworthiness Assurance Center
Infrastructure Assurance and NDI Department
Sandia National Labs

Experimenter Briefing and Information

Introduction

The Sandia National Labs' FAA Airworthiness Assurance NDI Validation Center (AANC), under contract to the Federal Aviation Administration's William J. Hughes Technical Center, is conducting an experiment to assess flaw detection in composite laminate aircraft structures. The Composite Laminate Flaw Detection Experiment, including a set of 15 composite laminate test specimens containing engineered flaws, will travel to airlines, third party maintenance depots, aircraft manufacturers, and NDI developer labs to acquire flaw detection data. The experiment will require approximately 2 to 4 days of each inspector's time. In general, inspectors will be asked to locate and size hidden flaws in the test specimens. After a sufficient number of inspectors have completed the experiment (using standard pulse-echo UT), industry-wide performance curves will be established that determine: 1) how well current inspection techniques (PE-UT) are able to reliably find flaws in composite laminate structure, and 2) the degree of improvements possible through the integration of more advanced NDI techniques and procedures. The inspections will emphasize flaw detection methods applicable to solid laminate structures ranging from 12 plies to 64 plies thick. The results will be published as industry-wide performance measures and all links to specific aircraft maintenance depots will be permanently removed.

Inspectors will gain experience and feedback on the implementation of your inspections on representative aircraft structure. No individual inspector's names will be linked to any experiment results. Similarly, no organization's name will be linked to any group of experiment results. However, results will be made available to potential users and they will be able to compare the results of competing inspection techniques and systems.

The inspectors will receive feedback on how they performed in the experiment. This will come in the form of tabulated results indicating the number of flaws correctly detected, the number of flaws missed, the number of false calls made, and the ability of the inspector to accurately size the flaws they detected. We can also provide feedback on the type of flaws that were detected and missed so that the inspector will learn what types of flaws they have trouble detecting. It is important to note that the feedback to the inspectors is kept confidential. In the final aggregate results, we ensure that the participants are always kept anonymous so that there is no way to correlate any results to a specific person or airline.

Background

The inspection category for evaluation in this experiment is the inspection for representative disbonds, interply delaminations, and "simulated" impact flaws in solid laminate composite structures. The test articles are modeled after the general range of construction scenarios found on commercial aircraft. The test program is intended to evaluate the technical capability of the inspection procedures, process and the equipment (i.e., NDI technique). Evaluation of inspector specific or environment specific factors associated with performing this inspection are not the primary objective of this experiment. However, notice will be taken by the experiment monitor if such factors seem to influence results or if unplanned events occur which could impact the results of the inspection. Specific notice will be taken if issues such as deployment or maneuverability adversely affect the outcome of the inspection.

For this experiment a set of test specimens containing engineered flaws have been manufactured. The inspections will be conducted on a series of panels and Bullnose specimens of different sizes. These panels will be placed on a foam frame to support the entire perimeter of the panel and the Bullnose specimens will be placed on a flat surface to produce uniform boundary conditions across all experimenters. You will be asked to inspect each test specimen and provide any information you can about the presence of applicable flaws. If you determine that flaws are present, you should then provide size and shape information about each detected flaw. The results should be marked directly on the test specimen using only markers provided by the experiment monitors. *Inspectors should use any positive indications to find flaws as small as 1/4″ in diameter.* Experimenters should work at a pace that is comfortable for them. Although monitors will note start and stop times for your inspection, time to inspect is a secondary variable of the experiment. Inspectors should take whatever time is necessary to assure that any and all flaws in the test specimens are found.

1. TEST SPECIMENS AND THE FLAW DETECTION EXPERIMENT

Engineered Specimens - Engineered specimens have been manufactured that mimic the inspection applications of interest and include realistic flaws found in those structures. Specific information on the construction of the test panels follows. Experimenters will be told the configuration of each panel they inspect and be provided with drawings for reference.

- **Laminate Type** - carbon graphite
- **Laminate Thickness** - Panels have 12 (~.078″), 20 (~.130″), 24 (~.156″) and 32 (~.229″) plies.
- **Paint** - All panels are painted as per current aircraft specifications.
- **Substructure Thicknesses –** .075″, .125″, .192″, .225″, and .250″
- **Tapered Area Ranges –** 12-20 (.50″ step), 20-32 (.50″ step), 12-20 (.25″ step)
- **Specimen Deployment -** During testing, panels will be placed on a flat surface to support the entire footprint.
- **Flaw Detection** - Inspectors should use any positive indications to find flaws as small as 1/4″ in diameter.
- **Inspection Device –** For the most part, the inspector will utilize their own NDI equipment. We will provide acceptable inspection devices (UT probes) to be used for this testing (meet Boeing/Airbus specs) and the inspectors will make the final choice based on availability and familiarity with that equipment. Some testing with non-standard devices may also be conducted in order to form a basis of comparison with results obtained using the recommended pulse echo UT devices.
- There are two separate experiments. There is a Thin Laminate Skin experiment with skins ranging from 12-20 plies (0.078″ to 0.130″ thick) and total thickness extending to 62 plies (0.406″) when substructure is considered. There is also Thick Laminate Skin experiment with 32 ply skins (0.21″ thick) and total thickness extending to 58 plies (0.377″) when substructure is considered.

Equipment Calibration and Familiarization - Each blind inspection process will be preceded by inspections on appropriate training/feedback specimens supplied by the experiment monitors. The inspector will be given information on the manufactured flaws present in the training/feedback specimens and will be allowed to use them for check-out of their inspection equipment. The training/feedback specimens will have similar construction as the blind test specimens and include similar flaws. Thus, they also can be used to allow inspectors to become familiar with an inspection device and learn about a specific equipment's response for various solid laminate composite structures and flaws within those structures. Figures A-1 thru A-5 show the flaw profiles of all the training/feedback specimens.

Figure A-6 is a drawing of various cross-sectional views of the 12 ply training/feedback specimen showing how the pillow inserts and Graphoil inserts are used to simulate interply delaminations, flat bottom holes are used to simulate the presence of an air gap, and pull tabs are used to simulate the presence of an air gap between the laminate and the bonded substructure. The training/feedback specimens will be used as a training tool prior to starting the experiment and will also be used by inspectors during the course of the experiment to set-up their equipment.

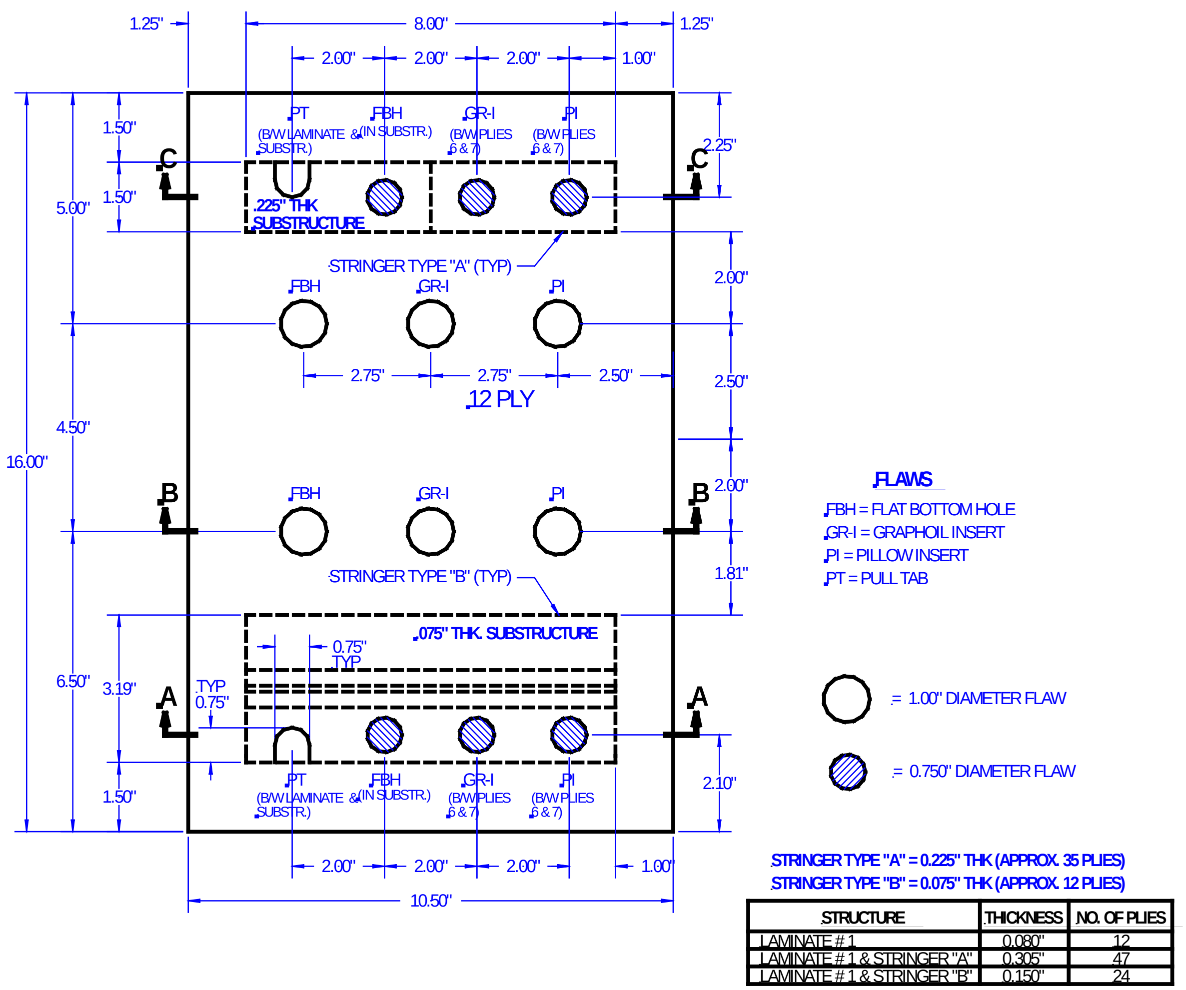

STRUCTURE	THICKNESS	NO. OF PLIES
LAMINATE # 1	0.080"	12
LAMINATE # 1 & STRINGER "A"	0.305"	47
LAMINATE # 1 & STRINGER "B"	0.150"	24

Figure A-1. Final Design of 12 Ply Training/Feedback Specimen

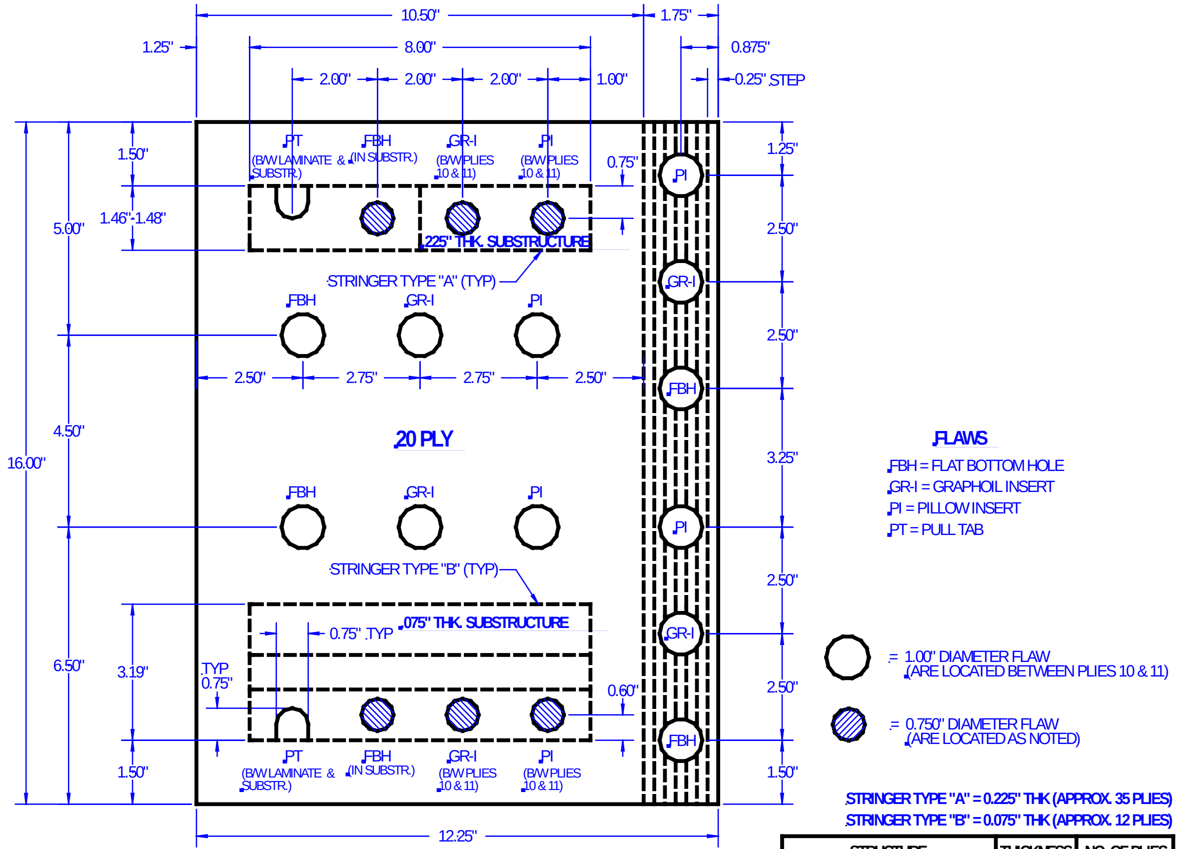

STRUCTURE	THICKNESS	NO. OF PLIES
LAMINATE # 2	0.130"	20
LAMINATE # 2 & STRINGER "A"	0.355"	55
LAMINATE # 2 & STRINGER "B"	0.205"	32

Figure A-2. Final Design of First 20 Ply Training/Feedback Specimen with Taper

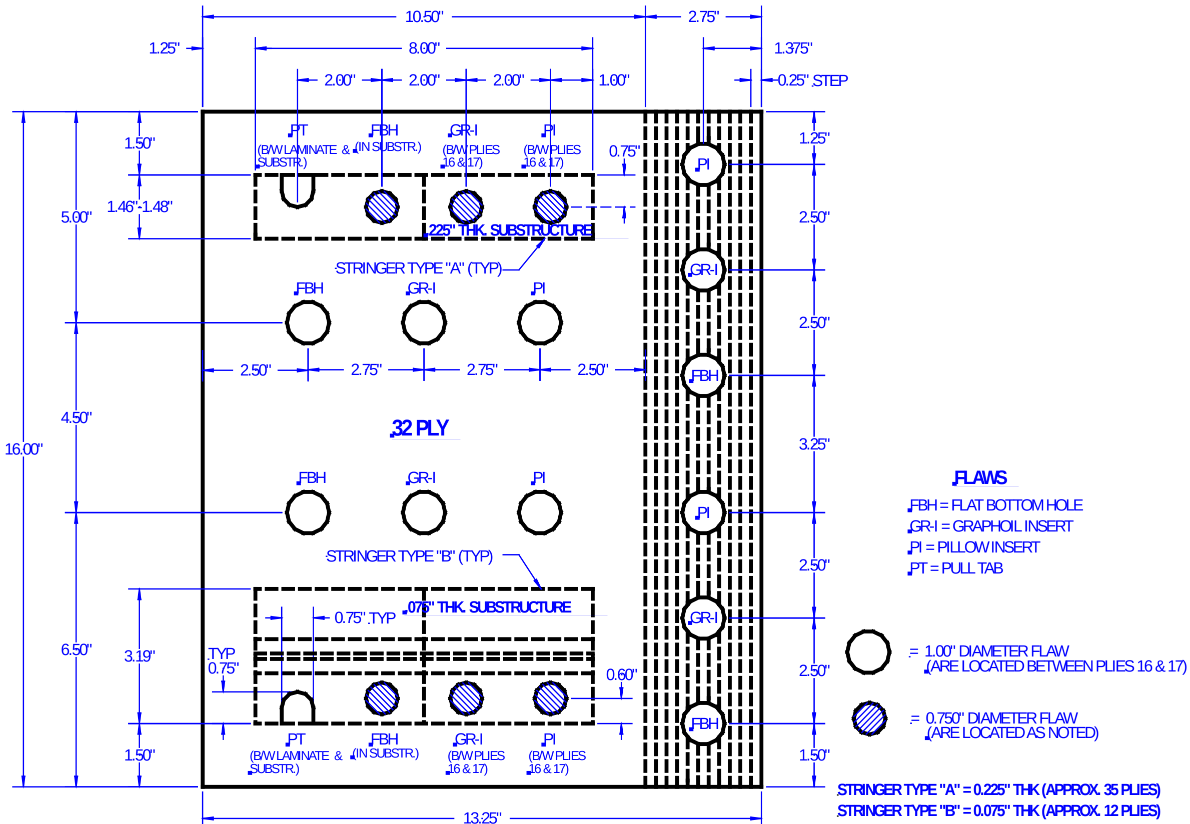

STRUCTURE	THICKNESS	NO. OF PLIES
LAMINATE # 3	0.208"	32
LAMINATE # 3 & STRINGER "A"	0.433"	67
LAMINATE # 3 & STRINGER "B"	0.283"	44

Figure A-3. Final Design of 32 Ply Training/Feedback Specimen with Taper

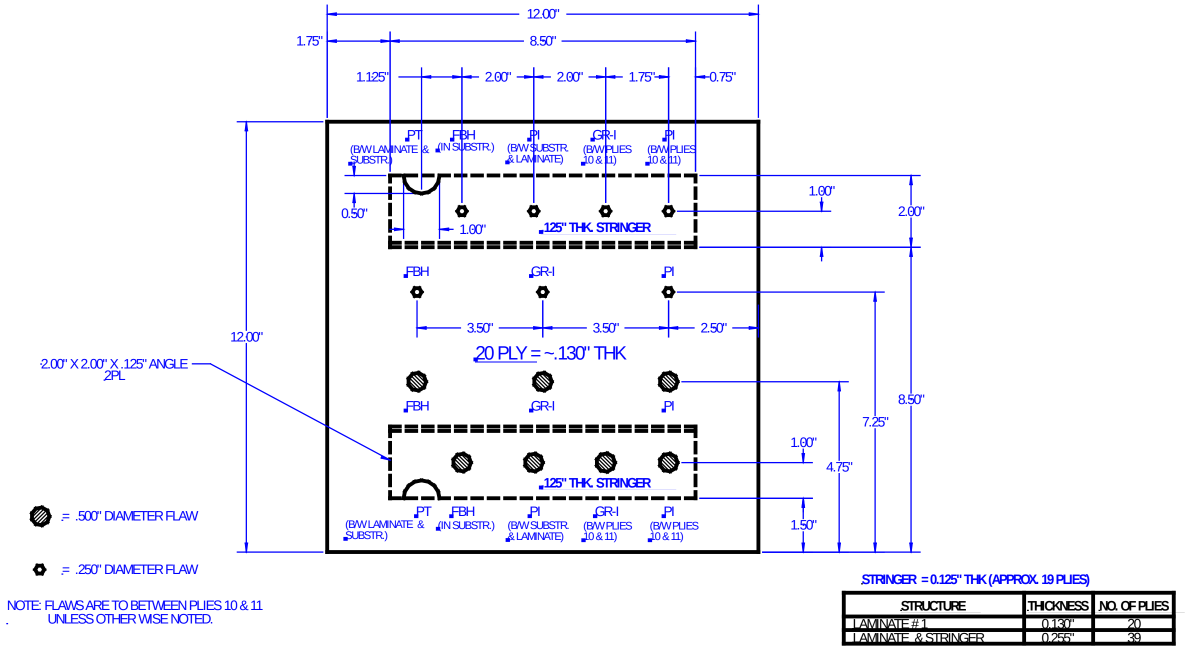

STRUCTURE	THICKNESS	NO. OF PLIES
LAMINATE # 1	0.130"	20
LAMINATE & STRINGER	0.255"	39

Figure A-4. Final Design of second 20 Ply Training/Feedback Specimen without Taper and Different Substructure and Smaller Flaws

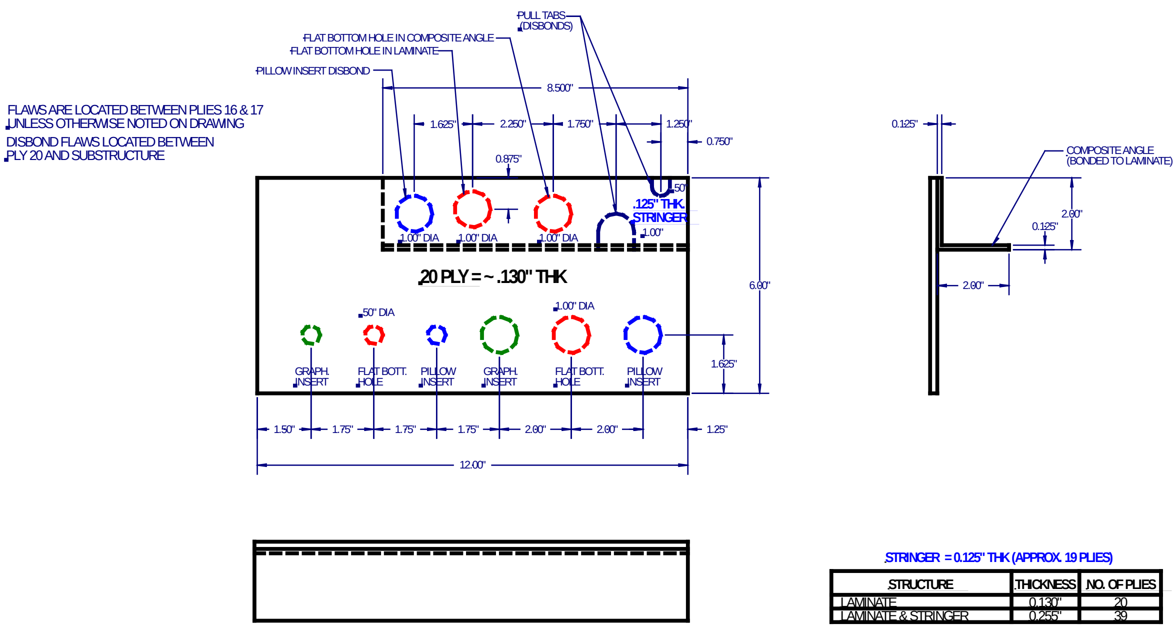

STRUCTURE	THICKNESS	NO. OF PLIES
LAMINATE	0.130"	20
LAMINATE & STRINGER	0.255"	39

Figure A-5. Final Design of third 20 Ply Training/Feedback Specimen

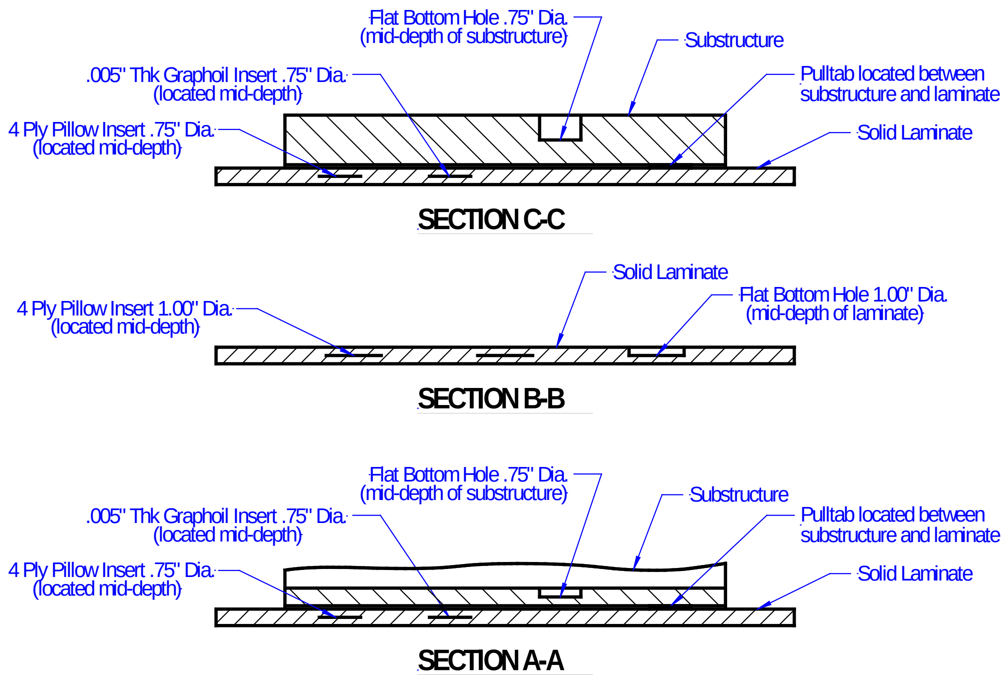

Figure A-6. Cross Section Views of 12 Ply Training/Feedback Specimen Showing the Locations of the Different Flaws

2. PERFORMANCE METRICS

Multiple performance attributes will be discussed in the final report for this experiment. These are given in the table below and are briefly discussed following the table. Quantitative metrics (standards applied to events that can be numerically counted or quantified) will be applied when appropriate but many of the performance attributes will be discussed using qualitative metrics (standards that rely on human judgments of performance). Where practical, qualitative assessments will be based on predetermined criteria to ensure grading consistency. The intent is to provide useful summaries of the major factors that would influence the user communities' perception of the viability of the technique or specific equipment. Because different users may have different priorities, we will not rank or prioritize the various measures.

<u>Quantitative Metrics</u> - objective standards applied to events that can be numerically counted or quantified.

<u>Qualitative Metrics</u> - subjective standards that rely on human judgments of performance; where practical, qualitative assessments will be based on predetermined criteria to ensure grading consistency.

STRUCTURED EXPERIMENT EVALUATION CRITERIA
1. Accuracy and Sensitivity
2. Data Analysis Capabilities
3. Versatility
4. Portability
5. Complexity
6. Human Factors
7. Inspection Time

1. Accuracy and Sensitivity
   Accuracy is the ability to detect flaws reliably and correctly in composite structures and repairs without overcalling (false calls). Sensitivity is the extent to which the inspection system responds to flaws as a function of size, type, and location (e.g., proximity to repair edges, underlying or adjacent structural elements) in the structure.

   Test results will be graded to evaluate the accuracy of quantitative measurements and to assess qualitative measurement parameters. The test results will identify hits (calls with any amount of overlap between the call and the solution), misses (no call for an area of a known flaw), false calls (call with no overlap of a flaw), degree of overlap between experimenter calls and actual flaw areas, and accuracy of quantitative call.

2 Data Analysis Capabilities
   Data analysis capabilities define how well the inspection system and process can correctly characterize flaws. Analysis capabilities include, but are not limited to, the ability to identify the flaw size (e.g., lateral extent), flaw location, and flaw type (i.e., distinguish between disbonds and delaminations). Quantitative aspects of the data analysis capabilities are provided by evaluating the accuracy and sensitivity as discussed above. Also, the repeatability, reliability, degree of automation, data storage and retrieval capabilities and constraints, and subjective interpretation requirements are considered when assessing the data analysis capabilities.

3. Versatility
   Versatility is the capability of the inspection system to be easily adapted for application to varying inspection tasks and conditions (e.g., varying surface conditions, specimen orientations and accessibility). Versatility is primarily assessed using qualitative metrics, such as calibration and equipment reconfiguration requirements to address differing inspection applications. Furthermore, variations in system performance due to changes in the surface condition (e.g., paint variations, front and/or back surface contaminants, surface scratches or dents), and specimen configuration (e.g., accessibility and orientation).

4. Portability
   Portability is the capability of the inspection system to be easily moved and used in standard aircraft inspection applications. Portability is assessed using qualitative metrics such as the inspection system's size, weight, apparent ease of use in each evaluated inspection application, and inspection restrictions (i.e., limitations created by power requirements, tethering or remote control issues, safety, or other factors that may restrict equipment usage). Equipment storage and shipment requirements will also be considered when evaluating the system portability.

5. Complexity
   Complexity is the intricacy of the tasks required to perform the inspections and data analysis. The inspection system should be suitable for use by qualified airline NDI personnel. Also, the inspection process should be efficient, repeatable, and reliable. Complexity is assessed using qualitative metrics, such as: the number of people required to perform the inspection; the number and difficulty of the range of tasks required for the inspection (including setup, calibration, system reconfiguration for changing inspection requirements, data acquisition, and data analysis); the number of simultaneous tasks required; tasks requiring unusual manipulative skills (as compared to traditional inspection needs) or which place the inspector in awkward positions that may be uncomfortable; and tasks that require advanced interpretative skills (including calibration, data acquisition, and data analysis - both qualitative and quantitative).

6. Human Factors
   For purposes of this evaluation, human factors include procedures or equipment (hardware or software) related inspection elements that may act as a source of human error. Environmental factors such as temperature, noise, and lighting level will not be considered. The Human Factors criterion is assessed subjectively considering: man-machine interface issues (e.g., data presentation clarity and ease of interpretation, presentation speed, layout and usability of knobs and dials, opportunities for operational or interpretative errors, glare effects, safety to the inspector and others in the surrounding area, etc.); written procedure usability (e.g., clarity, correctness, correlation to tasks actually performed); inspector education, training (initial and recurring) and experience requirements; objective versus subjective calibration, inspection, and analysis processes.

7. Inspection Time
   Inspection time is assessed quantitatively. Set up, clean up, inspection, and analysis time will be measured. This includes re-calibration and equipment reconfiguration time to move to differing inspection applications.

3. Experimenter Flaw Calls and Data Logging

The purpose of this experiment is to determine the capability of various inspection methods to detect and measure flaws in solid laminate composite aircraft structure. The Composite Laminate Flaw Detection Experiment will travel to airlines, third party maintenance depots, aircraft manufacturers, and NDI developer labs to acquire flaw detection data.

For this experiment a set of test specimens containing engineered flaws has been manufactured. The inspections will be conducted on a series of panels and Bullnose specimens of various sizes. These panels will be placed on a foam frame to support the entire perimeter and the Bullnose specimens will be placed on a flat surface to produce uniform boundary conditions across all experimenters. You will be asked to inspect each test specimen and provide any information you can about the presence of applicable flaws. If you determine that flaws are present, you should then provide size and shape information about each detected flaw. If possible, the results can be marked directly on the test specimen using only the markers provided by the experiment monitors.

If instructed by the experiment monitors, inspection results can also be marked on a full-scale sheet of tracing paper. Registration points/lines should be used on the tracing paper to assure location accuracy of the flaws. Also, test specimen numbers should be logged onto each log sheet. Note: if providing C-scan or other signal data as final results, you should identify flawed area and size (x and y dimension if at all possible on the scan image). Figure A-7 shows a sample set of flaw marks on one of the solid laminate test specimens. This study would like to assess performance for flaws as small as 1/4″ in diameter. Inspectors should use any positive indications to find flaws as small as 1/4″ in diameter. It is not necessary to track small anomalies, such as porosity, that are less than 1/4″ in length.

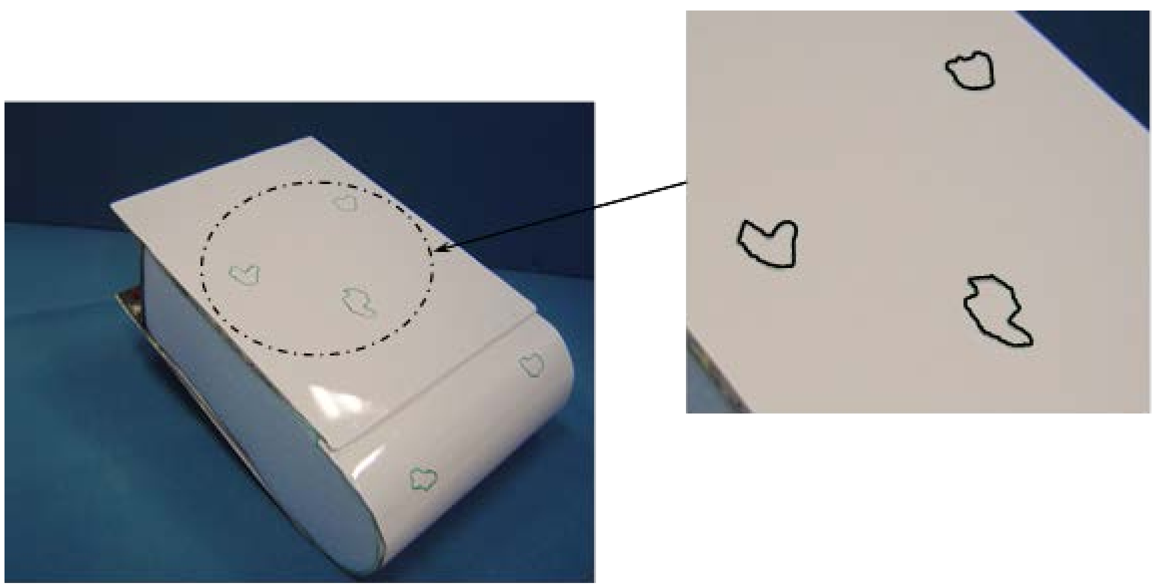

Figure A-7. Sample Set of Inspector's Flaw Marks on a Solid Laminate Test Specimen

<u>Typical Signals and Flaw Calls</u>

Figures A-8 through A-11 show a series of representative ultrasonic signals that may be produced during a pulse-echo UT inspection of a solid laminate structure. Figure A-8 shows signals that might be expected from an inspection on a co-cured laminate (skin and substructure cured at the same time) as the transducer engages flaws at various depths in the structure. Figure A-9 shows a similar set of signals stemming from an inspection on a secondarily-bonded laminate (skin and substructure cured separately and bonded in another process). Note that the secondary bond creates a bond line signal that will appear in time before the back wall signal.

Figures A-10 and A-11 show two different signals corresponding to flaws in the laminate. In Figure A-10, the back wall signal disappears, or is reduced drastically, while a new intermediate signal between the front and back wall appears. In Figure A-11, the back wall signal is reduced significantly (approximately 30%) while a new, substantial, intermediate signal appears between the front and back wall. Normally, one would use a drop in the back wall signal below 20% Full Screen Height (FSH) as an indication of a flaw. However, due to the nature of this study and the desire to detect flaws as small as 0.25″ there may be instances where the back wall signal drops significantly (perhaps 50% FSH) but not below the 20% FSH threshold. This may be due to the fact that the UT transducer has a larger footprint than the 0.25″ flaw. Thus, the transducer is actually covering an area that is both flawed (center region with disruption of UT signal) and unflawed (outer region with no disruption in UT signal). However, as shown in Figure A-11, there will also be a large intermediate signal (in the 80% FSH range) that appears between the front and back wall. When this is accompanied by a non-uniform or unusual reduction in the back wall signal, it could indicate the presence of a small delamination. A schematic of the signal travel through the flawed and unflawed regions beneath the transducer is shown in Figure A-12. UT waves at points (A) and (C) are unaffected by the presence of the small delamination flaw but the UT waves at point (C) interact with the delamination. These waves around point (C) cause the back wall signal to be reduced and also create an intermediate signal between the front and back wall. Inspectors should utilize the small flaws in the feedback panels in order to understand the type of signals associated with these flaws. This will be helpful in interpreting the flaw signals in this experiment.

Specimen Deployment

During the inspections, the various panels will be placed on a foam frame to support the entire perimeter and the Bullnose specimens will be placed on a flat surface to produce uniform boundary conditions across all experimenters. The test specimens should not be turned over at any time. The foam frame, supplied, should be assembled as per Figure A-13 to support the panels properly. The order of inspections will be set forth by the experiment monitors. The inspection order may be varied, but once started on a specific panel the inspector will be expected to complete that panel before moving onto another. The test specimens and the training/feedback specimens are painted.

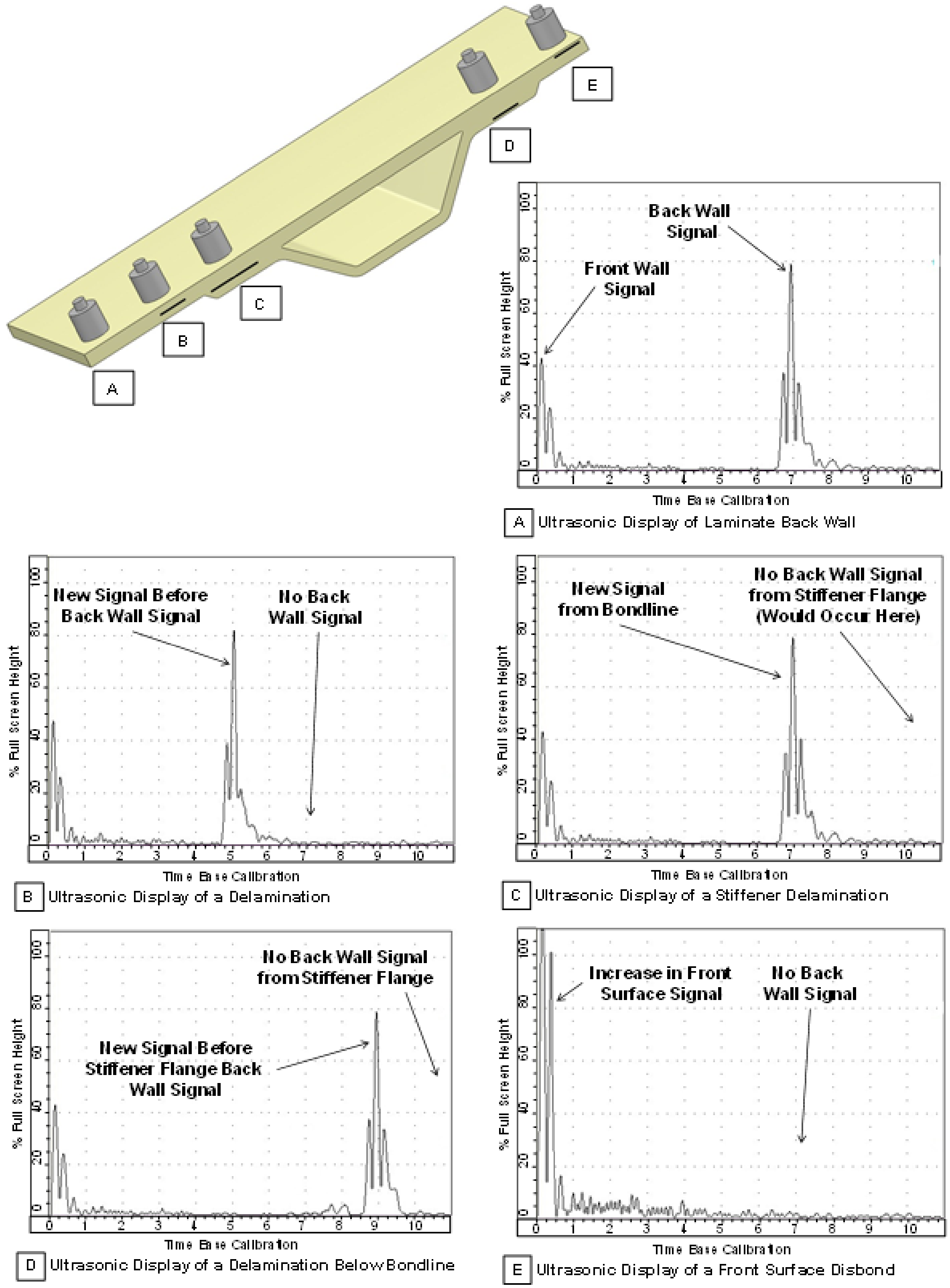

Figure A-8. Delamination Indications at Different Structure Thicknesses for Co-Cured Substructures

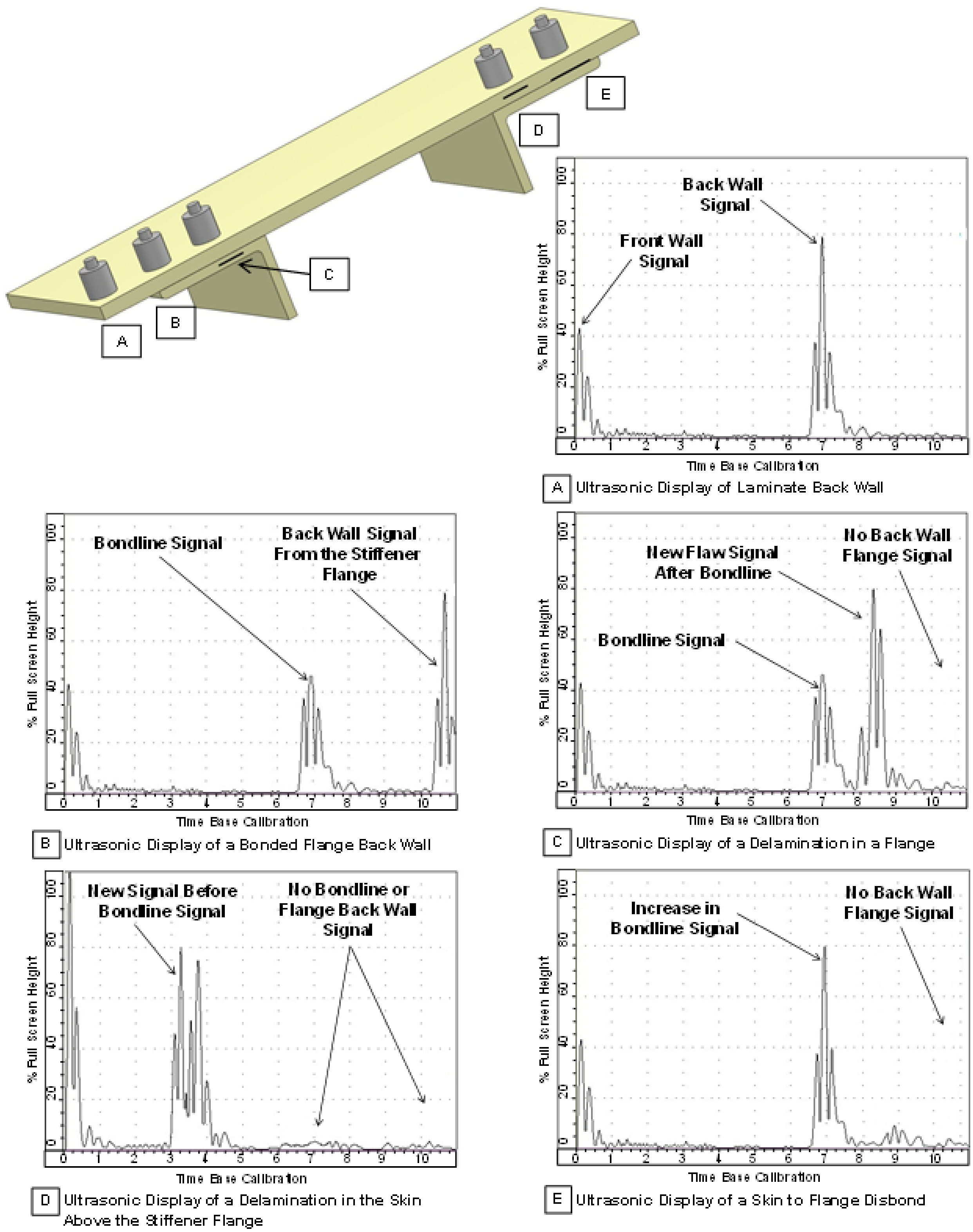

Figure A-9. Delamination Indications at Different Structure Thicknesses for Secondarily Bonded Substructures

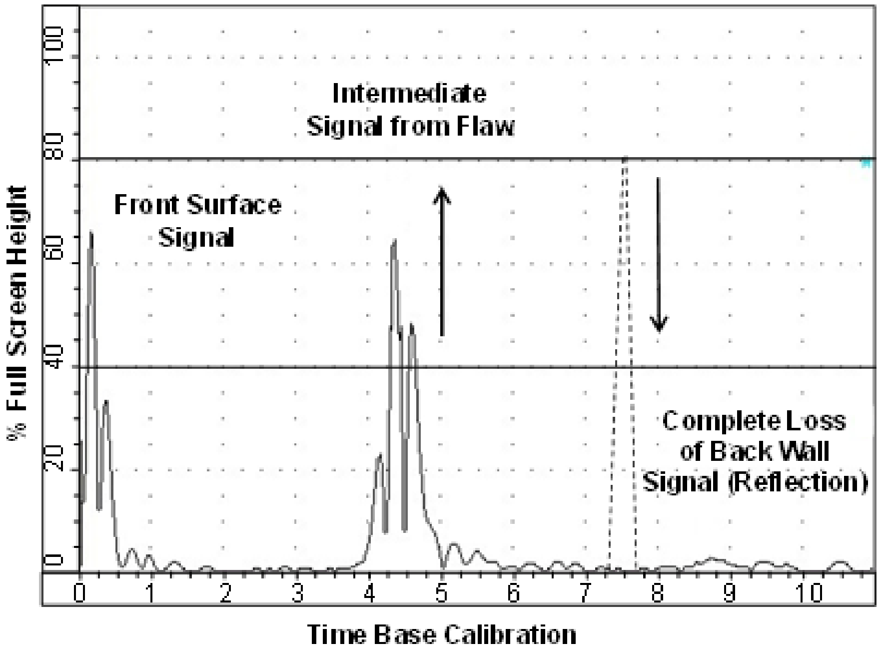

Figure A-10. Intermediate Peak and Reduction of Back Wall Signal Indicating a Flaw

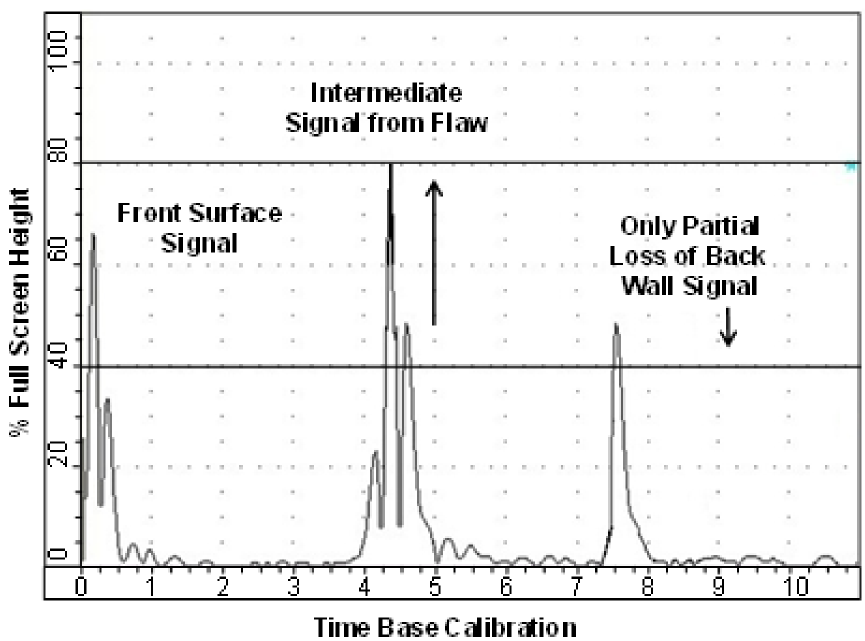

Figure A-11. Intermediate Peak with Only a Partial Reduction in Back Wall Signal that May Indicate a Small Flaw

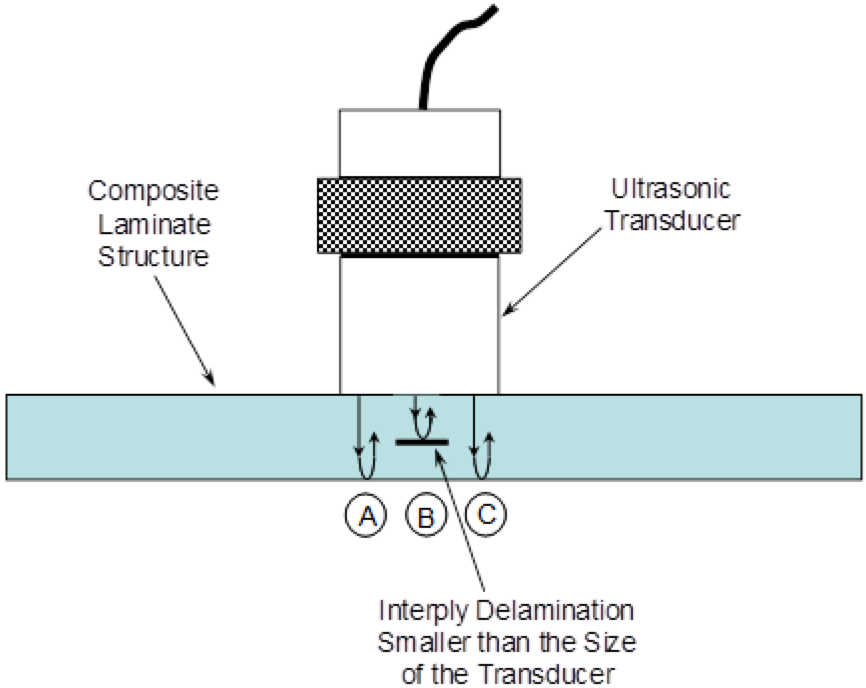

Figure A-12. Schematic Showing Reflection of Pulse-Echo UT Signals When the Flaw is Smaller than the Diameter of the UT Probe

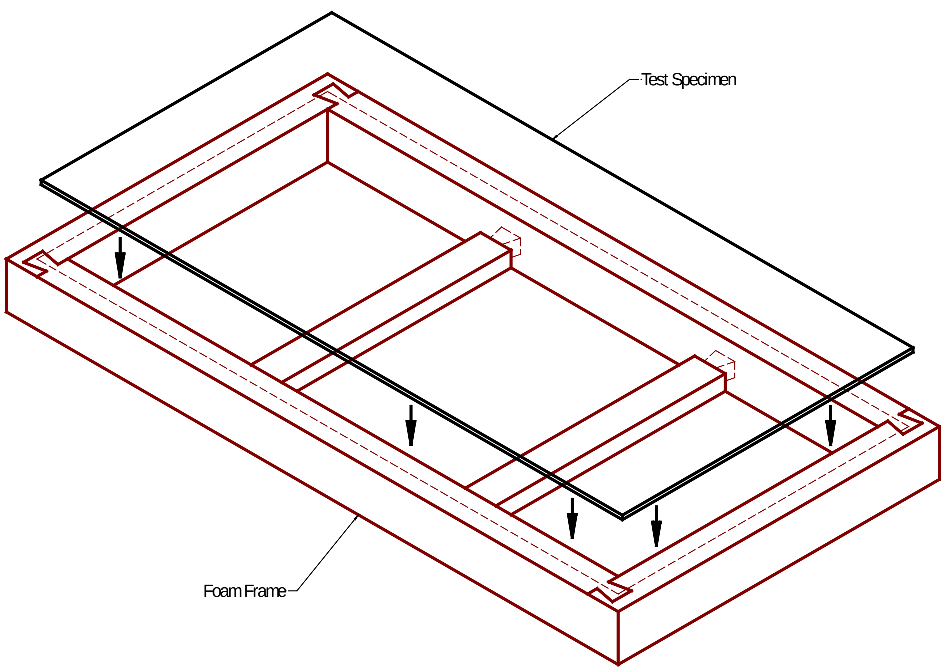

Figure A-13. During Inspections, Place Each Panel Such That it is Supported Around its Perimeter by a Foam Frame. This will Provide Uniform Boundary Conditions.

Additional guidance for inspectors performing this experiment are as follows:

- Experimenters should work at a pace that is comfortable for them. Although monitors will note start and stop times for your inspection, time to inspect is a secondary variable of the experiment.

- Applicable procedures from OEM manuals will be provided as a reference tool. Inspectors should use their own judgment as to how to perform the inspection (i.e., a strict procedure will not be enforced).

- Inspection coverage should be 100% of the panel with the exception of a small .50″ band around the perimeter of the panels where edge effects may create problems.

- The Solid Laminate Training/Feedback Specimens, or equivalent, should be used to set-up the equipment. Minor equipment adjustments stemming from in-situ calibration on the parts being inspected are allowed.

- Inspectors should draw the entire size/shape of the flaw (i.e., delineate the edges).

- Training/feedback specimens should be used as an aid to determine where to make flaw call edges. This is based on the diameter of the probe and how much of the probe needs to be over the flaw in order to react/detect.

- Inspectors do not need to determine the type of flaw just the location, size, and shape of the suspected anomaly.

- <u>Inspectors should ignore any visual clues</u> (surface anomalies in the paint or small surface marks) and to avoid using these as flaw detection aids. Such anomalies may be intentionally planted to add complexity to the inspection. <u>Inspectors should only make a call on those flaws that are highlighted by their inspection device.</u>

Test results will be graded to evaluate the accuracy of quantitative measurements and to assess qualitative measurement parameters. The test results will identify hits (calls with any amount of overlap between the call and the solution), misses (no call for an area of a known flaw), false calls (call with no overlap of a flaw), and the degree of overlap between experimenter calls and actual flaw areas. Figure A-14 is a grading parameter drawing that shows how the hits-misses-false calls results will be graded. Percentage of flaw covered will be another variable of primary interest. Error in lateral extent of flaw and maximum linear extent of overcall are variables of secondary concern and are not currently being considered as part of the grading plan.

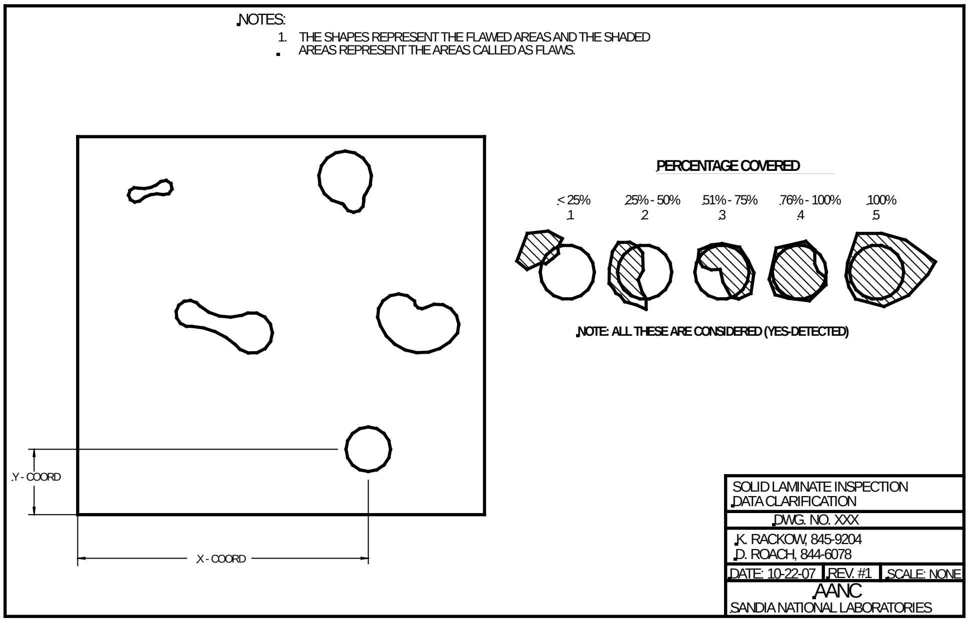

Figure A-14. Schematic Showing the Sizing Categories Comparing Experimenter Flaw Calls with Actual Flaw Information

4. Sample NDI Procedures for Pulse Echo Ultrasonic Inspection of Solid Laminate Composite Structures

Boeing and Airbus inspection procedures for solid laminate structures are provided as reference during the experiment. The procedures are for general deployment of NDT equipment that is relevant to this flaw detection experiment. The NDI procedures are included here as general information to aid inspectors in preparing for the flaw detection experiment. It is not expected that these procedures are sufficient to train an inexperienced inspector. Rather, they provide additional background and guidance to inspectors who are already familiar with the equipment and have experience in performing this type of solid laminate composite inspection. The Solid Laminate NDI feedback specimens provided with this experiment can be used in lieu of, or in addition to, the NDI standards described in the Boeing and Airbus inspection procedures.

APPENDIX B—Solid Laminate Experiment—Experiment Briefing

(presentation provided to inspectors prior to starting experiment)

Composite Laminate Flaw
Detection Experiment

Experiment Briefing

- The purpose of this experiment is to determine the capability of various inspection methods to detect and measure flaws in composite solid laminate aircraft structure. The Composite Laminate Flaw Detection Experiment will travel to many airlines and third party maintenance depots but it is not an evaluation of individual inspectors or particular companies.

- This effort will also identify the factors influencing composite inspections so that improved methods and procedures can be developed.

- You will be inspecting for representative disbonds, interply delaminations, and impact flaws in solid laminate composite structures. The test articles are modeled after the general range of construction scenarios found on commercial aircraft.

- Inspections will be conducted on a series of test panels and structures. The flat panels will be placed on a foam frame and the Bullnose specimens will be placed on a flat surface to produce uniform boundary conditions across all experimenters. You will be asked to inspect each test specimen and provide any information you can about the presence of flaws. If you determine that flaws are present, you should then provide size and shape information about each detected flaw. The results should be marked directly on the test specimen with the provided marking device.

- At no time should the inspector look at the underside of the blind test specimens. All references to test specimen structural configuration should be done by reviewing drawings provided for each specimen type. Note: two drawings will be provided for each specimen type. The first one will show the structural configuration of the panel in the orientation it is being inspected (painted side up with dark triangle marked in upper right-hand corner). The second drawing is an Isometric of the panel if the bottom side of the panel was turned up (just to show structural details that are on underside).

- When you have completed your inspection of the panel do not remove the panel from the inspection frame. Call on your experiment monitor to remove the test panel and provide the next panel.
- We will be recording the equipment make and model, probe information, and various settings that are used during the inspections, so if at any time you change probes, frequency or other pertinent settings during your inspections please call it to our attention so that we can record them.

- There are spray bottles available if you would like to mix the couplant with water to dilute it and then spray on the test specimens for coupling purposes.

- There are two separate experiments. There is a Thin Laminate Skin experiment [1] with skins ranging from 12-20 plies (0.078″ to 0.130″ thick) and total thickness extending to 62 plies (0.406″) when substructure is considered. There is also Thick Laminate Skin experiment [2] with 32 ply skins (0.21″ thick) and total thickness extending to 58 plies (0.377″) when substructure is considered.

- Inspectors can complete the Thin Laminate Skin experiment in 3 days. There are 11 specimens in this experiment. Inspectors can complete the Thick Laminate Skin experiment in 1 to 2 days. There are 4 specimens in this experiment.

- Experimenters should work at a pace that is comfortable for them; time to inspect is a secondary variable of the experiment. Inspectors should take whatever time is necessary to assure that any and all flaws in the test specimens are found.

- Test Specimens
  - → **Material Type** - carbon graphite
  - → **Laminate Thicknesses** - Panels have 12 (~.078″), 20 (~.130″), 24 (~.156″), and 32 (~.229″) plies.
  - → **Substructure Thicknesses** – .075″, .125″, .192″, .225″, and .250″
  - → **Tapered Area Ranges** – 12-20 (.50″ step), 20-32 (.50″ step), and 12-20 (.25″ step)
  - → **Paint** - All panels are painted as per current aircraft specifications.
  - → **Flaw Detection** - Inspectors should use any positive indications to find flaws as small as 1/4″ in diameter.
  - → **Inspection Device** – You may use any inspection device that you would normally use to inspect composite laminate structures.

- Each blind inspection process should be preceded by inspections on appropriate solid laminate training/feedback specimens supplied by the experiment monitors. You will be given information on the manufactured flaws present in the training/feedback specimens. The training/feedback specimens have the same construction as the blind test specimens and include similar flaws.

- Inspectors may need or choose to use alternate probes due to: a) variation and extremes in thickness, and b) our desire to find flaws as small as ¼″ diameter. The training/feedback specimens allow inspectors to try probes of various sizes and frequencies so that they can optimize their equipment before performing the blind inspections.

- The figure below shows a sample set of flaw marks on one of the solid laminate composite test specimens. This study would like to assess performance for flaws as small as 1/4″ in diameter. Inspectors should use any positive indications to find flaws as small as 1/4″ in diameter. It is not necessary to track small anomalies, such as porosity, that are less than 1/4″ in length.

- Experimenters should try various transducers on the feedback panels (known flaw profiles) provided in this experiment to determine the best transducer to use for each laminate thickness. Existing Boeing and Airbus procedures reference the use of UT transducers in the range of 1-10 MHz (1, 2.25, 5, 10 MHz are all listed). The transducer diameters are listed as 0.5″ and 0.25″ in diameter. The required flaw detection listed in the Boeing procedures is 5/64″ dia. Both the Boeing and Airbus procedures are contained in the "Experimenters Information Packet."

- An inspector will complete all specimens (11) for the 12-20 ply experiment or 4 specimens for the 20-32 ply experiment and will be asked to finish all of a specific specimen design (i.e., Bullnose, Complex Taper) before moving on to the next specimen type.

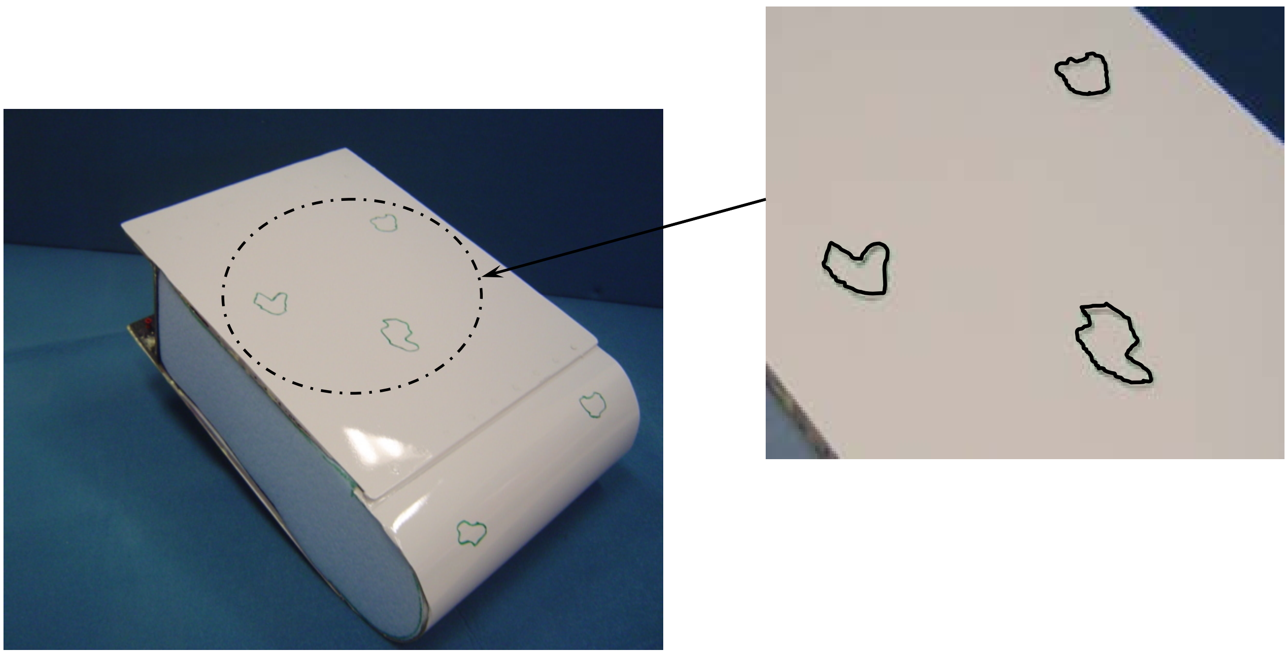

- Additional guidance for inspectors performing this experiment are as follows:
  → Experimenters should work at a pace that is comfortable for them. Although monitors will note start and stop times for your inspection, time to inspect is a secondary variable of the experiment.
  → Applicable procedures from OEM manuals will be provided as a reference tool. Inspectors should use their own judgment as to how to perform the inspection (i.e., a strict procedure will not be enforced).
  → Inspection coverage should be 100% of the panel with the exception of a small .50″ band around the perimeter of the panels where edge effects may create problems.
  → The Solid Laminate Training/Feedback Specimens provided should be used to set-up the equipment. Minor equipment adjustments stemming from in-situ calibration on the parts being inspected are allowed.
  → Inspectors should draw the entire size/shape of the flaw (i.e., delineate the edges).
  → Inspectors do not need to determine the type of flaw just the location, size, and shape of the suspected anomaly.

→ Inspectors should ignore any visual clues (surface anomalies in the paint or small surface marks) and to avoid using these as flaw detection aids. Such anomalies may be intentionally planted to add complexity to the inspection. Inspectors should only make a call on those flaws that are indicated by their inspection device.

→ Training/Feedback Specimens should be used as an aid to determine where to make flaw call edges. This is based on the diameter of the probe and how much of the probe needs to be over the flaw in order to react/detect.

- Go through the series of A-scan signals in Experimenter Information Packet to clarify flaw calls.

- Test results will identify hits (calls with any amount of overlap between the call and the solution), misses (no call for an area of a known flaw), false calls (call with no overlap of a flaw), and the degree of overlap between experimenter calls and actual flaw areas.

- You will be provided with feedback to indicate how you performed - percentage of flaws found, how well you sized the flaws, and number of false calls made. Inspectors will gain experience and feedback on the implementation of your inspections on representative aircraft structure. No individual inspector's names will be linked to any experiment results. Similarly, no organization's name will be linked to any group of experiment results. However, results of all participants will be combined and potential users will be able to compare the results of competing inspection techniques and systems.

- We can also provide feedback on the type of flaws that were detected and missed so that the inspector will learn what types of flaws they have trouble detecting. It is important to note that the feedback to the inspectors is kept confidential. In the final aggregate results, we ensure that the participants are always kept anonymous so that there is no way to correlate any results to a specific person or airline.

- A series of Boeing and Airbus inspection procedures, relevant to this flaw detection experiment, are included in your "Experimenter Information Packet." Use them as you see fit. They provide information on equipment set-up and scan patterns for typical solid laminate inspections.

APPENDIX C—SOLID LAMINATE EXPERIMENT—EXPERIMENT MONITOR DATA ACQUISITION SHEETS

SOLID LAMINATE INSPECTION TIMING RESULTS AND PANEL DISTRIBUTION (12-20 PLY)														
Panel Description	Panel Inspection Order (random)	Start Time 1	Stop Time 1	Elapsed Time 1	Start Time 2	Stop Time 2	Elapsed Time 2	Start Time 3	Stop Time 3	Elapsed Time 3	Start Time 4	Stop Time 4	Elapsed Time 4	Total Elapsed Time
Complex Taper 1-A														
Complex Taper 1-B														
Complex Taper 2-A														
Complex Taper 2-B														
Simple Taper 1-A Upper														
Simple Taper 1-A Lower														
Simple Taper 2-A Upper														
Simple Taper 2-A Lower														
Bullnose 1														
Bullnose 2														
Bullnose 3														
													Total	

Inspector Name: ______________________ Date: ____________

Company: ____________________________

Inspection Method: _____________________

Note: Multiple start and stop times for a single test specimen are provided in case the inspector needs to take a break(s) before completing inspection of a single specimen.

Figure C-1. Solid Laminate Inspection Timing Results and Panel Distribution (12-20 Ply)

SOLID LAMINATE INSPECTION TIMING RESULTS AND PANEL DISTRIBUTION (20-32 PLY)														
Panel Description	Panel Inspection Order (random)	Start Time 1	Stop Time 1	Elapsed Time 1	Start Time 2	Stop Time 2	Elapsed Time 2	Start Time 3	Stop Time 3	Elapsed Time 3	Start Time 4	Stop Time 4	Elapsed Time 4	Total Elapsed Time
New 32 - 1														
New 32 - 2														
New 32 - 3														
New 32 - 4														
													Total	

Inspector Name: ______________________ Date: ____________

Company: ____________________________

Inspection Method: _____________________

Note: Multiple start and stop times for a single test specimen are provided in case the inspector needs to take a break(s) before completing inspection of a single specimen.

Figure C-2. Solid Laminate Inspection Timing Results and Panel Distribution (20-32 Ply)

EQUIPMENT CALIBRATION

Name of inspector/facility: ____________________

Inspector Number: ____________

12-20 or 20-32 ply Experiment: ____________

Inspectors Experience: Overall NDI - ____________ NDI of Composites - ____________

Record the technique to be used : ____________________

Record equipment information :

Manufacturer: ____________________

Model: ____________ Serial #: ____________________

Certification Date: ____________________

Record probe or other ancillary equipment information:

Manufacturer: ____________________

Reference #: ____________________

Record any other accessory information: ____________________

____

____

____

____

Ask the participant to provide specific equipment set/up or calibration settings. Examples of the type of information to be provided could include some of the following:

Gain: horizontal _____vertical _____ meter ____________

Frequency (kHz) ____________

Filtering ____________

Calibration Level ____________

____________ Inspection threshold

Coil output impedance ____________

Digitization ____________

Figure C-3 (sheet 1). Experiment Monitor Data Acquisition Sheet

Equipment calibration performed: YES NO (circle one)

Record calibration standard information:

a) Solid Laminate Composite Ref. Stds. were used: YES NO (circle one)
b) Other Ref. Stds. used (if so, list)____

____

c) Is calibration standard used referenced in NDT manual? YES NO (circle one)
d) How long did it take to calibrate the equipment? ________________________

Note any difficulties encountered during equipment calibration.

____

____

____

____

Note any innovative procedures or practices used for equipment calibration.

____

____

Figure C-3 (sheet 2). Experiment Monitor Data Acquisition Sheet

INSPECTION

Name of inspector/facility: ______________________________

Device Deployed ______________________

Experience, background information (including experience on device deployed). ________

____

____

____

List NDI devices used at the facility for composite inspections: ____________________

____

____

____

Note any difficulties encountered during the inspection. ____________________

____

____

____

____

Note any innovative procedures or practices used during the inspection of this specimen.

____

____

____

____

INSPECTION DATA LOGGING

Figure C-4 (sheet 3). Experiment Monitor Data Acquisition Sheet

ANALYSIS

Name of inspector/facility: ____________________

Did the operator/inspector follow pre-set criteria for flaw identification? Yes No

If Yes, describe the criteria; If No, describe how the decision was made.

____

____

____

____

Note any difficulties encountered during the analysis of this specimen?

____

____

____

____

Note any innovative procedures or practices used for analysis?

____

____

____

____

Figure C-5 (sheet 4). Experiment Monitor Data Acquisition Sheet

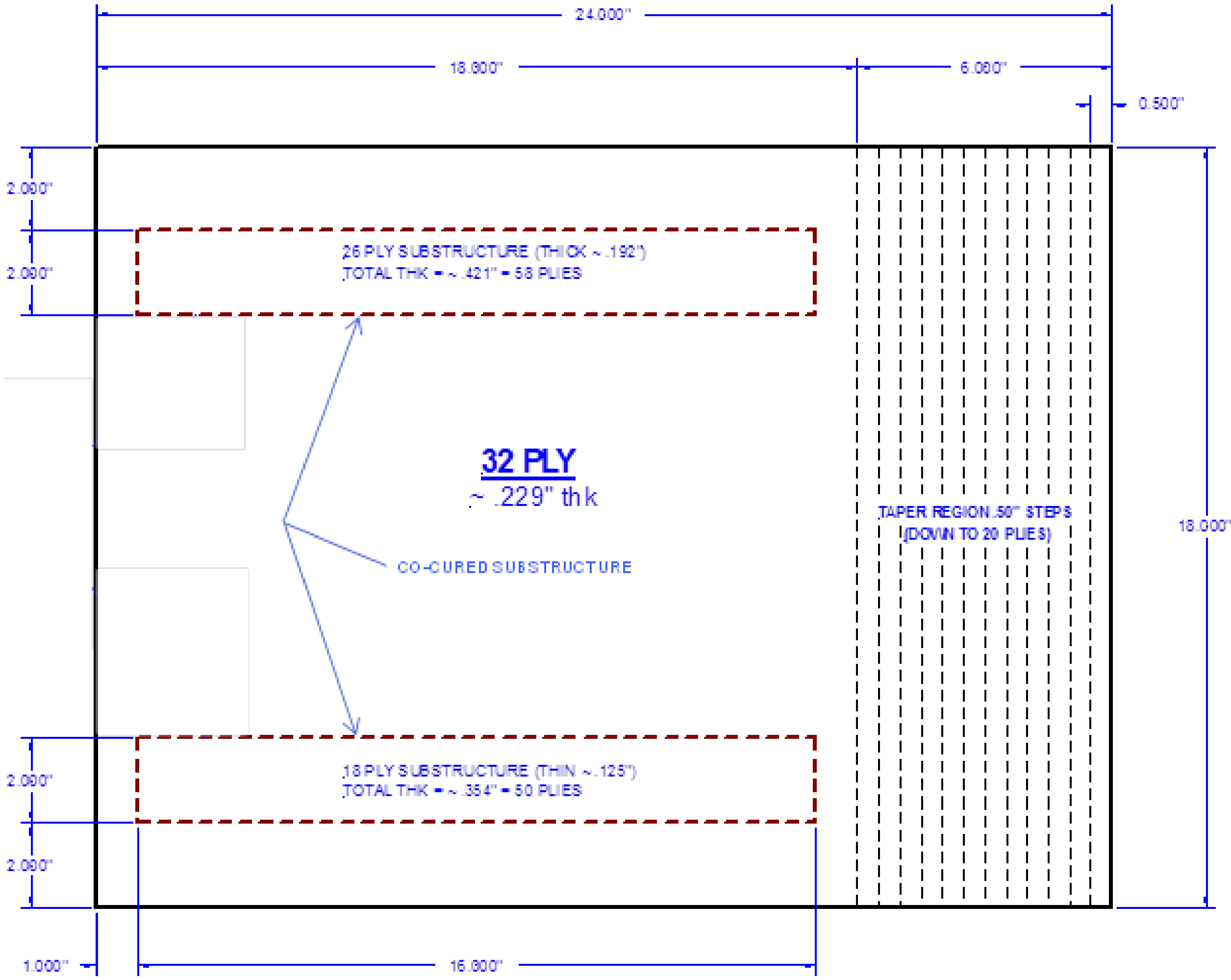

Figure D-1. Simple Taper 20-32 Ply Specimen—4 Panels, All the Same Size, But With Different Flaw Profiles

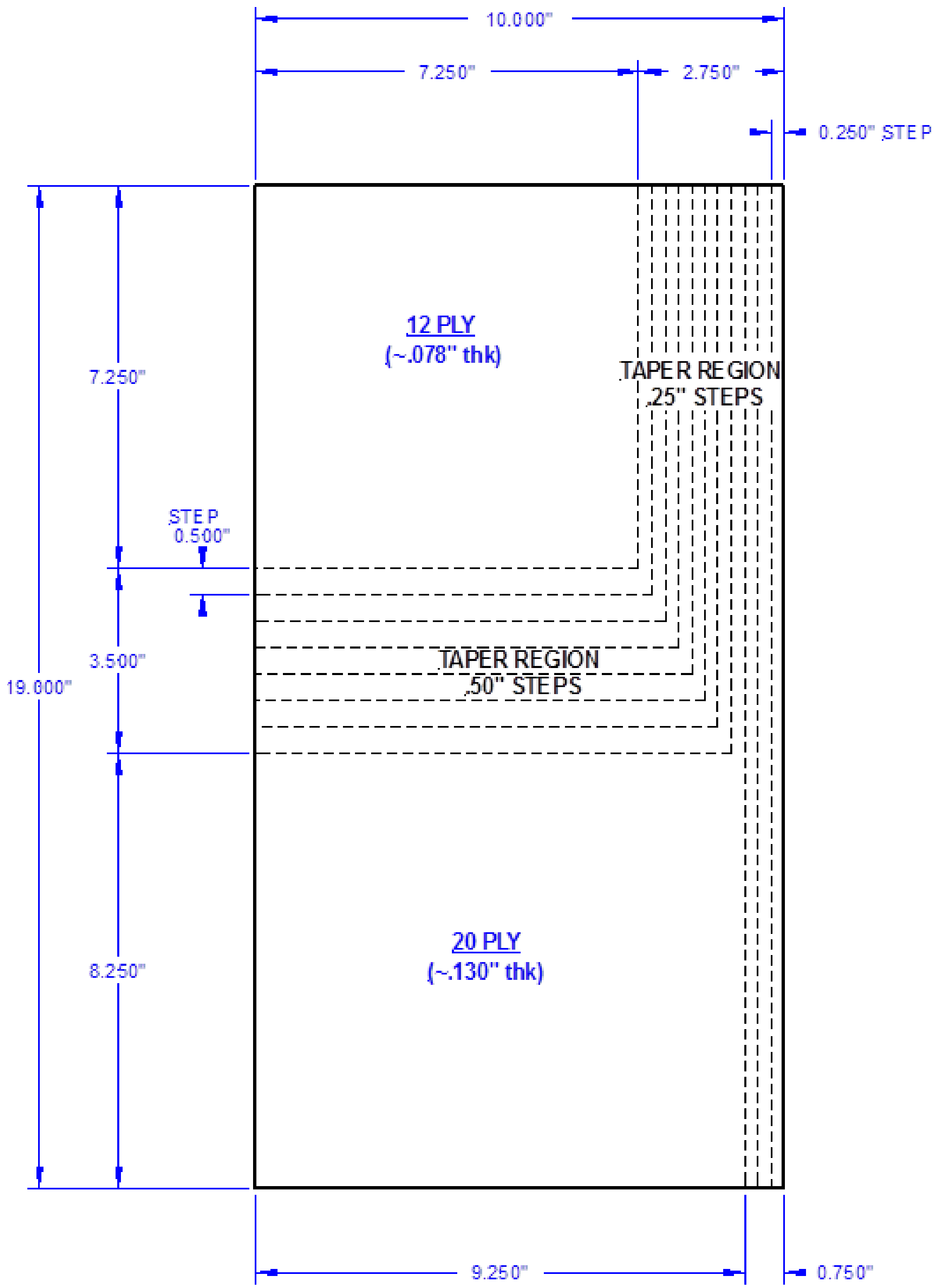

Figure D-2. Complex Taper 12-20 Ply Specimen—4 Panels, All the Same Size, But With Different Flaw Profiles

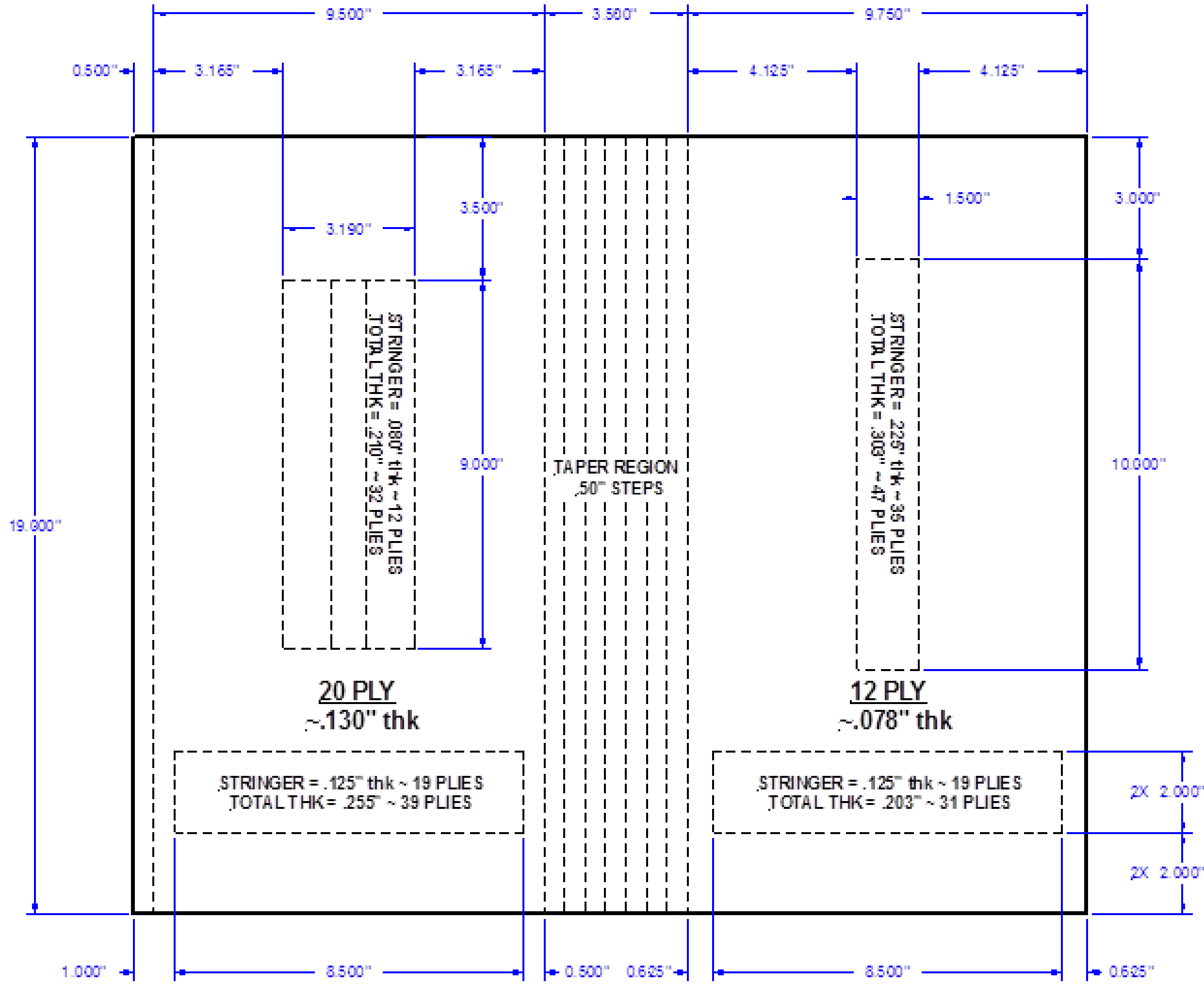

Figure D-3. Simple Taper 12-20 Ply Specimen—4 Panels, All the Same Size, But With Different Flaw Profiles

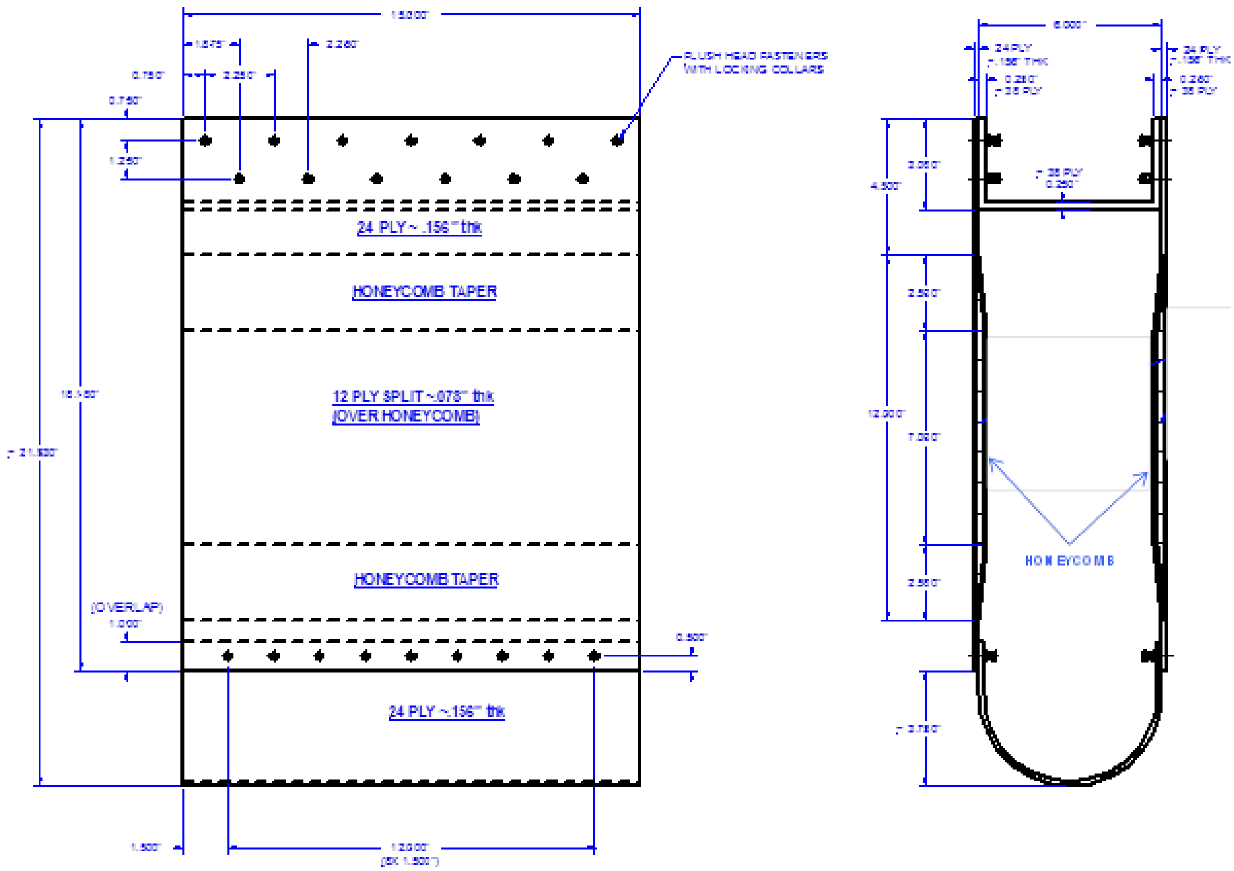

Figure D-4. Bullnose 12-20 Ply Specimen—3 Panels, All the Same Size, But With Different Flaw Profiles

APPENDIX E—RAMP DAMAGE CHECK EXPERIMENT—SETUP AND OPERATION PROCEDURES FOR GE® BONDTRACER™ AND OLYMPUS NDT 35 RAMP DAMAGE CHECK DEVICES

GE Bondtracer™
Set Up Procedure
Initial Set Up

<u>Step 1</u>: Connect the probe cable to the probe connector located on the top panel of the GE Bondtracer™.
<u>Step 2</u>: Connect the probe to the other end of the cable.
<u>Step 3</u>: Press the **[ON/OFF]** button to power on the unit. The Bondtracer™ will start an internal self-check and lights all the LED's in a chase pattern. The blue LED remains lit as long as the Bontracer™ is on.
Note: If the Bondtracer™ fails the self-check, the working LEDs blink for 10 seconds, and then the Bondtracer™ will power down. The blue power LED will begin to flash when about 30 minutes of run time remain on the batteries. The Bondtracer will shut down automatically when the battery level is too low to provide proper operation.

<u>Step 4</u>: Find a **GOOD** area next to the visible discrepancy on the aircraft or composite structure for calibration.
<u>Step 5</u>: Apply ultrasonic couplant to the **GOOD** area, place the probe on the surface, and then press the **CAL** button for 1 second. If the calibration is successful, A solid yellow LED indicates a calibration has been stored and the probe is coupled **(See Figure E-1)**. A flashing yellow LED indicates that a calibration has been stored, and that the probe is currently uncoupled.

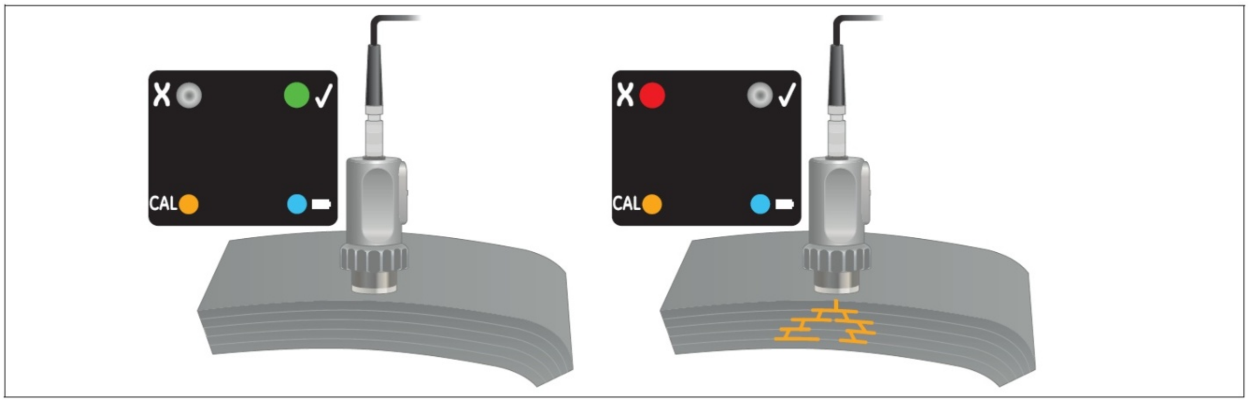

Figure E-1

NOTE: ***If the yellow LED is off, reapply couplant, recouple with the area, and then press the CAL button again.***
<u>Step 6</u>: To test a piece of suspect material with the calibrated Bondtracer™, couple the probe to the suspect area. It compares the amplitude and TOF (Time Of Flight) with the values from the known-good material **(CAL)** and delivers a **PASS** or **FAIL** result **(See Figure E-1)**.

➔ If the amplitude and TOF of the signal from the area being inspected are within the defined limits, the green LED will illuminate, indicating a “**PASS**.”

➔ If the amplitude and TOF of the signal from the area being inspected is less than the defined limits, the red LED will illuminate, indicating a “**FAIL**.”

➔ If the amplitude and TOF of the signal from the area being inspected is greater than the defined limits, the red LED and yellow LED will blink, indicating an “**ABOVE CALIBRATED RANGE**.”

CAUTION

Call a trained nondestructive testing technician if you get confusing readings or indications of subsurface damage (delaminations).

Key Items on the Use of the GE Bondtracer™ are as Follows:

- It should be used with a straight edge
- It should only be scanned from two directions
- It should be scanned parallel to the stiffeners
- It should be scanned toward the damage from each of the two directions
- If both directions produce a red light, the user is permitted to map out the size of the damage, again using scans that are in parallel paths and approaching the defect from opposing directions
- It should not be used within 1 inch of a fastener hole
- If confusing indications are obtained, the user should call NDT (after checking for proper couplant, the delay line coupling, etc.).

Key Things to Know about How it Operates:

- It identifies areas that appear thinner than the null location, or lack a back surface echo of sufficient amplitude.
- It will be "above calibrated range” when both the red and yellow LED’s blink.
- If you calibrate on a thin area, then scan into a thick area, delaminations lying beyond the calibration thickness will not be detected. It is mitigated by the requirement to null and scan toward the damage from two directions, and by the blinking red and yellow LED’s "above calibrated range” warning given by the instrument.

Olympus NDT 35RDC
(Ramp Damage Checker)
Set Up Procedure
Initial Set Up

Step 1: Connect the transducer cable to the transducer connector located on the top panel of the Panametrics 35RDC.
Step 2: Connect the transducer to the other end of the cable.
Step 3: Press the **[ON/OFF]** key to turn on the gage.
Step 4: Approximately 3 seconds after the gage is turned on, your screen will say "**Cal to Start**".
Step 5: Find a **GOOD** area next to the visible discrepancy on the aircraft or composite structure for calibration.
Step 6: Apply ultrasonic couplant to the **GOOD** area, place the probe on the surface, and then press the **CAL** button. If the calibration is successful, the unit will display **SUCCESSFUL**, and then displays **GOOD** while coupled to the calibration location **(see Figure E-2)**.

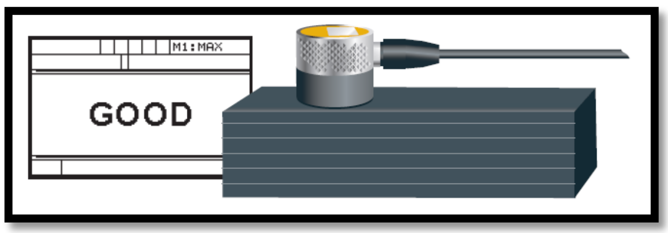

Figure E-2

NOTE: ***The unit will display one of two messages: SUCCESSFUL or CAL FAIL. In a CAL FAIL condition, reapply couplant, recouple with the area, and then press the CAL key again. A unit that does not calibrate may be an indication that the transducer cable is defective, the transducer is not functioning properly, or the calibration area is outside the measurement range of the instrument.***

Step 7: Index from the calibration area toward the area of possible damage. If the area is **GOOD**, your screen will indicate **GOOD** as shown in ***Figure E-3***. If the display shows **BAD**, there may be damage present as shown in ***Figure E-4.***

NOTE: If the transducer is scanned over an area of greater thickness than the calibration point, the gage displays **BEYOND CAL THICKNESS** as shown in ***Figure E-5***. If this occurs, recalibrate to the thickness currently within your scanning zone.

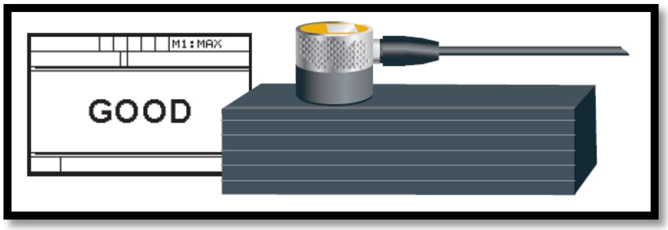

Figure E-3

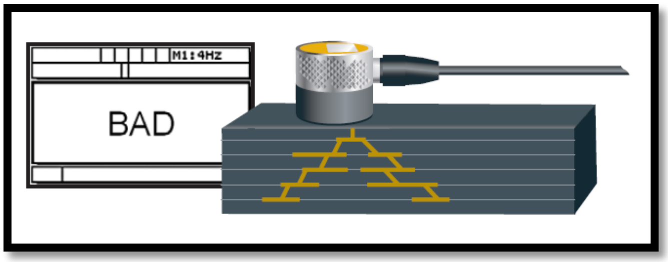

Figure E-4

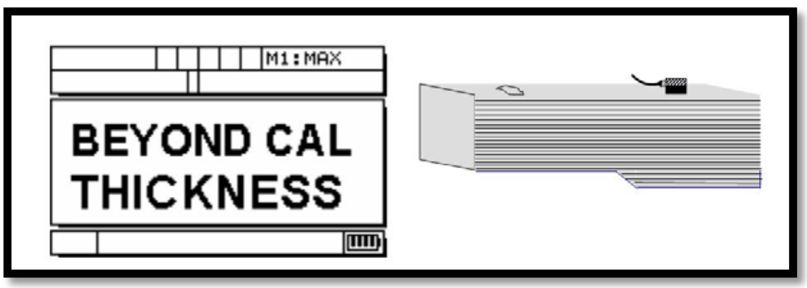

Figure E-5

<u>Key Items on Use of the RDC are as Follows:</u>

- It should be used with a straight edge
- It should only be scanned from two directions
- It should be scanned parallel to the stiffeners
- It should be scanned toward the damage from each of the two directions.
- If both directions produce a BAD Indication, the user is permitted to map out the size of the damage, again using scans that are in parallel paths and approaching the defect from opposing directions
- It should not be used within 1 inch of a fastener hole
- If confusing indications are obtained, the user should call NDT (after checking for proper couplant, the delay line coupling, etc.).

<u>Key Things to Know about How it Operates:</u>

- It identifies areas that appear thinner than the null location, or lack a back surface echo of sufficient amplitude.
- It will say "beyond calibration thickness" (35RDC) if you move into a thicker area
- If you calibrate on a thin area, then scan into a thick area, delaminations lying beyond the calibration thickness will not be detected. It is mitigated by the requirement to null and scan toward the damage from two directions, and by the "beyond calibration thickness" warning given by the instruments.

CAUTION

Call a trained nondestructive testing technician if you get confusing readings or indications of subsurface damage (delaminations).

APPENDIX F—RESULTS FROM AVIATION INDUSTRY SURVEY OF COMPOSITE NDI TRAINING

Aviation Industry Survey of Composite NDI Training

Thomas Rice
Dennis Roach
FAA Airworthiness Assurance NDI Validation Center
Sandia National Laboratories

F.1 Introduction

The aircraft industry continues to increase its use of composite materials, most notably in the area of principle structural elements. This expanded use, coupled with difficulties associated with damage tolerance analysis of composites, has placed greater emphasis on the application of accurate nondestructive inspection (NDI) methods. Inspecting these composite structures is a critical element in assuring their continued airworthiness. Typical damage encountered in composite structures includes: (1) disbonds and delaminations stemming from normal flight loads, (2) fluid ingress, (3) impact damage, (4) lightning strikes, (5) deterioration from contact with fluids, such as paint strippers or hydraulic fluids, and (6) extreme heat and ultraviolet exposure. Each of these elements can produce hidden damage that may be difficult to visually detect, yet are detrimental to the strength of the structure.

The Federal Aviation Administration (FAA) Airworthiness Assurance NDI Validation Center (AANC) at Sandia National Laboratories, in conjunction with the Commercial Aircraft Composite Repair Committee Inspection Task Group (CACRC-ITG), recently completed a study to assess conventional and advanced inspection methods as applied to flaw detection in solid composite laminate aircraft structures. The results from the Composite Laminate Flaw Detection Experiment, also referred to as the Solid Laminate Experiment (SLE), are being published in a Department of Transportation report as industry-wide performance measures [F-1]. The SLE experiment assessed the ability of conventional NDI techniques, as deployed at aircraft maintenance facilities, to detect voids, disbonds, delaminations, and impact damage in adhesively bonded composite aircraft structures. A series of solid laminate, carbon composite specimens with statistically relevant flaw profiles were inspected using conventional, handheld pulse echo ultrasonics (PE UT) to evaluate the sensitivity and repeatability of this inspection. The primary factors affecting flaw detection in laminates were included in the SLE study: material type, flaw profiles, presence of complex geometries like taper and substructure elements, presence of fasteners, secondarily bonded joints, and environmental conditions. The SLE program used airline personnel to study probability of detection (POD) in the field and to formulate improvements to existing inspection techniques.

After a sufficient number of inspectors had completed the experiment, industry-wide performance curves were established to determine how well current inspection techniques are able to reliably find flaws in composite laminate structure. In total, over 70 inspectors from 14 airlines and 2 Maintenance and Repair Organizations (MRO) participated in this experiment. The test program was intended to evaluate the technical capability of the inspection procedures and the equipment (i.e., the NDI method). Evaluation of inspector-specific or environment-specific factors associated with performing the inspections were not the primary objective of the experiment; however, key insights regarding measures to improve inspection performance were obtained. The inspections emphasized flaw detection methods applicable to solid laminate structures ranging from 12-plies to 64-plies thick. Overall, the results from the SLE study produced input and recommendations to the FAA regarding guidance (e.g., Advisory Circular [AC]) that can enhance the composite inspection process. Thus, the SLE study was driven by a desire to improve aircraft safety. Airlines and OEMs can use these results to guide NDI deployment and training, to define what flaws/damage can be reliably found by inspectors, and to reduce the human factors issues to produce improved NDI performance in the field.

For an inspector deploying handheld, PE UT methods, the overall $POD_{[90/95]}$ levels for solid laminate composite structures occur when the flaw, or damage, is approximately 1.0″ in diameter ($POD_{[90/95]}$ = 1.0″). Although this is in alignment with the industry-desired flaw detection capabilities, it was also observed that the inspector performance varied for the same set of test specimens. Some inspection scenarios showed a larger spread in individual inspector results than others. These results brought about an interest in understanding one of the key factors in inspector performance—NDI training.

Successful efforts to transition inspectors from “average” to “good” or “outstanding” performance levels will have a significant effect on $POD_{[90/95]}$ levels. Possible measures to achieve this include: increased training, apprenticeships, exposure to representative inspections, enhanced procedures, inspector teaming, and awareness training on inspection obstacles. The survey discussed in this report was conducted in an effort to understand and define the NDI training practices currently being carried out to prepare inspectors for composite laminate inspections. With these results in hand, it is then possible to propose improvements in composite NDI training practices.

The main drivers for this “Composite NDI Training” survey were to: (1) understand the general nature of the training available for NDI of composites, (2) identify the similarities and differences in training among the major aircraft maintenance depots, and passenger and cargo airlines, (3) determine the needs with respect to composite NDI training, as defined by the aviation industry, (4) identify additional training and/or training aids that will help propel inspectors from average to good and outstanding categories to improve composite NDI performance [F-1], and (5) translate these results into actions for aviation industry teams and airline training departments to facilitate improvements.

Training programs for aircraft inspectors are based on, and guided by, a number of industry nondestructive testing training, qualification, and certification documents [F-2 through F-6]. Thus, the aircraft maintenance depots have similar foundations for their training programs. However, there is sufficient leeway to allow airlines to customize their training programs and to expand their training beyond the minimum requirements. AC 65-31A [F-2] states that “Nondestructive testing is defined as inspections, tests, or evaluations that may be applied to a structure or component to determine its integrity, composition, electrical or thermal properties, or dimensions without causing a change in any of these characteristics. Qualified personnel are required for reliable performance of nondestructive testing. Both the performance of tests and the interpretation of results require skill and must be accomplished by trained personnel." Thus, it is important to understand how aircraft maintenance facilities qualify and train their inspectors. This survey used the information found in references [F-2 through F-6], combined with the potential, additional training brought on by composite laminate inspection requirements, to formulate a series of questions related to composite NDI training. It is believed that the results compiled in this report will help formulate critical NDI training, whether developed in-house or by industry support groups such as the CACRC, that can improve inspector performance and, thus, improve the POD and reliability of composite laminate inspections.

F.2 Composite NDI Training Survey Results

F.2.1 Background Information

Twenty airline (passenger and cargo) and MROs were contacted by phone to participate in the Composite NDI Training Survey. Once an organization agreed to participate, an invitation letter and survey were e-mailed to them directly. See section 4 of this appendix for a copy of the participant survey. The participant locations consisted of 17 unique companies, some with multiple locations. Two locations from Delta Air Lines and United Airlines were chosen to include locations of former airlines that recently merged with these two carriers. Of the 20 unique locations, 16 locations responded with a completed survey (80% participation). Table F-1 lists the participating companies in alphabetical order, along with their completed survey status. Figure F-1 shows the completed survey respondents organized by their aviation category. To understand more about the individuals who completed the survey, Figure F-2 shows the breakdown of the individual respondents by their job title. Table F-2 is a list assigning a respondent number to each response received. The respondent numbers will be used throughout this report to link answers from each question to the respondent category.

Table F-1. Composite NDI Training Survey Participants

Composite NDI Training Survey Participants	
Company	Completed Survey
AAR-ASI (Indy)	Yes
American Airlines® (Tulsa)	Yes
Aviation Technical Services, Inc (Seattle)	Yes
Delta Airlines (Atlanta)	Yes
Delta Airlines (MN)	Yes
FedEx® (Indy)	Yes
FedEx (Los Angeles)	Yes
Goodrich Aerostructures (Chula Vista)	Yes
Kalitta Air LLC (Michigan)	Yes
Rohr Aero Services LLC (Alabama)	Yes
Southwest Airlines® (TX)	Yes
Timco (Georgia)	Yes
United Airlines® (Houston)	Yes
United Airlines (San Francisco)	Yes
UPS® (KY)	Yes
US Airways (PA)	Yes

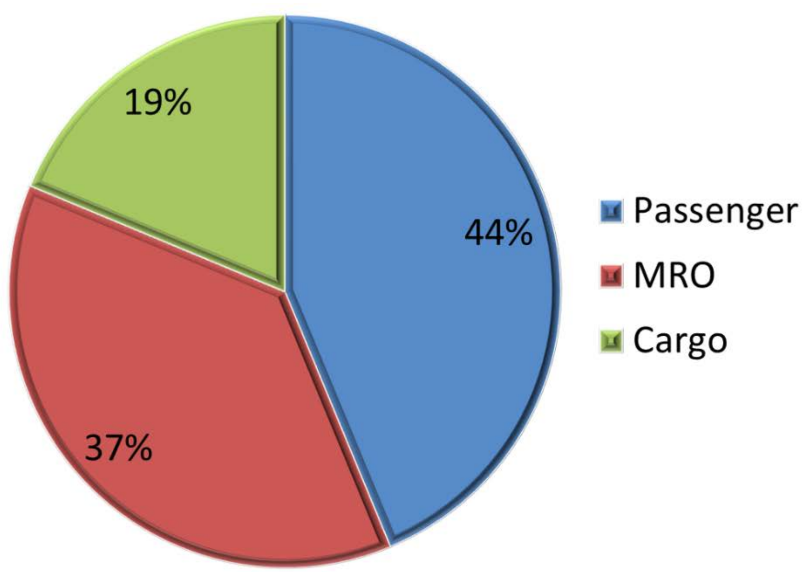

Figure F-1. Survey Respondents (16)—Organized by Aviation Category

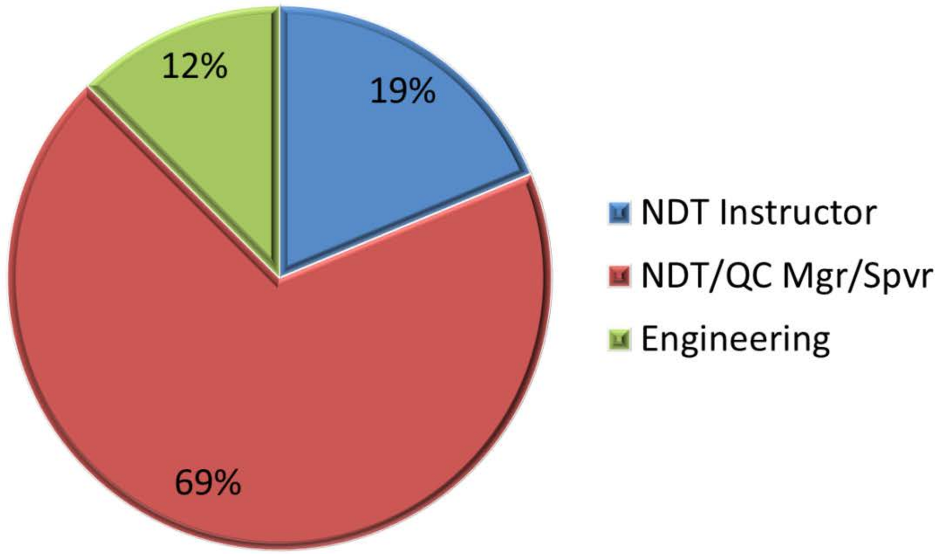

Figure F-2. Survey Respondents (16)—Organized by Job Title

Table F-2. Survey Respondents Aviation Category

Respondents Aviation Category	
Respondent #	Category
1 (P)	Passenger
2 (P)	Passenger
3 (P)	Passenger
4 (P)	Passenger
5 (P)	Passenger
6 (P)	Passenger
7 (P)	Passenger
8 (M)	MRO
9 (M)	MRO
10 (M)	MRO
11 (M)	MRO
12 (M)	MRO
13 (M)	MRO
14 (C)	Cargo
15 (C)	Cargo
16 (C)	Cargo

F.2.2 Survey Results

The following are the results based on survey questions sent to the various airline and MROs that participated in the Composite NDI Training Survey. In the aggregate results, all survey participants were kept anonymous from their responses so that it would not be possible to correlate any results to a specific person or participating company. Please note that, for some of the following questions, the respondents were asked to check all that apply. Figures F-3 through F-58 show the results of each of the individual survey questions.

Question 1: Describe the general NDI training programs at your company.

> **Respondent 1 (Passenger):** We use ATA specification 105 guideline for training, qualifying, and certifying personnel to the minimum requirement for inspection of aircraft, power plant and components.
>
> **Respondent 2 (P):** We have a comprehensive program that includes classroom instruction, OJT, recurrent training and performance assessments in accordance with industry standards. The methods include ET, IR, MT, PT, UT and X-ray.
>
> **Respondent 3 (P):** NDT training is accomplished in accordance with the company Nondestructive Test Training Manual, which is based on ATA Spec.105. Course outlines are maintained for all NDT training courses and qualification levels, based primarily ASNT CP-105.
>
> **Respondent 4 (P):** Our program complies with NAS-410 and ATA 105
>
> **Respondent 5 (P):** Our company has classroom training followed by OJT with level 1s, level 1 and level 2. All methods require written exams and practical assessments. We also require recurrent classroom training every 2 years and random assessments at any time.
>
> **Respondent 6 (P):** We use NAS 410 and ATA105 as guides. We have 4 qualifications, level I limited, level I, Level II and Level III.
>
> **Respondent 7 (P):** We use ATA 105 2012 edition
>
> **Respondent 8 (Maintenance):** Our training and certification program is our own based on SNT-TC-1A and ATA 105 Documents for ET, MT, PT, UT and RT.
>
> **Respondent 9 (M):** We use a combination of in-house and outside NDT contractors to obtain our current NDT training programs.

Respondent 10 (M): We use a combination of the training hours and experience between the three major NDT standards ASNT TC-1A, NAS 410 and ATA-105 so that all of our customers' requirements are met.

Respondent 11 (M): Classroom and OJT training for the following methods: ET, UT, PT, and MT. This is done to meet the intent of NAS-410 and ATA-105 NDT certification standards.

Respondent 12 (M): Designed in accordance with NAS410 requirements.

Respondent 13 (M): No Response

Respondent 14 (Cargo): Provided by local vendor. ASNT III qualified ET, UT, PT and MT. RT is provided by different vendor for film Interpretation only.

Respondent 15 (C): We used guide lines from ATA-105. 1) All class room trainings from outside vendor (Hellier…), 2) In house OJT

Respondent 16 (C): Our NDT Training Program is derived from the ATA Specification 105 and modified to meet the scope of our operation. The training of unqualified NDT personnel will consist of initial formal training in the particular inspection technique either in–house or vendor contracted. This training will consist of theory and hands–on training necessary to impart the knowledge level of the NDT inspection method. Practical hands–on training will consist of equipment set up, and demonstrating accepted techniques using equipment standards. The NDT methods we use to support both line maintenance and wheel and brake shop operations are Ultrasonic, Eddy Current, Magnetic Particle and Penetrant inspections.

Question 2: Indicate how your NDI training program is implemented.

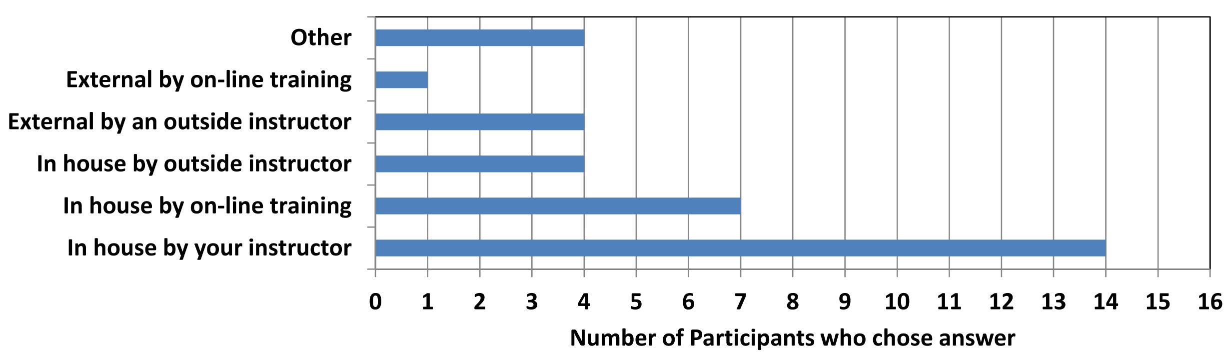

Figure F-3. Chart Showing How the Aviation Industry Implements Their NDI Training Programs (Aviation Industry—All Respondents)

Responses provided for "other" in question 2:

Respondent 2 (P): OEM training at their facility when offered.

Respondent 5 (P): OEM when offered.

Respondent 6 (P): We've used most of the above methods to get the training information out; self-directed internet, in house level I class with OJT and outside vendor level I and II theory training then bring the student in for OJT. Using an outside vendor for general theory and in house OJT works well. We also use an outside vendor to train re-current training to our customized course. We wrote it to be particular to aircraft inspections.

Respondent 15 (C): In-house OJT by experienced inspectors.

Question 3: What type of formal documentation is obtained from the instruction?

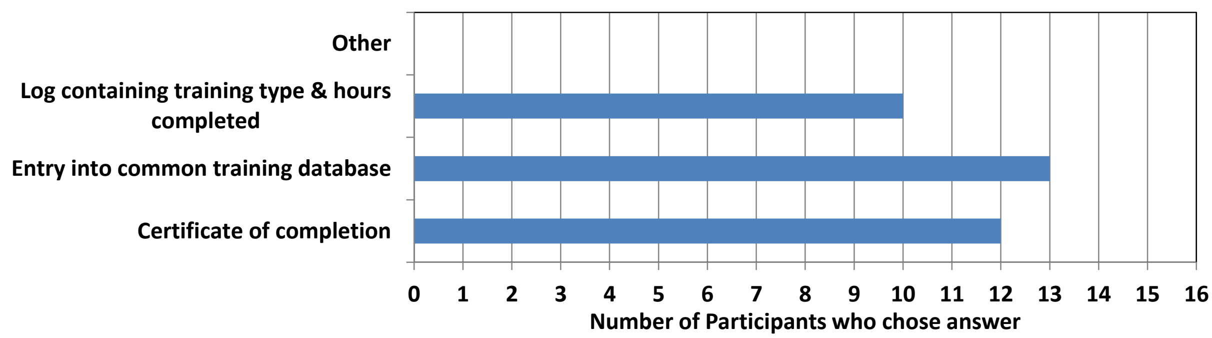

Figure F-4. Chart Showing Type of Formal Documentation the Aviation Industry Obtains From Instruction (Aviation Industry—All Respondents)

Comment provided for question 3:

Respondent 6 (P): If an outside source is used, using their training course, they will provide a certificate. We will give credit for the person as accomplishing either Level I or Level II classroom.

Question 4 (Laminate Composites): What NDI techniques does your company employ to inspect composites?

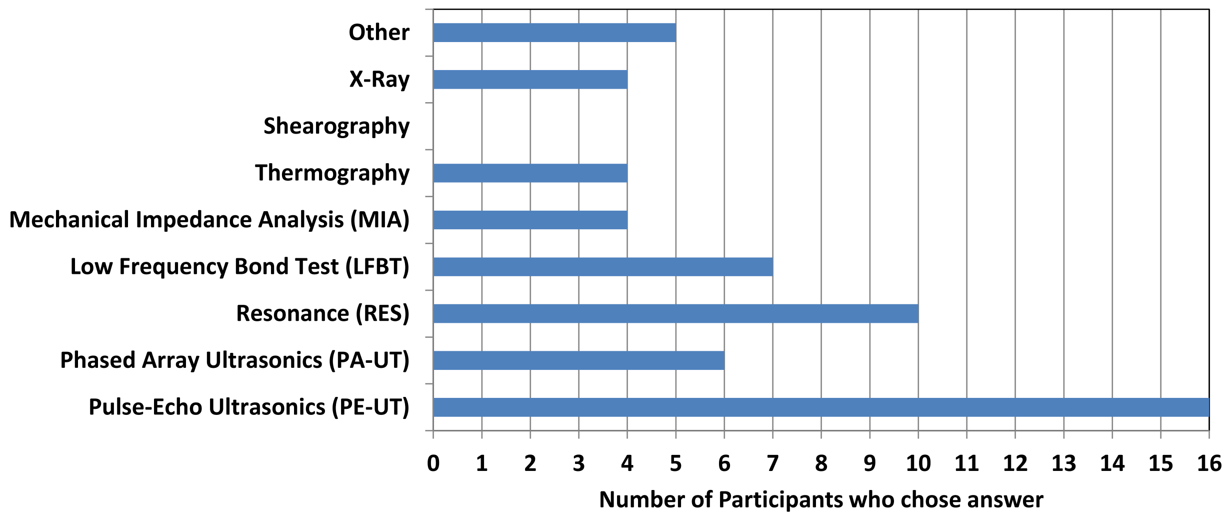

Figure F-5. Chart Showing the NDI Techniques That Are Used by the Aviation Industry to Inspect Laminate Composites (Aviation Industry—All Respondents)

Responses provided for "other" in question 4 (Laminate Composites):

Respondent 3 (P): Air Coupled TTU and Manual TTU.

Respondent 8 (M): Through Transmission (TTU).

Respondent 10 (M): Through Transmission (TTU).

Respondent 11 (M): Through Transmission Ultrasonics (contact technique) and tap test (coin test).

Respondent 13 (M): Through Transmission (TTU).

Question 4 (Honeycomb Composites): What NDI techniques does your company employ to inspect composites?

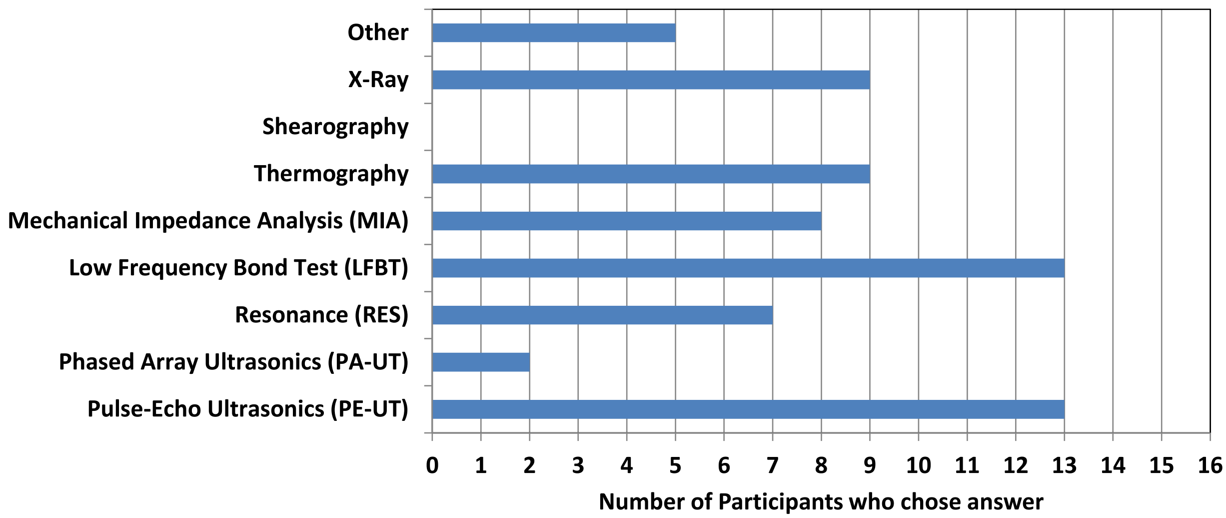

Figure F-6. Chart Showing the NDI Techniques That Are Used by the Aviation Industry to Inspect Honeycomb Composites (Aviation Industry—All Respondents)

Responses provided for "other" in question 4 (Honeycomb Composites):

Respondent 3 (P): Air Coupled TTU.

Respondent 6 (P): Mostly Tap Testing due to the number of plies involved in the repairs we do in-house.

Respondent 10 (M): Through Transmission (TTU).

Respondent 11 (M): Through Transmission Ultrasonics (contact technique) and tap test (coin test).

Respondent 13 (M): Through Transmission (TTU).

Question 5: Do inspectors also receive general composite training to understand composite materials, plies, lay-ups, scarfed repairs, composite design, composite processing, etc.?

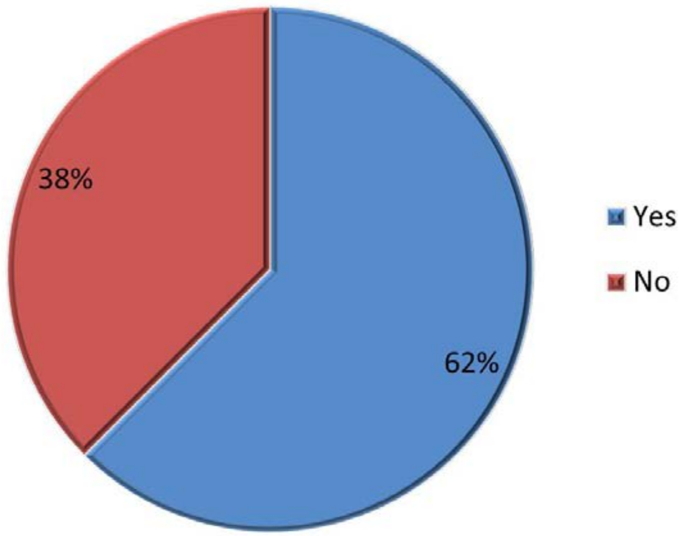

Figure F-7. Chart Showing Percentage of the Aviation Industry That Provide Inspectors With General Composite Training (Aviation Industry—All Respondents)

Tabulated Responses provided for “yes” in question 5:

Table F-3. Table Showing General Composite Training Structure (Aviation Industry—10 Respondents Answered “Yes” to Question 5)

Question 5 – (If Yes)		
Respondent #	How Many Hours/Year	How Many Classes/Year
1 (P)	80	2
2 (P)	No general composite training	NA
3 (P)	40	1
4 (P)	No general composite training	NA
5 (P)	No general composite training	NA
6 (P)	24	One Time Training
7 (P)	40	1
8 (M)	Limited & not structured	As needed
9 (M)	Initial qualification only	NA
10 (M)	24	As needed
11 (M)	Did not specify	Did not specify
12 (M)	40	1
13 (M)	No general composite training	NA
14 (C)	No general composite training	NA
15 (C)	40	1
16 (C)	No general composite training	NA

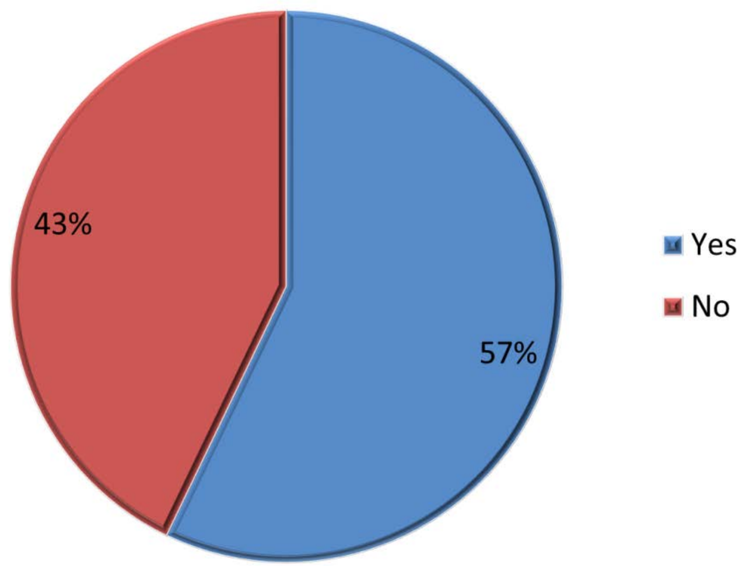

Figure F-8. Chart Showing Percentage of Passenger Respondents That Provide Inspectors With General Composite Training (Passenger Category Respondents Only)

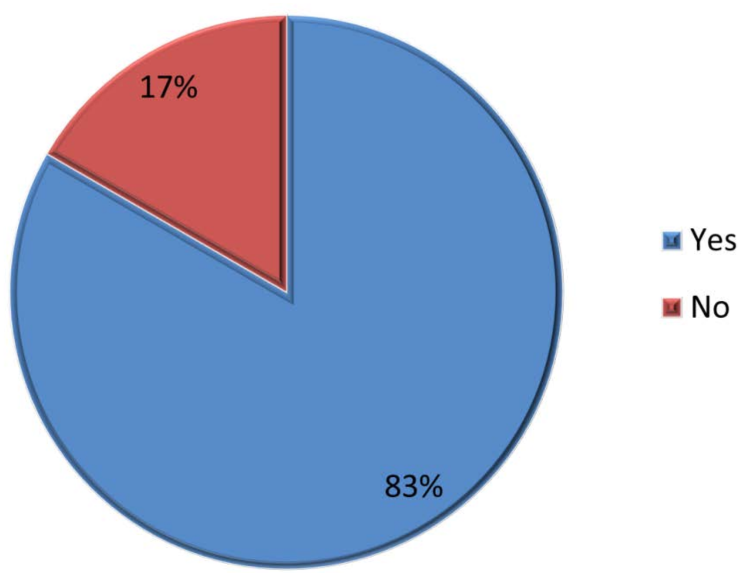

Figure F-9. Chart Showing Percentage of MRO Respondents That Provide Inspectors With General Composite Training (MRO Category Respondents Only)

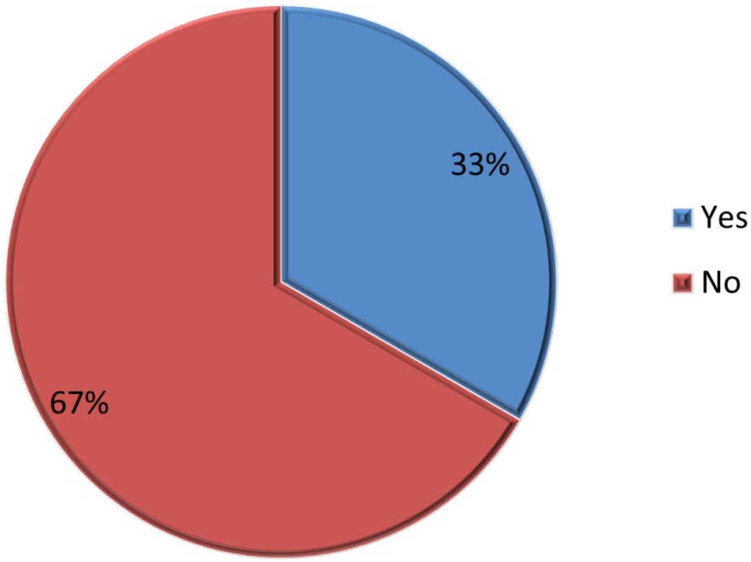

Figure F-10. Chart Showing Percentage of Cargo Respondents That Provide Inspectors With General Composite Training (Cargo Category Respondents Only)

Question 6: Do you have additional, specialized training specifically for inspectors who can perform composite inspections? [This would be above-and-beyond your normal NDI training.]

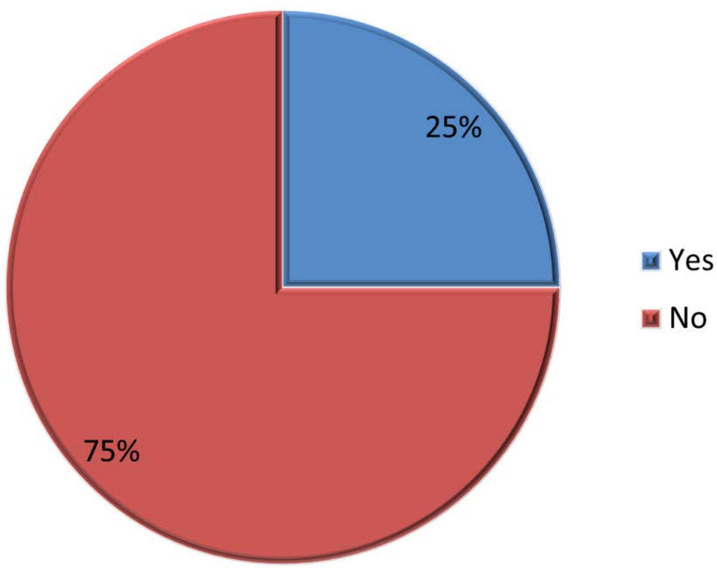

Figure F-11. Chart Showing Percentage of the Aviation Industry That Provides Inspectors With Additional, Specialized Training to Perform Composite Inspections (Aviation Industry—All Respondents)

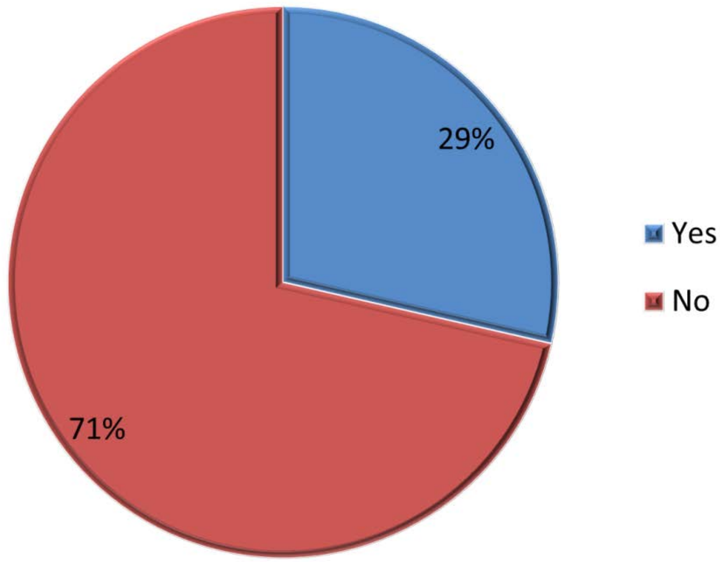

Figure F-12. Chart Showing Percentage of Passenger Respondents That Provide Inspectors With Additional, Specialized Training to Perform Composite Inspections (Passenger Category Respondents Only)

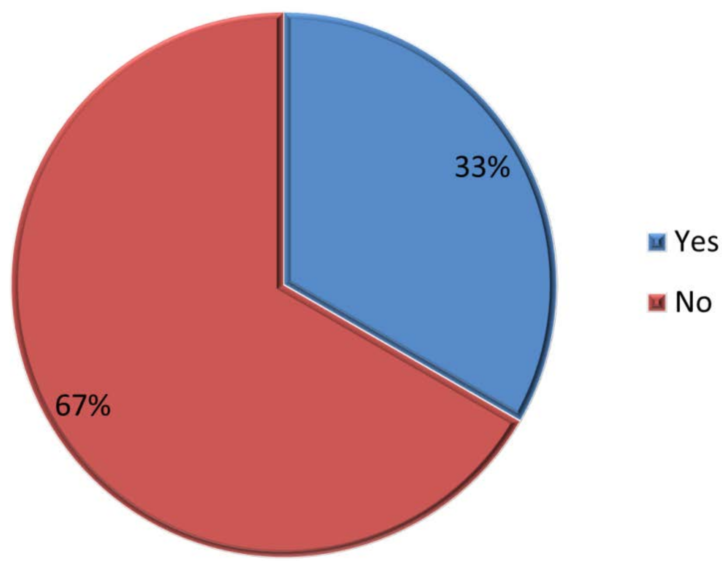

Figure F-13. Chart Showing Percentage of MRO Respondents That Provide Inspectors With Additional, Specialized Training to Perform Composite Inspections (MRO Category Respondents Only)

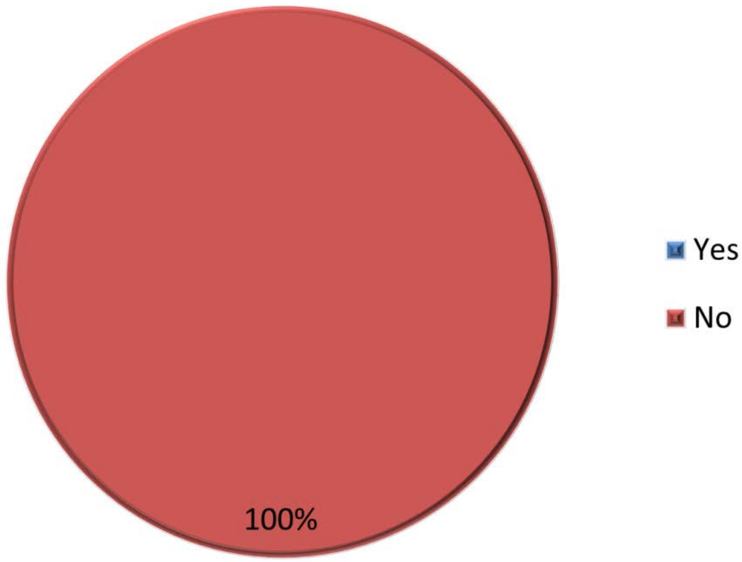

Figure F-14. Chart Showing Percentage of Cargo Respondents Who Provide Inspectors with Additional, Specialized Training to Perform Composite Inspections (Cargo Category Respondents Only)

Responses provided for “yes, please describe” in question 6:

> **Respondent 1 (P):** No description provided.
>
> **Respondent 3 (P):** Training in these areas has generally been provided by OEM’s (Airbus and Boeing) specific to certain inspections. Example: Airbus A320 elevator and rudder, Boeing 787 damage repair and assessment, 787 composite repair, 787 composite fan blade inspection. In-house courses in these areas have been further developed and implemented using OEM course material.
>
> **Respondent 8 (M):** We give hands on training with the Bondmaster™, Pulse Echo and TTU when inspections arise for composites in addition to that inserted in our L1 and L2 training program.
>
> **Respondent 10 (M):** Composite qualification is obtained through OJT for each technique PE, TTU, Pitch-Catch, Resonance and then further broken down to fiberglass, carbon fiber and type aircraft. No hours are assigned for OJT qualifications but are more toward performance based. A minimum is: observe task , perform task, and qualify.

Comment provided for question 6:

> **Respondent 11 (M):** This is part of initial qualification for certification.

Question 7: If the answer to the previous question is “Yes,” list the areas in which you provide <u>additional</u>, specialized NDI <u>training</u> for composite inspections (above and beyond Level I, II and

III NDI certification for composites). List how many total hours of specialized, composite NDI training inspectors complete and over what interval?

Respondent 1 (P): See tables below. (Respondent stated that the training for laminate and honeycomb composites is combined and is the reason for duplicate answers below.)

Table F-4. Respondent 1 for Laminate Composites

Laminate Composites			
Method	Total OJT Hours	Total Classroom Hours	Over What Time Period in Years
Pulse-Echo Ultrasonics (PE-UT)	400	40	N/A
Phased Array Ultrasonics (PA-UT)	160	80	N/A
Resonance (RES)	-	-	-
Low Frequency Bond Test (LFBT)	-	-	-
Mechanical Impedance Analysis (MIA)	-	-	-
Thermography	210	32	N/A
Shearography	-	-	-
X-Ray	400	40	N/A
Other (list)	-	-	-

Table F-5. Respondent 1 for Honeycomb Composites

Honeycomb Composites			
Method	Total OJT Hours	Total Classroom Hours	Over What Time Period in Years
Pulse-Echo Ultrasonics (PE-UT)	400	40	N/A
Phased Array Ultrasonics (PA-UT)	160	80	N/A
Resonance (RES)	-	-	-
Low Frequency Bond Test (LFBT)	-	-	-
Mechanical Impedance Analysis (MIA)	-	-	-
Thermography	210	32	N/A
Shearography	-	-	-
X-Ray	400	40	N/A
Other (list)	-	-	-

Respondent 3 (P): See tables below.

Table F-6. Respondent 3 for Laminate Composites

Laminate Composites			
Method	Total OJT Hours	Total Classroom Hours	Over What Time Period in Years
Pulse-Echo Ultrasonics (PE-UT)	-	-	-
Phased Array Ultrasonics (PA-UT)	20	40	1
Resonance (RES)	-	-	-
Low Frequency Bond Test (LFBT)	-	-	-
Mechanical Impedance Analysis (MIA)	-	-	-
Thermography	-	-	-
Shearography	-	-	-
X-Ray	-	-	-
Other (list)	-	-	-

Table F-7. Respondent 3 for Honeycomb Composites

Honeycomb Composites			
Method	Total OJT Hours	Total Classroom Hours	Over What Time Period in Years
Pulse-Echo Ultrasonics (PE-UT)	-	-	-
Phased Array Ultrasonics (PA-UT)	-	-	-
Resonance (RES)	-	-	-
Low Frequency Bond Test (LFBT)	-	-	-
Mechanical Impedance Analysis (MIA)	-	-	-
Thermography	-	-	-
Shearography	-	-	-
X-Ray	-	-	-
Other (list)	-	-	-

Respondent 6 (P): See tables below (Answered "no" to question 6, but provided data).

Table F-8. Respondent 6 for Laminate Composites

Laminate Composites			
Method	Total OJT Hours	Total Classroom Hours	Over What Time Period in Years
Pulse-Echo Ultrasonics (PE-UT)	-	-	-
Phased Array Ultrasonics (PA-UT)	-	-	-
Resonance (RES)	-	-	-
Low Frequency Bond Test (LFBT)	2-4	-	One time
Mechanical Impedance Analysis (MIA)	-	-	-
Thermography	-	-	-
Shearography	-	-	-
X-Ray	-	-	-
Other (list)	-	-	-

Table F-9. Respondent 1 for Honeycomb Composites

Honeycomb Composites			
Method	Total OJT Hours	Total Classroom Hours	Over What Time Period in Years
Pulse-Echo Ultrasonics (PE-UT)	-	-	-
Phased Array Ultrasonics (PA-UT)	-	-	-
Resonance (RES)	-	-	-
Low Frequency Bond Test (LFBT)	-	-	-
Mechanical Impedance Analysis (MIA)	-	-	-
Thermography	-	-	-
Shearography	-	-	-
X-Ray	-	-	-
Other (list)	-	-	-

Respondent 8 (M): See tables below.

Table F-10. Respondent 8 for Laminate Composites

Laminate Composites			
Method	Total OJT Hours	Total Classroom Hours	Over What Time Period in Years
Pulse-Echo Ultrasonics (PE-UT)	-	8	-
Phased Array Ultrasonics (PA-UT)	Not yet	-	-
Resonance (RES)	-	-	-
Low Frequency Bond Test (LFBT)	-	-	-
Mechanical Impedance Analysis (MIA)	-	-	-
Thermography	NA	-	-
Shearography	NA	-	-
X-Ray	NA	-	-
Through Transmission	-	-	-

Table F-11. Respondent 1 for Honeycomb Composites

Honeycomb Composites			
Method	Total OJT Hours	Total Classroom Hours	Over What Time Period in Years
Pulse-Echo Ultrasonics (PE-UT)	-	-	-
Phased Array Ultrasonics (PA-UT)	-	8	-
Resonance (RES)	-	-	-
Low Frequency Bond Test (LFBT)	-	-	-
Mechanical Impedance Analysis (MIA)	-	-	-
Thermography	-	-	-
Shearography	-	-	-
X-Ray	-	-	-
Other (list)	-	-	-

Respondent 10 (M): See tables below.

Table F-12. Respondent 10 for Laminate Composites

Laminate Composites			
Method	Total OJT Hours	Total Classroom Hours	Over What Time Period in Years
Pulse-Echo Ultrasonics (PE-UT)	20	-	-
Phased Array Ultrasonics (PA-UT)	0	-	-
Resonance (RES)	10	-	-
Low Frequency Bond Test (LFBT)	20	-	-
Mechanical Impedance Analysis (MIA)	0	-	-
Thermography	0	-	-
Shearography	0	-	-
X-Ray	0	-	-
Other (list)	0	-	-

Table F-13. Respondent 10 for Laminate Composites

Honeycomb Composites			
Method	Total OJT Hours	Total Classroom Hours	Over What Time Period in Years
Pulse-Echo Ultrasonics (PE-UT)	0	-	-
Phased Array Ultrasonics (PA-UT)	0	-	-
Resonance (RES)	0	-	-
Low Frequency Bond Test (LFBT)	20	-	-
Mechanical Impedance Analysis (MIA)	0	-	-
Thermography	10	-	-
Shearography	0	-	-
X-Ray	0	-	-

Question 8: Do inspectors receive additional training related to composite repair inspection?

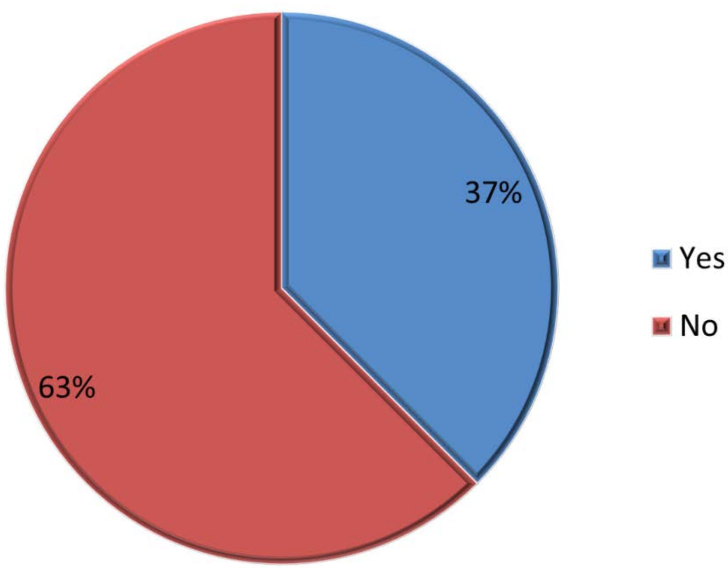

Figure F-15. Chart Showing Percentage of the Aviation Industry That Provides Additional Training Related to Composite Repair Inspection (Aviation Industry—All Respondents)

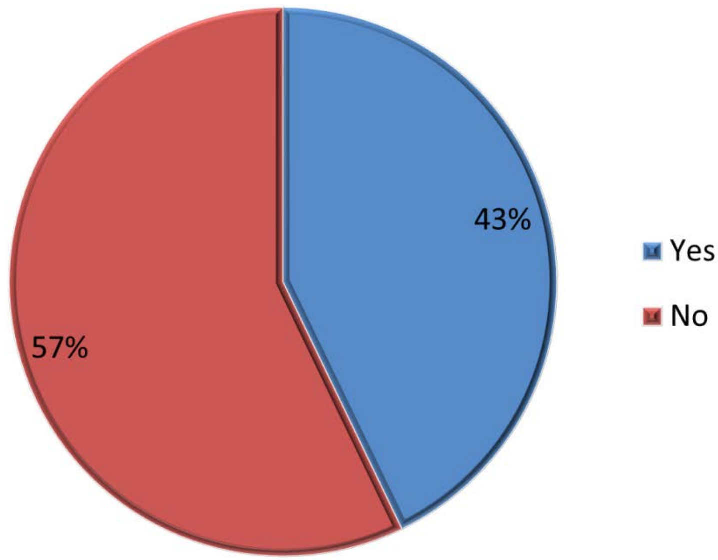

Figure F-16. Chart Showing Percentage of the Passenger Respondents That Provide Additional Training Related to Composite Repair Inspection (Passenger Category Respondents Only)

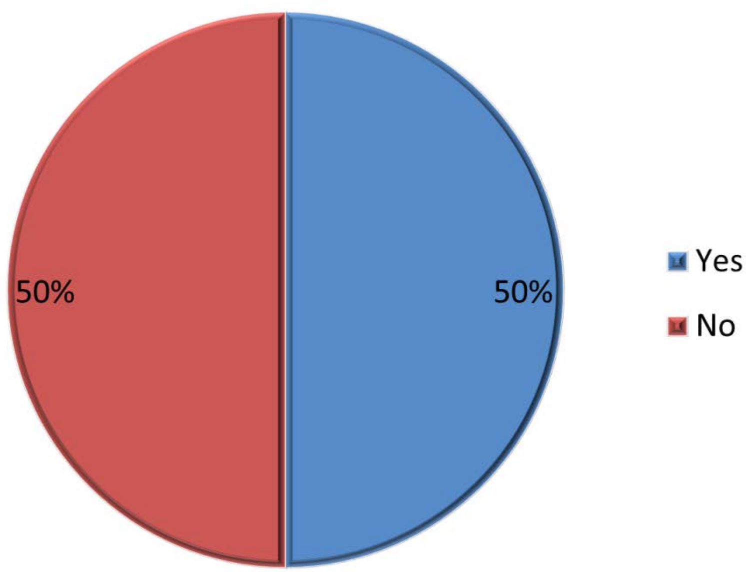

Figure F-17. Chart Showing Percentage of the MRO Respondents That Provide Additional Training Related to Composite Repair Inspection (MRO Category Respondents Only)

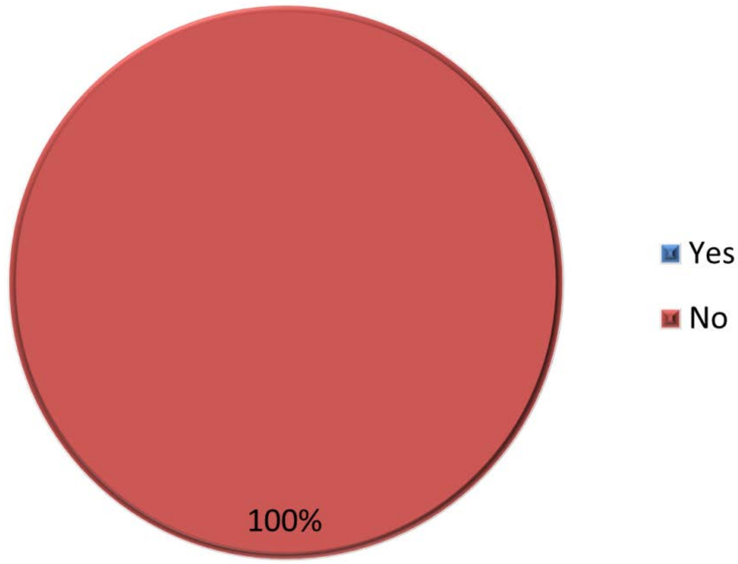

Figure F-18. Chart Showing Percentage of the Cargo Respondents That Provide Additional Training Related to Composite Repair Inspection (Cargo Category Respondents Only)

Responses provided for “yes, please specify” in question 8:

Respondent 1 (P): Airbus composite and Boeing 787 composite.

Respondent 3 (P): OEM training for composite repair.

Respondent 6 (P): 24 hours.

Respondent 8 (M): As certain repairs require inspections, OJT is provided.

Respondent 9 (M): Answered “Yes”, but did not specify.

Respondent 10 (M): As needed.

Question 9: Do you have inspectors assigned specifically to the composite shop that conduct your composite inspections?

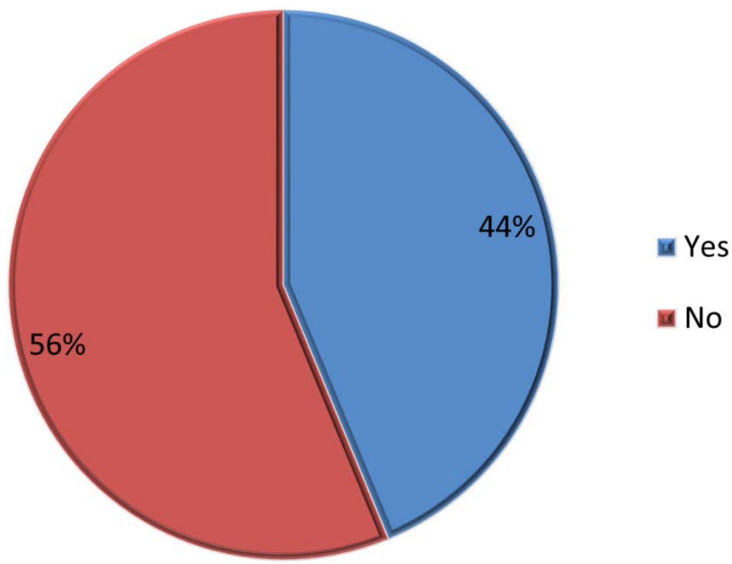

Figure F-19. Chart Showing Percentage of the Aviation Industry That Has Inspectors Assigned Specifically to the Composite Shop That Conducts Composite Inspections (Aviation Industry—All Respondents)

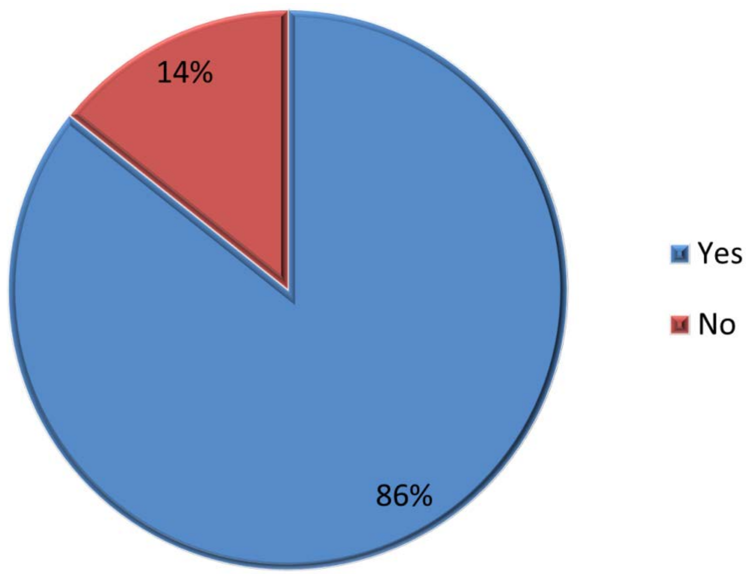

Figure F-20. Chart Showing Percentage of the Passenger Respondents That Have Inspectors Assigned Specifically to the Composite Shop That Conducts Composite Inspections (Passenger Category Respondents Only)

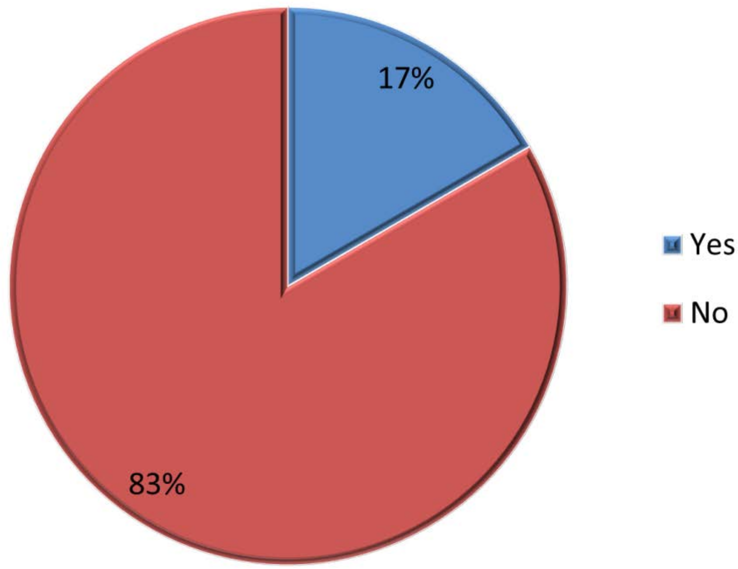

Figure F-21. Chart Showing Percentage of the MRO Respondents That Have Inspectors Assigned Specifically to the Composite Shop That Conducts Composite Inspections (MRO Category Respondents Only)

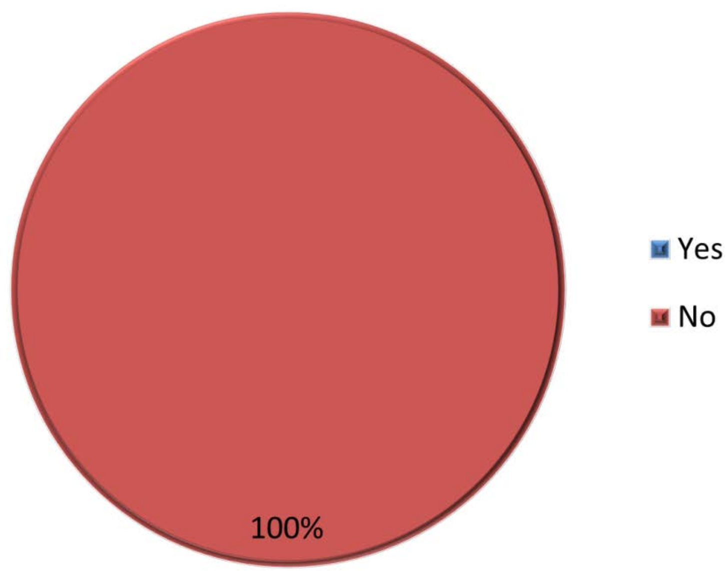

Figure F-22. Chart Showing Percentage of the Cargo Respondents That Have Inspectors Assigned Specifically to the Composite Shop That Conducts Composite Inspections (Cargo Category Respondents Only)

Responses provided for "If 'Yes,' do inspectors accomplish other inspection tasks such as receiving inspections? (If so, list them)" in question 9:

Respondent 1 (P): Receiving Inspection, Electrical Shop, Seat Shop and Heavy Check.

Respondent 2 (P): Eddy current, visual and Thermography.

Respondent 4 (P): No.

Respondent 5 (P): No.

Respondent 6 (P): Yes, our Inspectors have to be qualified for all areas including NDT. All Inspectors at our airline are qualified to inspect the repairs

Respondent 7 (P): No.

Respondent 9 (M): No.

Question 10: Does your company provide instruction on the use of NDI scanning systems (production of C-Scan images), for example the Boeing MAUS system?

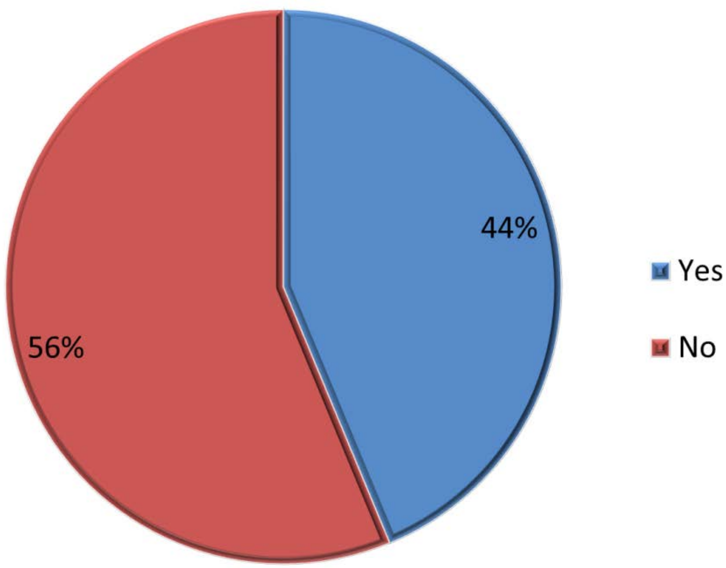

Figure F-23. Chart Showing Percentage of the Aviation Industry That Provides Instruction on the Use of NDI Scanning Systems (Aviation Industry—All Respondents)

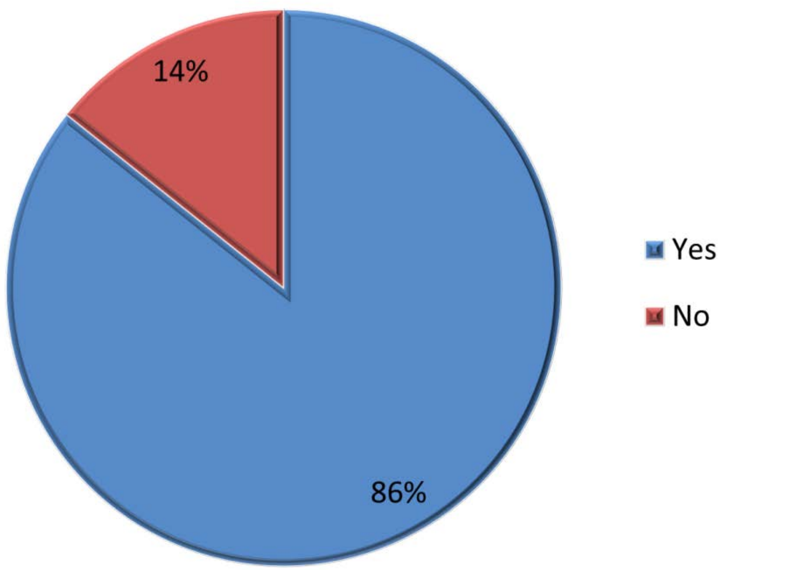

Figure F-24. Chart Showing Percentage of the Passenger Respondents That Provide Instruction on the Use of NDI Scanning Systems (Passenger Category Respondents Only)

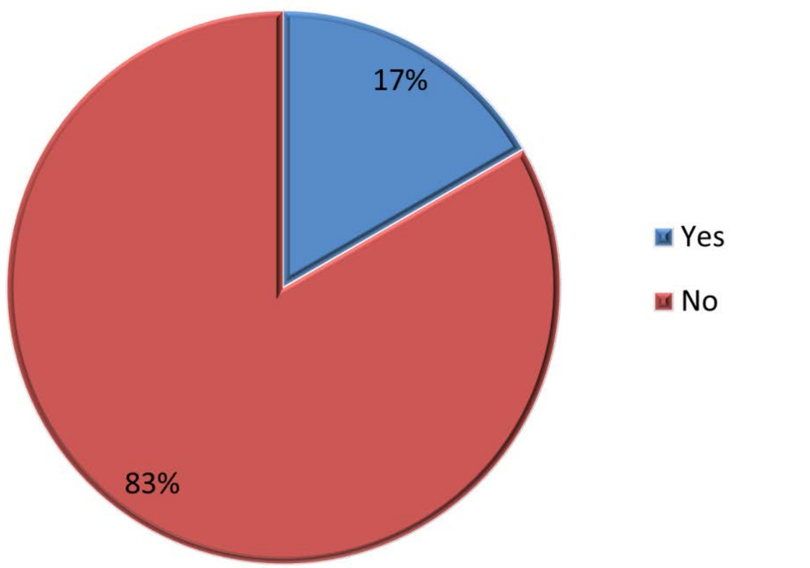

Figure F-25. Chart Showing Percentage of the MRO Respondents That Provide Instruction on the Use of NDI Scanning Systems (MRO Category Respondents Only)

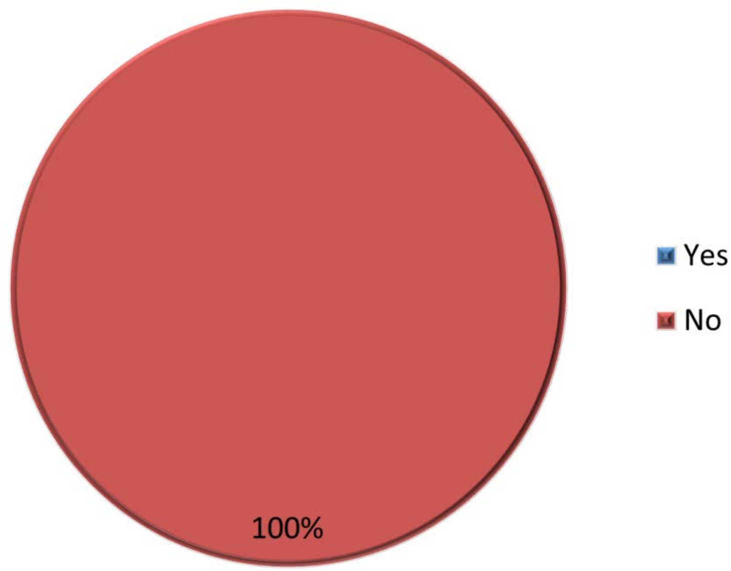

Figure F-26. Chart Showing Percentage of the Cargo Respondents That Provide Instruction on the Use of NDI Scanning Systems (Cargo Category Respondents Only)

Responses provided for "If 'Yes,' please explain and list the systems" in question 10:

Respondent 1 (P): Olympus OmniScan C-Scan images.

Respondent 2 (P): We have a MAUS system that was used for eddy current C-Scans. We are exploring the possibility of using C-Scan bond testing.

Respondent 3 (P): Omniscan MX C-scan.

Respondent 4 (P): .Answered "Yes", but did not list systems.

Respondent 5 (P): We currently use the MAUS for ET and resonance and are in the research phase of using the MAUS for bond testing..

Respondent 6 (P): Olympus Eddy Current Array is our method to detect chem. mill cracking in the 737 fuselage. We also use Phased Array UT for chem. mill crack verification and scribe line crack detection. Sector Scan None on composites.

Respondent 8 (M): AUSS V at our other facility (Automated Ultrasonic Scanning System, the predecessor to the MAUS V).

Comment provided for question 10:

Respondent 11 (M): Not at this time, I would require additional training for specialized systems, such as C-scan, MAUS, Phased Array.

Question 11: Has your NDI training curriculum been updated to accommodate composite inspections?

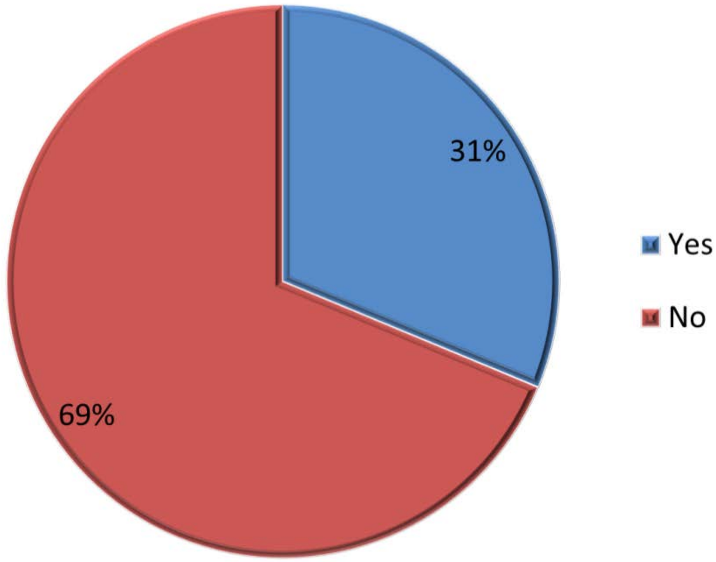

Figure F-27. Chart Showing Percentage of the Aviation Industry That Has Updated Their NDI Training Curriculum to Accommodate Composite Inspections (Aviation Industry—All Respondents)

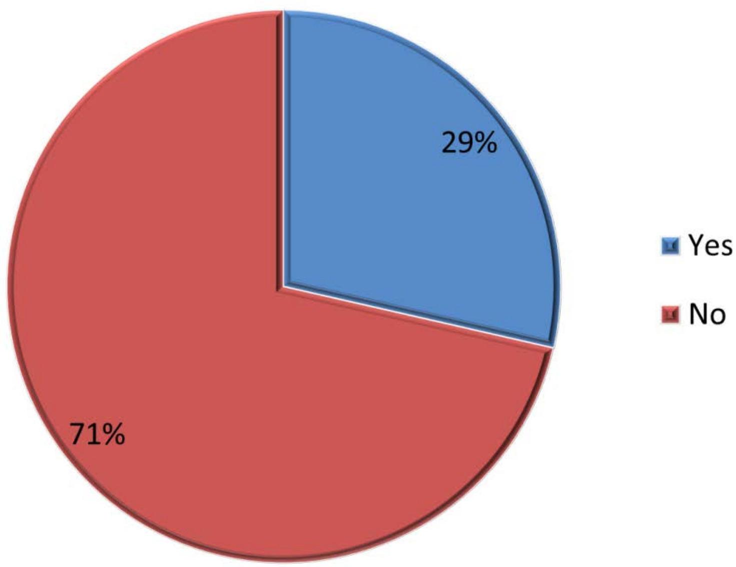

Figure F-28. Chart Showing Percentage of the Passenger Respondents That Have Updated Their NDI Training Curriculum to Accommodate Composite Inspections (Passenger Category Respondents Only)

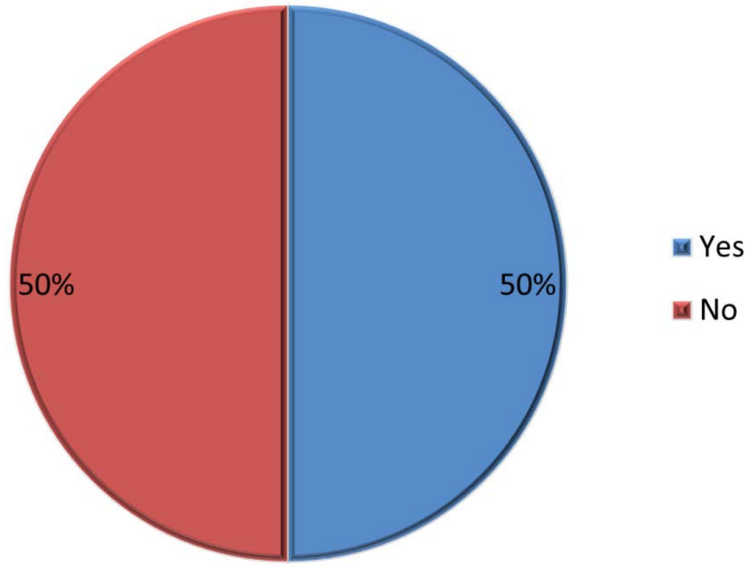

Figure F-29. Chart Showing Percentage of the MRO Respondents That Have Updated Their NDI Training Curriculum to Accommodate Composite Inspections (MRO Category Respondents Only)

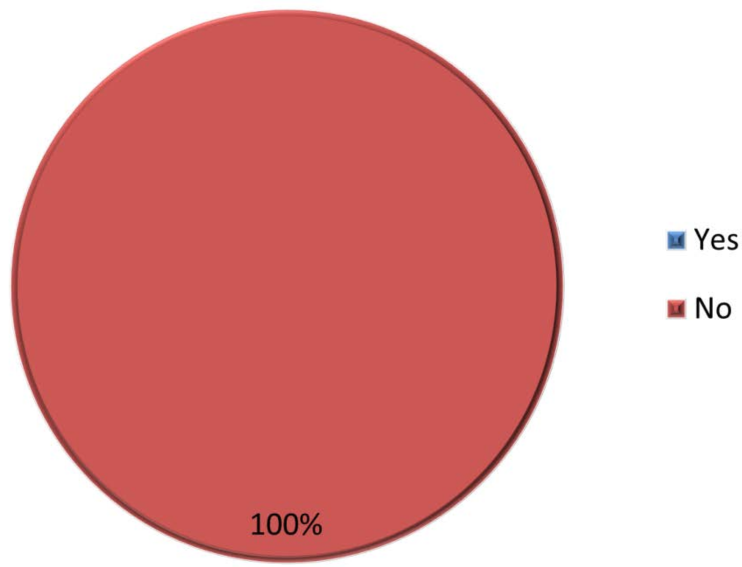

Figure F-30. Chart Showing Percentage of the Cargo Respondents That Have Updated Their NDI Training Curriculum to Accommodate Composite Inspections (Cargo Category Respondents Only)

Responses provided for "If 'Yes,' please explain what you have added" in question 11:

> **Respondent 1 (P):** Ramp Damage Checker, A-Scan, C-Scan damage assessment, A-Scan bonded repair and C-Scan bonded repair.

Respondent 8 (M): Will upgrade our training program with upgraded equipment.

Respondent 9 (M): We have specifications that detail the composite inspection requirements. The specific exams cover the use of the fabrication and composite inspection requirements.

Respondent 10 (M): Answered “Yes”, but did not explain what was added.

Respondent 3 (P): 787 Damage and Repair Assessment, A320 Elevator and Rudder Inspections, GEnX fan blade (bird strike) UT.

Comment provided for question 11:

Respondent 11 (M): Until directed otherwise, see question 6.

Question 12: Does your company use any of the following standards as criteria for your NDI training program? If so, which one(s)?

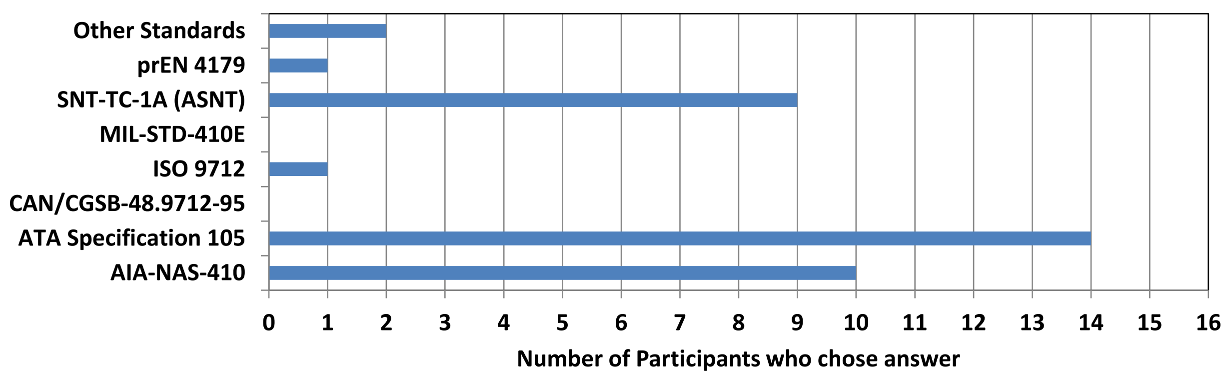

Figure F-31. Chart Showing the Standards Used by the Aviation Industry for Their NDI Training Programs (Aviation Industry—All Respondents)

Responses provided for “Other” in question 12:

Respondent 6 (P): FAA AC 165, Same as old ATA 105.

Respondent 9 (M): Our facilities are Nadcap accredited.

Question 13: Qualification of inspectors to perform tasks is usually based on an examination and/or other demonstration of proficiency. Do you have <u>additional</u>, special inspector <u>qualification</u>/<u>certification</u> to qualify personnel for conducting composite inspections, in addition to your normal qualification program?

Responses provided for “If ‘yes,’ please explain local methods” in question 13:

Respondent 3 (P): (Considered a “yes” in figure F-32) We have a change pending to this policy—future answer will be yes, additional certification via training will be required for 787 repair assessment.

Respondent 10 (M): All initial inspections for inspectors regardless if it is for composites has to have OJT and the OJT record shows which methods and techniques he/she is qualified on and is not related to level.

Comment provided for question 13:

Respondent 11 (M): No, we use the standards checked in the previous question.

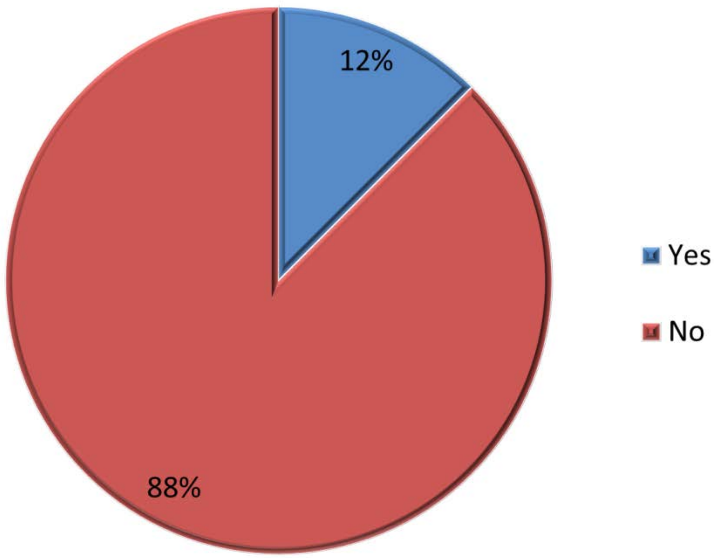

Figure F-32. Chart Showing Percentage of the Aviation Industry That Has Additional, Special Inspector Qualification/Certification to Qualify Personnel for Conducting Composite Inspections (Aviation Industry—All Respondents)

Question 14: Do any of the following enter into decisions on <u>qualification</u> to perform certain inspections (e.g., composite damage inspections) or is qualification solely based on formal inspector ratings such as ASNT Level II or Level III?

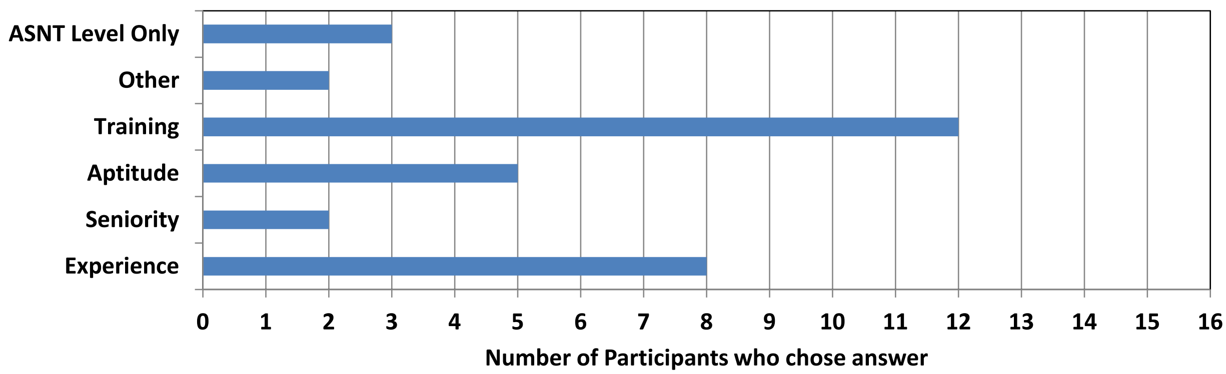

Figure F-33. Chart Showing the Qualifications Used by the Aviation Industry to Perform Certain Inspections, Such as Composite Damage Inspection (Aviation Industry—All Respondents)

Responses provided for "other" in question 14:

> **Respondent 3 (P):** Additional training requirement revision is pending.
>
> **Respondent 6 (P):** We have several Inspectors with a limited rating, our limited rating is only after the Inspector has the 40 hour theory course and demonstrates the ability to perform the particular inspection.

Comment provided for question 14:

> **Respondent 2 (P):** UT Level I or II Inspectors are considered qualified.
>
> **Respondent 5 (P):** Level I or II.
>
> **Respondent 11 (M):** Must be minimum Level 1 with specific authorization to use the appropriate UT wave mode and equipment for composite inspections.

Question 15: If experience level is a factor in determining qualification to perform certain inspections, do you use some sort of apprentice program to expose newer inspectors to such inspections?

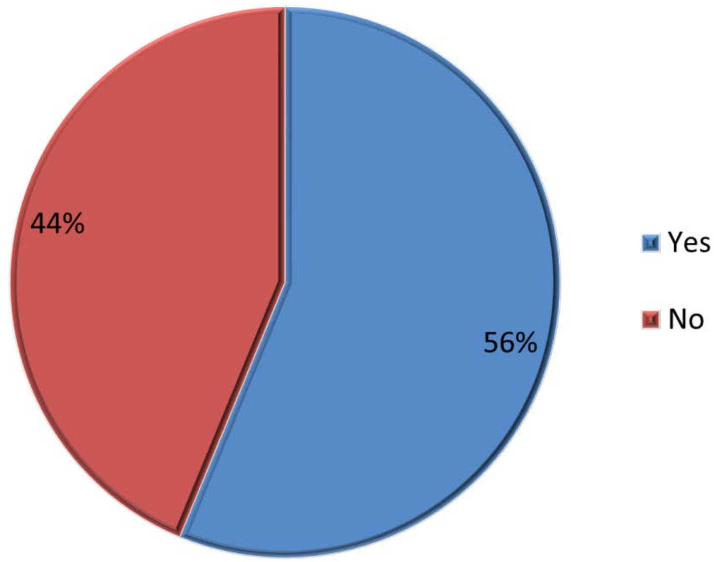

Figure F-34. Chart Showing Percentage of the Aviation Industry That Has Some Sort of Apprentice Program to Expose Newer Inspectors to Certain Types of Inspections (Aviation Industry—All Respondents)

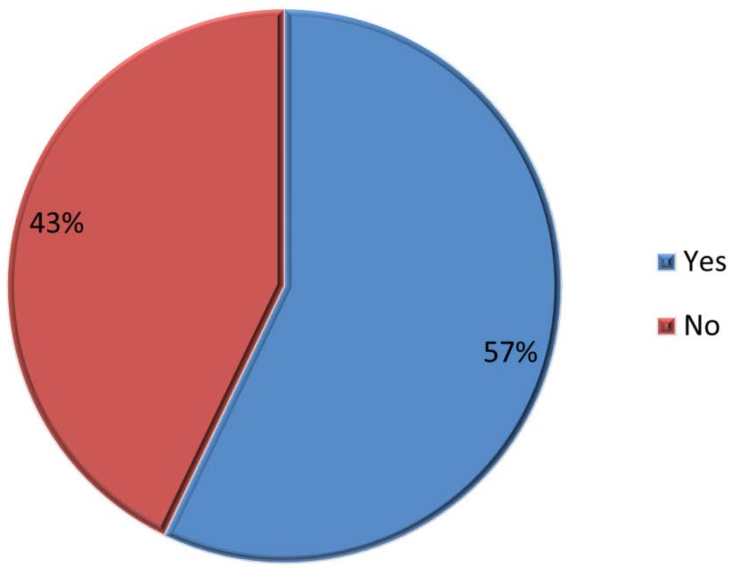

Figure F-35. Chart Showing Percentage of the Passenger Respondents That Have Some Sort of Apprentice Program to Expose Newer Inspectors to Certain Types of Inspections (Passenger Category Respondents Only)

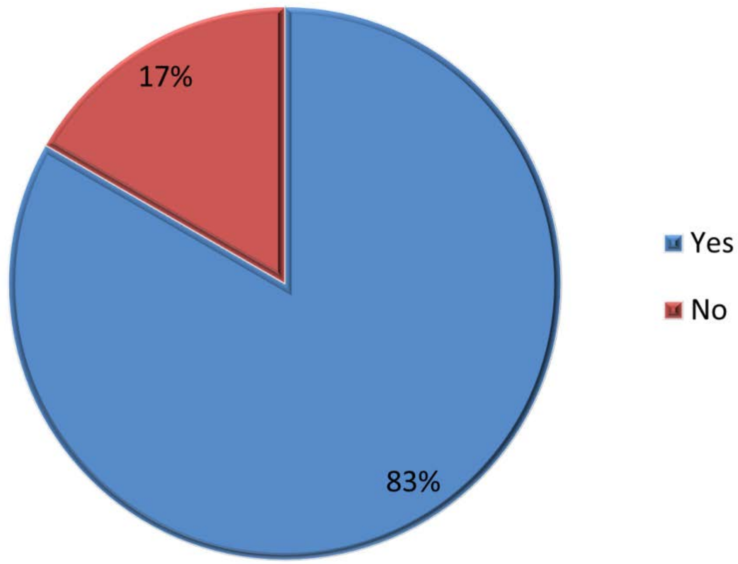

Figure F-36. Chart Showing Percentage of the MRO Respondents That Have Some Sort of Apprentice Program to Expose Newer Inspectors to Certain Types of Inspections (MRO Category Respondents Only)

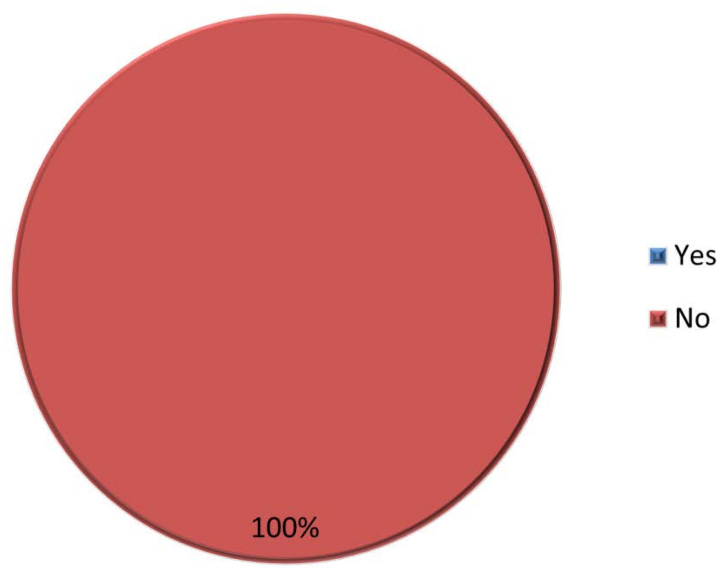

Figure F-37. Chart Showing Percentage of the Cargo Respondents That Have Some Sort of Apprentice Program to Expose Newer Inspectors to Certain Types of Inspections (Cargo Category Respondents Only)

Responses provided for “If ‘yes,’ please explain the program” in question 15:

Respondent 1 (P): All new inspectors receive the qualification code Level I special, which means they will be under the guidance of a Level II until they become task qualified.

Respondent 2 (P): We have an OJT program for new inspectors to learn inspections where they get additional training.

Respondent 5 (P): Basically the inspectors are trainees until they receive an adequate amount of OJT hours to obtain a level 1s.

Respondent 6 (P): Our program starts with the limited or special rating. Inspectors attend the method course then get specific training on the inspections they can perform. They do this until they gain enough hours of experience to be graduated to level I. They can’t become level I until they have the hours and pass a practical on techniques they have not held a previous qual. for.

Respondent 8 (M): Yes, if what you mean is, does our training program use trained Level II's to give additional hands on training as inspections arise in composites.

Respondent 10 (M): A new inspector will be assigned to the Level III for his initial 10 percent of level I experience and can begin inspecting after OJT qualification is accomplished.

Respondent 11 (M): See Question 6, inspectors may start NDT as a trainee, composite inspection and the ultrasonic techniques used are just a part of the qualification process to become a Level 1.

Respondent 12 (M): OJT with senior personnel observation and sign off.

Respondent 13 (M): Trainee: under direct supervision and does not have accept or reject authority. Level I: has accept/reject authority and can independently perform inspections after a level II or higher has witnessed and sign their training record as successfully accomplished that specific inspection.

Question 16: In your opinion, do Level I, II, and III training/qualifications provide the necessary expertise for both metal and composite NDI or should additional training take place for composite inspections?

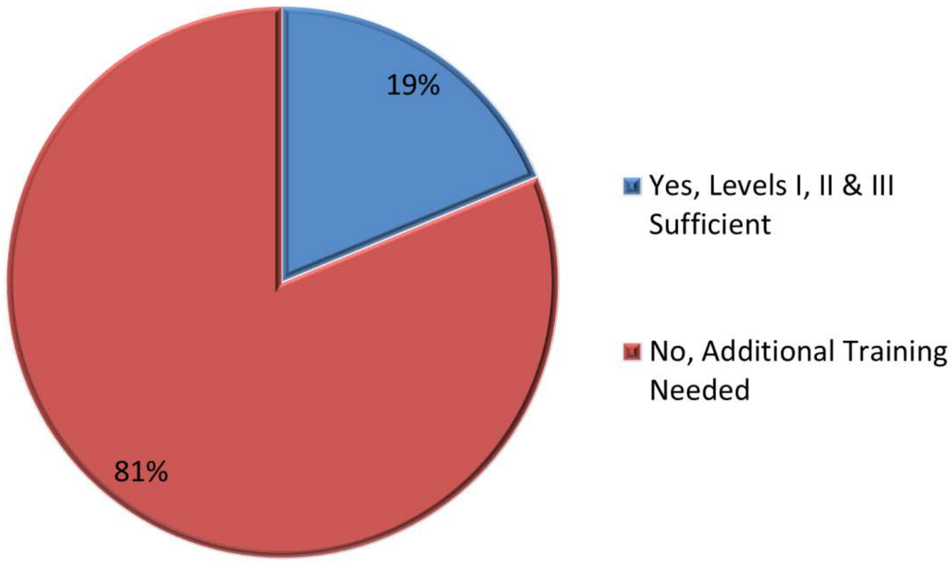

Figure F-38. Chart Showing Percentage of the Aviation Industry That Thinks Level I, II, and III Training/Qualification Provides the Necessary Expertise for Both Metal and Composite NDI (Aviation Industry—All Respondents)

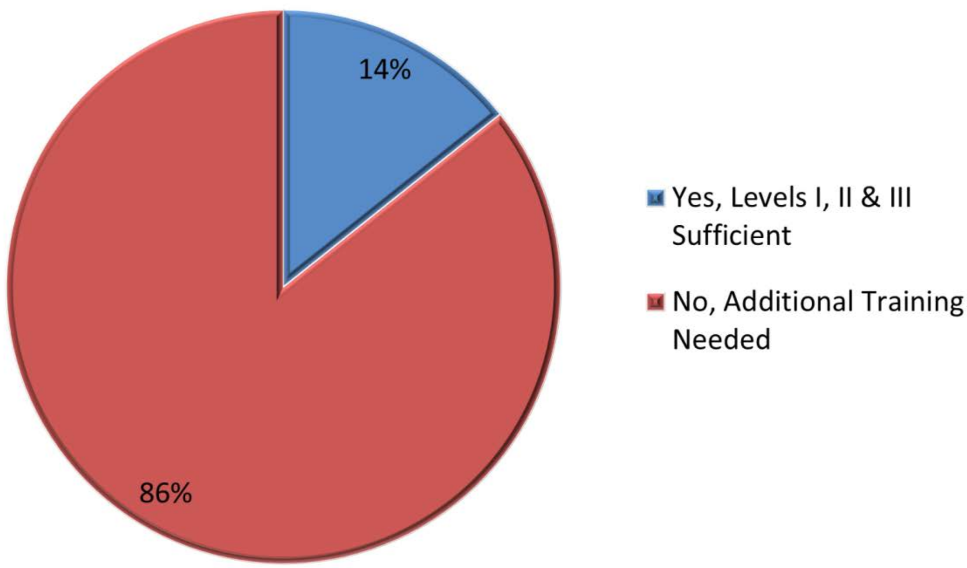

Figure F-39. Chart Showing Percentage of the Passenger Respondents That Think Level I, II, and III Training/Qualification Provide the Necessary Expertise for Both Metal and Composite NDI (Passenger Category Respondents Only)

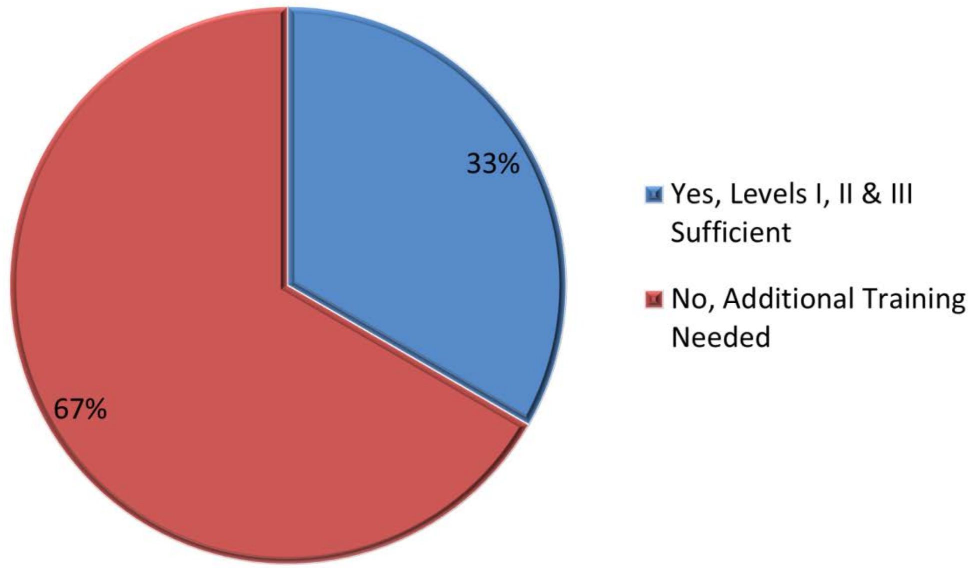

Figure F-40. Chart Showing Percentage of the MRO Respondents That Think Level I, II, and III Training/Qualification Provides the Necessary Expertise for Both Metal and Composite NDI (MRO Category Respondents Only)

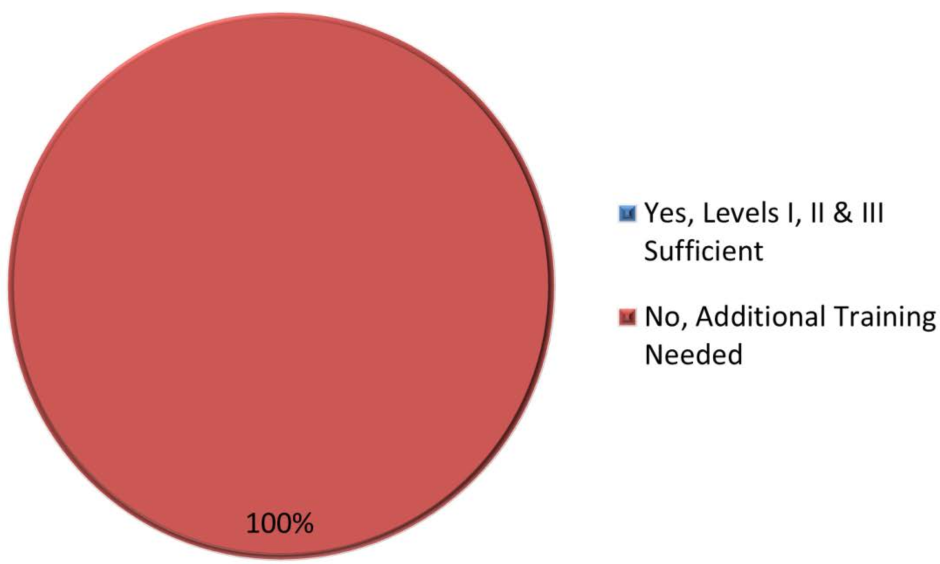

Figure F-41. Chart Showing Percentage of the Cargo Respondents That Think Level I, II, and III Training/Qualification Provide the Necessary Expertise for Both Metal and Composite NDI (Cargo Category Respondents Only)

Comments provided for question 16:

> **Respondent 6 (P):** I've tried a lot of methods to train Inspectors, all Inspectors are different. The easiest is to use very little theory unless it pertains to the technique. Most Inspectors were mechanics before they became an Inspector so theory puts them to sleep. Our latest method is to send Inspectors to 40 hours theory for the method then bring them in for OJT. The OJT is over the procedure. I write addendums (cheat sheets) on how to arrive at the Boeing procedure calibrations using our equipment. It doesn't replace the procedure but helps them with the correct setups. I add the particular theory or the WHY to this addendum and everyone ends up at the same result.
>
> **Respondent 8 (M):** The program should be updated with new equipment and technology.

Question 17: Should there be additional inspector ratings (i.e., Level I – III) for new NDI methods, such as shearography, that currently do not exist? (If yes, what methods?)

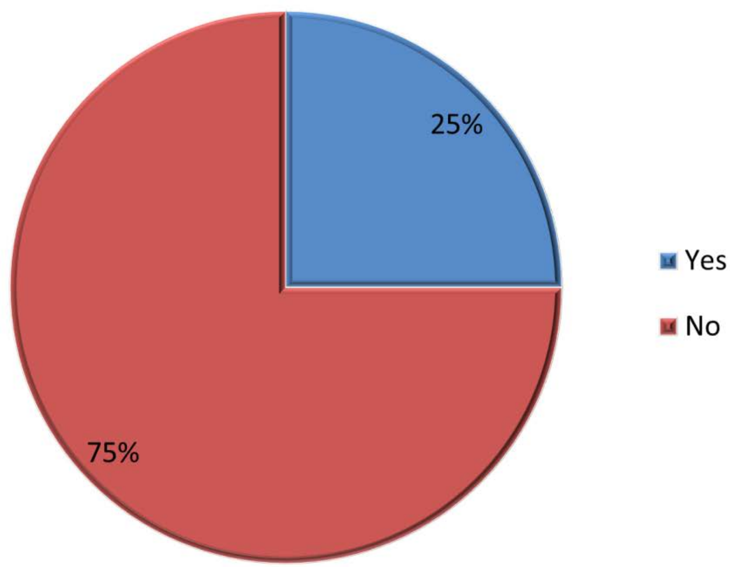

Figure F-42. Chart Showing Percentage of the Aviation Industry That Thinks There Should Be Additional Inspector Ratings for New NDI Methods (Aviation Industry—All Respondents)

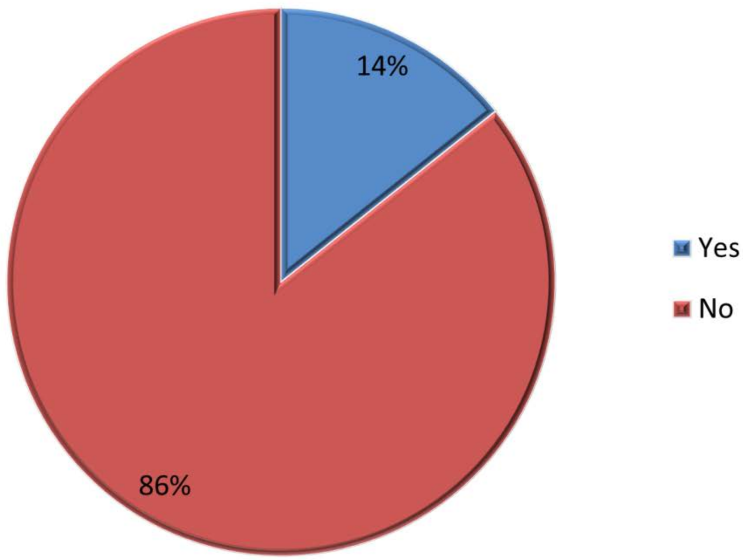

Figure F-43. Chart Showing Percentage of the Passenger Respondents That Think There Should Be Additional Inspector Ratings for New NDI Methods (Passenger Category Respondents Only)

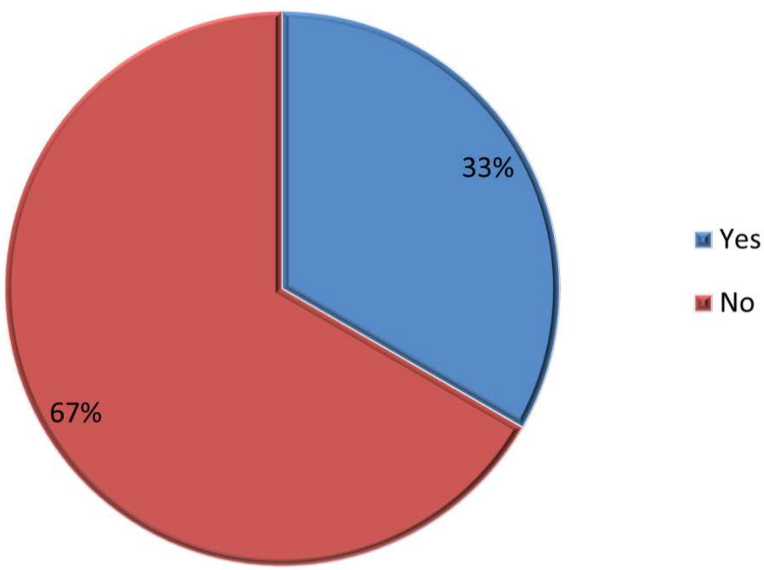

Figure F-44. Chart Showing Percentage of the MRO Respondents That Think There Should Be Additional Inspector Ratings for New NDI Methods (MRO Category Respondents Only)

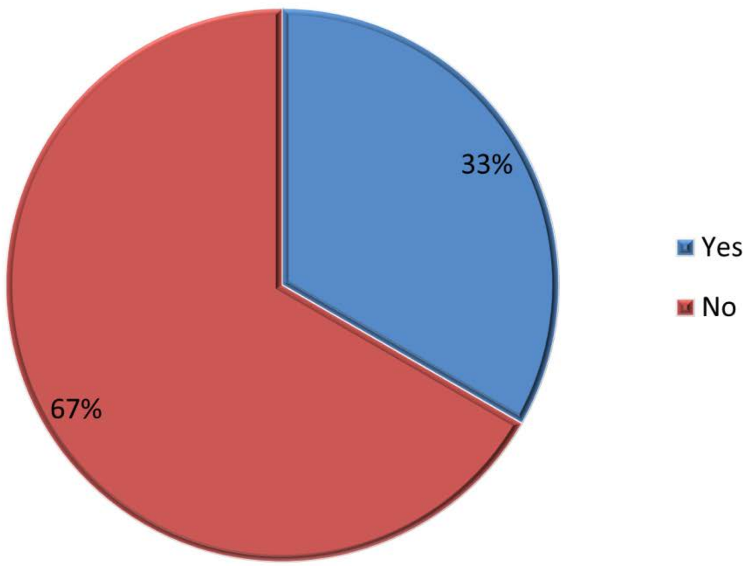

Figure F-45. Chart Showing Percentage of the Cargo Respondents That Think There Should Be Additional Inspector Ratings for New NDI Methods (Cargo Category Respondents Only)

Responses provided for “If ‘yes,’ list the methods” in question 17:

Respondent 6 (P): No methods listed.

Respondent 9 (M): No methods listed.

Respondent 11 (M): Shearography, Thermography, if we were to use these methods, training and experience hours would have to be met in accordance with the qualification/certification standards that we use (NAS-410 and ATA-105).

Respondent 14 (C): No methods listed.

Comments provided for question 17:

Respondent 3 (P): Ratings already exist for new methods, though we currently are not using.

Respondent 10 (M): No, Unless new methods become a main method like Eddy Current or Ultrasonics they should be more like a special qualification because a person may never get the hours to level up.

Question 18: What percentage of your NDI inspectors are qualified to inspect composites?

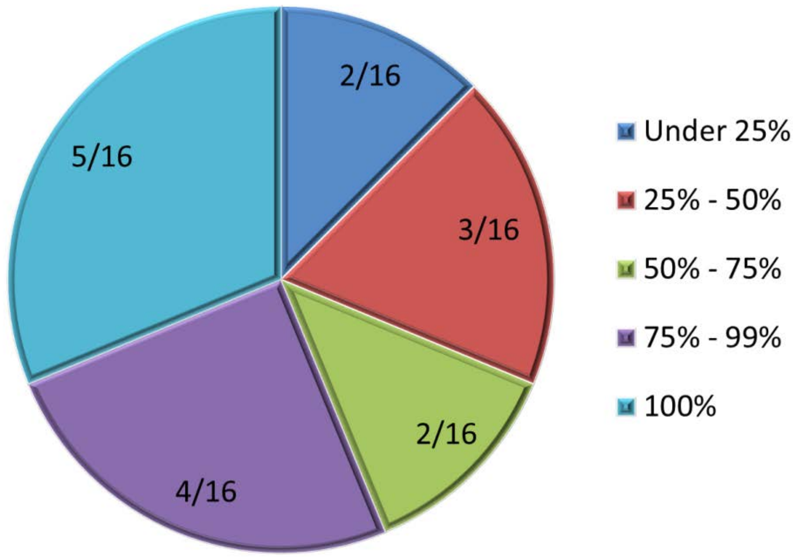

Figure F-46. Chart Showing Percentage Breakdown of NDI Inspectors Within Each Company Who Are Qualified to Inspect Composites (Aviation Industry—All Respondents)

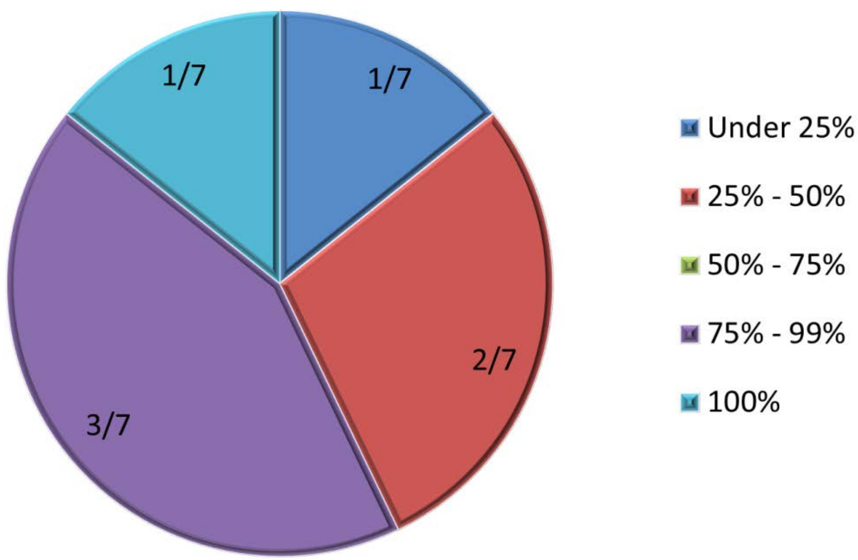

Figure F-47. Chart Showing Percentage Breakdown of NDI Inspectors Within Each Company Who Are Qualified to Inspect Composites (Passenger Category Respondents Only)

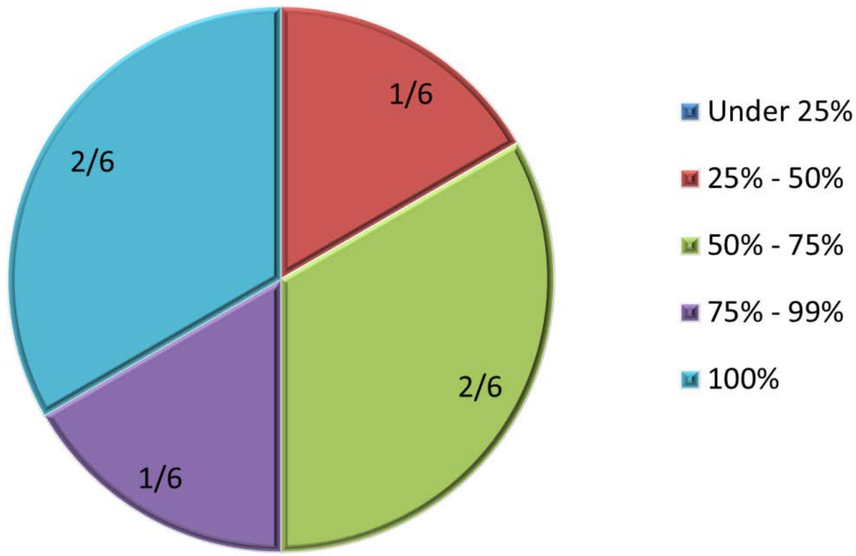

Figure F-48. Chart Showing Percentage Breakdown of NDI Inspectors Within Each Company Who Are Qualified to Inspect Composites (MRO Category Respondents Only)

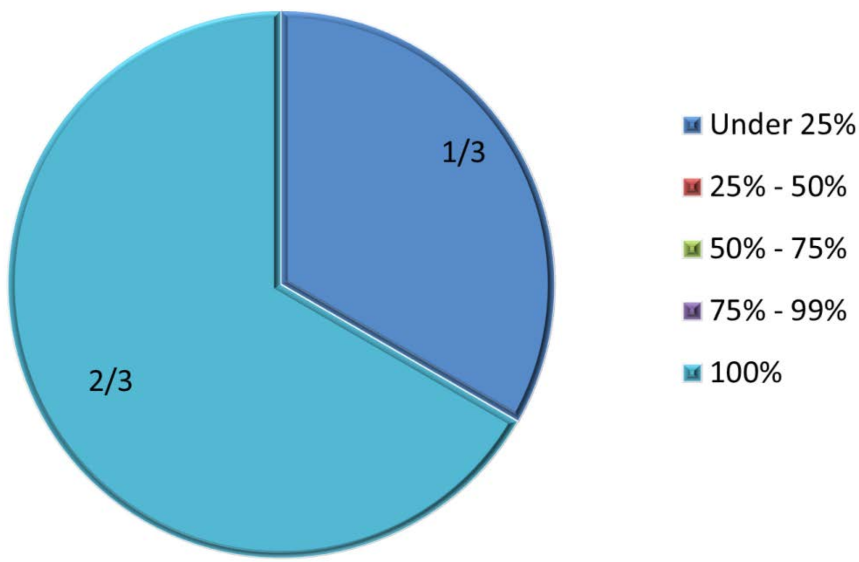

Figure F-49. Chart Showing Percentage Breakdown of NDI Inspectors Within Each Company Who Are Qualified to Inspect Composites (Cargo Category Respondents Only)

Comments provided for question 18:

> **Respondent 2 (P):** UT Level I or II are considered qualified unless there is a special requirement called out by the OEM.

Question 19(A): In your company, can a mechanic deploy a simple "Go/No-Go" (or "Green Light/Red Light") device, such as the Olympus Ramp Damage Checker or GE Bondtracer™ instrument, to conduct composite inspections?

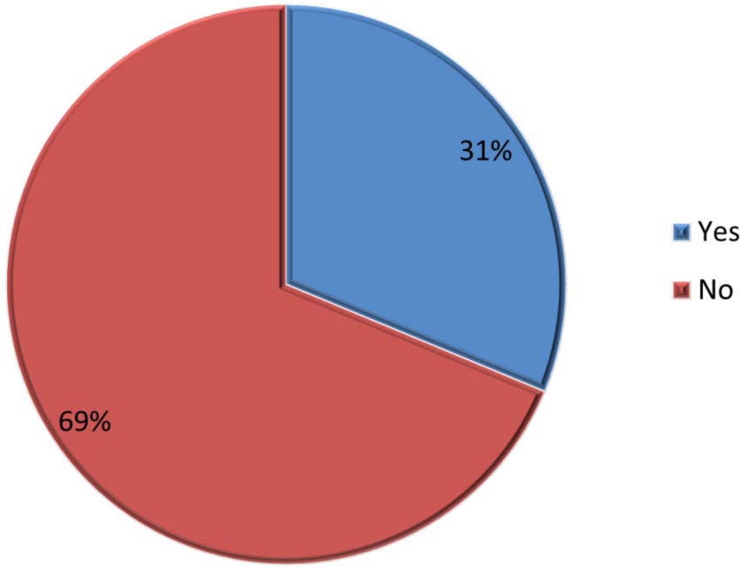

Figure F-50. Chart Showing Percentage of the Aviation Industry Where a Mechanic Can Deploy a Simple "Go/No-Go" Device to Inspect Composites (Aviation Industry—All Respondents)

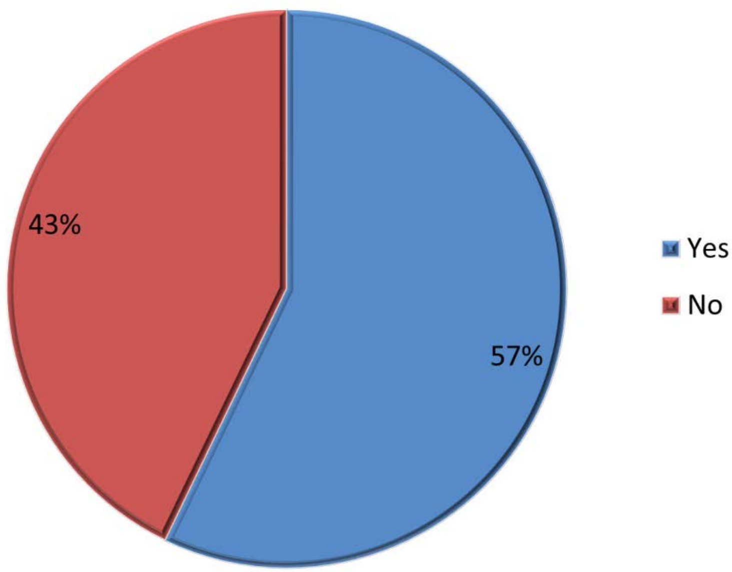

Figure F-51. Chart Showing Percentage of the Passenger Respondents Where a Mechanic Can Deploy a Simple "Go/No-Go" Device to Inspect Composites (Passenger Category Respondents Only)

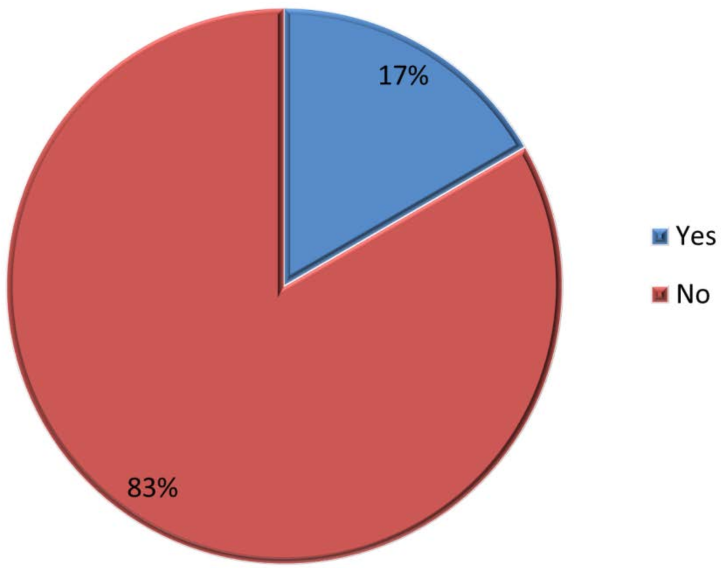

Figure F-52. Chart Showing Percentage of the MRO Respondents Where a Mechanic Can Deploy a Simple "Go/No-Go" Device to Inspect Composites (MRO Category Respondents Only)

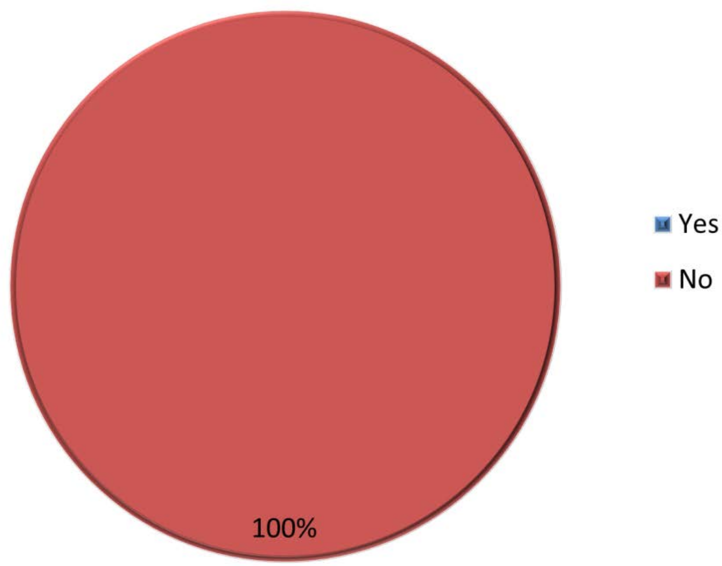

Figure F-53. Chart Showing Percentage of the Cargo Respondents Where a Mechanic Can Deploy a Simple "Go/No-Go" Device to Inspect Composites (Cargo Category Respondents Only)

Comments provided for question 19(A):

Respondent 8 (M): No, but is an option in the future.

Respondent 11 (M): We currently do not have those instruments here.

Question 19(B): Would there be management-labor issues associated with a mechanic doing inspector functions?

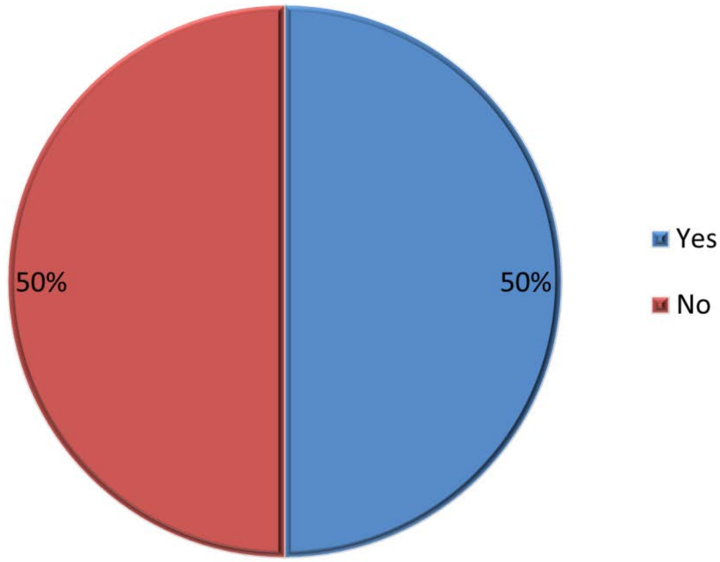

Figure F-54. Chart Showing Percentage of the Aviation Industry Where There Would Be a Management-Labor Issue Associated With a Mechanic Doing Inspector Functions (Aviation Industry—All Respondents)

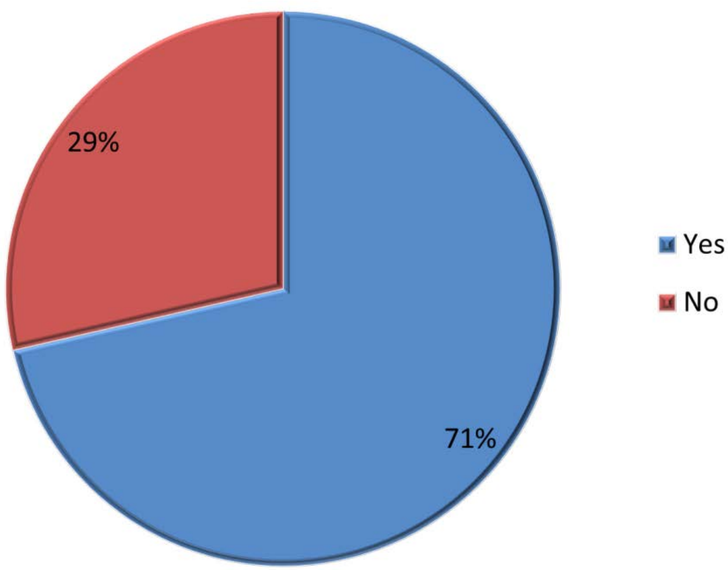

Figure F-55. Chart Showing Percentage of the Passenger Respondents Where There Would Be a Management-Labor Issue Associated With a Mechanic Doing Inspector Functions (Passenger Category Respondents Only)

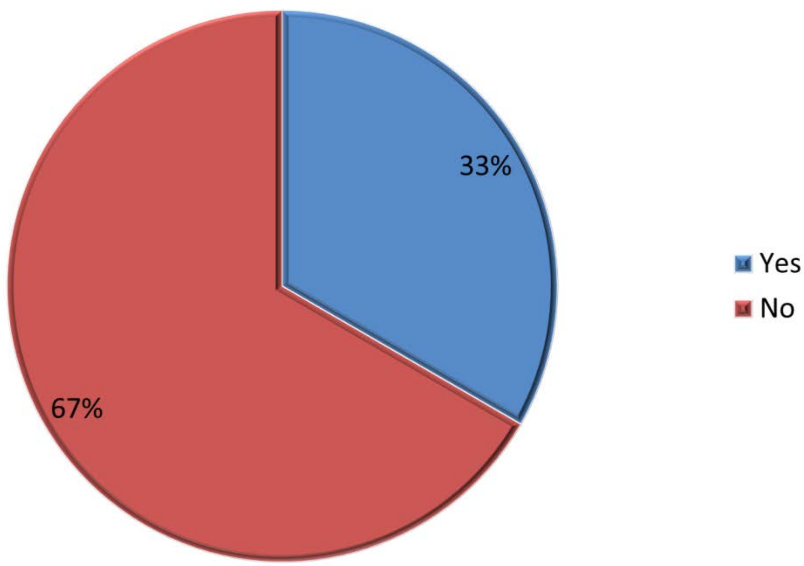

Figure F-56. Chart Showing Percentage of the MRO Respondents Where There Would Be a Management-Labor Issue Associated With a Mechanic Doing Inspector Functions (MRO Category Respondents Only)

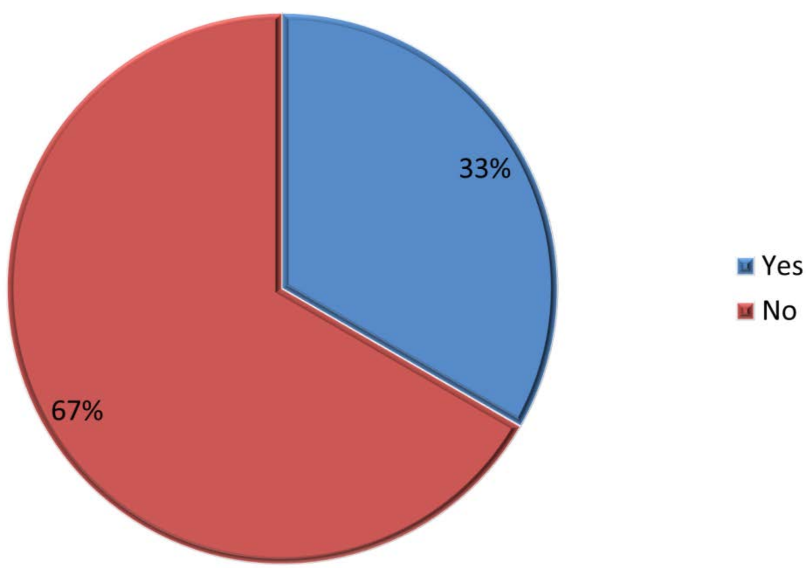

Figure F-57. Chart Showing Percentage of the Cargo Respondents Where There Would Be a Management-Labor Issue Associated With a Mechanic Doing Inspector Functions (Cargo Category Respondents Only)

Comments provided for question 19(B):

> **Respondent 3 (P):** Possibly, still exploring issue.

Question 19(C): How much and what type of training should the mechanics receive?

Respondent 1 (P): Base knowledge of how ultrasonic sonic work and the use of the instrument.

Respondent 2 (P): Mechanics that do NDT inspections should have the same training as inspectors doing the equivalent level of inspection.

Respondent 3 (P): Basic overview on RDC use, minimum 4 hours.

Respondent 4 (P): No response provided.

Respondent 5 (P): Mechanics that accomplish inspections should have the same amount of training required as an inspector.

Respondent 6 (P): At least what the Inspector receives if the mechanic is utilized for NDT Inspections.

Respondent 7 (P): Basic training.

Respondent 8 (M): "Please describe" depends on the simplicity of the unit and on the knowledge of the mechanic. Is he a structures person trained in composites, or is he a wrench turning mechanic with little composite knowledge?

Respondent 9 (M): We do not allow mechanics to perform NDT inspections. The facility has a bargain for work force. It would violate the Union contract.

Respondent 10 (M): No response provided.

Respondent 11 (M): If a Level I special is used then approximately 25% of required experience and training is needed compared to a full Level 1(400 experience hours and 40 hour classroom).

Respondent 12 (M): At least 40 hours of basic bond practices.

Respondent 13 (M): No response provided.

Respondent 14 (C): Only familiarization training for the simple go/no-go device.

Respondent 15 (C): 40 hrs or more on basic honeycomb composite structures.

Respondent 16 (C): None at this time.

Question 19(D): Should there be recurrent training for mechanics? Please describe what type of recurrent training and how often.

Respondent 1 (P): Yes, yearly.

Respondent 2 (P): Recurrent requirements should be the same for everyone doing the same level of inspection.

Respondent 3 (P): Yes, same as initial training.

Respondent 4 (P): No response provided.

Respondent 5 (P): Yes, same as inspectors.

Respondent 6 (P): Yes.

Respondent 7 (P): Yes, 4 hours.

Respondent 8 (M): No, If this is a go-no go unit with little or no real set-up. If a signal must be analyzed yes.

Respondent 9 (M): No response provided.

Respondent 10 (M): No response provided.

Respondent 11 (M): Level 1 special would require annual recurrent training.

Respondent 12 (M): No.

Respondent 13 (M): No response provided.

Respondent 14 (C): No.

Respondent 15 (C): Yes, Once a year or more, if new material or technology.

Respondent 16 (C): None at this time.

Question 20: What are your ideas for improvements to training programs and inspector qualifications in order to perform composite inspections?

Respondent 1 (P): Have a limit on how many inspectors are trained to perform composite inspections because of the limited amount of NDI that is needed.

Respondent 2 (P): More emphasis put on the Bondmaster™ and training with it.

Respondent 3 (P): Due to critical nature of 787 repairs, training has been developed specific to the Omniscan MX for C-scans. In addition, change has been proposed to require the additional training and qualification to conduct these inspections.

Respondent 4 (P): We are in the process of developing a Composite NDT training course for our NDT inspectors. It should be finished by the end of the year.

Respondent 5 (P): There should be more training for Bondmaster and resonance inspections.

Respondent 6 (P): More OJT and specific setup sheets. I've learned the more you write down for the inspector to follow the better. As far as qualification goes, the hours required by the specifications are generic. One person could be proficient in just a few hours others never.

Respondent 7 (P): Recurrent every 3 years.

Respondent 8 (M): It should be part of the normal qualification and certification program for the method, if the formal training or experience hours need to be increased that should be determined by the companies level III. The degree of composite inspection is different for each airline or repair station.

Respondent 9 (M): More mentoring and on the job training. This requires Leaderships buy-in.

Respondent 10 (M): No improvements listed.

Respondent 11 (M): As the qualification/certification standards are currently written there seems to be an emphasis meeting certain training (classroom) and experience hours. Regarding composite inspection as it relates to ultrasonics (instrumented NDT inspection) this becomes part of the qualification process used to certify inspectors for composite inspection.

However, basic ultrasonics does not specifically address composite inspection, but only covers the wave modes that may be encountered. This is where OJT or experience hours are important, because of the need to learn how different instruments and procedures are used.

That being said the focus is on inspection, not how a composite material is made. Perhaps additional training in the construction of composites would aid an inspector in the accomplishment of this kind of inspection.

Respondent 12 (M): Basic bond practices should be required training.

Respondent 13 (M): No improvements listed.

Respondent 14 (C): No input at this time.

Respondent 15 (C): Training provided by material/equipment OEMs.

Respondent 16 (C): Increase knowledge of composite structures. Clarification on what reference standards are applicable to inspecting repairs.

Question 21: In what areas is additional guidance needed to help ensure comprehensive composite training programs for the aviation industry? (Check all that apply)

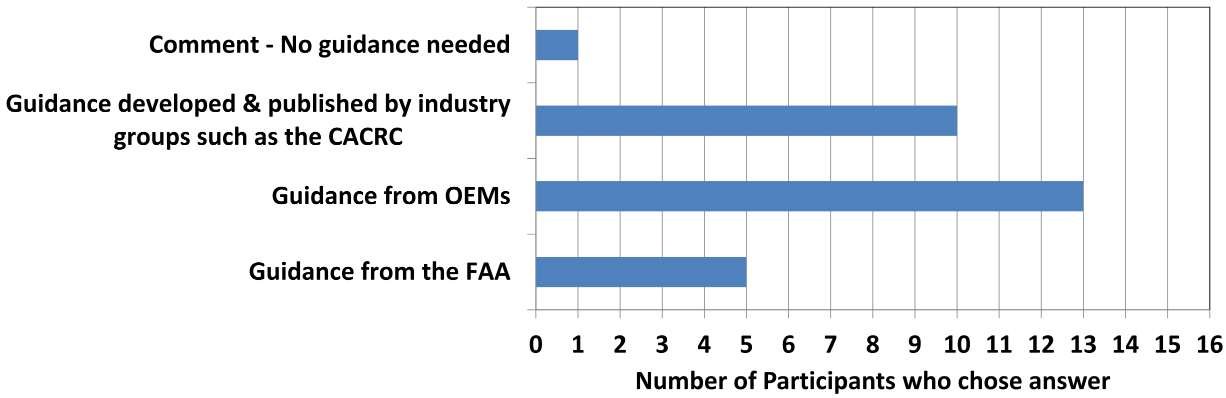

Figure F-58. Chart Showing the Areas Chosen by the Aviation Industry for Additional Guidance to Help Ensure Comprehensive Composite Training Programs (Aviation Industry—All Respondents)

Question 22: Please list, in the order of their importance, areas where additional guidance/information is needed for comprehensive composite inspection training programs.

Respondent 1 (P):

a. Manuals
b. Instrument

Respondent 2 (P):

a. Bond line detection of fiberglass repairs using PE
b. Better understanding of the Bondmaster
c. Resonance inspection
d. UTPA on composites

Respondent 3 (P):

a. Repair assessment
b. Damage assessment
c. R&D methods

Respondent 4 (P):

a. Pulse Echo UT
b. Resonance
c. Low Frequency Bond Testing

d. Mechanical Impedance Analysis
e. Thermography

Respondent 5 (P):
a. Bondmaster
b. Resonance

Respondent 6 (P):
a. Lots of hands on
b. Detailed Instructions
c. Specific Training for task

Respondent 7 (P): Nothing listed.

Respondent 8 (M):
a. Upcoming technologies in the basic methods of UT IAW OEM Data
b. Composite structure and repair technology
c. Post repair inspection and limitations
d. Upcoming technologies in the non-basic techniques such as shearography, thermography and limitations
e. OEM criteria for writing individual techniques for specific parts to be inspected IAW OEM SPM

Respondent 9 (M):
a. Fabrication reference standards
b. Validation of reference standards
c. Standardization of equipment
d. Evaluation of indications

Respondent 10 (M):
a. With the new composite material used in repairs that require additional information to be documented in the post repair inspection the information is hidden in other sections of the SRM other than the repair section, it is only seen by the mechanic as he processes though the repair steps at the end of the repair. And then it references to another SRM section where the post repair requirements are called out. What happens is if the mechanic had this information up front the repair records would be more detailed so the inspector has all of the necessary information to setup a good procedure, maps ,number of plies, direction, everything. This is necessary to make a judgment of how much porosity in the repair area which is becoming more as important has disbonds or delaminations.

Respondent 11 (M):
a. Specialized Equipment
b. Standards used for instrument "set-up"
c. Composite Structures and how they are made

Respondent 12 (M):

a. Where and when inspections need to be performed

Respondent 13 (M): Training guidance is adequate.

Respondent 14 (C):

a. OEM
b. FAA

Respondent 15 (C):

a. OEM Training
b. OJT
c. Recurrent Training

Respondent 16 (C):

a. Instructional videos of pulse echo and bondtest composite inspections
b. Clarification between pre preg and wet layup inspections.

F.3 Conclusion

The use of composites will continue to grow because of the associated engineering and economic benefits. This survey shows that some training issues are being addressed at airlines and MROs to accommodate the transition to increased inspection of composite structures. However, the survey also revealed that additional training is deemed necessary by the airline/MROs and that they are interested in obtaining guidance on such training from the FAA, OEMs, and aviation industry working groups.

F.3.1 Conclusions Summarized for Each Question

- Question 1—Training programs at the aircraft maintenance depots are based on the industry documents represented in ATA-105, with inspector qualification based on ASNT and NAS 410.

- Question 2—This survey shows that the majority of airlines and MROs still provide some or all of their NDI training in-house by their own instructors. Of the two companies that don't use their own instructors, one uses primarily an outside instructor in-house and the other uses an outside instructor at external locations. Only two respondents mentioned OEM training. Online training seems to be a growing part of the overall NDI training programs within the industry.

- Question 3—Formal training documentation seems to be very consistent within the industry. Most companies document their instruction via entry into a common training database. It should be noted that 38% (6 out of 16 respondents) of the respondents use all three types of documentation listed: certificate of completion, entry into a common training database, and a log containing training type and hours completed.

- Question 4—The NDI techniques employed for inspecting laminate composites by the industry is very broad. The survey highlights the fact that every company still uses conventional PE UT for inspecting laminate composites, but many are also using more advanced methods. Twenty-five percent or more of the industry also use X-Ray, thermography, mechanical impedance analysis (MIA), low frequency bond test, and phased array UT. Five of the companies listed through-transmission ultrasonics (TTU) as one of their “other” methods and 63% of the respondents also use resonance testing to inspect laminate composites. At this time, none of the respondents use shearography for inspecting laminate composites.

- Question 5—NDI techniques employed by industry for honeycomb composite inspection are also very broad. PE UT and low frequency bond testing are used by 81% (13 out of 16 respondents) of the industry. X-ray and thermography are used by 56% of the industry, along with 44% or more using resonance and MIA to inspect honeycomb composites. TTU and even tap testing were listed as “other” methods for honeycomb composite inspections. Only two respondents use phased array UT and shearography is not currently being used by any of the respondents for inspecting honeycomb composites.

- Question 6—Two-thirds of the industry provides general composite training to understand composite materials, plies, lay-ups, scarfed repairs, composite design, and processing. See table F-3 in the results section under question 5 showing the general composite training structure reported by those who provide this training.

- Question 7—The survey shows that 25% (4 out of 16 respondents) of the industry provides additional, specialized training specifically for inspectors who can perform composite inspections. From a different perspective, responses to this question also show that 75% of the industry provides no additional specialized training specifically for composite inspections, above and beyond Level I, II, and III certification.

- Question 8—For those in the industry who provide specialized instruction specifically for inspectors performing composite inspections (Reference Question 6), the training is varied, ranging from very little training to a great deal of structured training (see the tables generated by the respondents in the results section under question 7).

- Question 9—As far as composite repair inspection, 37% (6 out of 16 respondents) of the industry reported that inspectors receive additional training for this type of inspection. The type of training specified was listed as coming from OEMs’ OJT, as needed and structured.

- Question 10—The industry reported that 44% (7 out of 16 respondents) have inspectors assigned specifically to the composite shop that conducts composite inspections. The majority of the respondents who answered “Yes” come from the passenger category, totaling 83% (6 out of 7 respondents).

- Question 11—Instruction provided for the use of NDI scanning systems (for example, the Boeing MAUS system) was reported by 44% (7 out of 16 respondents), with the majority of those company's respondents coming from the passenger category, with 83% (6 out of 7 respondents) providing instruction on the use of NDI scanning systems. The systems listed by the respondents were mainly the MAUS system and the OmniScan system, with one respondent listed the AUSS-V (the predecessor to the MAUS V).

- Question 12—The industry reported that 31% (5 out of 16 respondents) of the respondents have updated their NDI training curriculum to accommodate composite inspections.

- Question 13—This survey shows that the majority of the aviation industry uses the ATA-105 standard as the criterion for their NDI training programs, along with AIA NAS-410 and ASNT-TC-1A, to a lesser extent. The responses to this question correlate very well with the written answers provided in question 1.

- Question 14—A majority (86%) of the industry does not have additional, special inspector qualification/certification to qualify personnel to conduct composite inspections. Most companies use the normal qualification program for general NDI inspection as qualification for composite inspection.

- Question 15—Training and experience seem to be the main factors used to qualify an inspector to perform certain inspections, such as composite damage inspections.

- Question 16—Experience being a factor in determining qualification to perform certain inspections, the industry reported that 56% (9 out of 16 respondents) of the aviation industry uses an apprentice program to expose newer inspectors to such inspections. OJT, under the guidance of a Level II or III, was listed as an example to expose newer inspectors to certain types of composite inspections (see other apprentice program descriptions provided by respondents in question 15).

- Question 17—The survey shows that 81% (13 out of 16 respondents) of the respondents think additional training should take place for composite inspections and do not think that Level I, II, and III training/qualifications alone provide the necessary expertise.

- Question 18—Only 25% of the industry thinks there should be additional inspector ratings for new NDI methods.

- Question 19—From the industry respondents, 31% (5 out of 16 respondents) stated that 100% of their NDI inspectors are qualified to inspect composites. The data also shows that 69% (11 out of 16 respondents) reported that 50%-100% of their NDI inspectors are qualified to inspect composites. Two respondents reported that less than 25% of their NDI inspectors are qualified to inspect composites.

- Question 19(A)—Concerning the use of a go/no-go device, 31% (5 out of 16) of the industry respondents reported that a mechanic can use a simple device such as the Olympus Ramp Damage Checker or the GE® BondTracer™ to conduct composite inspections. Four of the 5 respondents who reported that a mechanic can use this type of device were from the passenger category, equaling 57% (4 out of 7) of the passenger respondents.

- Question 19(B)—As far as management labor issues associated with a mechanic doing inspector functions, 50% (8 out of 16 respondents) stated there would be labor issues. An interesting data point from the passenger category is that 71% (5 out of 7 respondents) stated there would be management labor issues associated with a mechanic doing inspector functions, even though 57% of the passenger respondents reported it was acceptable for a mechanic to use such a device.

- Question 19(C)—For the question asking what type of training a mechanic should receive, the answers varied from basic training to mechanics should receive the same training that an inspector receives.

- Question 19(D)—50% of the respondents reported that mechanics doing composite inspections with a go/no-go device should receive some kind of recurrent training.

- Question 20—Various ideas for improvements to inspector composite NDI training were received. Some of the suggestions included more specific instrument training, limiting the number of inspectors who are trained to perform composite inspections, more mentoring and OJT, training related to how composites structures are made, and clarification on which reference standards should be used for inspecting composite repairs. Some of the respondents mentioned that they have developed, or are in the process of developing, their own training courses related to composite NDI training.

- Question 21—The respondents requested additional guidance to help ensure comprehensive composite training programs with the breakdown as follows: 81% requested more guidance from the OEMs, 63% would like more guidance that is developed and published by industry groups, and 31% requested more guidance from the FAA. Only one respondent mentioned that no guidance was needed.

- Question 22—The areas where additional guidance is needed for comprehensive composite inspection training programs varied widely. The general overall requests for guidance centered around specific instrument information, guidance on specific methods, repair inspections, composite construction training, and more OEM information.

F.4 Composite NDI Training Survey

The following is the actual survey sent to airlines and MROs:

Composite NDI Training Survey

Please provide information for the following questions regarding your company's composite NDI training program. Please feel free to use this document and add your answers under each question. If you have any NDI Training description document files that you want to pass on to us to provide additional information on your programs, please feel free to do so. These documents will be kept strictly confidential and the information will only be used in a compiled set of results for industry training. *As a participant, the compiled survey results will be sent to you.*

(Note: For questions that have multiple answers, please check all that apply)

Please refer any questions to: Tom Rice
Sandia National Laboratories
(505) 844-7738

1. Describe the general NDI training programs at your company.

2. Indicate how your NDI training program is implemented.
   a. ____ In house by your instructor
   b. ____ In house by on-line training (in house generated material)
   c. ____ In house by an outside instructor
   d. ____ External by an outside instructor
   e. ____ External by on-line training (externally generated material)
   f. ____ Other, please specify

3. What type of formal documentation is obtained from the instruction?
   a. ____ Certificate of completion
   b. ____ Entry into common training database
   c. ____ Log containing training type and hours completed
   d. ____ Other, please specify
4. What NDI techniques does your company employ to inspect composites

Laminate Composites:

a. ____ Pulse-Echo Ultrasonics (PE-UT)
b. ____ Phased Array Ultrasonics (PA-UT)
c. ____ Resonance (RES)
d. ____ Low Frequency Bond Test (LFBT)
e. ____ Mechanical Impedance Analysis (MIA)
f. ____ Thermography
g. ____ Shearography
h. ____ X-Ray
i. ____ Other, please specify

Honeycomb Composites:

a. ____ Pulse-Echo Ultrasonics (PE-UT)
b. ____ Phased Array Ultrasonics (PA-UT)
c. ____ Resonance (RES)
d. ____ Low Frequency Bond Test (LFBT)
e. ____ Mechanical Impedance Analysis (MIA)
f. ____ Thermography
g. ____ Shearography
h. ____ X-Ray
i. ____ Other, please specify

5. Do inspectors also receive general composite training to understand composite materials, plies, lay-ups, scarfed repairs, composite design, composite processing, etc.?

a. ____ Yes

If yes, how many hours/year?	
If yes, how many classes/year?	

b. ____ No

6. Do you have additional, specialized training specifically for inspectors who can perform composite inspections? [This would be above-and-beyond your normal NDI training.]

    a. ____ No

    b. ____ Yes, please describe (no limit on length)

7. If the answer to the previous question is "Yes," list the areas in which you provide additional, specialized NDI training for composite inspections (above and beyond Level I, II and III NDI certification for composites). List how many total hours of specialized, composite NDI training inspectors complete and over what interval?

Laminate Composites			
Method	Total OJT Hours	Total Classroom Hours	Over What Time Period in Years
Pulse-Echo Ultrasonics (PE-UT)			
Phased Array Ultrasonics (PA-UT)			
Resonance (RES)			
Low Frequency Bond Test (LFBT)			
Mechanical Impedance Analysis (MIA)			
Thermography			
Shearography			
X-Ray			
Other (list)			
Honeycomb Composites			
Method	Total OJT Hours	Total Classroom Hours	Over What Time Period in Years
Pulse-Echo Ultrasonics (PE-UT)			

Phased Array Ultrasonics (PA-UT)			
Resonance (RES)			
Low Frequency Bond Test (LFBT)			
Mechanical Impedance Analysis (MIA)			
Thermography			
Shearography			
X-Ray			
Other (list)			

8. Do inspectors receive additional training related to composite repair inspection?
   a. ____ No
   b. ____ Yes (Please specify)

9. Do you have inspectors assigned specifically to the composite shop that conduct your composite inspections?
   a. ____ No, we don't have composite shop inspectors vs. other heavy maintenance inspectors.
   b. ____ Yes

   If "Yes," do inspectors accomplish other inspection tasks such as receiving inspections? (If so, list them) _______________

10. Does your company provide instruction on the use of NDI scanning systems (production of C-Scan images), for example the Boeing MAUS system?
    a. ____ Yes, please explain and list the systems

    b. ____ No

11. Has your NDI training curriculum been updated to accommodate composite inspections?

a. ____ Yes, please explain what you have added.

b. ____ No

12. Does your company use any of the following standards as criteria for your NDI training program? If so, which one(s)?

    a. ____ AIA-NAS-410, Aerospace Industries Association, National Aerospace Standard, NAS Certification & Qualification of Nondestructive Test Personnel.

    b. ____ ATA Specification 105, Air Transport Association, Guidelines for Training and Qualifying Personnel in Nondestructive Testing Methods.

    c. ____ Canadian National Regulations contained in CAN/CGSB-48.9712-95, Qualification and Certification of Nondestructive Testing Personnel

    d. ____ International Standards Organization (ISO) document; ISO 9712, Nondestructive Testing-Qualification and Certification of Personnel

    e. ____ MIL-STD-410E, Military Standard, Nondestructive Testing Personnel Qualification and Certification

    f. ____ American Society for Nondestructive Testing, Inc. (ASNT), Recommended Practice SNT-TC-1A, Personnel Qualifications and Certification in Nondestructive Testing

    g. ____ European Standard prEN 4179, Qualification and Approval of Personnel for Nondestructive Testing

    h. ____ Other standards, please specify

13. Qualification of inspectors to perform tasks is usually based on an examination and/or other demonstration of proficiency. Do you have <u>additional</u>, special inspector <u>qualification</u>/<u>certification</u> to qualify personnel for conducting composite inspections, in addition to your normal qualification program

    a. ____ Yes, please explain local methods

    b. ____ No, we use the standards checked in the previous question

14. Do any of the following enter into decisions on qualification to perform certain inspections (e.g., composite damage inspections) or is qualification solely based on formal inspector ratings such as ASNT Level II or Level III?
    a. ____ Experience
    b. ____ Seniority
    c. ____ Aptitude
    d. ____ Training
    e. ____ Other, please specify
    f. ____ Qualification is based solely on ASNT Level

15. If experience level is a factor in determining qualification to perform certain inspections, do you use some sort of apprentice program to expose newer inspectors to such inspections?
    a. ____ Yes, please explain the program (no limit on length)

    b. ____ No

16. In your opinion, do Level I, II, and III training/qualifications provide the necessary expertise for both metal and composite NDI or should additional training take place for composite inspections?
    a. ____ Yes, Level I, II, and III training/qualification is sufficient
    b. ____ No, additional training should take place for composite inspections

17. Should there be additional inspector ratings (i.e., Level I – III) for new NDI methods, such as shearography, that currently do not exist?
    a. ____ Yes, list the methods

    b. ____ No

18. What percentage of your NDI inspectors are qualified to inspect composites?
    a. ____ Under 25%

b. ____ 25% - 50%

c. ____ 50% - 75%

d. ____ 75% - 99%

e. ____ 100%

19. (A) In your company, can a mechanic deploy a simple “Go/No-Go” (or “Green Light/Red Light”) device, such as the Olympus Ramp Damage Checker or GE Bondtracer™ instrument, to conduct composite inspections?

    a. ____ Yes

    b. ____ No

    (B) Would there be management-labor issues associated with a mechanic doing inspector functions?

    a. ____ Yes

    b. ____ No

    (C) How much and what type of training should the mechanics receive?

    Please describe (no limit on length).

    (D) Should there be recurrent training for mechanics?

    Please describe what type of recurrent training and how often (no limit on length).

20. What are your ideas for improvements to training programs and inspector qualifications in order to perform composite inspections? Please specify (no limit on length).

21. In what areas is additional guidance needed to help ensure comprehensive composite training programs for the aviation industry? (check all that apply)

    a. ____ Guidance from the FAA
    b. ____ Guidance from OEMs
    c. ____ Guidance developed and published by industry groups such as the Commercial Aircraft Composite Repair Committee

22. Please list, in the order of their importance, areas where additional guidance/information is needed for comprehensive composite inspection training programs.

    a. ____

    b. ____

    c. ____

    d. ____

    e. ____

Please provide the following responder information:

Name:

Email:

Title:

Company:

In the final aggregate results, we ensure that the survey participants will be kept anonymous so that it is not possible to correlate any results to a specific airline or MRO. We are merely trying to assemble a summary of industry training practices. **No individual responder's name will be linked to any survey results.** Similarly, no organization's name will be linked to any survey information.

Please return this survey to Tom Rice.

Mail to:
Sandia National Laboratories
Attn: Tom Rice
P.O. Box 5800, MS-0615
Albuquerque, NM 87185

Email to:
tmrice@sandia.gov

F-1. Roach, D.P., Rice, T.M., and Rackow, K.A., “A Quantitative Assessment of Conventional NDI Techniques for Detecting Flaws in Composite Laminate Aircraft Structures,” FAA Report DOT/FAA/TC-15/4, Publication date TBD.

F-2. U.S. Department of Transportation, Federal Aviation Administration, Advisory Circular 65-31A, “Training, Qualification, and Certification of Nondestructive Inspection (NDI) Personnel,” April 25, 2003.

F-3. Berry, F.C., “ASNT Recommended Practice for Nondestructive Testing Personnel Qualification and Certification (SNT-TC-1A) and its Use,” Nondestructive Testing Standards-A Review, ASTM STP 624, Harold Berger, Ed., American Society for Testing and Materials, 1977, pp. 53-62.

F-4. American Society for Nondestructive Testing, Inc. (ASNT), Recommended Practice SNT-TC-1A, “Personnel Qualifications and Certification in Nondestructive Testing,” 2011 edition.

F-5. Aerospace Industries Association, National Aerospace Standard, NAS-410, “NAS Certification & Qualification of Nondestructive Test Personnel,” 2008.

F-6. Air Transport Association of America, Inc., ATA Specification 105, “Guidelines for Training and Qualifying Personnel in Nondestructive Testing Methods,” Revision 2011.1.

APPENDIX G—DISTRIBUTION LIST FOR REPORT

Frances Abrams
AFRL/MLMP
2977 Hobson Way
Bldg 653, Rm 215
Wright-Patterson AFB, OH 45433-7739

Paul Acres
Lockheed-Martin Aero
Lockheed Blvd.
Bldg. 4, 1st Floor, Column 22C
Ft Worth, TX 76108

Dick Alberts
Digiray Corporation
317 Hartford Rd
Danville, CA 94526

Jay Amos
Cessna Aircraft Co.
P.O. Box 7704 M/S1
Wichita, KS 67277-7704

Ric Anderson
Air Transport Association
1301 Pennsylvania Avenue, NW
Suite 1100
Washington, DC 20004-1707

Jason Anzai
Aloha Airlines
P.O. Box 30028
Honolulu, Hawaii 96820

James Arnold
NDT Manager
Continental Airlines
4849 Wright Road
Houston, TX 77032

Brian Baggot
Laser Technology Inc.
1055 West Germantown Pk
Norristown, PA 19403

Eric Bartoletti
American Airlines
Maintenance & Engineering Center
3900 North Mingo Rd., MD 35
Tulsa, OK 74107-4854

Andrew Bayliss
British Airways
Aircraft Structures & Qual Standards
P.O. Box 10 B4 TBA S343
Hounslow, Middlesex
UNITED KINGDOM, TW6 2JA

Phil Berkley
GKN Westland Aerospace
Materials Laboratory
Box 103 Yeovil
BA20 2YB UNITED KINGDOM

Subra Bettadapur
NAVAIR 4.3.4.2
Bldg. 2188 MS-5
48066 Shaw Rd.
Patuxent River, MD 20670-1908

Wolfgang Bisle
AIRBUS Deutschland GmbH
Dept.: ESWNG / Testing Tech. Germany
Huenefeldstr. 1-5
28199 Bremen, GERMANY

James Bitner
NDT Engineering
19620 Russell Rd.
Kent, WA 98032

Bryce Boe
Raytheon Aircraft Co.
P.O. Box 85
Wichita, KS 67201-0085

Robert Bonaventura
Continental Airlines
HQJQC
Box 4623
Houston, TX 77210

Richard Bossi
Boeing Phantom Works
P.O. Box 3999 MC 2T-50
Seattle, WA 98124-2499

Susan Bowles
Defense Science Tech. Org.
P.O. Box 4331
Melbourne, Victoria 3001 AUSTRALIA

Rudy Braun
Boeing Canada Technology Ltd.
Winnipeg Division
99 Murray Park Road
Winnipeg, Manitoba R3J 3M6 CANADA

John Brausch
AFRL/MLSA
2179 12th Street, Bldg 652, Rm 122
Wright-Patterson AFB, Ohio 45433-7718

Nick Brinkhoff
Cessna Aircraft Co.
Box 7704
Wichita, KS 67277-7704

Al Broz
Chief Scientist and Technical Advisor
FAA NRS NDI
FAA New England, ANE 105N
12 New England Exec. Dev. Park
Burlington, MA 01803

Doug Burleigh
Goodrich
2845 Arcola Ave.
San Diego, CA 92117

Alistair Burns
Air New Zealand
Eng. Base, Geoffrey Roberts Road
Auckland International Airport
P.O. Box 53098
Auckland, NEW ZEALAND

Michael Canning
GKN Westland Aerospace
Avonmouth Rd.
Avonmouth, Bristol   BS11 9DU
UNITED KINGDOM

Steve Cargill
Aerospace Structural Integrity
8637 SE Sharon Street
Hobe Sound, FL 33455

LCDR Mark Carmel
Chief, HH-60J Engineering Branch
USCG Aircraft Repair and Supply Center
Elizabeth City, NC 27909

Jerry Carr
Corpus Christi Army Depot
P.O. Box 81325
Corpus Christi, TX 78468-1325

Eric Chesmar
United Airlines
Maintenance Operations - SFOEG
San Francisco Int'l Airport
San Francisco, CA 94128-3800

Francisco Coelho
TAP Air Portugal
P.O. Box 50194
Lisbon,1704 Lisbon Codex
PORTUGAL

Jack Conrad
American Airlines
Mail Drop 8948 Hangar
2000 Eagle Parkway
FT. Worth, TX 76161

Vicente Cortes
Airbus España
Materials & Processes
John Lennon S/N
28906 Getafe (Madrid), SPAIN

Ed Cosgro
Petroleum Helicopters, Inc.
P.O. Box 90808
Lafayette, LA 70509-0808

Ed Cuevas
FAA Rotorcraft Directorate
2601 Meacham Blvd
Ft Worth, TX 76137

Dave Cummins
GKN Westland Helicopters
Box 103 Yeovil
BA20 2YB UNITED KINGDOM

Wayne Davis
Manager, Aircraft Inspection
United Airlines - INDIQ
2825 W. Perimeter Rd.
Indianapolis, IN 46241

Marie-Anne De Smet
NDT Expert
1 Av Leon Foucault
Colomiers 31770 FRANCE

Juan Garcia Diaz
Head of NDT Department
IBERIA Airlines
IBERIA Dirección de Material
Zona Industrial # 2
Madrid, SPAIN 28042

Gerry Doetkott
Northwest Airlines
5101 Northwest Dr.
St. Paul, MN 55111-3034

Leo Dominguez
American Airlines/TAESL
2100 Eagle Parkway
MD 8361
Fort Worth, Texas 76177

Christopher Dragan
Air Force Institute of Technology
Ks. Boleslawa 6
P.O. Box 96
01-494 Warsaw, POLAND

Tommy Drake
Lockheed Martin Aeronautics - Fort Worth
Laser Ultrasonics Technology Center
One Lockheed Blvd.
MZ 6852 Bldg.4/1/23C
Fort Worth, TX 76108

Tom Dreher
Rolls Royce Engine
Indianapolis, IN

Marco Dube
Lufthansa Technik AG
Airframe Related Components WD51
Weg Beim Jager 193
22335 Hamburg, GERMANY

Philippe Dupont
Engineering Mgr.
Air France
Hangar H2
Le Bourget Overhaul Center
F93352 Le Bourget, FRANCE

Ewald Ekart
Lufthansa Technik
Dept. WF21
60546 Frankfurt, GERMANY

Emmanuel Enemouh
Univ. of Minnesota
Dept. of Mechanical Engineering
105 Voss-Kovach Hall
1305 Ordean Court
Duluth, Minnesota 55812-3042

Peter Feddern
NDT - Workshop Lead
Lufthansa Technik A.G.
Department: HAM WO 484
Weg Beim Jaeger 193
D-22335 Hamburg, GERMANY

Ernie Fidgeon
Air Canada
Air Canada Base 891
2450 Saskatchewan Ave
Winnipeg, MB R3C2N2 CANADA

Tom Flournoy
FAA WJ Hughes Technical Center
AAR-480
Atlantic City Int'l Airport, NJ 08405

Laurent Fontaine
Airbus Industries
1 Rond Point Maurice Bellonte
31707 Blagnac Cedex, FRANCE

Joe Gabris
Boeing
PO Box 516 MS S270-4360
St Louis, MO 63166-0516

Yolanda de Frutos Galindo
Airbus España
Materials & Processes
John Lennon S/N
28906 Getafe (Madrid) SPAIN

Jean-Baptiste Gambini
Airbus Industrie
1 Rond Point Maurice Bellonte
31707 Blagnac Cedex, FRANCE

Steve Galea
Aeronautical and Maritime Res. Lab
Defense Science Tech. Org
P.O. Box 4331
Melbourne, Victoria 3001   AUSTRALIA

Dave Galella
FAA WJ Hughes Technical Center
AJP-6360
Atlantic City Int'l Airport, NJ 08405

Donald Gauronski
United Parcel Service
A/C Maintenance - Quality Control
3121 East Jurupa Street
Ontario, CA 91761

Head of NDI
Bombardier Aerospace
P.O. Box 6087, Station Centre-ville
Montreal, Quebec
H3C 3G9 CANADA

Skeeter Gehring
Delta Air Lines
Dept. 521 NDT
2901 East 28th St.
DFW Int'l Airport, TX 75261

Marc Genest
Institute for Aerospace Research National
Research Council Canada
Building M-14 1200 Montreal Road,
Ottawa, ON, K1A 0R6
Canada

Bill Gerrish
Aerostructures Customer Support
BF Goodrich
850 Lagoon Dr
Chula Vista, CA 91910-2001

Don Gilbert
Lead Inspector
Alaska Airlines
PO Box 68900
Seattle, WA 98168

Robert Gleason
Director of Inspection
Northwest Airlines
5101 Northwest Dr.
St. Paul, MN 55111-3034

Jon Goo, VP of QA
Aloha Airlines
P.O. Box 30028
Honolulu, Hawaii 96820

Kim Graebner
Boeing
P.O. Box 7730, MS K84-40
Wichita, KS 67277-7730

Eric Grandia
Quality Material Inspection, Inc
3505 Cadillac Ave., #N-3
Costa Mesa, CA 92626

Irving Gray
NDE Technologies Inc.
1785 Sourwood Pl.
Charlottesville, VA 22911

Bert Groenewoud
Hans Kramer
Eng. & Maintenance (SPL/CF)
KLM Royal Dutch Airlines
P.O. Box 7700
1117 ZL Schiphol Airport
NETHERLANDS

Mike Gutierrez
Mgr. NDT Dept.
Federal Express
7401 World Way West
Los Angeles, CA 90045

Colin Hanna
Bombardier Aerospace
Materials and Processes Eng. Dept.
Airport Road, Belfast BT3 9DZ
UNITED KINGDOM

Pekka Hayrinen
Finnair
Helsinki-Vantaa -Airport
XU-28
Helsinki, Finland 01053

Pam Herzog
Air Force NDI Office
AFRL/MLS-OL
4750 Staff Drive
Bldg. 3230 Rm. 111
Tinker Air Force Base, OK 73145

John Hewitt
Airbus
Materials Laboratory
No. 1 Flight Shed
Filton, Bristol
BS99 7AR UNITED KINGDOM

Keith L. Hickman
Lockheed Martin
P.O. Box 650003 M/S SK-04
Dallas, TX 75265-0003

Colin Hockings
Qantas Airlines
NDT Section
C/- Central Stores M189
Mascot, AUSTRALIA 2020

Jim Hofer
Boeing
2401 E. Wardlow Road
M/C: C078-0113
Long Beach, CA 90807-4418

Ed Hohman
Bell Helicopter
PO Box 482
Fort Worth, TX 76101

Mike Hoke
ABARIS Training
5401 Longley Lane, Suite 49
Reno, NV 89511

Quincy Howard
NDT Engineer - Customer Services
The Boeing Company
P.O. Box 3707 M/S 04-EH
Seattle, WA 98124

David Hsu
Center for Nondestructive Evaluation
1917 Scholl Road
Iowa State University
Ames, IA 50011

David Huddleston
United Space Alliance
8550 Astronaut Blvd.
Cape Canaveral, FL 32920-4304

Larry Ilcewicz
Chief Scientist and Advisor
FAA NRS Composites
1601 Lund Ave. SW
ANM-115N
Renton, WA 98055

Russell Jones
National Resource Specialist NDI
FAA National Headquarters
800 Independance Ave S.W.
Washington, DC 20591

David Jonker
Head of Technical Services
GAMCO
PO Box 46450
Abu Dhabi, UNITED ARAB EMIRATES

Birgit Junker
Vestas Wind Systems A/S
Quality and Enviromental Dept.
6940 Lem St.
Smed Hansens Vej 27 DENMARK

Tony Kepczyk, SQNLDR
Royal Australian Air Force
DGTA - DAIRMAINT
RAAF Base Hangar 410
Amberley, Queensland 4306
AUSTRALIA

Chris Kirby
NDT Solutions
Dunston Innovation Center
Dunston Road
Chesterfield S41 8NG
UNITED KINGDOM

Rene Klieber
Manager Non Destructive Testing
SR Technics Ltd
CH-8058 Zurich Airport
SWITZERLAND

Slawomir Klimaszewski
Air Force Institute of Technology;
ul. Ks. Boleslawa 6
P.O. Box 96
01 - 494 Warsaw, POLAND

Bryan Knowles
Southwest Airlines
2832 Shorecrest Dr
DAL-2MX
Dallas, TX 75235-1611

Jeff Kollgaard
Boeing
P.O. Box 3707, MS 2T-42
Seattle, WA 98124-2207

Hans Kramer
Eng. & Maintenance (SPL/CF)
KLM Royal Dutch Airlines
P.O. Box 7700
1117 ZL Schiphol Airport
NETHERLANDS

Steve Krause
Delta Air Lines
NDT Shop
P.O. Box 20706
Atlanta, GA 30320-6001

Lloyd Landburg
Quality Control NDT Analyst
Southwest Airlines
2832 Shorecrest Dr DAL/2MX
Dallas, TX 75235

Eric Le Nir
Air France
Hangar H2
Le Bourget Overhaul Center
F93352 Le Bourget, FRANCE

Tony Lewis
US Airways
Flight Service/Composites Shop
5535 Wilkinson Blvd.
Charlotte, NC 28226

Eric Lindgren
SAIC/Ultra Image International
Two Shaw's Cove, Suite 101
New London,CT 6320

Gregory Linkert
Technical Specialist NDT
Northwest Airlines
7500 Airline Drive
Minneapolis, MN 55450

Maria Lodeiro
Centre for Materials Measurement
National Physical Laboratory
Queens Rd.
Teddington, Middlesex
TW11 0LW UNITED KINGDOM

John Lundeen
NDI Engineer
Naval Air Warfare Center, Aircraft Div
Bldg. 2188, MS-5
Patuxent River, MD 20670

Pekka Manninen
Finnair
Finnair Oyj
PL 15, EN / 28
Helsinki-Vantaa Airport, FIN - 01053
FINLAND

John Marchant
British Airways
NDT & EHM Unit Heathrow Airport
P.O. Box 10 North Block Annexe TBD
Hounslow, Middlesex TW6 2JA
UNITED KINGDOM

Rod Martin
Chief Executive Officer
Materials Engineering Research Lab
Tamworth Road
Hertford, SG13 7DG
UNITED KINGDOM

Greg Marshall
Bell Helicopter
PO Box 482
Fort Worth, TX 76101

Sergio Mayer
Embraer
Av. Brigadeiro Faria Lima, 2170
1227-90 San Jose dos Campos – SP
BRAZIL

Glae McDonald
US Airways
5020 Hangar Rd.
Charlotte, NC 28219

John McNamara
New Mexico State
Civil Engineering Dept.
MSC 3CE / Box 30001
Las Cruces, NM 88003-8001

Alexander Melton
Northwest Airlines
NDT Dept. C8843
1914 Benjamin Street NE
Minneapolis, MN 55418-4810

Bill Miller
Transport Canada
330 Sparks Street Tower C
Ottawa, Ontario K1A ON5 CANADA

Scott Miller
Alaska Airlines-SEAMQ
P.O. Box 68900
Seattle, WA 98168

Tom Moran
Air Force Research Labs
Material & Mfg Directorate
2230 10th St
AFRL/MLLP
Wright-Patterson AFB, OH 45433-7817

Matt Moye
Air Force NDI Office
AFRL/MLS-OL
4750 Staff Drive
Bldg. 3230 Rm. 111
Tinker Air Force Base, OK 73145

Andy Murphy
Royal Air Force St Athan
Barry, Vale of Glamorgan CF62 4WA
UNITED KINGDOM

Sergio Nascimento
TAP Air Portugal
Maintenance & Engineering
P.O. Box 50194
Lisbon, 1704-801 PORTUGAL

Gwen Nguyen
Gov’t Indus. Data Exchange Program
P.O. Box 8000
Corona, CA 91718-8000

Cu Nguyen
FAA WJ Hughes Technical Center
AAR-480
Atlantic City Int'l Airport, NJ 08405

Carol Novea
Air Force Research Laboratory
2179 12th St., Bldg. 652, Rm. 124
Wright-Patterson AFB, OH 45433-7707

Marv Nuss
FAA
ACE-113
901 Locust
Kansas City, MO 64016

John O’Connell
Cargolux Airlines Int'l S.A.
Luxembourg Airport,
Findel, Luxembourg L-2990
LUXEMBOURG

Paul Oulton
United Airlines SFOIQ
San Franciso Intl Airport
San Francisco, CA 94128

Georgios Papageorgiou
Olympic Airways
Athens International Airport, Tech. Base
OA.TD/IC
Spata-Athens, 19019 GREECE

Rob Pappas
FAA WJ Hughes Technical Center
AJP-6360
Atlantic City Int’l Airport, NJ 08405

Marvin Paschal
American Airlines
Mail Drop 8948 Hangar
2000 Eagle Parkway
Ft. Worth, TX 76161

Kieren Patten (head)
Paul Guilfoyle (deputy)
Shannon Aerospace
Non Destructive Testing
Shannon Airport
Shannon, Co. Clare IRELAND

Fred Perkins
Syncretek - Shearography
6679 McLean Drive
McLean, VA 22101

John Petrakis
FAA
800 Independence Av, SW
Washington, DC 20591

Wilfried Pieles
AIRBUS Deutschland GmbH
Dept.: ESWNG / Testing Tech. Germany
Huenefeldstr. 1-5
28199 Bremen, GERMANY

David Piotrowski
Delta Air Lines
Department 572
PO Box 20706
Atlanta, GA 30320-6001

Rob Pitts
Naval Aircraft Materials Lab
Fleetlands Gosport
Hampshire
PO130FL UNITED KINGDOM

Richard Rachowiecki
British Airways
Non Destructive Testing
North Block Annex TBD E148
PO Box 10
Heathrow Airport
Hounslow, Middlesex TW 6 2JA
UNITED KINGDOM

Bernd Rackers
Airbus Deutschland GMBH
Hunefeldstrasse 1-5
21899 Bremen, GERMANY

Doug Ragsdale
Soutwest Airlines
Maintenance Control X-5929
2832 Shorecrest Dr
DAL-2MX
Dallas, TX 75235-1611

Tom Reep
Zetec
1370 NW Mall Street
Issaquah, WA 98027

Kevin Rees
U.S. Army Aviation & Missiles Command
ATTN: AMSAM-MMC-VS-EC
Corpus Christi, TX 78419

Jeff Register
Northwest Airlines
5101 Northwest Dr.
St. Paul, MN 55111-3034

Al Riffal
America West Airlines
4000 E. Sky Harbor Blvd.
Phoenix, AZ 85034

Paul Risso
Manager, Aircraft Inspection
United Airlines - SFOIQ
San Francisco Int'l Airport
San Francisco, CA 94128

Mark Rodekuhr
BF Goodrich Aerospace
8200 Arlington Ave.
Riverside, CA 92503-0428

Olaf Ronsdorf
Lufthansa Technik AG
Customer Engrg FRA WI 21
Phein Main Airport
60546 Frankfurt, GERMANY

Don Roth
NASA Glenn ResearchCenter
M.S. 6-1
RM. 117E, Bldg. 6
21000 Brookpark Road
Cleveland, OH 44135

Jean Rouchon
Ministry of Defence
CEAT – 23 Avenue Henri Guillaumet
31056 Toulouse Cedex FRANCE

Bob Saathoff
Cessna Aircraft Company
P.O. Box 7704 M/S1
Wichita, Kansas 67277

Engin Sabuncu
Cessna Aircraft Company
Pawnee Engineering
5800 E. Pawnee
Wichita, KS 67218

Adam Sawicki
Boeing Company
P.O. Box 16858 Mail Code P38-13
Philadelphia, PA 19142

Christine Scala
Aeronautical and Maritime Res. Lab
DSTO
P.O. Box 4331
Melbourne, Victoria 3001 AUSTRALIA

George Schneider
Sikorsky Aircraft Corp.
6900 Main Street
P.O. Box 9729
Stratford, CT 066615-9129

Philip Schnubb
First Air
3257 Carp Road
Carp, Ontario K0A 1L0 CANADA

Bob Schroeder
Inspection Supervisor
United Parcel Service
750 Grade Lane
Louisville, KY 40213

Steve Shepard
Thermal Wave Imaging
845 Livernois
Ferndale, MI 48220

Luiz Siegmann
VARIG Airlines
Engineering and Maintenance
Augusto Severo, 851 – POABS
Porto Alegre RS, 90240-480 BRAZIL

Vilmar da Silva do Valle
Embraer
Av. Brigadeiro Faria Lima, 2170
1227-90 San Jose dos Campos – SP
BRAZIL

Jesse A. Skramstad
NDT Solutions, Inc.
1682 County Road K
New Richmond, WI 54017

Fred Sobeck
FAA NRS Aging Aircraft
FAA Flight Standards
AFS 330D
800 Independence Ave. SW
Washington, DC 20591

Holger Speckmann
AIRBUS Deutschland GmbH
Dept.: ESWNG / Testing Tech. Germany
Huenefeldstr. 1-5
28199 Bremen GERMANY

Giancarlo Spera
NDT Engineering Dept.
Alitalia
Areoporto Leonardo da Vinci
Piazza Almerico da Schio
Fiumicino (Rome), 50 ITALY

Bob Stakenborghs
Evisive, Inc.
1925 Ryder Ave.
Baton Rouge, LA 70808

Robert Stevens
United Airlines
San Francisco Int'l Airport - SFOEP
NDT Process Engineering
San Francisco, CA 94128-3800

Larry Sullivan
Goodrich Aerostructures
850 Lagoon Dr. mz 107P
Chula Vista, CA 91910-2098

Paul Swindell
FAA WJ Hughes Technical Center
AJP-6360
Atlantic City Int'l Airport, NJ 08405

Vasu Thirumalai
Applied Aerospace Structures Corp.
3437 South Airport Way
P.O. Box 6189
Stockton, CA 95206

Darrell Thornton
UPS
750 Grade Lane
Louisville, KY 40213

Alain Tissenier
Airbus Industries
1 Rond Point Maurice Bellonte
31700 Blagnac FRANCE

Gustav Tober
AIRBUS Deutschland GmbH
Dept.: ESWNG / Testing Tech. Germany
Huenefeldstr. 1-5
28199 Bremen, GERMANY

John Tomblin
Wichita State Univ.
1845 Fairmount
Wichita, KS 67260-0044

John Tyson
Trilion Quality Systems
241 Atlee Rd.
Wayne, PA 19087

K. Dick Vaughn
Rocky Mountain Composites
301 W. 3000 N.
Spanish Fork, UT 84660

Victor Vilents
PK Design
Sevanskaya st. 3 app 170
Moscow 115516 RUSSIA

Jon Voeller
OC-ALC/MANPO
B3001 Post 2V106
Tinker AFB, OK 73145-3030

Stephen Ward
SW Composites
HC68 Box 15G
Taos, NM 87571

Patrick Walter
Texas Christian University
Engineering Dept., Box 298640
Ft. Worth, TX 76129

Richard Watkins
Delta Air Lines
NDT Shop
P.O. Box 20706
Atlanta, GA 30320-6001

Guenter Wehmann
AIRBUS Deutschland GmbH
Dept.: ESWNG / Testing Tech. Germany
Huenefeldstr. 1-5
28199 Bremen, GERMANY

Brian Williams
British Airways
NDT - Heathrow Airport
North Block Annex TBD E148
PO Box 10
Hounslow, Middlesex, TW6 2JA
UNITED KINGDOM

Scott Williams
Southwest Airlines
2620 George Street
Pearland, TX 77581

William Winfree
Mail Stop 231
3b East Taylor Street
NASA Langley Research Center
Hampton, VA 23681-0001

Buzz Wincheski
Mail Stop 231
3b East Taylor Street
NASA Langley Research Center
Hampton, VA 23681-0001

Roy Wong
Bombardier Aerospace
P.O. Box 6087, Succursale, Centre-ville
Montreal, Quebec H3C 3G9 CANADA

Roman Wottle
Head of Mechanics & NDT Workshop
Austrian Airlines
Austrian Base / TDWM
Vienna Airport, A-1300 AUSTRIA

Nancy Wood
The Boeing Company
PO Box 516
Mailcode 1021111
St. Louis, MO 63166

John Vogt
The Nordham Group
11200 E. Pine St.
Tulsa, OK 74116

Jun Yamanaka
Japan Airlines International
M1 Bldg.
3-5-1, Haneda Airport
Ota-ku, Tokyo 144-0041 JAPAN